Magnesium Transport in the Heart

by

Hasan Almulla

A thesis submitted to the Faculty of Medicine at
The University of Edinburgh for the Degree of

Doctor of Philosophy

The University of Edinburgh - 2002
Edinburgh, Scotland

DECLARATION

Unless specifically mentioned otherwise, the work presented in this thesis has been conducted by myself. This thesis has not been submitted for any other degree or professional qualification except as specified.

Hasan Almulla

Dedicated to

the soul of my father and to my mother

for their infinite love and support

ABSTRACT

The Na^+-dependence of Mg^{2+} transport in isolated rat ventricular myocytes was investigated using the Mg^{2+} fluorescent dye mag-fura-2. The dye was used in dual excitation mode (340 nm/ 380 nm) and was calibrated *in vitro*. Free cytosolic Mg^{2+} concentration ($[Mg^{2+}]_i$) in quiescent ventricular myocytes was 0.75 ± 0.05 mM (mean ± S.E.M., n = 77). Myocytes were loaded with Mg^{2+} by superfusion with a high $[Mg^{2+}]$ solution that was both Na^+- and Ca^{2+}-free. On changing to a physiological solution, $[Mg^{2+}]_i$ returned to pre-load levels. This reduction was found to depend on the presence and concentration of external Na^+ ($[Na^+]_o$) where, increasing $[Na^+]_o$ increased the rate constant of $[Mg^{2+}]_i$ reduction. The relationship between $[Na^+]_o$ and $[Mg^{2+}]_i$ reduction is well described by a straight line of slope 1.02 ± 0.10 mM^{-1} (mean ± S.E., n = 20). This $[Mg^{2+}]_i$ reduction is inhibited by imipramine (200 μM).

The rate of $[Mg^{2+}]_i$ elevation above resting levels was also dependent on $[Na^+]_o$ and $[Mg^{2+}]_o$. Decreasing $[Na^+]_o$ or increasing $[Mg^{2+}]_o$ increases the maximum rate of $[Mg^{2+}]_i$ elevation. $[Mg^{2+}]_i$ elevation was not inhibited by imipramine (200 μM), in cells loaded such that $[Mg^{2+}]_i$ was at least 2 mM.

In order to investigate the involvement of the Na^+/Ca^{2+} exchanger in the regulation of $[Mg^{2+}]_i$, cells were treated with KB-R7943, an inhibitor of the reverse mode of the Na^+/Ca^{2+} exchanger. $[Mg^{2+}]_i$ reduction in Mg^{2+}-loaded myocytes was insensitive to KB-R7943 (20 μM). However, the same concentration of the drug inhibited $[Mg^{2+}]_i$ elevation, but only when applied at modest Mg^{2+} loads ($[Mg^{2+}]_i < 2$ mM).

The possible electrogenicity of Mg^{2+} transport was investigated by depolarising the cell, either by high $[K^+]_o$ or by patch clamping. Cell depolarisation increased the rate constant of $[Mg^{2+}]_i$ reduction in Mg^{2+}-loaded myocytes and decreased the maximum rate of $[Mg^{2+}]_i$ elevation in cells superfused with the high $[Mg^{2+}]$ solution.

The results suggest that Mg^{2+} is expelled from these cardiac cells through an imipramine- and Na^+-sensitive sarcolemmal Mg^{2+} transporter, possibly a Na^+/Mg^{2+} antiport in which, the influx of one Na^+ ion is required for the extrusion of one Mg^{2+} ion. Also, some Mg^{2+} uptake probably occurs through reversal of the putative antiport, but almost certainly other uptake mechanisms exist, possibly including the Na^+/Ca^{2+} exchanger, at least under the experimental conditions used in this study.

ACKNOWLEDGEMENT

Praise be to Allah for enabling me to complete this work, and for granting me this opportunity to explore new dimensions in my career. Throughout my time at Edinburgh University, there have been many people who have offered support and friendship to make my experience a successful and an enjoyable one.

A great debt of thanks is owed to my research supervisors, Drs. David Ellis and Peter W. Flatman. I feel extremely lucky to have worked with such wonderful and sincere scientists. Dave and Peter, I cannot thank you enough for your intelligent guidance, encouragement, kindness and above all trust. You have allowed me to become the best scientist I can be. Our discussions were always enlightening, even if not immediately so. I am indebted to you for everything that you have taught me.

I am very grateful to the Ministry of Health in Bahrain for sponsoring this work. My thanks to Ms. Batool Al Muhandis, Dean of the College of Health Sciences, former Dean, Dr. Faisal Al Hamar and Ms. Mona Bu Hazza, Chair of the Integrated Sciences Division for their support.

My friends provided much needed moral support. My old friends, Abdul Rahman Al Shaikh and Maher Alkhan, helped me in ways they can never imagine. My thanks to Jassim Mohammed who has been a true friend over many years and last but not least my gratitude to Dr. Omar Elahmer who, although lost most of the badminton games to me, has won my utmost respect and friendship. I am proud to have such friends.

My deepest thanks and gratitude to my brother-in-law Talal Hijris for all the great moments we had during his stay in the UK. I am forever grateful for his encouragement, appreciation of my work and friendship. I am indebted to my cousin Ahmed Al Rayes for all his patience and relentless support. I owe my cousin much more than can be said. I am honoured to have him as family and friend.

My love and thanks to my family for their enduring faith in me. My parents' love and support have seen me through every hurdle in my life. They have provided me with the opportunities in life that have allowed me to fulfil my ambitions. To my brothers and sisters and their beautiful kids, I love you all so much. I would not have been able to do any of this without you.

TABLE OF CONTENTS

LIST OF FIGURES

LIST OF TABLES

$[ion]_i$	Ion concentration inside (cytosolic)
$[ion]_o$	Ion concentration outside (extracellular)
$[ion]_t$	Total ion concentration (ionised + bound)
ADP	Adenosine diphosphate
ANT	Adenine nucleotide translocase
APTRA	*O*-aminophenol *N,N,O*-triacetic acid
ATP	Adenosine triphosphate
BSA	Bovine serum albumin
cAMP	Cyclic adenosine monophosphate
cDNA	Cyclic deoxyribonucleic acid
DAT	Dopamine transporter
DHP	Dihydropyridine
DIDS	4,4′-diisothiocyanatostilbene-2,2′-disulphonic acid
E_m	Membrane potential
E_r	Reversal potential
GDP	Guanosine diphosphate
GTP	Guanosine triphosphate
I_{ion}	Ion current
I_m	Membrane current
ISME	Ion-selective microelectrode
K_d	Dissociation constant
KBR	KBR-7943 mesylate
mOsm	Milli-osmole per litre
MTP	Mitochondrial permeability transition pore
NET	Noradrenaline transporter
NMDA	N-methyl-D-aspartate
NMR	Nuclear magnetic resonance
BAPTA	1,2-Bis(2-aminophenoxy)ethane-tetraacetic acid
PT	Permeability transition
SERT	Serotonin transporter

The history of magnesium (Mg^{2+}) research probably begins in 1618 in a farm in the small town of Epsom, southwest of London, where a farmer noticed that his cows refused to drink from a certain mineral well. Once he tasted the bitterness of the water, he couldn't blame the cows for not drinking it. But he also discovered that the water had some positive healing effects on scratches and rashes on the skin. The well at Epsom became a worldwide commercial success that could not keep up with the demand, and so industrialists turned to wells at Limington and Portsea Island to work out the "bitter salts". The product, which was then, as now, called Epsom salt, regardless of its origin, was nothing but magnesium sulphate.

Following its isolation in 1808 by Sir Humphrey Davy and until the first quarter of the twentieth century, scientists were mainly concerned with the chemical nature and pharmacological effects of Mg^{2+}. Thereafter, the work conducted over the period from 1926 to the 1960's established the basis of our current knowledge of the role of Mg^{2+} in health and disease (Durlach, 1988).

Today Mg^{2+} is recognised as an essential element in vast and diversified fields. It is used either as pure metal, in alloys with other metals, or with other salts in fields such as aeronautics, automobile industry, solar power, agriculture, textiles, and even explosives.

Its importance in living organisms has been recognised for decades. In plants, it has a pivotal role in photosynthetic activities, whereas in animals, Mg^{2+} is involved in almost every cellular function, including enzymatic catalysis, energy transfer, reproduction and movement. In the human, its role cannot be overemphasised. In fact the lack of Mg^{2+} in the body can lead to serious consequences that could, in the extreme case, lead to disorientation, convulsions and eventually death.

Our knowledge of Mg^{2+} function and regulation in living organisms has developed vastly in the past twenty years. Mg^{2+} research has benefited immensely from the

extraordinary advancements and technical developments in biology, chemistry, optics, microscopy, and most importantly computing and microelectronics.

This thesis has been organised in eight chapters, with references cited listed in alphabetical order at the end. **Chapter 1** is a general introduction to the role of Mg^{2+} in physiology, techniques used in the measurement of Mg^{2+} in living tissue and the current status of Mg^{2+} research in the heart. In **Chapter 2**, description of the materials and methods used throughout the study is given. **Chapters 3 to 6** describe the experiments. Each chapter has been organised into four sections: an Introduction, the Materials and Methods, the Results and the Discussion. Although the results of each set of the experiments were discussed separately at the end of each of the four chapters, a general discussion of all the results, a model for the possible mechanisms involved in regulating Mg^{2+} transport in cardiac myocytes and potential future work is presented in **Chapter 7**.

CHAPTER 1

GENERAL INTRODUCTION

1.1 OVERVIEW

There is increasing interest in the role of magnesium in health and disease. During the past two decades the physiological and biological functions of Mg^{2+} received greater attention, contesting the prevalent view that Mg^{2+} is a dormant cation with little functional importance, and setting the scene for more elaborate research into the mechanisms and various biological interactions that regulate Mg^{2+}, both at the cellular and organismal levels.

Significant evidence for the importance of Mg^{2+} in cells came to light in the late 1960s to early 1970s following reports that Mg^{2+} modulates the tension generated by frog and crayfish skeletal muscle (Reuben *et al.*, 1971; Brandt *et al.*, 1972; Ford & Podolsky, 1972; Kerrick & Donaldson, 1972) and that it has a central role in the regulation of ionic movements across the axolemma of the giant squid axon (Brinley & Mullins, 1968; Brinley, 1973; Brinley *et al.*, 1977). Much of the work that followed focused on the function and distribution of Mg^{2+} in various cell types and homeostatic mechanisms involved in regulating its concentration.

Today Mg^{2+} is known to have a central role in biological activities within the cell. Mg^{2+} is required for the activation of hundreds of enzymes (Flatman, 1984; Prescott *et al.*, 1988), among them are ATPases, kinases and phosphatases involved in phosphorylation and dephosphorylation (Wacker, 1969; Beyenbach, 1990). Mg^{2+} is important for key cellular processes such as glycolysis, oxidative phosphorylation and protein synthesis (Bronzetti *et al.*, 1995), and is required for substrate formation such as Mg.ATP and Mg.GTP (Rude & Oldham, 1990). It participates in stabilising the structure of DNA and initiating its synthesis. Many studies have shown that Mg^{2+} is essential for cell division in different types of cells (e.g. McKeehan & McKeehan, 1980). It is involved in the regulation of mitosis where it helps trigger the condensation of chromatin (Staron, 1985), it stimulates the assembly of microtubules (Grover & Hamel, 1994), it is needed for the insertion of proteins into membranes (Prescott *et al.*, 1988), it preserves the bilayer fluidity (Amler *et al.*, 1987), and it serves as a key activator of adenylate cyclase which, together with Mg^{2+} and ATP,

acts as a substrate for the synthesis of cAMP, a key regulator of cardiac activity (White & Hartzell, 1989).

The clinical significance of Mg^{2+} as an important intracellular cation has been suggested for decades. Experimental and epidemiological studies have linked hypomagnesemia with conditions such as ischemic heart disease, hypertension and atherosclerosis (Whang, 1993; Fox *et al.*, 2001). Mg^{2+} therapy may also influence the clinical outcome in certain medical and emergency conditions such as acute myocardial infarction (e.g. Herzog & Serebruany, 1996; Rabbani & Antman, 1996), and arrhythmias and cardiogenic shock following cardiopulmonary bypass (Storm & Zimmerman, 1997). In addition, there is evidence that hypomagnesemia plays an important role in the pathogenesis of diabetes mellitus (e.g. Paolisso & Barbagallo, 1997), pre-eclampsia/eclampsia (Frakes & Richardson, 1997) and stroke (Ascherio *et al.*, 1998; Saris *et al.*, 2000).

If Mg^{2+} deficiency is truly linked to some or all of the clinical conditions mentioned above, then Mg^{2+} should provided a cheap and effective form of treatment. However, there is still controversy on the beneficial effects of Mg^{2+} supplementation or infusion of Mg^{2+} salts in the management of certain medical conditions. For example disagreement still exists on the benefit of infusion of Mg^{2+} following myocardial infarction. The LIMIT-2 study of 1992 was the first large-scale randomised trial to show a statistically significant decrease in total mortality of the magnesium-treated group (Woods *et al.*, 1992; Woods & Fletcher, 1994). However, these findings were not substantiated by a much larger study, the ISIS-4, which showed no survival benefit from intravenous magnesium supplementation (ISIS-4 Collaborative Group, 1991). In a more recent evaluation of the efficacy of magnesium therapy, Hennekens *et al.* (1996) suggested that the null findings in the ISIS-4 study were probably attributed to the longer time between the start of myocardial reperfusion and the achievement of therapeutic serum magnesium concentrations.

It appears that despite a wealth of clinical experience with the use of intravenous magnesium salts in the management of various medical conditions, the principal

mechanism by which Mg^{2+} acts is still controversial. Shechter *et al.* (1990) suggested that the cardioprotective effect of magnesium is more of a general myocardial protective effect than one solely due to reduction of arrhythmias. The authors postulated that among the possible mechanisms involved were coronary vasodilatation, reduction of the catecholamine effect in myocardial tissue and calcium-magnesium interaction at the cellular level preventing ischemic accumulation of calcium in cardiac mitochondria.

However, the implementation of Mg^{2+} therapy needs to be based on sound understanding of the mechanisms that regulate Mg^{2+} at the cellular level. This can only be achieved under controlled experimental conditions. In particular, basic knowledge of how ionised and total intracellular magnesium concentrations are regulated is essential for the understanding of the pathogenesis and pharmacodynamics of magnesium in various diseases. In the heart such knowledge is still lacking, and a Mg^{2+} transporter has not been isolated or cloned from the plasma membrane of heart cells. It is even not known whether Mg^{2+} uptake and extrusion occur through the same or different transport pathways.

Research in this field has gained increasing attention in the last 20 years. The emergence of new techniques for the measurement and monitoring of the concentration of various ions and their distribution within the cells and the patch clamp technique has significantly enhanced our understanding of the role of Mg^{2+} in influencing various cellular functions. Electrophysiological studies of the effect of Mg^{2+} on the movement of ions such as Ca^{2+}, Na^{+} and potassium (K^{+}), across the cell membrane through channels, carriers and pumps have been most rewarding in this regard. A brief review of Mg^{2+} influences on channels is presented in the next section.

1.2 Effect of Mg^{2+} on channels

In order to understand the interactions between Mg^{2+} and various transport systems, it is important to discuss the effects Mg^{2+} has on some of the most intensively studied channels, namely Ca^{2+}, K^{+} and Na^{+} channels.

1.2.1 Effect of Mg^{2+} on Ca^{2+} channels

Ca^{2+} entry through voltage-dependent calcium channels is critical for both electrical and chemical signalling. Cardiac muscle contains two major types of Ca^{2+} channels, L- and T-type (Bean, 1989). T-type Ca^{2+} channels are most prominent in atrial cells and Purkinje fibres. They are characterised by low conductance (~8 pS in 110 mM Ba^{2+}), transient openings, insensitivity to 1,4-dihydropyridines (DHPs) and activation at more negative membrane potentials, compared to the L-type channels (Bers, 1991). Their function in the heart is not fully understood, although they appear to have a prominent role in pacemaker activity (Bean, 1989; Hirano *et al.*, 1989; Huser *et al.*, 2000).

The second class of Ca^{2+} channel is the L-type channel. They are abundant in the ventricles and atria and are the main route of Ca^{2+} influx into cardiac cells. In isolated mammalian ventricular myocytes, the density of L-type Ca^{2+} channels has been estimated from single channel and whole cell Ca^{2+} current (I_{Ca}) measurements to be 3-5/μm^2 (Tsien *et al.*, 1983; McDonald *et al.*, 1986). I_{Ca} is rapidly activated by depolarisation to –40 mV, reaching a peak in approximately 2 to 7 msec, depending on E_m and surface potential (Hille, 1992a). L-type channels carry Ca^{2+} during the plateau phase of the action potential and can be activated by cAMP. They are often characterised by their sensitivity to DHPs. Most DHPs act as Ca^{2+} channel blockers (e.g. nifedipine and nitrendipine), while some DHPs act as Ca^{2+} channel agonists (e.g. (-)Bay K 8644). In addition to DHPs, at least two other classes of drug interact specifically with L-type Ca^{2+} channels, namely phenylalkylamines, such as verapamil, D600, D888 and D890, and benzothiazipines, such as diltiazem (e.g. Bers, 1991). In addition to being modulated by drugs and hormones, Ca^{2+} influx through the L-type channel is also affected by the concentration of other ions, mainly Na^+ and Mg^{2+}.

A third major class of Ca^{2+} channel in mammalian heart muscle is the sarcoplasmic reticulum (SR) Ca^{2+} release channel (Ryanodine receptor). These channels are responsible for release of Ca^{2+} stored in the SR in response to Ca^{2+} influx through L-

type Ca^{2+} channels during cell contraction, a mechanism usually referred to as Ca^{2+}-induced Ca^{2+} release. Mg^{2+} affects all three types of Ca^{2+} channels mentioned above.

Effect of Mg^{2+} on L-type Ca^{2+} channels

Mg^{2+} block of L-type Ca^{2+} channels is well established (Campbell *et al.*, 1988; Hartzell & White, 1989; Wu & Lipsius, 1990; Hall & Fry, 1992; Zhang *et al.*, 1995). Mg^{2+} elicits dose-dependent inhibition of L-current in cardiac myocytes. Whole-cell voltage clamp recordings from isolated cat atrial myocytes (Wu & Lipsius, 1990) and rat and rabbit ventricular myocytes (Hall & Fry, 1992) indicate that an increase in external Mg^{2+} concentration ($[Mg^{2+}]_o$) is associated with a decrease in I_{Ca} and a shift of channel activation towards more positive membrane voltages.

Ca^{2+} channel conductance is also affected by $[Mg^{2+}]_i$. In frog ventricular myocytes, I_{Ca} significantly decreases on increasing $[Mg^{2+}]_i$, from 0.3 mM to 3 mM, provided the channel is activated by cAMP (White & Hartzell, 1988). Similar inhibitory effects on I_{Ca} and shortening of action potential duration are also seen in guinea pig ventricular myocytes. Increasing $[Mg^{2+}]_i$ to 9.4 mM almost totally inhibits I_{Ca} in these cells (Agus *et al.*, 1989).

Effect of Mg^{2+} on T-type Ca^{2+} channels

Permeation mechanisms have been studied most thoroughly for L-type channels. Many of the basic features are also present in T-type Ca^{2+} channels, including high permeability to monovalent cations and block by millimolar concentrations of divalent cations (Hagiwara *et al.*, 1988; Lux *et al.*, 1990). Although Ca^{2+} and Ba^{2+} carry comparable inward currents through T-type channels, the channel is actually selective for Ca^{2+} over Ba^{2+} (Serrano *et al.*, 2000). Some studies have suggested that, compared to L-type channels, Mg^{2+} blocks T-type channels with similar or even more potency (Wu & Lipsius, 1990; Serrano *et al.*, 2000). 1 mM $[Mg^{2+}]_o$ strongly blocks inward currents carried by 2 mM Ba^{2+}, while a weaker block is observed of currents carried by 2 mM $[Ca^{2+}]_o$, suggesting that Mg_o^{2+} selectively blocks currents carried by Ba^{2+} (Serrano *et al.*, 2000). Mg^{2+} block of T-current may play a physiological role, since 1 mM $[Mg^{2+}]_o$ produces modest inhibition of Ca^{2+} inward

current (Serrano *et al.*, 2000). The block is stronger at more negative potentials, where significant Ca^{2+} entry can occur through T-channels following an action potential (Wu & Lipsius, 1990). In cardiac cells, Mg^{2+} block of T-current has been suggested to play a role in the antiarrhythmic effect of elevated $[Mg^{2+}]_o$ (Wu & Lipsius, 1990).

The effect of Mg^{2+} on Ca^{2+} channels is believed to be by mechanisms other than simple surface charge screening (Fry & Proctor, 1993; Serrano *et al.*, 2000). Fry & Proctor (1993) have suggested that Mg^{2+} block is brought about by slow permeation by Mg^{2+} of Ca^{2+} channels, as indicated by a low flux of Mg^{2+} current measured through Ca^{2+} channels.

Effect of intracellular Mg^{2+} on sarcoplasmic reticular Ca^{2+}-release channels

Intracellular Mg^{2+} (Mg_i^{2+}) modulates the Ca^{2+}-release channel found in heavy SR vesicles. The rate of Ca^{2+} efflux is stimulated by micromolar cytosolic Ca^{2+} concentrations and millimolar concentrations of ATP. Mg^{2+} in millimolar concentrations shifts the Ca^{2+}-dependence of Ca^{2+} efflux rate to higher calcium concentrations (Meissner & Henderson, 1987). In other words, in the presence of high $[Mg^{2+}]_i$, higher cytosolic Ca^{2+} concentrations are needed to stimulate Ca^{2+} release through these channels. Since Ca^{2+} release from the SR is closely related to the magnitude of muscle contraction in the heart, the modulation of SR Ca^{2+} release by $[Mg^{2+}]_i$ will also influence muscle contractile function. In isolated canine SR vesicles, raising $[Mg^{2+}]_i$ inhibits Ca^{2+}-induced Ca^{2+} release (Meissner & Henderson, 1987). Regulation of $[Mg^{2+}]_i$ within a narrow range is therefore vital to the control of SR Ca^{2+} release and hence muscle contractile function.

1.2.2 Effect of intracellular Mg^{2+} on K^+ channels

Mg_i^{2+} interferes with the outward movement of K^+, blocking outward currents (inward rectification) through several K^+ channels including the inward rectifier K^+ channel, the ATP-dependent K^+ channel, the delayed K^+ rectifier channel and the muscarinic K^+ channel. The effect of Mg_i^{2+} on currents carried by some of these channels is of major importance in producing the normal cardiac action potential.

The effect of Mg^{2+} is more pronounced at potentials more positive than the resting potential, when rectification occurs. Inward rectification of K^+ channels is a phenomenon during which the conductance of the channel is greatly reduced at depolarised potentials. It results from block by Mg^{2+} of a K^+ channel in its open state, thereby delaying repolarisation and prolonging action potential duration. The voltage-dependence has been explained by the increase in the apparent affinity of the channel to Mg^{2+} at more positive potentials. As the membrane potential becomes more negative, the block by Mg^{2+} is relieved allowing K^+ to exit the cell, thereby removing the block. The affinity of the binding site to Mg^{2+} has a dissociation constant of approximately 10 μM at positive potentials (Matsuda *et al.*, 1987). Hence, at normal $[Mg^{2+}]_i$ (~ 0.8 mM) the degree of rectification is maximal.

Effect of intracellular Mg^{2+} on inward rectifier K^+ current (I_{K1})

Inwardly rectifying K^+ channels are mostly found in the ventricles and Purkinje fibres. I_{K1} is responsible for the final phase of repolarisation (phase 3) and maintenance of the resting membrane potential. I_{K1} increases the rate of repolarisation when the membrane potential reaches –40 mV with a maximum channel conductance at around the resting membrane potential (Shimoni *et al.*, 1992). Mg_i^{2+} at physiological concentrations, blocks I_{K1} in a voltage-dependent manner resulting in rapid closure of the channel during depolarisation; it allows K^+ to enter during cell hyperpolarisation (Matsuda *et al.*, 1987).

Effect of intracellular Mg^{2+} on ATP-sensitive K^+ current (I_{KATP})

Mg_i^{2+} was also found to influence a set of K^+ channels that are inhibited by low intracellular concentrations of ATP (Findlay, 1987). ATP-sensitive K^+ channels have been reported in cardiac and skeletal muscle. Activation of the channels requires agents such as ADP, GDP, and GTP in addition to Mg^{2+}. However, these agents together with Mg^{2+} will also induce block of the channel at depolarised potentials. Mg^{2+} plays a dual role where it promotes channel opening at hyperpolarized potentials and block at depolarised potentials. Activation of this K^+ channel usually occurs under ischemic conditions where cellular ATP is low and ADP is high, and $[Mg^{2+}]_i$ is high. The increase in $[Mg^{2+}]_i$ causes the ATP-sensitive channel to rectify

which results in a negative conductance slope at positive potentials (Horie *et al.*, 1987).

Effect of intracellular Mg^{2+} on delayed rectifier current (I_K)

The I_K operates throughout the plateau phase of the cardiac action potential and is the major determinant of the plateau duration. In guinea pig ventricular myocytes, the I_K can be separated by dofetilide, a class III antiarrhythmic drug, into two components, the rapidly activating component (I_{Kr}) and the slowly activating component (I_{Ks}). Mg_i^{2+} has been shown to cause a dose-dependent decrease in total I_K. Both components are inhibited by an increase in $[Mg^{2+}]_i$ to a similar extent (Williams & Beatch, 1997). While Mg_i^{2+} has little effect on the activation and deactivation kinetics of I_K, increasing $[Mg^{2+}]_i$ shifts activation of I_K towards more positive values (Williams & Beatch, 1997). The sensitivity of the delayed rectifier channel to Mg_i^{2+} of approximately 20 nM, reported by Williams & Beatch (1997), suggests that small changes to the normal physiological $[Mg^{2+}]_i$ in mammalian ventricular myocytes, will have negligible effect on I_K.

1.2.3 Effect of Mg^{2+} on Na^+ channels

An increase in $[Mg^{2+}]_o$ is associated with decreased Na^+ permeability in skeletal muscle. In addition to Na^+ channel block, elevated divalent cation concentration affects the kinetics of sodium ionic and gating currents and results in a shift in the time courses of channel activation and inactivation (Hahin & Campbell, 1983). Mg^{2+} is less effective in producing these changes than similar concentrations of Ca^{2+}. This was attributed to different binding affinities of the two ions to fixed membrane surface charges around the channel pore, which in turn reduces the local effective Na^+ concentration. The difference between Ca^{2+} and Mg^{2+} in influencing Na^+ channel properties suggests that specific binding to the channel occurs (Hahin & Campbell, 1983; Fry & Proctor, 1993).

1.3 DISTRIBUTION OF Mg^{2+} IN THE BODY AND WITHIN THE CELL

Mg^{2+} is the second most abundant cation within cells, where its amount is exceeded only by K^+ (Flatman, 1991; Heaton, 1993). It is estimated that the total body store of magnesium is approximately 21 to 28 gram (Whang *et al.*, 1994). Of the total body magnesium, 65% is in the mineral phase of the bones, of which only 30% is exchangeable, about 34% is in the intracellular compartment and only 1% is present in the extracellular space (Levine & Coburn, 1984; Paolisso & Barbagallo, 1997). The concentration of plasma Mg^{2+} has been estimated to range between 0.65 and 1.20 mM (Quamme, 1993; Whang *et al.*, 1994). Almost 80% of total plasma magnesium is in the freely ionised form while the rest is bound to plasma proteins or partially immobilised by association with anions in solution (Rouilly *et al.*, 1990).

Within the cell, the distribution of magnesium was the focus of intensive research, aiming at exploring its compartmentation characteristics, and the physiological role it plays within a specific compartment. Total cellular magnesium concentration ($[Mg]_t$) is between 5 and 30 mM depending on the cell type (e.g. Romani & Scarpa, 1992b). It has been estimated that about 60% of the total magnesium is present in the cytosol, 38% in mitochondria and 2% distributed among the sarcoplasmic reticulum, the nucleus and bound to other cellular components (Garfinkel *et al.*, 1986; Günther, 1986).

The $[Mg]_t$ in rat ventricular myocytes is about 17 mM (Page & Polimeni, 1972), less than 10% of that is in the free ionised state (e.g. Flatman, 1991). $[Mg^{2+}]_i$, in cardiac cells has been estimated by many workers using different techniques (Table 1.1). Most reports suggest $[Mg^{2+}]_i$ in cardiac cells is between 0.47 and 0.85 mM. Much higher values were reported in non-mammalian species. In the giant squid axon $[Mg^{2+}]_i$ is around 3 mM, in barnacle muscle between 4 and 6 mM, and 1 to 4 mM in Escherichia coli (from a review by Flatman (1984)). It is this fraction, which is believed to be the physiologically active moiety. Most Mg_i^{2+} is bound to ATP as Mg.ATP complex and ATP is almost saturated by Mg^{2+} at physiological levels (Flatman, 1991). Other stores of Mg_i^{2+} include the mitochondria, where, in the heart,

about 40% of the $[Mg]_t$ is present. The majority of mitochondrial Mg^{2+} is present in the matrix with a free ion concentration for Mg^{2+} of 0.8 mM (Jung & Brierley, 1994).

It is believed that the effects of Mg^{2+} on the various cell functions mentioned above are mediated, at least partly, through the ionised moiety of the total cell magnesium. In keeping with this view, sound and reliable methods for the measurement of $[Mg^{2+}]_i$ are required in order to assess its physiological role and mechanisms involved in its regulation. Various techniques have been employed to measure $[Mg^{2+}]_i$ and $[Mg]_t$. The following is a brief summary of those techniques, and their advantages and limitations.

Table 1.1. Estimates of $[Mg^{2+}]_i$ in heart muscle.

Mean $[Mg^{2+}]_i$ (mM)	*Model*	*Method*	*Reference*
0.82	Rat	Mag-fura-2	(Handy *et al.*, 1996)
0.85	Rat	^{31}F – NMR/^{31}P – NMR	(Murphy *et al.*, 1989)
0.71	Rat	Mag-fura-2	(Tashiro & Konishi, 2000)
0.72	Guinea-pig	ISME - ETH 5214	(Buri *et al.*, 1993)
0.51	Chicken	Mag-fura-2	(Freudenrich *et al.*, 1992b)
0.47	Chicken	Mag-fura-2	(Quamme & Rabkin, 1990)
0.66	Sheep	Mag-fura-2	(Gow *et al.*, 1995)
0.56	Chicken	^{19}F-NMR	(Romani & Scarpa, 1992)
0.85	Ferret	ISME - ETH 5214	(Hall *et al.*, 1991)
0.48	Chicken	Mag-fura-2	(Freudenrich *et al.*, 1992a)

1.4 TECHNIQUES FOR THE MEASUREMENT OF $[Mg^{2+}]$

Mg^{2+} is present in all living cells either in the free ionised form or bound to macromolecules such as ATP, RNA and Mg^{2+}-activated enzymes (e.g. Reid & Cowan, 1990). For an understanding of the distribution of intracellular Mg^{2+} between free and bound forms and the regulation of cytosolic Mg^{2+}, reliable and accurate measurements of both total and free intracellular magnesium are essential. Magnesium research has been hampered in the past by the lack of suitable methods to investigate perturbations of cellular Mg^{2+} under controlled experimental conditions. However, several techniques have been developed to measure free and total cellular magnesium concentrations. $[Mg^{2+}]_i$ can be measured using ion-selective microelectrodes (ISME), fluorescence spectrophotometry, nuclear magnetic resonance (NMR) spectrophotometry, null point for plasma membrane permeabilisation and radiotracer methods. $[Mg]_t$ is more commonly measured using atomic absorption (AA) and NMR spectrophotometry but also by electron probe x-ray microanalysis. This section describes the methods mentioned above with particular emphasis on fluorescence spectrophotometry, since it was the method used for measuring $[Mg^{2+}]_i$ throughout this study.

1.4.1 Mg^{2+}-selective microelectrodes

Ion-selective microelectrodes measure the activity of a given ion in solution. It must be remembered though that the activity of an ion in solution is different from its total concentration. For example, in a solution that contains 150 mM NaCl, NaCl would fully ionise so that the concentration of Na^+ ions would be 150 mM. However, because of the mutual electrostatic repulsion between the similarly charged species and attraction between anions and cations the mobility of the ion is reduced. Due to the existence of these inter-ionic forces, the activity of the Na^+ ions in solution, or their effective concentration, is less than their total concentration. The intracellular activity of an ion, usually denoted a_i, is calculated by multiplying the total concentration of the ion by an activity coefficient that is calculated according to the valency and total concentration of the ion and number and valency of other ionic species in the solution. ISMEs are normally calibrated in solutions that mimic the

intracellular environment. Therefore, provided the activity coefficient inside the cell and outside is nearly the same, the value read from the calibration curve will be the intracellular free ion concentration.

Ion-selective microelectrodes are usually glass micropipettes plugged at the tip with a selectively permeable membrane sealing a small volume of the permeant ion. The selectively permeable membrane can be a specific type of glass or, more common recently, an organic compound. Because the organic membrane filling at the tip of the electrode does not provide electrical interactions for ions as water does, ions can only enter the membrane phase if they bind to a specific carrier molecule (ionophore) in the membrane solution. Specific ionophores are available for specific ions, including Na^+, K^+, H^+, Ca^{2+}, Mg^{2+} and Cl^-. They promote the transfer of hydrophilic ions into and across a hydrophobic region, and thus a potential across the membrane between the inner filling solution and the external solution being measured (usually the cytosol) is generated. Because ion-selective microelectrodes also record the membrane potential in addition to the intracellular ion changes, the voltage due to the membrane potential (measured by a second reference electrode) needs to be subtracted from the combined signal registered by the ISME. Only then can ion activity be determined.

Ion-selective microelectrodes have been frequently used to measure $[Mg^{2+}]_i$ in a wide range of preparations. The early Mg^{2+}-selective microelectrodes used the neutral ionophore ETH-1117. The selectivity of ETH-1117 resin for Mg^{2+} over K^+ and Na^+ ions was not high (Lanter *et al.*, 1980). ETH-1117-filled ion-selective microelectrodes have been used to measure $[Mg^{2+}]_i$ in ferret and guinea pig muscles (Fry, 1986) and registered a mean value of 2.4 ± 0.2 mM at 36 °C. Introduction of the resin ETH-5214 (Hu *et al.*, 1989) permitted more accurate measurements of $[Mg^{2+}]_i$, since the new resin is less susceptible to interferences by K^+ and Na^+ ions. Using ETH-5214, Buri & McGuigan (1990) estimated $[Mg^{2+}]_i$ in isolated ferret ventricular muscle at about 0.85 mM, much lower than that registered using ETH-1117. Using Mg^{2+}-selective microelectrodes to measure $[Mg^{2+}]_i$ has a number of

advantages over other methods, such as NMR and fluorescence spectrophotometry, but also has its own limitations (Table 1.2).

Table 1.2. Advantages and limitations of ion-selective microelectrodes

Advantages	*Limitations*
1. Exclusion of cell organelles	1. Better suited to large cells
2. Permits measurement of two or more ions simultaneously	2. Specificity occasionally inadequate
3. Direct measurement of ion activity	3. Extremely sensitive to electrical interference
4. Good response time	4. May require some degree of manipulative skills
5. Low cost of equipment	5. Invasive nature of measurement, especially when used on single cells

1.4.2 Atomic absorption spectrophotometry (AAS)

In AAS, an element in its atomic form is introduced into a light beam of appropriate wavelength causing the atom to absorb light (atomic absorption) and enter an excited state. At the same time there is a reduction in the intensity of the light beam, which can be measured and directly correlated with the concentration of the elemental atomic species. This is carried out by comparing the light absorbance of the unknown sample with the light absorbance of known calibration standards.

A typical atomic absorption spectrophotometer consists of an appropriate light source (usually a hollow cathode lamp containing the element to be measured), an absorption path (usually a flame but occasionally an absorption cell), a monochromator (to allow transmission of light of appropriate wavelength) and a detector.

The most common form of AAS is called flame atomic absorption. In this technique, a solution of the element of interest is drawn through a flame in order to generate the element in its atomic form. At the same time, light from a hollow cathode lamp is passed through the flame and atomic absorption occurs. The flame temperature can be varied by using different fuel and oxidant combinations; for example, a hotter flame is required for those elements which resist atomisation by tending to form refractory oxides.

This technique has proven superior in terms of sensitivity and selectivity. It allows measurement $[Mg]_t$ rather than $[Mg^{2+}]_i$. Its sensitivity to Mg^{2+} of 1 μM or better requires determination of the relatively high intracellular $[Mg^{2+}]$ under artificially low extracellular $[Mg^{2+}]$. This method can be applied to either effluent from the tissue or cell suspension solutions. Successive measurements are usually required to estimate uptake/release of Mg^{2+} from the tissue under study over a certain period of time.

AAS has frequently been used to measure Mg^{2+} fluxes in various tissue types, including intact hearts and isolated cardiac myocytes (Romani & Scarpa, 1990; Romani *et al.*, 1992; Romani *et al.*, 1993a), hepatocytes (Romani & Scarpa, 1992a; Romani *et al.*, 1993b; Fagan & Romani, 2001), squid axon (Caldwell-Violich & Requena, 1979), and red blood cells (Flatman & Lew, 1980; Féray & Garay, 1986; Féray & Garay, 1988; Flatman & Smith, 1990; Flatman & Smith, 1991). Advantages and limitations of AAS are summarised Table 1.3.

Table 1.3. Advantages and limitations of atomic absorption spectrophotometry

Advantages	*Limitations*
1. Principles of measurement are straightforward and well-understood	1. Measures $[Mg]_t$ in a sample rather than $[Mg^{2+}]_i$
2. Very high sensitivity and selectivity	
3. Sample throughput is high as each measurement can take only seconds when the instrument is calibrated	
4. Applicability over a wide range of concentrations for most elements	

1.4.3 Radiochemical determination

The use of radioisotopes is probably the most robust method in the measurement of ionic fluxes in tissue. The radioactive material can be injected into live animals, and radioactivity determined after a certain period of time in the organ or tissue under study (Page & Polimeni, 1972). More often, isolated cells are incubated with the radiolabeled cation and radioactivity determined in the cell pellet and suspension media by a scintillation analysis method (e.g. Romani *et al.* (1993a)).

There are two radioisotopes for Mg^{2+}, $^{27}Mg^{2+}$ and $^{28}Mg^{2+}$. Unfortunately, there are serious limitations to the use of these isotopes. Mg^{2+} radioisotopes have very short half-lives, 9.46 minutes and 20.9 hours for $^{27}Mg^{2+}$ and $^{28}Mg^{2+}$, respectively (Flik *et al.*, 1993). In addition, they are not commercially available. $^{27}Mg^{2+}$ can be produced by thermal neutron irradiation of ^{26}Mg. Experiments with $^{27}Mg^{2+}$ require laboratory facilities near the nuclear reactor.

$^{28}Mg^{2+}$ on the other hand is produced by photonuclear irradiation of PCl_3 (Polak, 1989) or by exposing strips of Li^+/Mg^{2+} alloy to thermal neutron flux of 1.3×10^{17} m^2 s^{-1} for 36 hours followed by dissolution of the irradiated alloy and purification

processes (Flik *et al.*, 1993). The determination of both isotopes can be performed by gamma-spectrophotometry and liquid scintillation counting (Flik *et al.*, 1993).

While no reports are available on the biochemical application of $^{27}Mg^{2+}$, experiments of Mg^{2+} transport processes carried out over a longer time span benefited from the relatively longer half-life of $^{28}Mg^{2+}$. The exchange of cellular Mg^{2+} with external $^{28}Mg^{2+}$ has been studied in rat left ventricle *in vivo* and in Langendorff hearts (Page & Polimeni, 1972), in isolated ventricular myocytes (Romani *et al.*, 1993a), in the giant squid axon (De Weer, 1976) and in fish (Flik *et al.*, 1993). $^{28}Mg^{2+}$ has also been employed to study the uptake and extrusion mechanisms in isolated mitochondria (Brierley *et al.*, 1987), while Günther (1986) used $^{28}Mg^{2+}$ to study the compartmentation characteristics of Mg^{2+} in the mitochondria. Although the use of radioisotopes is considered the ideal method to study ionic fluxes in tissue, the introduction of new techniques and the unavailability, short half-life and high cost of $^{28}Mg^{2+}$ resulted in the virtual disappearance of the technique in Mg^{2+} research.

1.4.4 Nuclear Magnetic Resonance Spectrophotometry (NMRS)

A number of small metabolites in cells exist in equilibrium between un-complexed and Mg^{2+}-complexed states. The shift in the resonance of such molecules upon Mg^{2+} complexation can be detected by NMRS to provide information on $[Mg^{2+}]_i$ in the cell. Metabolites that have been used in the determination of $[Mg^{2+}]_i$ include ATP, ADP, citrate, phosphocreatine and diphosphoglycerate (e.g. London, 1991). Since ATP is present at high levels in all cell types, it is often targeted in NMRS studies. ATP is an endogenous indicator in contrast to other reagents that need to be loaded into the cell and therefore are known as exogenous indicators.

Because only the β- and γ-phosphates of the ATP molecule are available for ionic binding, the chemical shift of the α-phosphate resonance is insensitive to metal ion complexation and thus can be used as an internal standard provided the pH_i, temperature and ionic strength remain unchanged (Gupta *et al.*, 1984).

$[Mg^{2+}]_i$ can be measured by ^{31}P NMR since the binding of Mg^{2+} to ATP causes an NMR chemical shift of the β-phosphate resonance of ATP relative to the α-phosphate resonance of ATP (Gupta *et al.*, 1984). The difference in the shift between the α and β phosphates of ATP corresponds to $[Mg^{2+}]_i$. Although there seems to be an agreement of the magnitude of chemical shift that results from complexation of Mg^{2+} with ATP (Murphy *et al.*, 1991a), the value calculated for $[Mg^{2+}]_i$ in the heart varied considerably. This was mainly attributed to different dissociation constant values used for the Mg.ATP complex (Wu *et al.*, 1981; Gupta *et al.*, 1984). However, there now appears to be an agreement on an $[Mg^{2+}]_i$ of about 1 mM in the heart as measured by ^{31}P NMR (Murphy *et al.*, 1991a).

Exogenous NMR indicators have also been used to measure $[Mg^{2+}]_i$. Levy *et al.* (1988) have synthesised three fluorinated (^{19}F) NMR indicators based on the chelator *O*-aminophenol *N,N,O*-triacetic acid (APTRA). These indicators are introduced into the cell as acetoxymethyl (AM) esters, which can freely permeate the plasma membrane. Once inside the cell, endogenous esterases cleave the esters and leave the negatively charged indicator trapped. APTRA and its fluorinated derivatives are structural analogues of the Mg^{2+} chelator EDTA and hence possess high affinity for Mg^{2+} ions (Levy *et al.*, 1988). When Mg^{2+} binds to the fluorinated NMR Mg^{2+} indicators (5F-APTRA and MF-APTRA), the fluorine undergoes an NMR chemical shift, which is then used to calculate $[Mg^{2+}]_i$ (equations can be found in Mota de Freitas & Dorus (1993) and London (1991)). ^{19}F NMR is more sensitive to changes in $[Mg^{2+}]_i$ than ^{31}PNMR. This is because the K_d for 5F-APTRA and MF-APTRA NMR indicators is between 0.6 and 0.9 mM, close to the measured $[Mg^{2+}]_i$ in many cells. In rat perfused heart, F-APTRA NMR studies estimated $[Mg^{2+}]_i$ at about 0.85 mM (Murphy *et al.*, 1989), close to values obtained using other techniques such as the fluorescent indicator mag-fura-2 (Handy *et al.*, 1996).

Although the NMR technique offers a non-invasive method to study the regulation of $[Mg^{2+}]_i$ *in situ*, it has its own limitations. ^{31}P NMR is not very sensitive to changes in $[Mg^{2+}]_i$ since intracellular ATP is already saturated with Mg^{2+}. There is a tendency for the estimated K_d to change with any pH_i or osmolarity shifts, which can result in

over or under estimates of $[Mg^{2+}]_i$ (Romani & Scarpa, 1992b). ^{19}F NMR is more sensitive to alterations in $[Mg^{2+}]_i$, however, it is also more sensitive to changes in $[Ca^{2+}]_i$, which, if significant, could seriously affect $[Mg^{2+}]_i$ measured values (Mota de Freitas & Dorus, 1993). Provided perturbations in $[Ca^{2+}]_i$ are avoided, ^{19}F NMR can be used reliably in the study of $[Mg^{2+}]_i$ regulation, especially in intact tissue.

1.4.5 Energy dispersive electron probe microanalysis (EPMA)

This technique permits the determination of the cellular distribution of Mg^{2+} (Somlyo *et al.*, 1985; Bond *et al.*, 1987), and is both specific and quantitative. EPMA is very effective in determining the spatial localisation of Mg^{2+} within cell structures. However EPMA measures $[Mg]_t$ rather than $[Mg^{2+}]_i$. In addition the sample has to be subjected to cryopreservation, cryosectioning and freeze-drying, all of which are technically demanding and require, as in the case of NMR, expensive instrumentation. This technique has been used to measure $[Mg]_t$ changes in cells from ventricular trabeculae (Johnson *et al.*, 1997) and isolated cardiac myocytes (Wendt-Gallitelli & Isenberg, 1989).

1.4.6 Fluorescence spectrophotometry

Fluorescence is a form of luminescence in which light is emitted from molecules for a very short period of time (10^{-8} s) following absorption of light. Fluorescence is the result of a three-stage process that occurs in certain molecules (generally polyaromatic hydrocarbons or heterocycles) called fluorophores or fluorescent dyes or indicators. A fluorescent indicator is a molecule designed to localise within a specific region of a biological specimen or to respond to a specific stimulus, such as certain light wavelengths. Emitted light can be detected using a special microscope set-up designed to filter, detect, amplify and record the emitted light from a biological sample. The three stages of fluorescence are explained below.

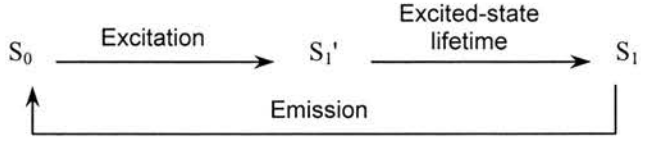

Excitation:

A photon of energy is supplied by an external source such as an incandescent lamp or a laser and absorbed by the indicator, creating an excited (unstable) electronic singlet state (S_1').

Excited-state lifetime:

The indicator remains in the excited state for a finite time (typically 1–10 nanoseconds). During this time, the indicator undergoes conformational changes and is also subject to a multitude of possible interactions with its molecular environment. As a result of these processes two important events take place. First, the energy of S_1' is partially dissipated, yielding a relaxed singlet excited state (S_1) from which fluorescence emission originates. Second, not all the molecules initially excited by absorption (Stage 1) return to the ground state (S_0) by fluorescence emission. The fluorescence quantum yield is the ratio of the number of fluorescence photons emitted (Stage 3) to the number of photons absorbed (Stage 1).

Emission:

A photon of energy is emitted, returning the indicator to its ground state S_0. Due to energy dissipation during the excited-state lifetime, the energy of this photon is lower, and therefore of longer wavelength, than the excitation photon. The difference in energy or wavelength is called the Stokes's shift. The Stokes's shift is fundamental to the sensitivity of fluorescence techniques because it allows emission photons to be detected against a low background, isolated from excitation photons. Therefore, according to Stokes's law, emission or fluorescence is only possible to detect if there is enough separation between the excitation and emission spectra. Fortunately this is almost always the case with most fluorochromes.

The intensity of the fluorescence signal is dependent on a number of factors, including optical path length, solute concentration, the fluorescence quantum yield of the dye, the excitation source intensity and fluorescence collection efficiency of the instrument. Unfortunately, the fluorescence intensity decreases with time due to a phenomenon referred to as "photobleaching" or "fading". Under high-intensity

illumination conditions, the irreversible destruction or photobleaching of the excited indicator becomes the factor limiting fluorescence detectability. Storing the dye-containing biological sample in a dark place and decreasing the intensity of the excitation light can reduce photobleaching. Fluorescence intensity can also decrease due to dye leakage from the sample over the time course of an experiment. Fluorescence detection sensitivity is also compromised by background signals (known as autofluorescence), which may originate from endogenous sample constituents and various optics used by the fluorescence setup, or from unbound or non-specifically bound indicators (referred to as reagent background). To determine the concentration of an ion accurately, background fluorescence has to be subtracted from the measured signal before any calculation of the ion concentration is carried out.

With certain dyes, for example the Ca^{2+} indicators fura-2 and indo-1, the Mg^{2+} indicator mag-fura-2, and pH indicators BCECF and SNARF, the free and ion-bound forms of fluorescent ion indicators have different emission/excitation spectra. With this type of indicator, the ratio of the optical signals obtained at two different excitation or emission wavelengths can be used to monitor and calculate ion concentrations following subtraction of background fluorescence. Ratiometric measurements reduce or eliminate variations of several factors in the measured fluorescence intensity, including indicator concentration, excitation path length, and excitation intensity and detection efficiency. Artifacts that are eliminated include photobleaching and leakage of the indicator, variable cell thickness, and non-uniform indicator distribution within cells (due to compartmentation) or among populations of cells (due to loading efficacy variations).

Mag-fura-2 as a Mg^{2+} indicator

The emergence of new fluorescent indicators which have improved affinity for Mg^{2+}, has proved very useful in the determination of $[Mg^{2+}]_i$. Fluorescent indicators for Mg^{2+} include FURAPTRA (mag-fura-2), mag-indo-1, and mag-quin-2, amongst which mag-fura-2 is probably the most frequently used indicator. It is insensitive to pH_i and $[Ca^{2+}]$ values within the physiological range (Raju *et al.*, 1989), and permits

ratiometric fluorescence measurement, analogous to the Ca^{2+} indicator fura-2. Since this study employs mag-fura-2 as the fluorescent dye of choice to measure $[Mg^{2+}]_i$, a more elaborate presentation of its chemical and fluorescence properties, practical utilisation as a probe for $[Mg^{2+}]_i$, and its advantages and disadvantages are presented in the following section.

Chemical properties of mag-fura-2

The method used to synthesise mag-fura-2 is similar to that used by Grynkiewicz (1985) to synthesise the calcium indicator fura-2. Raju *et al.* (1989) modified the structure of the Mg^{2+} chelator APTRA, previously modified by Levy *et al.* (1988) for use as ^{19}F NMR indicator for $[Mg^{2+}]_i$, to include a fluorescent chromophore.

Following a series of complex reactions, two forms of the fluorescent dye can be produced, the free acid and the tetra-acetoxymethyl (AM) ester. The free acid is cell impermeant, most commonly used for *in vitro* calibration, whereas the AM ester is relatively lipophilic, and therefore can cross biological membranes. It provides a relatively non-invasive method for loading cells with the fluorescent dye. Mag-fura-2 AM ester can be introduced into the cytosol by incubating it with the cell suspension at a final concentration of 1.5-5 μM for 20-40 minutes at room temperature (Quamme & Rabkin, 1990; Freudenrich *et al.*, 1992b; Buri *et al.*, 1993; Gow *et al.*, 1995; Handy *et al.*, 1996). Once inside the cell, the AM ester is hydrolysed by intracellular esterases leaving the free acid form of the dye, which is not capable of crossing the cell membrane, trapped inside the cell. Failure to cleave all the AM esters can result in high ion-insensitive fluorescence, leading to overestimation of the free cytosolic ion concentration (Williams *et al.*, 1999).

Intracellular distribution of mag-fura-2

When using fluorescent indicators to measure the concentration of an ion within the cytosol, it is usually assumed that the indicator is homogeneously distributed within the cytosol and equally responsive to the intracellular ion concentration. However, AM esters and their hydrolysis products are capable of accumulating in any membrane-enclosed intracellular structure such as the mitochondria.

Compartmentation is usually more pronounced at higher loading temperatures (Slayman *et al.*, 1994). Compartmentation can seriously affect the reliability of ion concentration measurement, especially in cells where intracellular organelles occupy a significant percentage of cell volume. The extent of compartmentation can be assessed by image analysis, using techniques such as laser confocal microscopy, as well as fluorimetrically using membrane permeabilisation reagents, such as Triton X-100 (Raju *et al.*, 1989). Unfortunately, the distribution of fluorescent dyes such as mag-fura-2 within the cell when loaded as the AM ester has not been adequately studied. Disagreement remains on the distribution of the dye within the various cellular compartments. It has been estimated that in cardiac myocytes around 60 per cent of mag-indo-1 fluorescence is confined to the cytosol following AM ester loading at room temperature (Silverman *et al.*, 1994). The rest is believed to be localised in intracellular organelles, mainly the mitochondria. In smooth muscle cells, loaded at room temperature (22-25 °C) with mag-fura-2 AM ester, more than 80 per cent of the generated fluorescence arises from the cytosol (Tashiro & Konishi, 1997).

Fluorescence properties of mag-fura-2

When an indicator binds to the target ion, it undergoes a change. This can manifest in an increase or decrease in the quantum yield with little change in either the absorbance or fluorescence spectra, a shift of the fluorescence excitation spectra to shorter wavelengths with little shift in the emission maximum, or a shift in both excitation and emission spectra to shorter wavelengths (Haugland, 1999).

Unbound mag-fura-2 has its excitation maximum at 370 nm. On binding to Mg^{2+}, an excitation shift occurs with its maximum at 335 nm, and an "isosbestic point" forms at 346 nm (Raju *et al.*, 1989). The isosbestic point is defined as a wavelength point at which the indicator fluorescence is insensitive to ion binding. For indicators such as fura-2 or mag-fura-2 that undergoes a spectral shift on ion binding, the fluorescence intensity resulting from excitation at the isosbestic point is directly proportional to the concentration of the dye in the sample and independent of the ion concentration. The emission maximum changes very little for both the bound and the unbound forms of the dye at 510 nm.

Complexation of mag-fura-2 with Mg^{2+} causes a decrease in fluorescence intensity at 370 nm and an increase at 335 nm, similar to the excitation spectra of fura-2 (Hurley *et al.*, 1992). Although this is true whether Mg^{2+} or Ca^{2+} binds to the dye, under normal resting conditions, the contribution of fluorescence originating from binding of the dye to Ca^{2+} is less than 2%, and even if $[Ca^{2+}]_i$ has risen to 1 μM, its contribution to the total fluorescence intensity would not exceed 10% (Raju *et al.*, 1989), assuming a basal $[Mg^{2+}]_i$ of 0.8 mM. Another important property of mag-fura-2 is its high quantum yield of 0.24 and 0.30 for the unbound and bound dye respectively. Therefore, only small concentrations of the dye are needed to achieve high fluorescence efficiency. In comparison, these values are much higher than those for other indicators such as quin-2, which has a quantum yield of only 0.029 and 0.14 for the unbound and bound forms (Tsien, 1980).

Dissociation constant of mag-fura-2

Since mag-fura-2 resembles in its molecular structure the Ca^{2+} indicator fura-2 (Grynkiewicz *et al.*, 1985; Raju *et al.*, 1989), it is expected that both exhibit a degree of similarity in their chemical and fluorescence properties (Grynkiewicz *et al.*, 1985; Raju *et al.*, 1989; Hurley *et al.*, 1992). The dissociation constant for Mg^{2+}-mag-fura-2 and Ca^{2+}-mag-fura-2 complexes were estimated to be 1.5 mM and 53 μM respectively, with a binding of one Mg^{2+}/Ca^{2+} to one dye molecule (Raju *et al.*, 1989). Mag-fura-2 has a greater binding affinity for Ca^{2+}, but since the resting $[Ca^{2+}]_i$ is in the order of 100 nM (Williamson *et al.*, 1983; Sheu *et al.*, 1984; Tsien, 1988; Bers *et al.*, 1990), the interference of fluorescence originating from calcium binding to mag-fura-2 is negligible. Therefore, unless the cell is spontaneously contracting or is stimulated to contract, or is influenced by conditions that result in considerable increases in $[Ca^{2+}]_i$, the measured fluorescence is assumed to be the result of Mg^{2+} complexation with mag-fura-2. Unfortunately, not all workers have reported the same K_d values for Mg^{2+}-mag-fura-2 complex. For example, Hurley *et al.* (1992) reported mean K_d values for Mg^{2+}-mag-fura-2 and Ca^{2+}-mag-fura-2 of 2.25 mM and 20.49 μM respectively. Quamme and Rabkin (1990) estimated Mg^{2+}-mag-fura-2 K_d at 1.4 mM and that for Ca^{2+}-mag-fura-2 of 60 μM. This discrepancy in K_d values for

both Ca^{2+}- and Mg^{2+}-mag-fura-2 complexes is probably due to differences in experimental conditions, such as temperatures and maximum levels to which cells were loaded with the ion under study to measure maximum fluorescence ratio (R_{max}), which could result in perturbation of cytoplasmic viscosity and hence affect binding properties of the fluorescent dye to either Ca^{2+} or Mg^{2+}.

Effect of pH_i on mag-fura-2 dissociation constant

The dissociation constant for mag-fura-2 is relatively insensitive to changes in pH_i within the normal physiological range (Raju *et al.*, 1989). However, the study by Howarth *et al.* (1995) suggests that when the pH_i is altered from 7.3 to either acidic (6.5) or alkaline (8.5) values, significant and variable differences in the dissociation constant values at 340 and 380 nm are observed. Their results show that greater sensitivity to pH_i shifts is observed at excitation wavelength 340 nm compared to 380 nm, with the most prominent effect observed at 335 nm. It appears though that mag-fura-2 is most sensitive to acidification when excited at 340 nm at 37 °C (Raju *et al.*, 1989; Howarth *et al.*, 1995). On the other hand, changes in pH_i in either direction have little effect on the K_d of mag-fura-2 at 22 °C (Lattanzio & Bartschat, 1991).

Calibration of mag-fura-2 and calculation of $[Mg^{2+}]_i$

Before ion concentrations can be calculated, the fluorescent dye must be calibrated. Ratiometric dyes such as mag-fura-2 can be calibrated either by measuring the fluorescence ratios of solutions of known $[Mg^{2+}]$ (*in vitro* calibration) or by loading the cells with the indicator and forcing maximum and minimum ratios (*in vivo* calibration) (Raju *et al.*, 1989).

The free acid analogue of the dye can be used to calibrate the dye *in vitro*, while loading the cell with the AM ester form permits *in vivo* calibration. Both calibrations make use of the same formula to calculate $[Mg^{2+}]_i$, while additional formulae can be used in the case of *in vitro* calibration, as will be discussed below.

The ion concentration is defined by the Grynkiewicz formula (Grynkiewicz *et al.*, 1985) as follows:

$[ion] = K_d \,.\, \beta \,.\, (R - R_{min})/(R_{max} - R)$, where:

K_d is the dissociation constant for mag-fura-2, β is the ratio of fluorescence intensities of the free to saturated mag-fura-2 at a single wavelength of 380 nm, R is the ratio of fluorescence at wavelengths 340 to 380 nm, R_{min} is the fluorescence ratio at wavelengths 340 to 380 nm for unbound mag-fura-2 (zero $[Mg^{2+}]$), and R_{max} is the ratio of fluorescence at wavelengths 340 to 380 nm for saturated mag-fura-2.

In vitro calibration

In vitro calibration is achieved using the free acid form (K^+ salt) of mag-fura-2. The dye is added to the calibration solution chosen to mimic the cytoplasmic composition of the cell under study, including ionic concentrations, pH_i, temperature and viscosity. R_{min} is obtained by measuring the fluorescence ratio of zero-$[Mg^{2+}]$ calibration solution (EDTA and EGTA are added to chelate trace Mg^{2+} and Ca^{2+} respectively) (Raju *et al.*, 1989; Quamme & Rabkin, 1990). R_{max} is obtained by using saturating $[Mg^{2+}]$ in the calibration solution to virtually saturate the dye and obtain the maximum fluorescence ratio. Ca^{2+} is often used to saturate mag-fura-2, since it has a higher binding affinity to Ca^{2+} than to Mg^{2+} (Raju *et al.*, 1989; Quamme & Rabkin, 1990). The K_d for Mg^{2+}-mag-fura-2 can be calculated from a Hill plot for individual fluorescence intensities (F) at 340 nm or 380 nm (log $(F\text{-}F_{min})/(F\text{-}F_{max})$) versus log $[Mg^{2+}]$ (Grynkiewicz *et al.*, 1985; Raju *et al.*, 1989; Howarth *et al.*, 1995). R has to be calculated after the subtraction of background fluorescence from individual data points. Background fluorescence is obtained by measuring the fluorescence signal from dye-free calibration solution. $[Mg^{2+}]_i$ can then be calculated directly from the above formula, assuming mag-fura-2 has the same K_d intracellularly. The advantage of using the formula to calculate $[Mg^{2+}]_i$ is that only two points are needed for calibration of the dye, R_{min} and R_{max}, which is especially useful in *in vivo* calibration, considering the difficulties involved in controlling $[Mg^{2+}]_i$.

The method described above can be modified to include data points between R_{min} and R_{max}, in which case either the Grynkiewicz formula or direct regression analysis of all data points can be used. This is carried out by preparing calibration solutions containing various [Mg^{2+}] (calibration standards). The fluorescence ratio is measured for each calibration standard and plotted against [Mg^{2+}] following subtraction of background fluorescence. Regression analysis of the data points is then carried out and $[Mg^{2+}]_i$ is read directly from the regression formula. This is considered again in the next chapter.

In vivo calibration

Cells are first loaded with the AM ester of mag-fura-2. They are then exposed to varying [Mg^{2+}], usually between 0 and 50 mM (Silverman *et al.*, 1994), in the presence of ionophores that increase the membrane permeability to divalent cations such as 4-bromo-A23187 or ionomycin (Silverman *et al.*, 1994) which doesn't result in significant autofluorescence as in the case of A23187. 4-bromo-A23187 is preferred since it is more effective than ionomycin in equilibrating cellular Mg^{2+} with external Mg^{2+} (Raju *et al.*, 1989; Tashiro & Konishi, 1997a).

Limitations of the Grynkiewicz formula

In assessing the reliability of $[Mg^{2+}]_i$ values retained by the Grynkiewicz formula, all elements of the formula should carefully be looked into. The three most important variables are R_{max}, K_d and β. As mentioned above, obtaining R_{max} requires saturation of mag-fura-2 with Mg^{2+}. *In vivo* fluorescence measurement of R_{max} assumes that Mg^{2+} has equilibrated across the cell membrane. However, none of the ionophores used for this purpose proved totally reliable in equilibrating Mg^{2+} across membranes, e.g. A23187 and ionomycin (Babcock *et al.*, 1976; Raju *et al.*, 1989). Using high Mg^{2+} concentrations to overcome this problem could change cytosolic osmolarity and hence influence mag-fura-2 K_d. *In vitro* estimation of R_{max}, although technically less demanding, suffers from the same difficulty of saturating mag-fura-2 without affecting the dye's K_d. In comparison, *in vivo* and *in vitro* estimates of R_{max} and R_{min} seem to agree within 10% (Raju *et al.*, 1989).

The third factor that has to be measured to use the formula is β. Since β is measured at a single wavelength (380 nm), changes of fluorescence efficiency due to dye leakage or photobleaching during the time between estimation of R_{min} and R_{max}, would ultimately change β value and results in an error in $[Mg^{2+}]_i$ estimates.

In conclusion, no single calibration method is error-free, however, these errors can be accommodated in most situations. There does not appear to be significant disagreement between *in vivo* and *in vitro* calibration methods in terms of $[Mg^{2+}]_i$ values obtained by the two methods (Raju *et al.*, 1989). In comparison to other methodologies used to monitor changes in $[Mg^{2+}]_i$, the fluorescent Mg^{2+} indicator mag-fura-2 is technically a less demanding and invasive method that permits monitoring of $[Mg^{2+}]_i$ for an extended period of time. The advantages and limitations of mag-fura-2 are shown in the Table 1.4.

Table 1.4. Advantages and limitations of mag-fura-2

Advantages	*Limitations*
1. Relatively non-invasive	1. Sensitivity to Ca^{2+}
2. Permits continuous monitoring of $[Mg^{2+}]_i$ for extended periods of time	2. Calibration occasionally inaccurate
3. Fast response time	3. Intracellular organelles cannot be entirely excluded
4. Can be applied to single cells, cell organelles or thin strips of muscle	4. Photobleaching and dye leakage increase noise-to-signal ratio

1.5 REGULATION OF $[Mg^{2+}]_i$ IN THE HEART

The movement of an ion across the plasma membrane of excitable cells is governed by the membrane permeability, the concentration of the ion on both sides of the membrane, and the membrane potential. These factors determine the routes by which an ion crosses the membrane in either direction.

The equilibrium of an ion moving through a simple pore in the plasma membrane of a polarised cell can be described by the Nernst equation. According to the Nernst equation, "ionic equilibrium potentials vary linearly with the absolute temperature and logarithmically with the ionic concentration ratio" (e.g. Hille, 1992b). The equilibrium potential of divalent cation S^{2+} (E_s) is:

$$E_S = \frac{RT}{2F} \ln \frac{[S^{2+}]_o}{[S^{2+}]_i}, \text{ where:}$$

R is the Gas constant, T the absolute temperature, F is Faraday's constant, $[S^{2+}]_o$ is the concentration of the ion outside, and $[S^{2+}]_i$ is the concentration of the ion inside. Therefore, according to the above equation, at a membrane potential equal to the equilibrium potential (E_s), the net flux of the ion S^{2+} should be zero, and the ion is said to be at electrochemical equilibrium. If the membrane potential is, however, more negative than E_s net ion *influx* should continue until electrochemical equilibrium is reached and vice versa.

The Nernst equation can therefore be used to calculate the equilibrium $[Mg^{2+}]_i$ at a given membrane potential and external $[Mg^{2+}]$. Total serum magnesium concentration is around 0.9 mM, 30% of which is bound to serum proteins or complexed with anions like bicarbonate, phosphate, sulphate, etc., leaving approximately 0.6 mM in the ionised form (Altura & Altura, 1995). Therefore, at a resting membrane potential of –80 mV, the expected $[Mg^{2+}]_i$ at electrochemical equilibrium would be about 240 mM at 37 °C. It can be concluded that $[Mg^{2+}]_i$ is maintained well below electrochemical equilibrium, and Mg^{2+} will tend to continuously enter the cell. Therefore, to explain the observed estimates of $[Mg^{2+}]_i$, some mechanism(s) must exist to remove Mg^{2+} from the cell against its

electrochemical gradient. While little is known about such mechanisms in heart cells, mechanisms have been suggested in other cell types. Before explaining the nature of the mechanisms responsible for the uptake and extrusion of Mg^{2+}, it is important to look into the chemistry and biochemistry of this divalent cation.

Compared to Ca^{2+}, Mg^{2+} ions are smaller, highly charged and have a much larger hydration shell in solution. The hydrated ion ($[Mg(H_2O_6)]^{2+}$) is formed from a cation that has a radius of 0.65 Å held in an octahedron surround of six water molecules, with a total radius for the hydrated ion of 2.10 Å (Williams, 1970; Williams, 1993). The high degree of attraction between Mg^{2+} and water molecules in the inner hydration shell results in a very slow exchange rate of water molecules on the shell for polar groups in the channel wall when the ion passes through a channel (10^4 times slower than other ions such as Na^+, K^+ or Ca^{2+}) (Flatman, 1991). Practically, this slow movement of Mg^{2+} through channels not only limits Mg^{2+} influx rate but also makes the distinction between channel and carrier behaviour difficult.

1.5.1 Mechanisms of Mg^{2+} uptake

There is evidence that Mg^{2+} does enter cells. Rogers and Mahan (1959) injected adult rats with $^{28}Mg^{2+}$ intraperitoneally and collected samples from various types of tissue at different intervals after the injection for analysis of $^{28}Mg^{2+}$ content. They found that the exchange reached complete equilibrium in the heart within 3 hours, while in rat skeletal muscle only 20% of total muscle magnesium equilibrated with $^{28}Mg^{2+}$ after 7 hours. Their study suggests that uptake of $^{28}Mg^{2+}$ by the heart, kidney and liver is faster than uptake in skeletal muscle, brain and testes. They also concluded that the uptake of Mg^{2+} has two components, a fast and a slow component with an exchange time of 1.2 and 25 hours in the "slow" organs, corresponding to the equilibration of free and bound magnesium respectively. In the case of the heart Mg^{2+} exchange occurs in a single process equivalent in time to the faster component in the "slow" organs (1.2 hours). Gilbert (1960) obtained similar results in isolated frog sartorius muscle using both non-radioactive Mg^{2+} and $^{28}Mg^{2+}$. In his study, muscle strips dissected from frog leg were immersed in Ringer's solution containing

high [Mg^{2+}], for 3 hours. Total muscle magnesium content was compared to control experiments in which the muscles were immersed in Ringer's solution containing 2 mM [Mg^{2+}]. It was found that the Mg^{2+} content of the muscle did not change over 5 hours of immersion in the control Ringer's solution while over the same period, the amount of Mg^{2+} in the muscle increased in a linear manner with the concentration of Mg^{2+} in the experimental Ringer's solution. The experiments with $^{28}Mg^{2+}$ provided evidence that the muscle cell membrane is permeable to Mg^{2+}. The author estimated that approximately 20% of total muscle magnesium is exchangeable in skeletal muscle.

In the heart, it has been shown that 98 ± 3 % of cellular Mg^{2+} in rat left ventricle is exchangeable while 2 to 3 % of cellular Mg^{2+} remains non-exchangeable (Page & Polimeni, 1972), and is believed to be the fraction of cellular Mg^{2+} tightly bound to myofibrillar actin (Weber *et al.*, 1969). Page & Polimeni (1972) found that the dependence of Mg^{2+} uptake by ventricular muscle on $[Mg^{2+}]_o$ was hyperbolic, with an apparent K_m value for a Mg^{2+} transporter of 0.57 ± 0.08 mM (n = 6), able to carry a maximum flux of 0.31 ± 0.04 mM kg^{-1} dry wt. min^{-1}. Their results were consistent with a carrier-mediated transport of Mg^{2+} across the sarcolemma of ventricular myocytes.

Further evidence for Mg^{2+} uptake by heart cells was obtained using Mg^{2+}-selective microelectrodes. Fry (1986) used Mg^{2+}-selective microelectrodes filled with the neutral ionophore ETH 1117 in ferret and guinea pig trabeculae. He reported a 0.8 mM increase in $[Mg^{2+}]_i$ in guinea pig papillary muscle superfused with a solution containing 10 mM $[Mg^{2+}]_o$, added to normal saline. Reducing $[Na^+]_o$ from 147 to 29.4 mM also resulted in a small increase in $[Mg^{2+}]_i$ in the same study. Hall *et al.* (1991) utilised the Mg^{2+}-sensitive resin ETH 5214 which has improved selectivity for Mg^{2+} over Na^+, K^+ and H^+, and measured a mean increase in $[Mg^{2+}]_i$ of 0.52 mM following superfusion of ferret ventricular papillary muscle strips with 10 or 20 mM $[Mg^{2+}]_o$ (added to normal Tyrode with no correction to osmolarity) for 10 minutes at 37 °C. The same effect was also noticed on reducing $[Na^+]_o$ to 20% of normal.

Also, Buri *et al.* (1993) used ETH 5214-filled microelectrodes to study the effect of changing $[Mg^{2+}]_o$ on the $[Mg^{2+}]_i$ of guinea pig ventricular papillary muscle. Superfusion of muscle with Tyrode's solution containing 10.5 or 20 mM $[Mg^{2+}]$ gave increases of 0.11 mM and 0.33 mM respectively. Reduction of $[Na^+]_o$ by 50% (to 77.5 mM) in the presence of 1 mM $[Mg^{2+}]_o$ and 1.8 mM $[Ca^{2+}]_o$ did not change $[Mg^{2+}]_i$ (see for example Fig. 2A in Buri *et al.* (1993)). In the same study, single ventricular myocytes loaded with mag-fura-2 showed a small increase in the fluorescence ratio when cells were exposed to Na^+-free Tyrode containing 1 mM $[Mg^{2+}]$. However, the same result was also obtained in the absence of extracellular Mg^{2+}.

More recently, Handy *et al.* (1996) succeeded in increasing $[Mg^{2+}]_i$ in mag-fura-2-loaded rat ventricular myocytes significantly above resting levels. This was achieved by replacing external Na^{2+} with either TMA or K^+ in Ca^{2+}-free conditions and at the same time increasing $[Mg^{2+}]_o$ from 1 to 5 mM. It was also possible to "clamp" $[Mg^{2+}]_i$ at the new elevated level for extended periods simply by reducing $[Mg^{2+}]_o$ back to 1 mM in the same solution.

It is not clear however, how Mg^{2+} crosses the plasma membrane. Studies on *Paramecium* revealed a Mg^{2+} current component, that cannot be attributed to K^+ or Na^+ entry, that was found to be specific to Mg^{2+} but manganese and cobalt can substitute as charge carriers. It was concluded from this study that the current is carried by a Mg^{2+} channel rather than a carrier (Preston, 1990). In another study on toad retinal rods (Nakatani & Yau, 1988), a conductive pathway that prefers divalent cations to monovalent cations was also demonstrated. The authors measured a Mg^{2+} current component, which accounts for up to 5% of the total current measured from rods under dark conditions. They calculated the relative probabilities for Na^+, Ca^{2+} and Mg^{2+} to permeate a light-sensitive conductance to be approximately 1: 12: 2.5 respectively. However, the authors concluded that Mg^{2+} influx might be an epiphenomenon, arising from the inability of the conductance to completely exclude Mg^{2+} while being permeable to both Na^+ and Ca^{2+}. Mg^{2+} may enter passively through cation channels or through other, as yet unknown route(s). There is evidence that

Mg^{2+} might enter through the L-type Ca^{2+} channel. Verapamil, a Ca^{2+}-channel blocker, inhibits Mg^{2+} influx in Mg^{2+}-depleted chick cardiac myocytes in the absence of alterations in $[Ca^{2+}]_i$ (Quamme & Rabkin, 1990). The authors found that $[Mg^{2+}]_i$ returned to normal baseline values on removal of verapamil. Similar findings were observed in rat cardiac myocytes, where verapamil significantly slowed the rate of Mg^{2+} "refill" in Mg^{2+}-depleted myocytes (Handy *et al.*, 1996). However, verapamil does not seem to inhibit elevation of $[Mg^{2+}]_i$ above resting levels in rat ventricular myocytes (Handy *et al.*, 1996). This may indicate that the pathways that return $[Mg^{2+}]_i$ to baseline in depleted cells are different from those that increase $[Mg^{2+}]_i$ above resting values.

Mg^{2+} might also enter cardiac myocytes through a putative Na^+/Mg^{2+} antiport (Handy *et al.*, 1996). The authors reported that $[Mg^{2+}]_i$ elevation was sensitive to imipramine, a tricyclic antidepressant that has been shown to inhibit Na^+/Mg^{2+} exchange in red blood cells (Féray & Garay, 1988). Application of 10 μM imipramine completely inhibited a rise in $[Mg^{2+}]_i$ when cells were superfused with a Na^+- and Ca^{2+}-free, solution containing 5 mM $[Mg^{2+}]$.

Much of the knowledge of the effect of imipramine on Na^+-dependent Mg^{2+} transport came from work on red blood cells (Féray & Garay, 1988; Flatman & Smith, 1990; Flatman & Smith, 1991). Ferret red blood cells can take up Mg^{2+} from the external medium under specific conditions, namely reduction of external $[Na^+]$ and elevation of $[Mg^{2+}]_o$ to more than 1 mM (Flatman & Smith, 1991). Mg^{2+} is believed to enter through reverse Na^+/Mg^{2+} exchange under conditions where the Na^+ gradient is outward and in the presence of more than 1 mM external $[Mg^{2+}]$. However, not all Mg^{2+} enters through a Na^+/Mg^{2+} antiport as evident from pharmacological studies by Flatman & Smith (1991). They report that approximately 80% of the Na^+-dependent Mg^{2+} uptake could be inhibited by imipramine (500 μM), amiloride (1 mM) or quinidine (500 μM), while the remaining 20% is believed to be through other, leak, pathways.

1.5.2 Mechanisms of Mg^{2+} removal

Whatever the routes through which Mg^{2+} enters the cell, mechanism(s) must exist to balance Mg^{2+} inward leak, and maintain $[Mg^{2+}]_i$ at around the measured values. Work in this area has established the existence of a Na^+-dependent Mg^{2+} efflux mechanism in human, chicken and ferret red blood cells (Féray & Garay, 1986; Günther & Vormann, 1989a; Flatman & Smith, 1990) consistent with a Na^+/Mg^{2+} antiport that extrudes intracellular Mg^{2+} in exchange for extracellular Na^+. It was found that a 1 Na^+: 1 Mg^{2+} stoichiometry in human red blood cells provides enough energy to drive the antiport, although 3 Na^+: 1 Mg^{2+} stoichiometry has also been suggested (Féray & Garay, 1988). Frenkel and co-workers (1989) concluded from their study on human red blood cells that the Na^+/Mg^{2+} antiport has an absolute requirement for ATP. However, Flatman (1991) argued against the need for ATP as a direct source of energy to drive the antiport but rather to catalyse Na^+-dependent Mg^{2+} efflux possibly by phosphorylating the protein.

The presence of a Na^+/Mg^{2+} antiport in the sarcolemma of cardiac cells is controversial. Experiments employing ISMEs provide evidence for and against the presence of a Na^+/Mg^{2+} antiport in ferret and guinea pig myocardium. Fry (1986) concluded that in guinea-pig heart Mg_i^{2+} is removed via a Na^+/Mg^{2+} antiport. The study measured changes in $[Mg^{2+}]_i$ and $[Na^+]_i$ using Mg^{2+}-selective microelectrodes filled with the ionophore ETH 1117. Raising $[Mg^{2+}]_o$ from 1 to 10 mM resulted in about a 3 mM decrease in $[Na^+]_i$ and 1 mM increase in $[Mg^{2+}]_i$. Inhibition of the Na^+ pump by ouabain increases both $[Na^+]_i$ and $[Mg^{2+}]_i$. Unfortunately, microelectrodes filled with ETH 1117 suffer from significant interference by Na^+, K^+ and H^+, therefore it is not ideal for monitoring $[Mg^{2+}]_i$ changes especially when $[Na^+]_i$ is also changing. In addition, inhibition of the Na^+ pump not only leads to accumulation of Na^+ in the cytosol but also Ca^{2+} due to inhibition of the Na^+/Ca^{2+} exchanger, with a consequent displacement of Mg^{2+} by Ca^{2+} from common intracellular binding sites. The net effect might be one of an apparent increase in $[Mg^{2+}]_i$ but not $[Mg]_t$.

Such experiments were later reinvestigated using microelectrodes filled with Mg^{2+} ionophore ETH 5214 and Na^+ ionophore ETH 227 (Buri *et al.*, 1993). It was found that upon reduction of $[Na^+]_o$ to 50% normal, replaced by either tetramethylammonium chloride (TMA) or *N*-methyl-D-glucamine (NMDG), a small increase in Mg_i^{2+} activity was recorded in TMA but not NMDG solution. It was concluded that the apparent rise in $[Mg^{2+}]_i$ was most probably due to TMA interference with the Mg^{2+}-selective microelectrode. This, together with the lack of a decrease in $[Na^+]_i$, was taken as evidence against the existence of a Na^+/Mg^{2+} antiport in guinea-pig papillary muscle.

Experiments by Freudenrich *et al.* (1992a) on cultured chicken heart cells did not support the existence of the putative Na^+/Mg^{2+} antiport. These experiments manipulated the $[Na^+]$ gradient and examined the subsequent effects on $[Mg^{2+}]_i$ in three different solutions, Na^+-free, Na^+-free and Mg^{2+}-free, and Na^+-free and Ca^{2+}-free. Since a rise in $[Mg^{2+}]_i$ as detected by mag-fura-2, was seen in the first and second but not the third solution, it was concluded that the increase in $[Mg^{2+}]_i$ was the result of displacement by Ca^{2+} of internal Mg^{2+} from common intracellular binding sites. Removal of Na^+ from the superfusate in the presence of Ca^{2+} may increase $[Ca^{2+}]_i$ through reversal of the sarcolemmal Na^+/Ca^{2+} exchanger, thereby resulting in a significant net $[Ca^{2+}]_i$ increase, that might interfere with mag-fura-2 fluorescence and/or displace bound intracellular Mg^{2+}. In addition Na^+-free superfusion increases $[H^+]_i$, resulting in displacement of both Mg^{2+} and Ca^{2+} bound to intracellular ligands such as ATP, ADP, troponin and myosin. It is estimated that 0.5 pH units acidification increases $[Mg^{2+}]_i$ by 0.1 mM, and contributes to about 10% of the total Na^+-free evoked $[Mg^{2+}]_i$ increase, the rest being attributed to Ca^{2+} influx (Freudenrich *et al.*, 1992a). Although this study suggests evidence against a Na^+/Mg^{2+} antiport it does, however, delineate the way in which Mg^{2+}, Ca^{2+} and H^+ may interact with each other intracellularly. In contrast to the study by Murphy *et al.* (1991a) in which $[Mg^{2+}]_i$ rose by twofold in Na^+-free solution, Silverman *et al.* (1994) observed only minor increases in $[Mg^{2+}]_i$ upon sustained increase in $[Ca^{2+}]_i$ to levels around 1 μM.

Evaluating the effect of Na_o^+ removal on pH_i in sheep Purkinje fibres, Ellis and Macleod (1985) found that Na^+-free solution inhibits pH_i recovery from acidification caused by approximately 15 minutes exposure to, and subsequent removal of, NH_4Cl. Replacing Na_o^+ by either TMA or K^+ can result in intracellular acidification either by inhibiting the sarcolemmal Na^+/H^+ exchanger or as a direct effect of Na_o^+ removal on other transport systems. The consequent increase in $[H^+]_i$ alters $[Ca^{2+}]_i$, and probably $[Mg^{2+}]_i$ by competing for common intracellular binding sites (Bers & Ellis, 1982).

To demonstrate movement of Mg^{2+} through a Na^+/Mg^{2+} antiport, it must be shown that Mg^{2+} can be driven out of the cell against its electrochemical gradient with a concomitant downhill movement of Na^+ or uphill Na^+ movement driven by Mg^{2+} entry down its electrochemical gradient (reversal of the antiport).

Both situations were addressed in the work of Handy and co-workers (1996). They showed that the increase in $[Mg^{2+}]_i$ caused by superfusion with 5 mM Mg^{2+}, Ca^{2+}- and Na^+-free solution, is most probably mediated through reversal of a putative Na^+/Mg^{2+} antiport. Although verapamil did not affect the rise, a Mg^{2+} channel cannot be ruled out. Also, increasing $[Na^+]_i$ by inhibiting the Na^+ pump by strophanthidin in Ca^{2+}-free Tyrode results in an increase in $[Mg^{2+}]_i$ at normal $[Mg^{2+}]_o$ of 1 mM, suggesting possible reversal of the Na^+/Mg^{2+} antiport.

In these experiments, $[Mg^{2+}]_i$ reduction was studied by superfusing Mg^{2+}-loaded cells with normal Tyrode, which contained 140 mM Na^+, 1 mM Ca^{2+} and 1 mM Mg^{2+}. Only when Na^+ was present in the superfusate did $[Mg^{2+}]_i$ recover to its basal levels, suggesting a relationship between internal Mg^{2+} and external Na^+. Imipramine was found to inhibit the Na^+-stimulated $[Mg^{2+}]_i$ reduction in these experiments, adding further evidence to the existence of a Na^+/Mg^{2+} antiport in cardiac myocytes. However, since the recovery was not complete in the presence of 25 μM verapamil, or absence of external Ca^{2+}, a role for Ca^{2+} in the recovery process cannot be ruled out. There is evidence for a Ca^{2+}/Mg^{2+} exchanger in liver plasma membrane vesicles

(LPM) (Cefaratti *et al.*, 1998). The authors propose the existence of two Mg^{2+} transporters, a Na^+/Mg^{2+} and a Ca^{2+}/Mg^{2+} exchanger. Their results indicate that Mg^{2+} efflux with Ca^{2+} is 63% less than that when Na^+ is the counter ion. It was also found that Mg^{2+} uptake occurs in LPM loaded with Na^+ but not with Ca^{2+}, suggesting reversibility of exchange through Na^+/Mg^{2+} but not Ca^{2+}/Mg^{2+}. Fluxes through both exchangers are inhibited by amiloride, imipramine and quinidine but not by Ca^{2+} channel blockers.

Recently, Tashiro & Konishi (2000) studied the Na^+-dependence of $[Mg^{2+}]_i$ reduction in Mg^{2+}-loaded rat ventricular myocytes. Their work confirms the observations by Handy *et al.* (1996) in that recovery of $[Mg^{2+}]_i$ is dependent on external Na^+ and can be completely inhibited by imipramine, although at much higher concentrations. The authors suggested the presence of an electroneutral Na^+/Mg^{2+} antiport that exchanges 2 Na^+ ions for each Mg^{2+} ion removed.

1.5.3 Aims and objectives

The main objective of this work is to investigate the mechanisms responsible for keeping $[Mg^{2+}]_i$ below its electrochemical equilibrium in isolated rat ventricular myocytes. To achieve that an, experimental protocol has to be developed to raise $[Mg^{2+}]_i$ above resting levels, in order to study $[Mg^{2+}]_i$ recovery back to basal values, which is believed to occur through a Na^+/Mg^{2+} antiport. The experiments presented in this thesis also aim to study the mechanisms responsible for the Mg^{2+}-loading. Specifically, the experiments were designed to study:

1. The Na^+-dependence of $[Mg^{2+}]_i$ reduction in Mg^{2+}-loaded, isolated rat ventricular myocytes.
2. The stoichiometry of the putative Na^+/Mg^{2+} antiport.
3. The routes through which Mg^{2+} enters the cell.
4. The Na^+- and Mg^{2+}-dependence of $[Mg^{2+}]_i$ elevation.
5. The effects of two drugs (imipramine and KB-R7943) on both $[Mg^{2+}]_i$ reduction and elevation.

CHAPTER 2

GENERAL MATERIALS AND METHODS

2.1 CHEMICALS

All chemicals were of analytical grade.

Table 2.1 below summarises the name and source of all chemicals used in this study in alphabetical order.

Table 2.1. List of chemicals used in the study

Name in the thesis	*Full name*	*Source*
BSA	Bovine serum albumin	Sigma
$CaCl_2$	Calcium chloride	Merck/BDH
Collagenase type-II	Collagenase type-II	Worthington, Biochemical Corp., USA
Creatine	Creatine	Sigma
DMSO	Dimethyl sulphoxide	Sigma
EDTA	Ethylenediamine tetraacetic acid	Sigma
EGTA	Ethylene glyco-bis(β-Aminoethyl ether) N,N,N`,N`-Tetra-acetic acid	Sigma
Glucose	Glucose	Merck/BDH
HCl	Hydrochloric acid	Merck/BDH
HEPES	(N-[2-Hyroxyethyl]piperazine-N`-[2-ethanesulfonic acid])	Sigma
Imipramine	10,11-dihydro-*N,N*-dimethyl-5*H*-dibenz[*b,f*]azepine-5-propanamine	Sigma
K-aspartate	L-aspartic acid (monopotassium salt)	Sigma
KBR	KB-R7943 mesylate	Tocris
KCl	Potassium chloride	Merck/BDH
KOH	Potassium hydroxide	Merck/BDH
Mag-fura-2 AM ester	Mag-fura-2 tetra-acetoxymethyl ester	Molecular Probes, USA/ Teflabs, USA
Mag-fura-2 free acid	Mag-fura-2 free acid (potassium salt)	Molecular Probes, USA/ Teflabs, USA
$MgCl_2$	Magnesium chloride	Merck/BDH
Mg.ATP	Magnesium ATP	Sigma
Mineral oil	Mineral oil	Sigma
NaCl	Sodium chloride	Merck/BDH

Name in the thesis	*Full name*	*Source*
Na_2HPO_4	Di-sodium hydrogen orthophosphate	Merck/BDH
NaH_2PO_4	Sodium dihydrogen orthophosphate	Merck/BDH
NaOH	Sodium hydroxide	Merck/BDH
Na-Pyruvate	Pyruvic acid (sodium salt)	Sigma
NMDG	N-methyl-D-glucamine	Sigma
Penicillin	Benzlypenicillin (sodium salt)	Sigma
Pluronic F-127	Pluronic F-127	Molecular Probes, USA
Procaine	p-Aminobenzoic acid diethylaminoethyl ester	Sigma
Protease	Protease (type XIV)	Sigma
Sodium pentobarbitone	Sodium pentobarbitone	Rhone Merieux, Harlow, UK
Streptomycin	Streptomycin sulphate	Sigma
Taurine	2-aminoethane sulphonic acid	Fluka Biochemika
TMA.Cl	Tetramethylammonium chloride	Merck/BDH

2.2 SOLUTIONS

Table 2.2 summarises the composition (in mM) of the solutions used for collection of the heart (the cardioplegic solution), for cell isolation, and the Normal Tyrode's used to superfuse the isolated cells.

Table 2.2. Composition of the cardioplegic, cell isolation and Tyrode's solutions. All concentrations are in mM.

Cardioplegic		*Cell isolation*		*Normal Tyrode (HCO_3^--free)*	
$CaCl_2$	1	Creatine	10	HEPES	10
Glucose	10	Glucose	10	KCl	6
HEPES	10	HEPES	5	NaCl	134
KCl	20	KCl	5.4	NaOH [c]	5.96
$MgCl_2$	1	$MgCl_2$	1	$CaCl_2$	1
Na_2HPO_4	4	Na Pyruvate	5	Glucose	10
NaCl	130	NaCl	130	$MgCl_2$	1
NaH_2PO_4	1	NaH_2PO_4	0.4		
NaOH [b]	5	NaOH [a]	5.8		
		Penicillin	0.02		
		Streptomycin	0.07		
		Taurine	20		
~ Osmolarity (mOsm)	350		347		320

[a] Used to adjust pH to 7.4 at 33 °C

[b] Used to adjust pH to 7.4 at 4 °C

[c] Used to adjust pH to 7.4 at 37 °C

A stock of cell isolation solution was prepared and kept at –20 °C until needed. A day before the experiment, 350 ml of the frozen solution was thawed and modified according to Table 2.3. The cardioplegic solution was gassed with 100% oxygen for approximately 10 minutes before use. Normal Tyrode was prepared by directly adding 1 mM $CaCl_2$, 1 mM $MgCl_2$ and 10 mM glucose to stock Tyrode immediately before use. For Ca-free Tyrode, $CaCl_2$ was simply omitted from the solution. The

solution used to raise $[Mg^{2+}]_i$ in isolated cells (so called **loading solution**) contained (in mM: $MgCl_2$ 30, KCl 6, TMA.Cl or NMDG 95, HEPES 10, glucose 10). The pH was adjusted to 7.4 at 37 °C using either 1 M KOH for TMA-containing solution, or 6 N HCl for NMDG-containing solution (final $[K^+]$ was 6 mM in both solutions). $[Mg^{2+}]_i$ was stabilised at high levels by superfusing the cell with a "**clamp solution**" which contained (in mM: $MgCl_2$ 1, KCl 6, TMA.Cl or NMDG 140, HEPES 10, glucose 10; pH 7.4 at 37 °C using 1 M KOH or 6 N HCl for TMA- or NMDG-containing solution respectively; final $[K^+]$ was 6 mM in both solutions). Wherever Na^+ was partly or totally removed from the solution, it was replaced in equimolar amounts by either TMA or NMDG.

In the cell isolation process six solutions were used as shown in Table 2.3 below.

Table 2.3. **Modifications made to the basic cell isolation solution**

Solution	*[Ca] (mM)*	*EGTA (mM)*	*Collagenase (mg ml^{-1})*	*BSA (mg ml^{-1})*
1	1.0			
2		0.1		
3	0.1		0.2 – 0.5	
4	0.17			20
5	0.5			20
6	1.0			20

2.3 ISOLATION OF VENTRICULAR MYOCYTES

All ventricular myocytes used in this study were isolated according to the method described by Levi *et al.*, 1992, with modifications (Handy *et al.*, 1996). Ventricular myocytes were isolated using a combination of enzymatic and mechanical dispersion. Hearts were collected from male albino *Sprague-Dawley* rats (mean body weight ± S.E.M., 295.10 ± 6.5 g, range 181-480 g, n = 77). Rats were anaesthetised by an intra-peritoneal injection of sodium pentobarbitone (120 mg Kg^{-1}). Since it is

crucial to obtain a good perfusion of the heart, 200 units heparin were also administered a few minutes before opening the thorax to prevent formation of coronary blood clots. Ice-cold cardioplegic solution was poured over the heart once the thorax was opened to slow the beating rate of the heart. The heart was quickly removed and placed in ice-cold cardioplegic solution. It was then gently compressed to empty as much blood from its chambers as possible, to try to prevent blood clots forming in its chambers, arteries and veins. It was then quickly transported to the laboratory (approximately 3 minutes).

The heart was placed in a dissection bath filled with the same cardioplegic solution, the aorta cannulated as quickly as possible and the heart mounted on a Langendorff perfusion system (Figure 2.1). In the Langendorff heart there is retrograde perfusion into the aorta. The solution closes the aortic valve and flows through both coronary arteries, and thus perfusion of cardiac tissue takes place. The perfusate finally drains into the right atrium, right ventricle and leaves the heart through the pulmonary artery and inferior and superior vena cava.

2.3.1 Langendorff perfusion of the heart

The heart was mounted on the Langendorff perfusion apparatus and perfused at a constant rate of 6 ml min^{-1} (g heart tissue)$^{-1}$ using a peristaltic pump (Minipuls 2, Gilson, France). Solutions used in perfusion, and time for each, are shown in Table 2.4. Solutions 1, 2 and 3 were placed in a water bath at 37 °C and gassed with 100% oxygen throughout the perfusion procedure. At the end of the perfusion protocol, the heart was taken off the Langendorff perfusion system and placed on a filter paper (Whatman International Ltd., 70 mm diameter) in a petri dish containing 5 ml oxygenated enzyme solution (solution 3). The atria were excised, ventricles opened longitudinally and 2-3 mm strips of ventricular muscle were gently cut around the circumference of the cavity.

Table 2.4. **Langendorff perfusion protocol**

Solution	*Time (min.)*	*Temperature (°C)*
1	10	Room
1	10	33
2	4	33
3	5	33
3 with recycling	~12	33

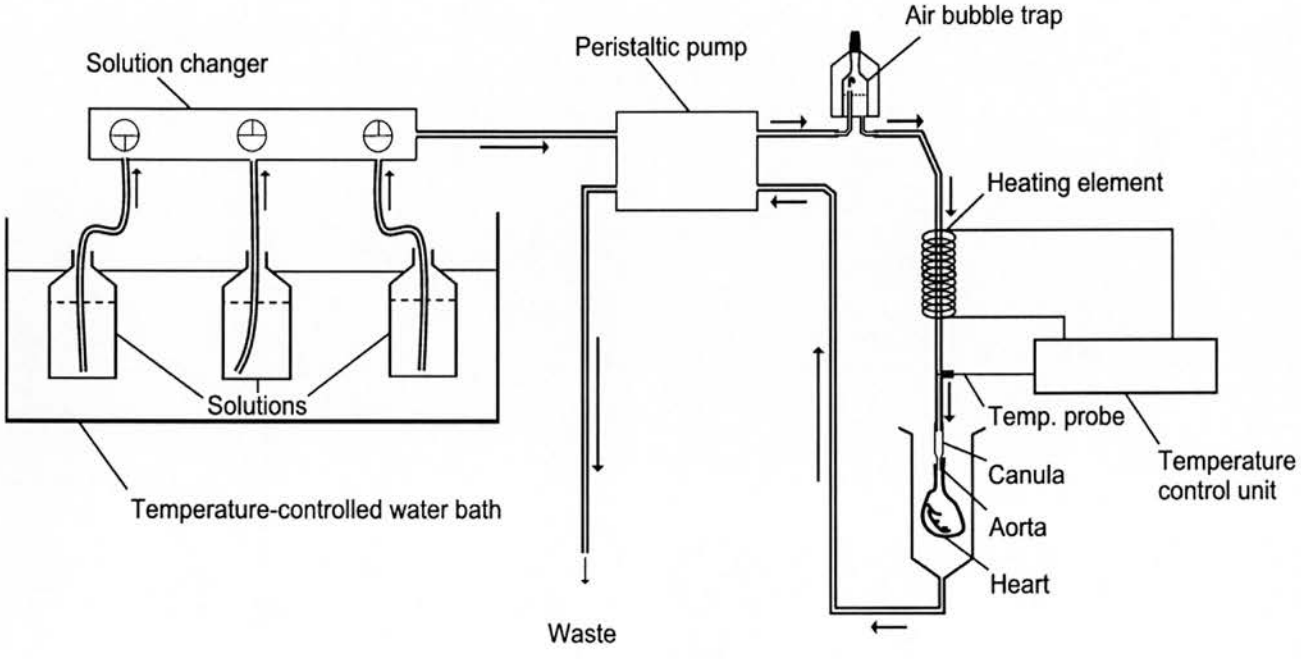

Figure 2.1. **Langendorff perfusion system**

Solutions used in retrograde perfusion of the heart were kept in a water bath at 37 °C. A manual solution changer was used to switch between solutions. Solutions were perfused at a constant rate of 6 ml min^{-1} (g heart tissue)$^{-1}$ using a peristaltic pump. An air bubble trap, positioned between the pump and the heart, ensured that no air bubbles entered the aorta. A temperature control unit set at 33 °C controlled the temperature of the solution being pumped into the heart. The cannulated heart itself was placed below the heating element, and the perfusate leaving it was collected and pumped out to waste.

2.3.2 Further digestion of the ventricles

The chopped heart was placed in a sterile plastic container containing 5 ml oxygenated solution 3 then shaken at a rate of 130 min^{-1} (Grant Instruments SS40-2) for 5-10 minutes at 37 °C. The supernatant was gently removed (to avoid further mechanical stress to isolated cells) using a 1.5 ml polyethylene transfer pipette (Sigma), filtered through a 200 μm mesh and added to 5 ml solution 4 (Table 2.3). The process was repeated until three to four test tubes each containing approximately 4 ml cell suspension and 5 ml solution 4 were obtained. In many preparations the first collection was discarded due to the relatively high percentage of dead cells.

2.3.3 Washing of the isolated ventricular myocytes

Isolated cells were washed with a medium containing progressively increased calcium concentrations of 0.17 mM, 0.5 mM and 1 mM. The washing procedure was carried out as follows: the tubes containing the isolated cell suspension were centrifuged at 30 *g*, at room temperature for 1 minute, the supernatant discarded and pellets from all four test tubes pooled into one. The pellet was re-suspended in 9 ml solution 4, and centrifuged under the same settings above. The procedure was repeated twice thereafter with solutions 5 and 6 (Table 2.3). The final pellet was re-suspended in 2 ml of filtered solution 6 (0.2 μm sterile filter unit, Sigma). Total cell yield was (mean ± S.E.M.) 2.03 ± 0.10 × 10^6 cells / g heart tissue (range 0.45 × 10^6 - 4.2 × 10^6, n = 77) with an average number of rods of 1.14 ± 0.08 × 10^6 / g heart tissue (range 0.18 × 10^6 – 2.7 × 10^6, n = 77). This gives an average rod percentage of 53.5 ± 2.1 % (range 12.7 – 77.7 %, n = 77). Washed isolated cells, suspended in filtered solution 6 were then incubated with 5 μg ml^{-1} protease for 30 minutes at 37 °C with continuous shaking. At the end of the incubation period the cells were washed once with normal Tyrode and re-suspended in filtered solution 6. Protease was used to both digest dead cells and "clean" cells' plasma membranes for better development of giga-seals (Hamill *et al.*, 1981) for electrophysiological studies.

2.4 DYE LOADING AND FLUORESCENCE MEASUREMENT

Mag-fura-2 AM ester was dissolved in dimethylsulphoxide with 5% (w/w) Pluronic-F127 to a final concentration of 1 mM and stored in aliquots of 70 µl at –20 °C until needed (Gow *et al.*, 1995). Isolated myocytes, re-suspended in 2 ml filtered solution 6, were loaded by incubation for 30 minutes with 5 µM mag-fura-2 AM ester at room temperature in the dark. The preparation was placed on a platform shaker (Stuart Scientific, UK), and gently shaken at 15 rev.min^{-1}. The cells were then washed twice with filtered normal Tyrode and re-suspended in 1 ml filtered solution 6. Loaded cells were stored at room temperature in the dark until required. Only cells that maintained a rod shape, sharp edges and well-defined striations were used for the experiments described.

A small volume of the final cell suspension (5-10 µl in solution 6) was introduced into a perspex perfusion chamber (Series 20, Warner Instrument Corp., Hamden, USA) containing normal Tyrode. Cells were allowed to adhere to the base of the perfusion chamber (slide cover thickness 0.08-0.12 mm, BDH No. 0) for a few minutes in non-flowing normal Tyrode before superfusion with the experimental solutions. To limit autofluorescence, the area around the cell – as seen on TV monitor – was shielded using a detector aperture (Nikon, Japan) placed between the emitted light beam and the photomultiplier tube (PMT), so that only the cell and the minimum cell-free area was visible. PMT voltage was set at 800 volts. Superfusion was then started at a rate of 3 ml min^{-1}. A set of three electronic solenoids (Lee Co., CT, USA) were used to switch between the solutions used in superfusing the cells.

The perfusion chamber exchange time was measured by switching between normal Tyrode and fluorescine-containing normal Tyrode. The 95% solution exchange time was 38 ± 2.3 seconds (n = 10). When measuring rates of $[Mg^{2+}]_i$ change, the first minute of recording following solution change was excluded from the calculations to allow for the bath exchange time. New batches of cells were used for each recording.

Fluorescence from mag-fura-2-loaded myocytes was measured according to the method previously described by Handy *et al.* (1996). Figure 2.2 shows the system setup. A rotating wheel fitted with 340 and 380 nm filters was used to alternately excite mag-fura-2-loaded cells at these two wavelengths. Emitted light from cells at wavelengths greater than 510 nm was measured using a spectrophotometry system (Cairn Research Ltd, Sittingbourne, UK) attached to an inverted microscope (Olympus IMT-2, Japan) and viewed with a 40× objective.

Digitised fluorescence signals were fed into a computer and were recorded and plotted in real time. Each point was averaged over 4 seconds while the excitation filters were illuminated at a rate of 8 Hz. At the end of each experiment, background fluorescence was measured by bringing a cell-free area of the cover slip into the field of view. This value was then subtracted from each data point prior to calculation of fluorescence ratio (340 nm / 380 nm). All experiments were carried out at 37 °C.

The strength of the fluorescence signal varied among different preparations and sometimes among cells within the same preparation. This was roughly assessed by the strength of the induced signals on an oscilloscope and the arbitrary values of the 340 nm and the 380 nm wavelengths on the computer monitor. A noisy trace suggested poor loading with mag-fura-2 AM ester. Only cells with relatively strong signals were used in the fluorescence measurement experiments.

2.5 Calibration of mag-fura-2

Mag-fura-2 was calibrated *in vitro* using mag-fura-2 free acid (K-salt). The free acid was dissolved in 1 mM HEPES buffer, pH 7.4 to a final concentration of 1 mM. Aliquots of 100 µl were stored at –70 °C until required.

On the day of the calibration, mag-fura-2 free acid was added to calibration standards to a final concentration of 5 µM. Calibration standards contained (in mM: KCl 140; NaCl 10; HEPES 10; variable $MgCl_2$, 0-15; EGTA 0.1); pH adjusted to 7.2 at 37 °C. 0.1 mM EDTA was added to the Mg-free standard to chelate contaminant Mg^{2+}.

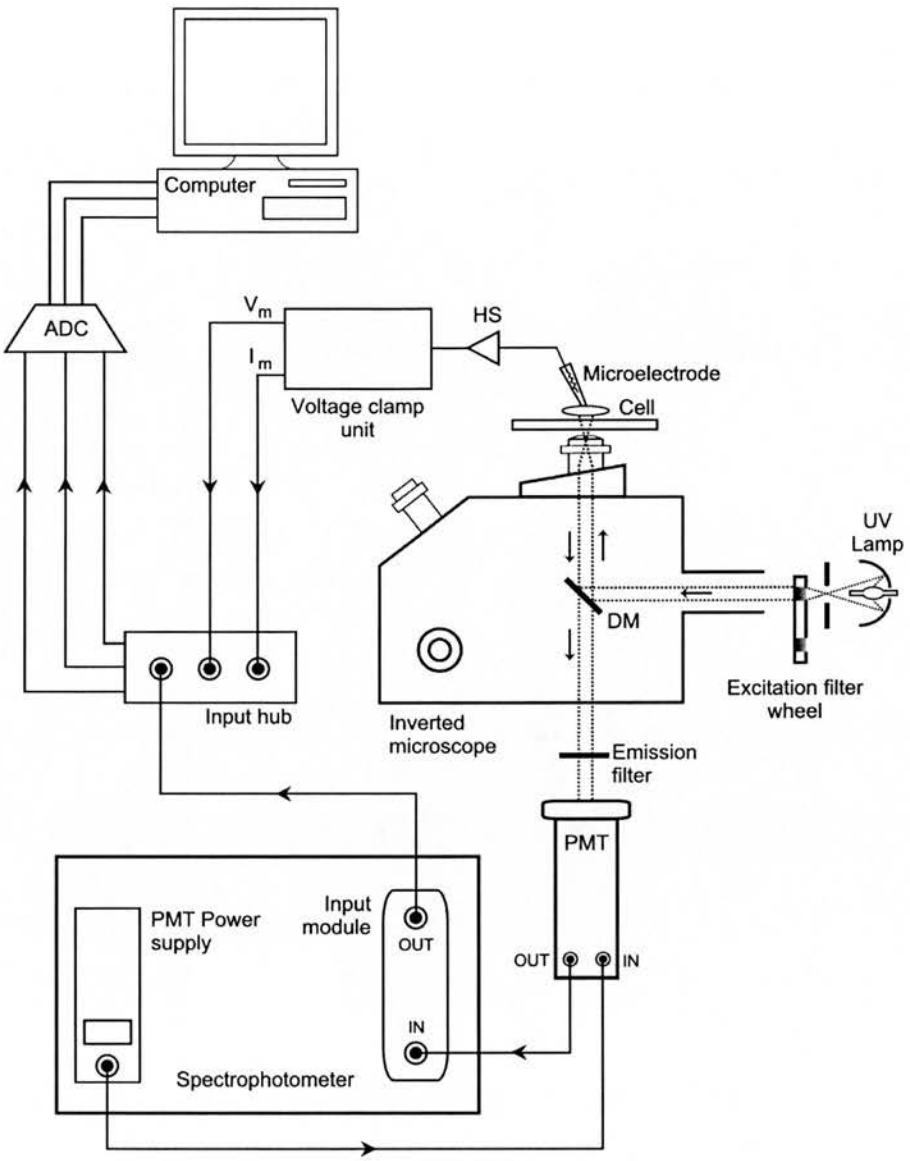

Figure 2.2. A system for the simultaneous recording of cell fluorescence, membrane potential and current.

A filter wheel is used to alternately excite a cell through the microscope objective lens. A dichroic mirror (DM), placed between the objective lens and excitation filters, reflects the excitation light (dotted line) onto the cell, and transmits longer wavelengths of the emitted fluorescence towards the photomultiplier tube (PMT). An emission filter, placed between the DM and PMT, allows emitted fluorescence at the peak emission wavelengths for the dye to be measured by the PMT. Cell membrane potential (E_m) and current (I_m) are measured via a microelectrode fitted on a head stage (HS) and attached to the cell. The fluorescence, E_m and I_m signals are fed into a computer following digitisation through an analogue-digital converter (ADC).

Droplets of 1 µl of calibration standards were placed onto the base of the perfusion chamber one at a time using a Hamilton syringe (Hamilton Company, USA), under 3-4 mm mineral oil. The platform supporting the perfusion chamber was heated (Heater Controller TC-344, Warner Instrument Crop., Hamden, USA) so that the oil temperature remained at 37 °C throughout the course of the recording.

Emitted light at 510 nm following excitation at 340 nm and 380 nm was recorded from the centre of each droplet under 40× magnification, with the fluorescence detector aperture set equal to an average size of a cardiac cell as seen on the TV monitor. The average of a two-minute recording was taken for each droplet. Background fluorescence was measured from droplets of the Mg-free (0.1 mM EDTA added) calibration solution that contained no dye. The ratio of fluorescence at 340 nm to 380 nm was plotted against $[Mg^{2+}]$, and $[Mg^{2+}]_i$ was derived directly from the calibration curve. A typical calibration curve is shown in Figure 2.3.

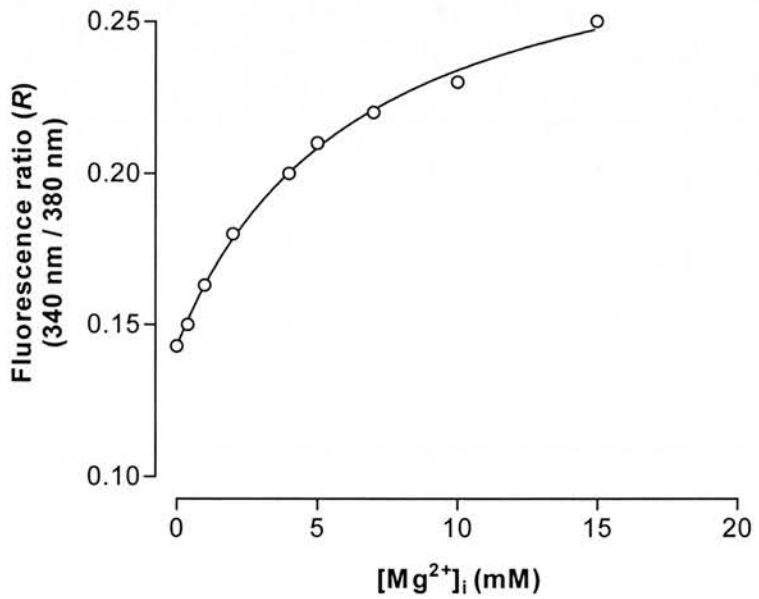

Figure 2.3. **Mag-fura-2 calibration**

Each data point represents the average of three calibration experiments. The line was fitted according to the equation: $[Mg^{2+}]_i = K_d.\beta.[R - R_{min})/ (R_{max} - R)]$, where $K_d.\beta = 6.34$, $R_{min} = 0.14$ and $R_{max} = 0.29$. Error bars are smaller than points. $R^2 = 0.99$.

2.6 MEMBRANE POTENTIAL RECORDING AND VOLTAGE-CLAMPING

In order to assess the effect of the various solutions used in the study on the resting membrane potential of isolated myocytes, the membrane potential was measured using high resistance sharp electrodes or low resistance patch pipettes. In other experiments the effect of cell depolarisation on Mg^{2+} transport was studied using the whole cell configuration of the voltage clamp technique. In these experiments only patch pipettes were used.

2.6.1 Pipette fabrication

Patch pipettes were pulled from borosilicate glass capillaries, internal diameter 1.15 mm, external diameter 1.55 mm (Garner Glass Company, Claremont CA, USA), using a computerised horizontal puller (Sutter Instrument Co. P-97, USA). Their tips were heat-polished producing pipette resistance in the range of 1.5-5 MΩ when filled with a solution designed to mimic the intracellular medium.

High resistance (sharp) glass electrodes were pulled from filamented borosilicate glass capillaries, external diameter 1.5 mm, internal diameter 0.86 mm (Clark Electromedical Instruments, Reading, England), using a vertical puller. Electrode resistance was in the range of 12 – 24 MΩ when filled with 3 mM KCl.

2.6.2 Mechanical set-up

The filled patch or high resistance microelectrode was mounted on a suction pipette holder connecting to a unity gain amplifier head stage (HS-2A, Axon Instruments Inc., USA), which was mounted on a hydraulic micromanipulator (Narishige MW-3, Japan). This, in turn, was mounted onto another manipulator for coarse movement (Narishige MN-2, Japan). The whole assembly was mounted on the inverted microscope.

2.6.3 Electronics set-up

The head stage was connected to a microelectrode voltage and current clamp unit (Axoclamp-2A, Axon Instruments Inc., USA). Recording of the membrane potential

was made in the bridge mode of the clamp unit using sharp or patch microelectrodes (see also Section 6.2). An analogue-digital converter (CED 1401, UK), was used to digitise signals from the clamp unit before being fed to a computer. In voltage clamp experiments, isolated cells were voltage-clamped using patch electrodes. Cells were voltage-clamped in the whole-cell configuration of the voltage clamp technique operating in the continuous mode (see also Section 6.2). In experiments where fluorescence and voltage signals were acquired simultaneously, both signals were digitised by the spectrophotometer's computer module.

2.7 SOFTWARE

The data for the membrane potential were captured using real-time data acquisition software (Spike 2 ver. 2 CED, UK) at a rate of 0.25 Hz. Further processing of the recorded membrane potential readings was carried out on Excel 2000 (Microsoft Corporation Inc., USA). In experiments where simultaneous recording of membrane voltage, membrane current and fluorescence signals was required, all the data were recorded using Cairn spectrophotometry software (Cairn ver, 5.2, Cairn Research Ltd, Sittingboune, UK), with further processing and plotting of data being carried out on MS Excel 2000 and Prism 3.0 (GraphPad Software Inc., USA). Schematic diagrams were produced using MS PhotoDraw 2000 (Microsoft Corporation, USA). Statistical analyses were carried out on SPSS for Windows release 10.0.5.

2.8 STATISTICAL ANALYSIS

The number of experiments (n) indicates the number of experiments carried on cells isolated from different hearts. Means of the rate of change of $[Mg^{2+}]_i$ or fluorescence ratio within cells were compared using the paired *t*-test for related samples. Similar statistical analysis was used to compare the means of change in the membrane potential. Where two or more means are compared to control mean, the one-way analysis of variance (ANOVA) test was used. Unless specified otherwise, all values

are expressed as mean ± S.E.M. Mean values were considered significantly different if the *P*-value was less than 0.05.

CHAPTER 3

SODIUM-DEPENDENCE OF MAGNESIUM REDUCTION

3.1 INTRODUCTION

Mg^{2+} leak into cardiac cells may be balanced by one or more of the following processes:

1. Sarcolemmal Mg^{2+} transporter(s)
2. Intracellular buffering, e.g. by ATP and other cellular constituents
3. Transport across cell organelles

The second and third processes could, in the short term, prevent a rise in $[Mg^{2+}]_i$ caused by Mg^{2+} influx and stabilise $[Mg^{2+}]_i$ at around the measured values. However, control of $[Mg^{2+}]_i$ ultimately depends on an active transport mechanism that removes Mg^{2+} against a large electrochemical gradient. Only the first proposed pathway for Mg^{2+} efflux will be considered here. Mg^{2+} may be removed via a channel or an antiport. Other possibilities are discussed elsewhere.

Extrusion through a channel

The only situation where Mg^{2+} can be extruded through a channel is when the net driving force acting on Mg^{2+} supports efflux rather than influx. This can be envisaged in a beating heart, where Mg^{2+} is extruded during systole when cells depolarise to values more positive than E_{Mg} (–7 mV), whereas influx of Mg^{2+} is expected to occur during diastole. Mg^{2+} influx during diastole must be balanced by efflux during systole, in the absence of other extrusion mechanism(s), otherwise a rise in $[Mg^{2+}]_i$ over the long term is inevitable. The possible existence and a role of such channels in the regulation of $[Mg^{2+}]_i$ in heart cells remain to be elucidated.

Extrusion through a Na^+/Mg^{2+} antiport

Günther and Vormann (1985), were first to report the existence of an amiloride-sensitive Na^+-dependent Mg^{2+} extrusion mechanism in the plasma membrane of chicken and turkey erythrocytes. Mg^{2+} efflux in Mg^{2+}-loaded chicken erythrocytes was found to depend specifically on $[Na^+]_o$. Mg^{2+} efflux was reversibly inhibited by amiloride at a half maximal concentration of 0.59 mM. Since then, an increasing

number of reports have suggested the presence of a similar mechanism in a many tissue types, including the heart (Fry, 1986; Handy *et al.*, 1996; Tashiro & Konishi, 2000)

Evidence for Na^+/Mg^{2+} exchange in the heart came from observations that reversing the Na^+ gradient across the sarcolemma (by removal of external Na^+) elevates $[Mg^{2+}]_i$. Conversely, reduction of $[Mg^{2+}]_i$ from high levels is stimulated by the presence of Na^+ in the bathing medium and is completely inhibited by its removal. Under these conditions Mg^{2+} will be moving against a large electrochemical gradient. These observations may be accounted for by a sarcolemmal Na^+-dependent Mg^{2+} exchange mechanism, possibly a Na^+/Mg^{2+} antiport.

In this chapter the Na^+-dependence of $[Mg^{2+}]_i$ reduction in Mg^{2+}-loaded cells was studied. The Mg^{2+} extrusion mechanisms were investigated by increasing $[Mg^{2+}]_i$ levels high enough to allow examination of recovery at two different $[Na^+]_o$ in the same cell, one being the test concentration while the other is the control.

A number of control experiments were carried out. These include the effect of the solutions used in the study on the resting membrane potential of quiescent myocytes, and the effects of Ca^{2+} transients during cell contraction on the determination of $[Mg^{2+}]_i$ from mag-fura-2 fluorescence. The effect of the solutions used in the present study on the resting $[Ca^{2+}]_i$ was also studied using the Ca^{2+}-sensitive dye fura-2. In addition, control experiments were conducted to examine the effect of changes in pH_i, evoked by NH_4Cl or propionic acid, on $[Mg^{2+}]_i$ measured using mag-fura-2.

3.2 MATERIALS AND METHODS

1. Loading isolated myocytes with Ca^{2+} indicator fura-2 AM ester: Fura-2 AM ester was dissolved in dimethylsulphoxide with 5% (w/w) Pluronic-F127 (Molecular Probes, Eugene, Texas, USA) to a final concentration of 1 mM, and stored in aliquots of 70 μM at –20 °C until required. Cells, suspended in solution 6 (Table 2.3), were incubated at room temperature with 5 μM fura-2 AM ester (Teflabs, Texas, USA) for 30-45 minutes in the dark. The preparation was gently shaken on a platform shaker at 15 rev.min^{-1}. After the incubation period, the cells were washed twice with normal Tyrode, and re-suspended in 3 ml filtered (0.2 μm filter unit, Sigma) solution 6. Loaded cells were stored at room temperature in a petri dish until required. Changes in $[Ca^{2+}]_i$ are expressed as per cent change in *R*.

2. Fura-2 fluorescence measurement: A similar method to the one used for mag-fura-2 was used. See General Materials and Methods (Section 2.4).

3. Stimulation of isolated ventricular myocytes: Isolated myocytes were stimulated to contract using an isolated stimulator (DS2, Digitimer Ltd., UK) driven by a digital timer (Digitimer 100, Digitimer Ltd., UK) at a rate of 1 Hz. Cells were stimulated to contract for at least 1 minute in normal Tyrode at 37 °C before recording was started.

3.3 RESULTS

3.3.1 Na^+-dependence of $[Mg^{2+}]_i$ reduction

A batch of isolated ventricular myocytes was introduced into the superfusion chamber containing normal Tyrode. The Na^+-dependence of Mg^{2+} reduction was investigated by increasing $[Mg^{2+}]_i$ above resting levels in a Na^+- and Ca^{2+}-free and high $[Mg^{2+}]$ solution before various "test" concentrations of Na^+ (28-98 mM) were introduced in the external solution. The removal of both external Na^+ and Ca^{2+} was found to be crucial for stimulating an increase in $[Mg^{2+}]_i$ above resting values (Handy *et al.*, 1996).The rate constant of $[Mg^{2+}]_i$ reduction in the test $[Na^+]_o$ was compared to that in 140 mM $[Na^+]_o$ within the same cell.

A typical experimental protocol is shown in Figure 3.1. The cell was initially superfused with normal Tyrode until the fluorescence signal stabilized (approximately 10 to 15 minutes). The solution was then changed to Ca^{2+}-free Tyrode for another 2 minutes. Increasing $[Mg^{2+}]_i$ was achieved by total replacement of external Na^+ with either TMA or NMDG and increasing $[Mg^{2+}]_o$ from 1 to 30 mM (see loading solution, page 41).

Once $[Mg^{2+}]_i$ was increased to high levels above normal, it was stabilised at this new level by changing to a similar solution but containing 1 mM $[Mg^{2+}]$ instead of 30 mM (see clamp solution, page 42). $[Mg^{2+}]_i$ was allowed to stabilise for about 5 minutes before changing to a solution containing various external Na^+ concentrations (test solution), in which either TMA or NMDG partly replaced Na^+ on an equimolar basis. Four external Na^+ concentrations were used: 28, 56, 70 and 98 mM. At this stage the presence of Na^+ in the superfusate caused $[Mg^{2+}]_i$ to begin to recover towards basal values in normal Tyrode. $[Mg^{2+}]_i$ was allowed to recover for a few minutes before switching to Ca^{2+}-free Tyrode containing 140 mM Na^+. $[Mg^{2+}]_i$ eventually recovered to its initial level in normal Tyrode and the experiment was stopped.

Resting $[Mg^{2+}]_i$ was 0.75 ± 0.05 mM (mean ± S.E.M., range 0.40 - 1.34 mM, n = 77). On changing to the high $[Mg^{2+}]$ loading solution, $[Mg^{2+}]_i$ rose to 4.75 ± 0.44 mM (range 1.80 - 9.30 mM, n = 20).

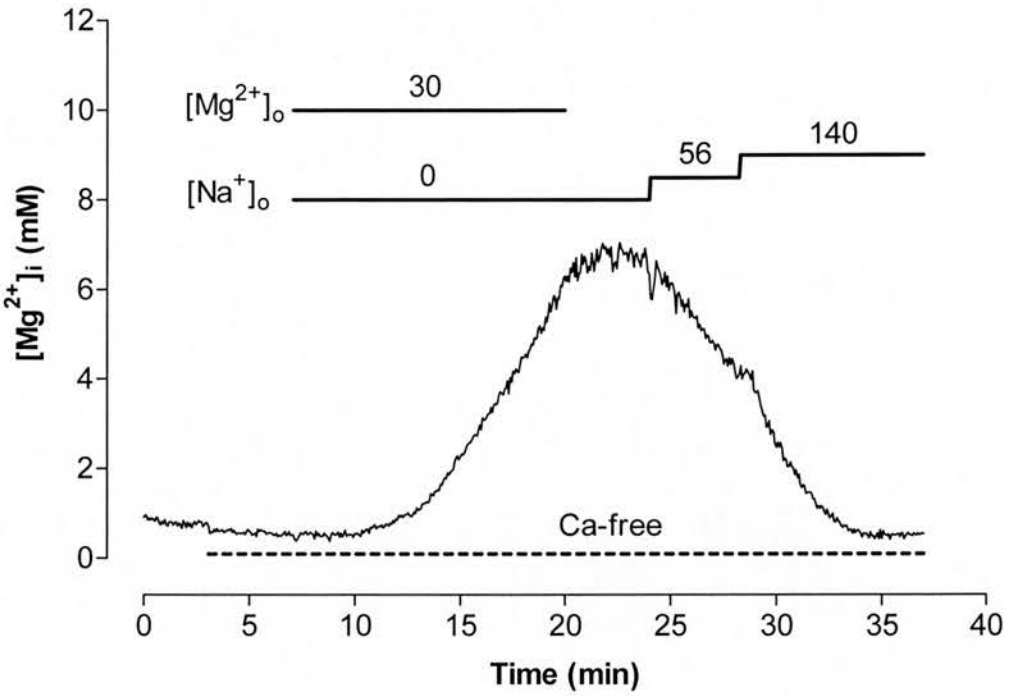

Figure 3.1. An experimental protocol for studying the Na^+-dependence of $[Mg^{2+}]_i$ reduction

A fluorescence trace depicting changes in $[Mg^{2+}]_i$ in a single ventricular myocyte. Dark bars represent solution changes and numbers on top are concentrations in mM. Where not specified (in mM: $[Ca^{2+}]_o$ 1, $[Na^+]_o$ 140, $[Mg^{2+}]_o$ 1). In this experiment, basal $[Mg^{2+}]_i$ was around 0.6 mM, and increased to 7 mM on superfusion with a Ca^{2+}- and Na^+-free solution containing 30 mM Mg^{2+} for 13 minutes. $[Mg^{2+}]_i$ was "clamped" at this concentration by reduction of $[Mg^{2+}]_o$ to 1 mM. $[Mg^{2+}]_i$ began to decline on adding 56 mM $[Na^+]$ to the superfusate. $[Na^+]_o$ was later increased to 140 mM until $[Mg^{2+}]_i$ recovered to the initial baseline level.

Since the aim of these experiments was to study the mechanism(s) responsible for $[Mg^{2+}]_i$ reduction, the rates of $[Mg^{2+}]_i$ elevation will not be presented here. However, it is clear that the increase in $[Mg^{2+}]_i$ follows a non-linear time course. This component of Mg^{2+} transport will be dealt with in more detail in Chapter 4. On returning to 140 mM Na^+_o Tyrode, $[Mg^{2+}]_i$ recovered to 0.76 ± 0.04 mM (range 0.40 - 1.10 mM, n = 20), the difference between $[Mg^{2+}]_i$ at the beginning of the experiment and at the end was not significant ($P > 0.05$). In all these experiments $[Mg^{2+}]_i$ recovered almost fully to its initial basal values only when Na^+ was introduced in the superfusate, indicating that $[Mg^{2+}]_i$ reduction was Na^+-dependent.

Examples of original fluorescence measurements depicting changes in $[Mg^{2+}]_i$ in single cardiac myocytes, where Mg^{2+} is believed to be removed from Mg^{2+}-loaded cells at $[Na^+]_o$ of 28, 56, 70, 98 and 140 mM are shown in Figure 3.2. Since the decrease in $[Mg^{2+}]_i$ on introducing Na^+ to the bathing solution is exponential, the maximum rate ($mM.min^{-1}$) and rate constant (min^{-1}) of $[Mg^{2+}]_i$ reduction at the test and 140 mM $[Na^+]_o$ were obtained using a semi-log plot (Figure 3.3). The rates of $[Mg^{2+}]_i$ change were measured The mean rate constant ratio of $[Mg^{2+}]_i$ reduction at external Na^+ concentrations of 28, 56, 70 and 98 mM compared to that at 140 mM are summarised in Table 3.1.

Table 3.1. **Mean rate constant ratios of $[Mg^{2+}]_i$ reduction (Test $[Na^+]_o$:140 mM $[Na^+]_o$)**

$[Na^+]_o$ (mM)	*Mean rate constant ratio ± S.E.M.*	*(n)*
28	0.18 ± 0.04	5
56	0.43 ± 0.02	5
70	0.50 ± 0.07	6
98	0.78 ± 0.11	4
140	1	20

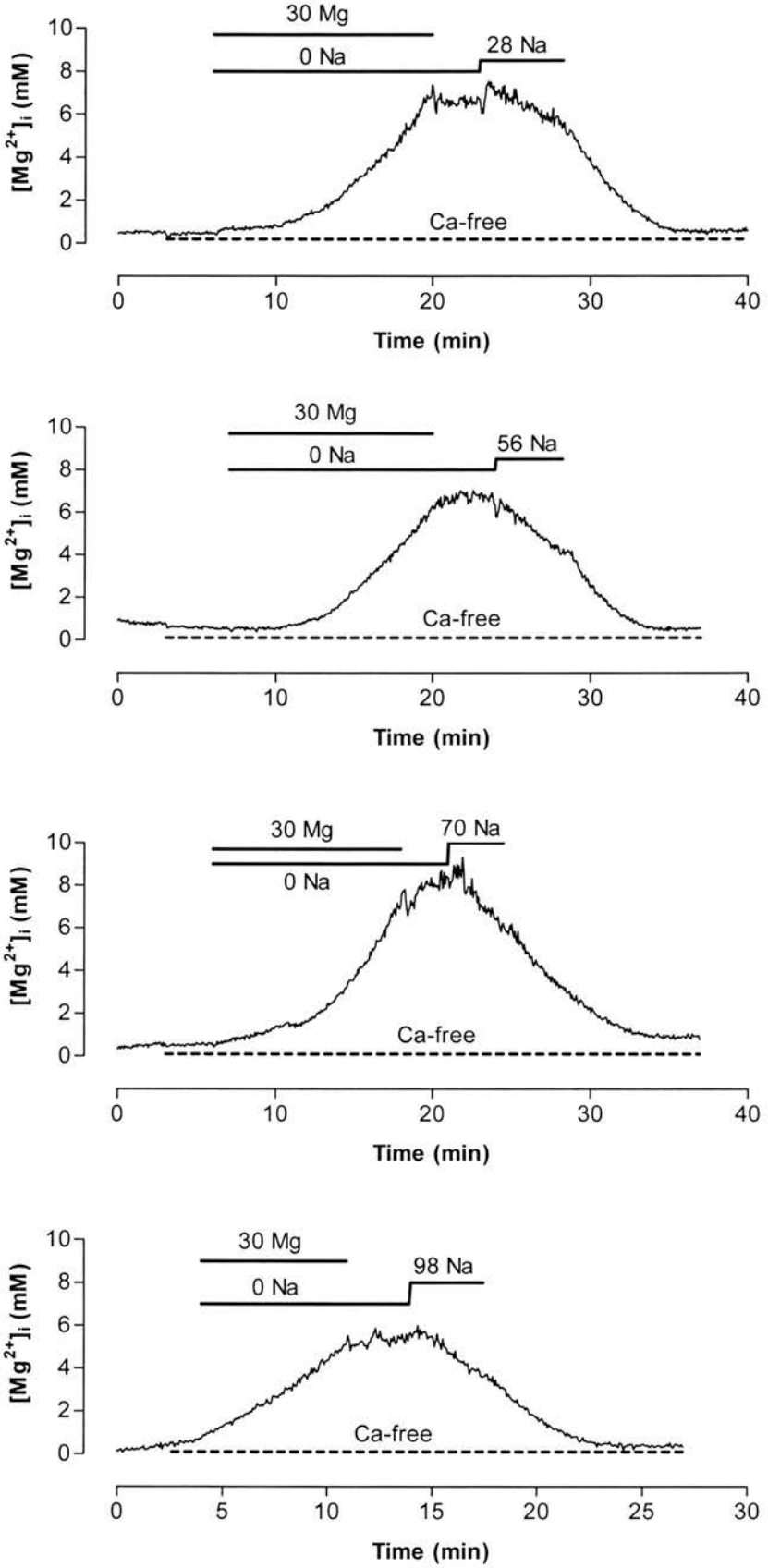

Figure 3.2. **$[Mg^{2+}]_i$ reduction in various $[Na^+]_o$ (28 to 98 mM).** Na^+ was replaced with equimolar amounts of TMA. All solutions are normal Tyrode unless otherwise indicated.

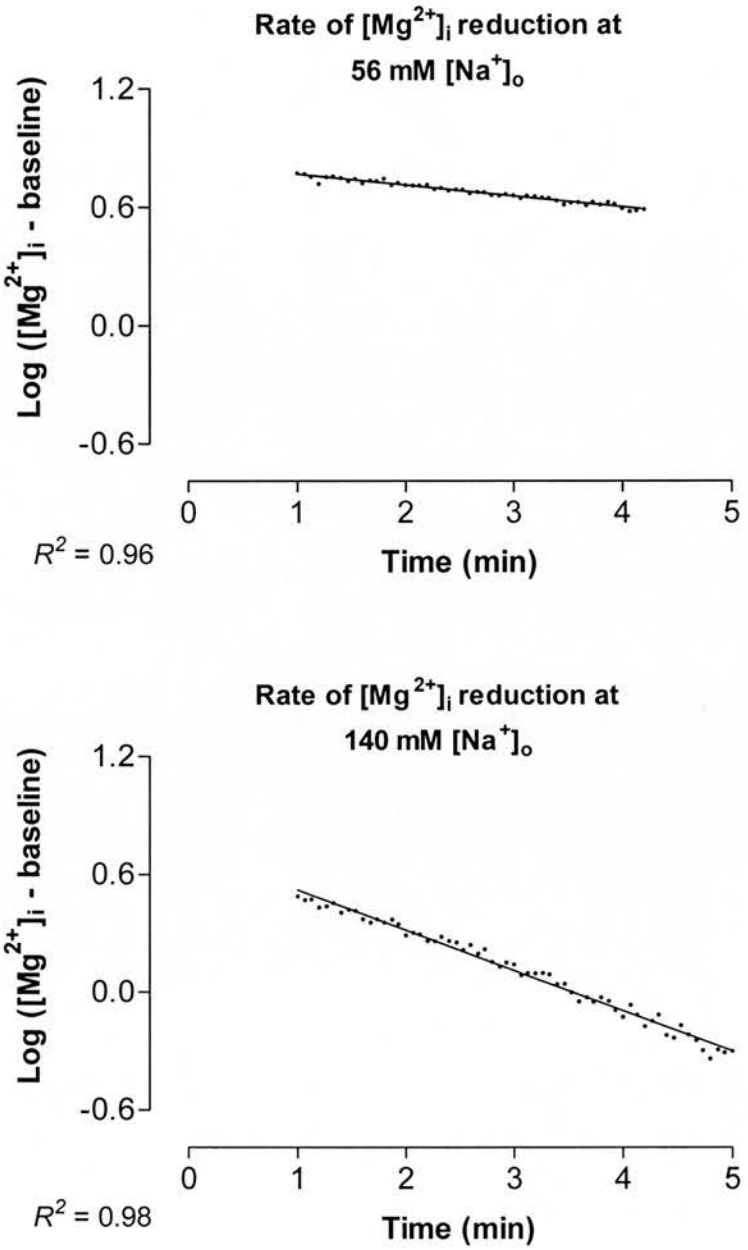

Figure 3.3. **Calculation of the rate of $[Mg^{2+}]_i$ reduction**

In experiments where $[Mg^{2+}]_i$ was recovering from a Mg^{2+}-load, $[Mg^{2+}]_i$ eventually reached a stable level that did not change any further with time. This "baseline level" was subtracted from $[Mg^{2+}]_i$ when calculating the rate of $[Mg^{2+}]_i$ reduction. The rate of $[Mg^{2+}]_i$ reduction at the test $[Na^+]_o$ (56 mM in this case) and 140 mM $[Na^+]_o$ was calculated by plotting $[Mg^{2+}]_i$ on a semi-log scale, following subtraction of baseline $[Mg^{2+}]_i$. The rate constant and maximum rate of $[Mg^{2+}]_i$ reduction at each $[Na^+]_o$ was obtained from the equation of the regression line fitted to the data points.

The mean rate constant of Mg^{2+} reduction in normal Tyrode (140 mM $[Na^+]_o$) was 0.35 ± 0.03 min^{-1} (range 0.11 – 0.69, n = 20). The relationship between $[Na^+]_o$ and mean rate constant ratios of $[Mg^{2+}]_i$ reduction appears to be linear (Figure 3.4A). The rate constant of $[Mg^{2+}]_i$ reduction at Na_o^+ test concentrations of 28, 56 and 70 mM were significantly lower than that at 140 mM ($P < 0.05$), while the difference between the rate of $[Mg^{2+}]_i$ reduction at 98 mM compared to that at 140 mM was not significant ($P = 0.1$).

The data were plotted on a log-log scale to estimate the co-operativity ratio for Na_o^+ and Mg_i^{2+} on a putative Na^+/Mg^{2+} antiport (Figure 3.4B). The line fitted to the data had a slope of 1.02 ± 0.10 mM^{-1} (mean ± S.E.), suggesting a 1 Na^+: 1 Mg^{2+} stoichiometry for the putative Na^+/Mg^{2+} antiport.

The data presented so far utilised rate constant ratios to describe the relationship between $[Na^+]_o$ and the rate of change in $[Mg^{2+}]_i$. Other parameters that were calculated and plotted against $[Na^+]_o$ include the maximum rates and rate constants of $[Mg^{2+}]_i$ reduction at the test and 140 mM $[Na^+]_o$. Maximum rates of reduction were dependent upon the extent of the initial rise in $[Mg^{2+}]_i$, and showed a wider scatter in the data points (Figure 3.5A) when compared to rate constants Figure 3.5B).

In summary, the results are consistent with a linear relationship between $[Na^+]_o$ and the rate of reduction in $[Mg^{2+}]_i$ where the influx of a single Na^+ ion is required for the extrusion of a single Mg^{2+} ion, possibly through a Na^+/Mg^{2+} antiport. As a consequence of such a model there will be a net loss of one positive charge carried by Mg^{2+}, and hence the rate of Mg^{2+} extrusion should be affected by changes in E_m and the putative transporter will be electrogenic. This voltage-dependence of Mg^{2+} transport will be dealt with in Chapter 6.

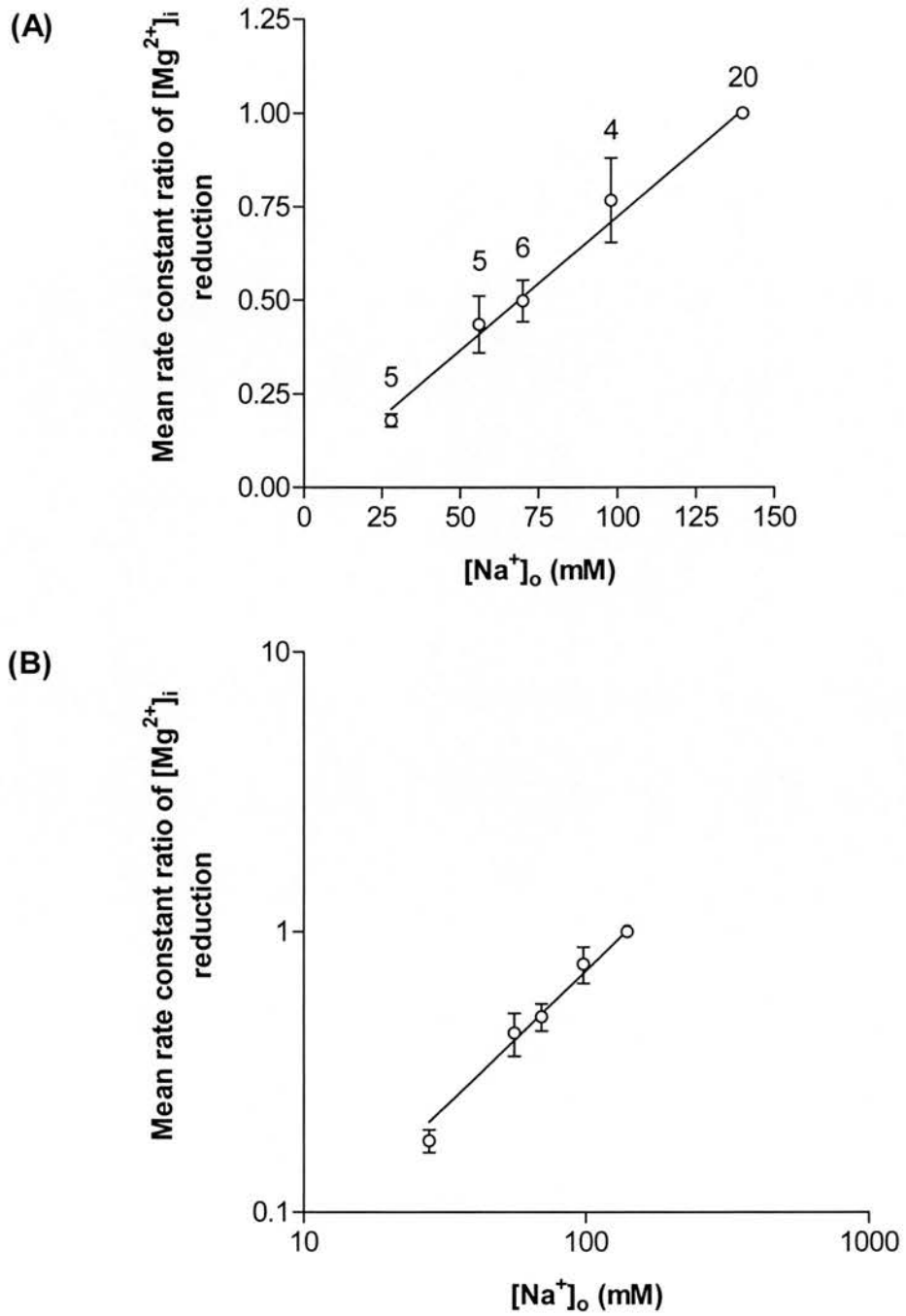

Figure 3.4. **$[Mg^{2+}]_i$ reduction from Mg^{2+}-loaded cells as a function of $[Na^+]_o$**

(A) Each point represents the mean ratio of rate constant of $[Mg^{2+}]_i$ reduction at the test $[Na^+]_o$ to the rate constant at 140 mM $[Na^+]_o$ for n (number on error bars) experiments. **(B)** Same data plotted on a log-log scale to obtain the co-operativity ratio for Na_o^+ and Mg_i^{2+} on a putative Na^+/Mg^{2+} antiport. The slope of the fitted linear regression line is 1.02 ± 0.1 mM^{-1}, $R^2 = 0.92$.

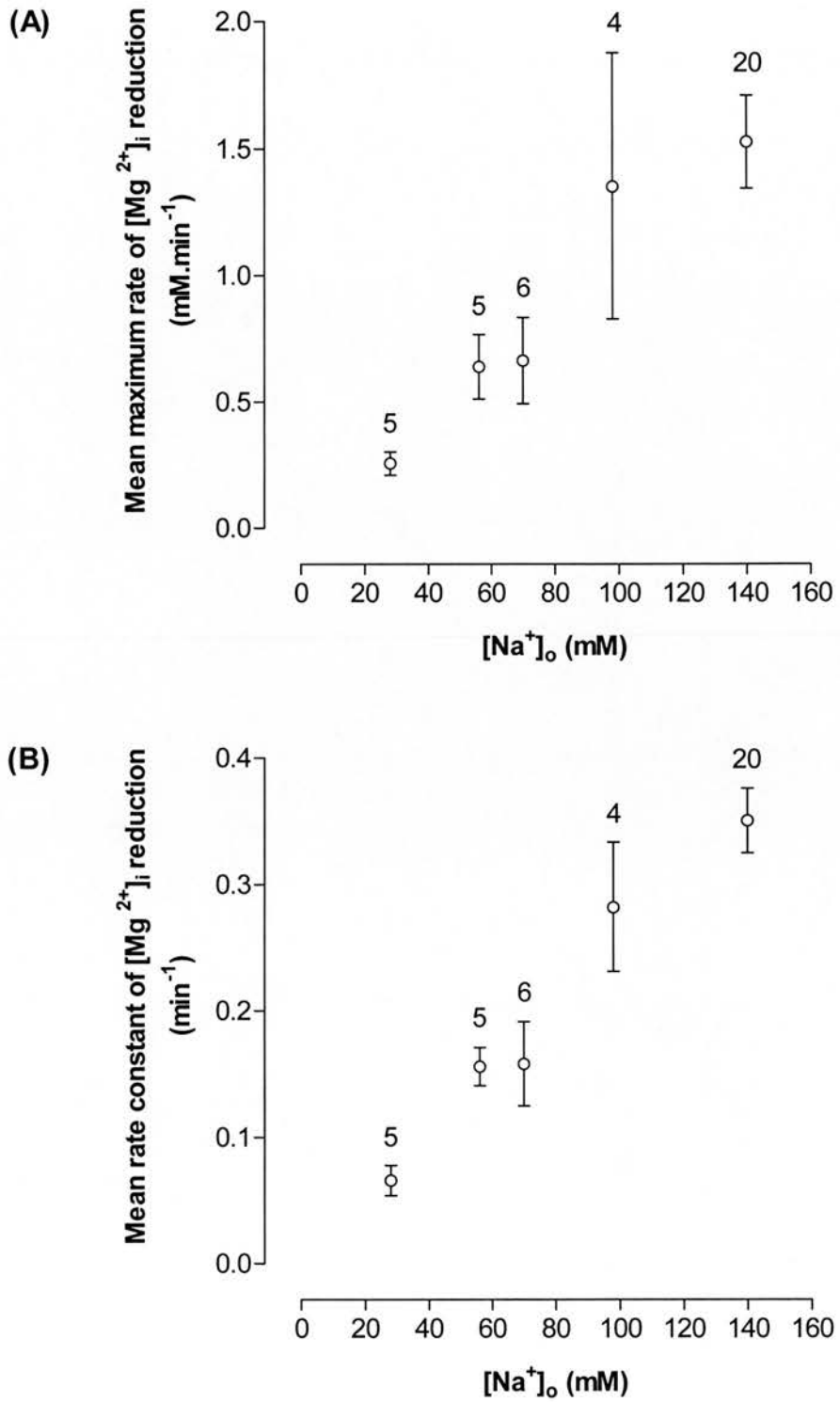

Figure 3.5. **Comparison between mean maximum rates (A) and mean rate constants (B) of $[Mg^{2+}]_i$ reduction at various $[Na^+]_o$**

Vertical bars are standard error of the mean (S.E.M).

3.3.2 Mg^{2+}-dependence of $[Mg^{2+}]_i$ reduction

$[Mg^{2+}]_i$ reduction in Mg^{2+}-loaded cells through a putative Na^+/Mg^{2+} antiport required external Na^+. However, in all of the experiments described so far $[Mg^{2+}]_i$ reduction was explored under conditions where $[Mg^{2+}]_o$ was 1 mM. Experiments to test whether external Mg^{2+} is required for the extrusion of Mg^{2+} through a Na^+/Mg^{2+} exchange mechanism(s) will be presented in this section.

Cells were first subjected to the Mg^{2+} loading solution. They were then superfused with either Mg^{2+}-free Tyrode or a similar solution containing 3 mM $[Mg^{2+}]$ (Figure 3.6). $[Mg^{2+}]_i$ recovered to levels close to the initial $[Mg^{2+}]_i$ in both solutions. There was no significant difference between initial $[Mg^{2+}]_i$ and $[Mg^{2+}]_i$ after full recovery at the end of the experiments in either case ($P > 0.05$). The rate constant of $[Mg^{2+}]_i$ reduction at 0 $[Mg^{2+}]_o$ was 0.23 ± 0.06 min^{-1} (range 0.16 – 0.30, n = 4), and that at 3 mM $[Mg^{2+}]_o$ was 0.16 ± 0.03 min^{-1} (range 0.15 – 0.20, n = 3). Although the mean rate of $[Mg^{2+}]_i$ reduction at 3 mM $[Mg^{2+}]_o$ was lower, the difference between rates of $[Mg^{2+}]_i$ reduction at 0 and 3 mM $[Mg^{2+}]_o$ was not significant ($P > 0.05$). Therefore, the results do not support a role for Mg_o^{2+} in Mg^{2+} extrusion from Mg^{2+}-loaded cells. Any slowing of the rate of $[Mg^{2+}]_i$ reduction in the presence of high $[Mg^{2+}]$ in the superfusate, could occur by reducing the electrochemical gradient available for Mg^{2+} extrusion through the putative Na^+/Mg^{2+} antiport or by inhibiting other Mg^{2+} efflux mechanism(s).

3.3.3 Effects of solutions on the membrane potential

Since the rates of Mg^{2+} reduction were measured in Ca^{2+}-free conditions and because of the possible electrogenicity of the putative Na^+/Mg^{2+} antiport, it was important to assess the membrane potential under conditions used in this study.

The membrane potential of quiescent ventricular myocytes initially bathed in normal Tyrode was measured using either high resistance (sharp) microelectrodes (10 – 24 MΩ) or patch microelectrodes (1.5 – 5 MΩ). The membrane potential in normal Tyrode was -74 ± 2.9 mV (range –95 to –55, n = 14).

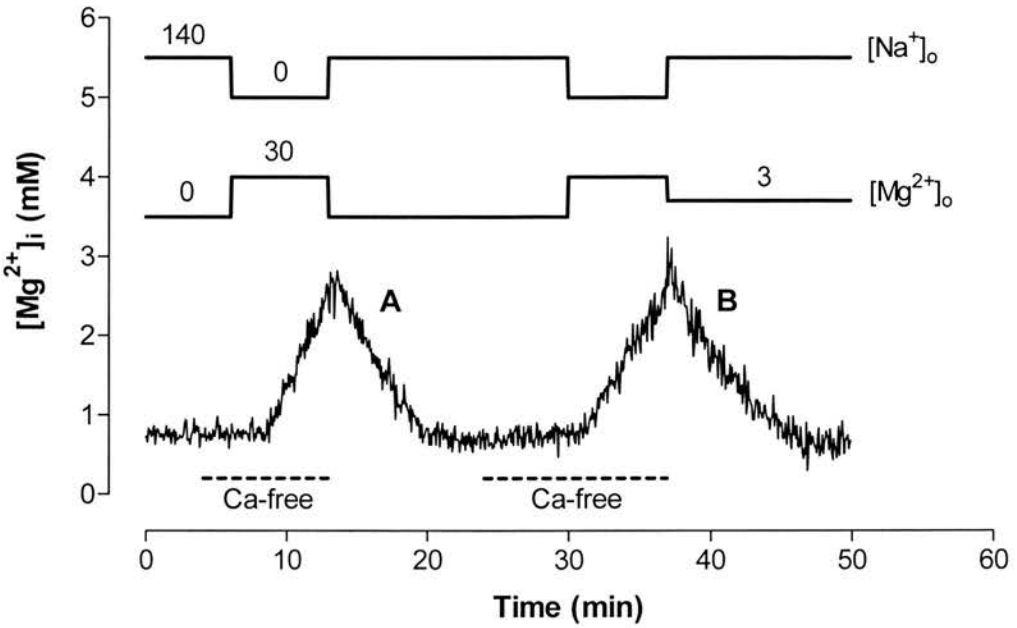

Figure 3.6. **Mg^{2+}-dependence of $[Mg^{2+}]_i$ reduction**

A dual Mg^{2+}-loading protocol in which $[Mg^{2+}]_i$ reduction was tested under two conditions: Mg^{2+}-free **(A)** and 3 mM $[Mg^{2+}]_o$ **(B)** Tyrode. Steps in bars on top represent the solution change and numbers are the concentrations in mM. $[Ca^{2+}]_o$ is 1 mM unless indicated otherwise.

On removal of external Ca^{2+}, there was an initial large depolarisation, which partially recovered to more negative values within 2-3 minutes (Figures 3.6 A & B). During superfusion with Ca^{2+}-free Tyrode solution, the membrane potential stabilised at a depolarised value of –38.0 ± 4.2 mV (range –67 to –20, n = 14); this depolarisation was statistically significant ($P < 0.05$).

Effect of Ca^{2+}-free, 5 mM [Mg^{2+}] Tyrode on the membrane potential

As mentioned above removal of Ca^{2+} from Tyrode solution resulted in significant depolarisation of the cell. However, if at the same time the concentration of another divalent cation, such as Mg^{2+} or Mn^{2+} is raised in the bathing solution, the depolarising effect of Ca^{2+} removal is attenuated to some extent (Deitmer & Ellis, 1978). Increasing [Mg^{2+}] in Ca^{2+}-free Tyrode from 1 to 5 mM caused the membrane potential to recover to –59 ± 1.3 mV (range –60 to –55, n = 4) (Figure 3.7A).

Effect of Ca^{2+}-free, Na^{+}-free, 5 mM [Mg^{2+}] on the membrane potential

In initial studies using the methods of Handy *et al.* (1996), Mg^{2+}-loading was achieved using a Na^{+}- and Ca^{2+}-free medium containing 5 mM [Mg^{2+}]. The effect of this solution on the membrane potential was assessed (Figure 3.7B). On changing to the loading solution the membrane potential stabilised at values close to the resting membrane potential normal Tyrode (–64.5 ± 2.6 mV; range –72 to –60, n = 4).

In conclusion, the depolarisation observed during superfusion with the Ca^{2+}-free Tyrode is significantly reduced when myocytes are superfused with the high [Mg^{2+}], Na^{+}-free loading solution. This restores the membrane potential close to the resting value in normal Tyrode. In later experiments $[Mg^{2+}]_o$ was increased to 30 mM to achieve better loading of cells with Mg^{2+}. Although the effect of this solution on the membrane potential was not examined in the present study, it would be expected to have better protective effects against cell depolarisation.

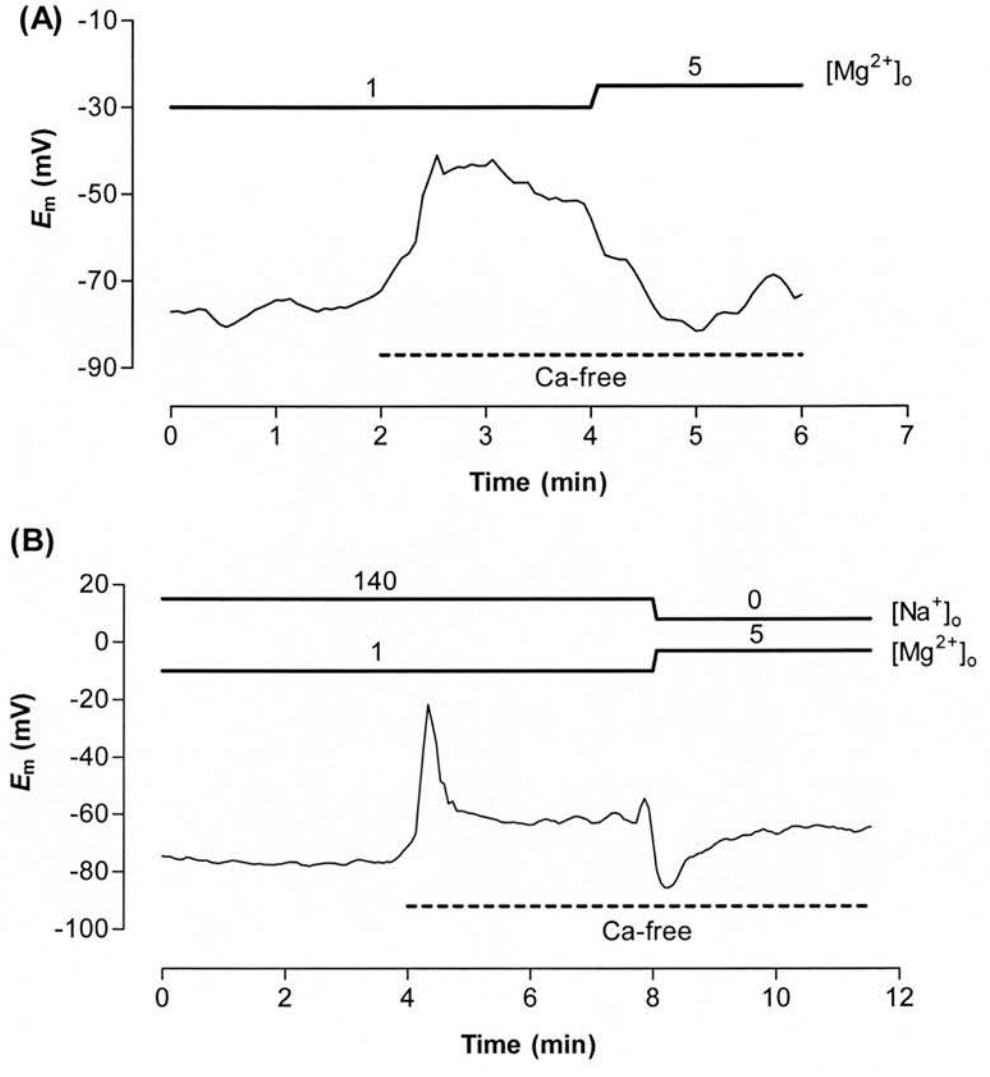

Figure 3.7. **Effect of Ca^{2+} removal and high $[Mg^{2+}]_o$ on the membrane potential**

(A) Membrane potential recording from a quiescent ventricular myocyte using a 5 MΩ patch pipette. The recording was carried out in the whole-cell configuration of the patch clamp technique. $[Na^+]_o$ was 140 mM throughout. On removal of external Ca^{2+}, the cell depolarised to approximately –40 mV. Increasing $[Mg^{2+}]_o$ from 1 to 5 mM restored the membrane potential to about –80 mV. **(B)** The cell transiently depolarised to about –20 mV on removal of external Ca^{2+}, but recovered to about –60 mV within 1 minute. On raising $[Mg^{2+}]_o$ to 5 mM while simultaneously removing external Na^+ (replaced with TMA), there was a rapid transient hyperpolarisation before the membrane potential stabilised at about –65 mV.

3.3.4 Interference by Ca^{2+} on mag-fura-2 fluorescence signal

Most if not all the current Mg^{2+} indicators are variants of Ca^{2+} indicators in which the structure of the Ca^{2+} chelator BAPTA, an aromatic analogue of the Ca^{2+}-sensitive chelator EGTA, is replaced by a triacetic acid analogue (e.g. Mason, 1999). Mag-fura-2 and the other Mg^{2+} indicators respond to Mg^{2+} concentrations in the range of about 0.1 to 10 mM (e.g. Mason, 1999). However, they also respond to high levels of intracellular Ca^{2+}. The dissociation constant of the Mg^{2+}-[mag-fura-2] complex is 1.5 mM, while that for the Ca^{2+}-[mag-fura-2] complexation is 53 μM (Raju *et al.*, 1989). The fluorescence signal measured from mag-fura-2-loaded myocytes was assumed to originate from the binding of cytosolic Mg^{2+} to the dye. However, due to the higher affinity of mag-fura-2 for Ca^{2+} in the micromolar range, significant increase in $[Ca^{2+}]_i$ during the experimental protocols used in this study could lead to interference by Ca_i^{2+} with the fluorescence signal measured from mag-fura-2-loaded myocytes.

To explore this possibility, experiments were designed to (1) obtain information on the magnitude of change in $[Ca^{2+}]_i$ during a typical Mg^{2+}-loading protocol, and (2) to investigate whether such change in $[Ca^{2+}]_i$ affects $[Mg^{2+}]_i$ as determined using mag-fura-2. The effect of Mg^{2+} loading on $[Ca^{2+}]_i$ was investigated by loading myocytes with the Ca^{2+}-sensitive indicator fura-2 as the AM ester. Cells were then subjected to a typical Mg^{2+} loading protocol. Figure 3.8A shows one such experiment. The cell was first superfused with normal Tyrode for at least 10 minutes (only 3 minutes is shown in Figure 3.8A) during which the fura-2 fluorescence ratio, *R*, remained unchanged at about 0.23, even after removing Ca^{2+} from the superfusate. A slight and slow increase in *R* was observed on increasing $[Mg^{2+}]_o$ from 1 to 30 mM in the absence of Ca^{2+} and Na^+ (loading solution). This increase continued over 10 minutes but stabilised after returning to the Ca^{2+}-free Tyrode. A larger transient rise in *R* was observed only on re-addition of Ca^{2+}. That transient began to recover within 3 minutes. *R* increased in the loading solution by a maximum of 0.02 and 0.04 from baseline values in normal Tyrode (n = 2, 2 hearts).

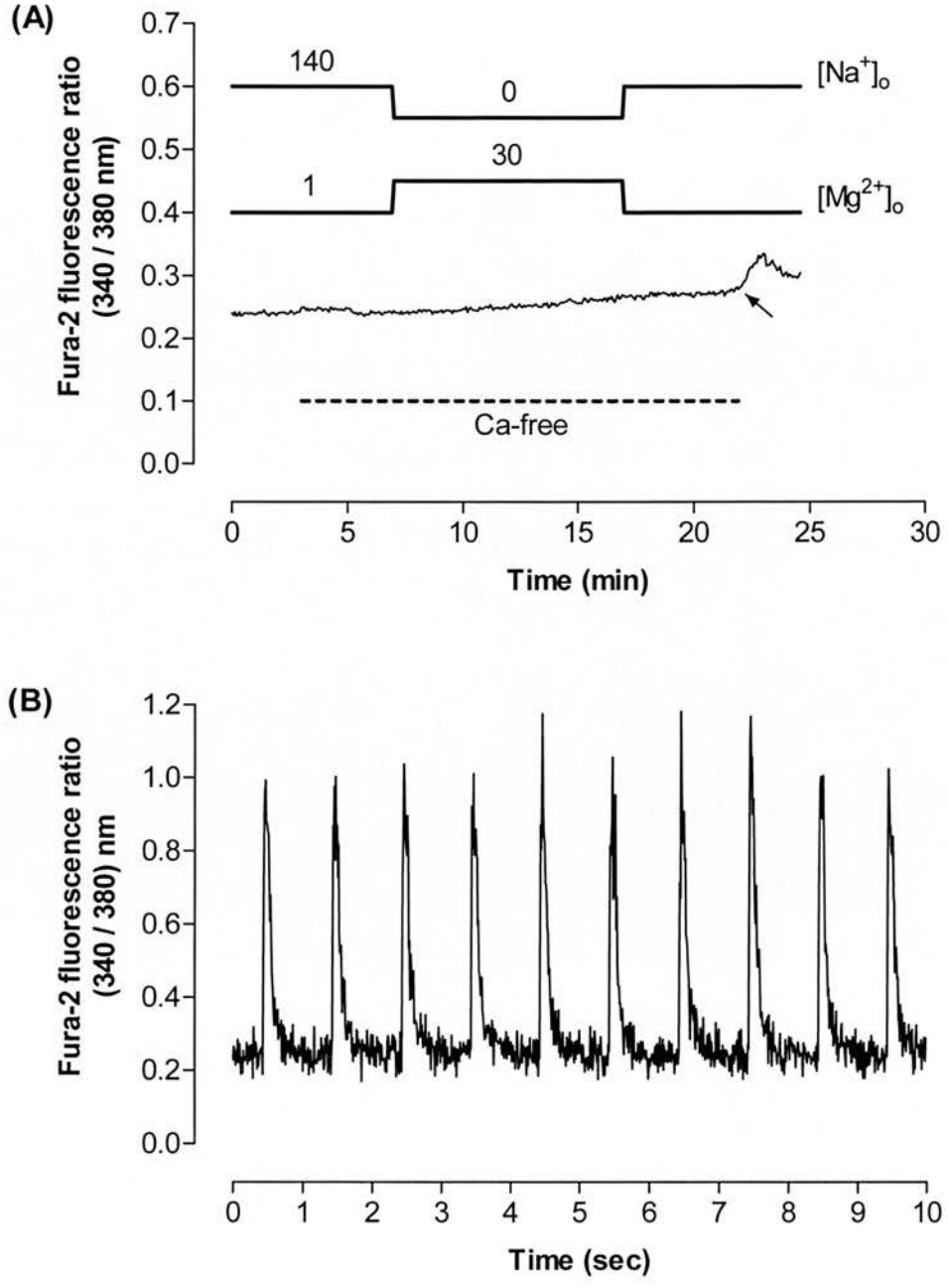

Figure 3.8. **Changes in $[Ca^{2+}]_i$ during the Mg^{2+}-loading protocol**

(A) Original recording from a myocyte loaded with fura-2 AM ester. The cell was subjected to a typical Mg^{2+}-loading protocol while quiescent. Changes in *R* were small during the Mg^{2+}-loading protocol. However, a larger transient rise (arrow) was observed only on re-addition of Ca^{2+} to the superfusate. That increase began to recover within less than 3 minutes. **(B)** Ca^{2+} spikes from the same myocyte, bathed in normal Tyrode at 37 °C, and stimulated to contract at a rate of 1 Hz. The cell was stimulated for at least 2 minutes before recording was started.

Since the change in R calculated from fura-2 fluorescence was not calibrated in order to determine change in $[Ca^{2+}]_i$, an alternative method was used to obtain information on the $[Ca^{2+}]_i$ during these experiments. This was achieved by electrically stimulating the same cell to contract prior to starting the Mg^{2+} loading protocol. The cell was stimulated to contract at a rate of 1 Hz in normal Tyrode. Contraction of myocytes was accompanied by a transient rise in R (Figure 3.8B) that averaged 0.83 ± 0.04 following subtraction of baseline R (mean of 120 transients from 2 cells obtained from 2 hearts). Since resting $[Ca^{2+}]_i$ in quiescent cardiac myocytes is approximately 0.1 μM and peaks at about 1 μM during the action potential, then the 0.83 increment increase in R corresponds roughly to 0.9 μM increase in $[Ca^{2+}]_i$. Although this calculation is approximate, it does provide a rough guide that can be used to obtain information on the increase in $[Ca^{2+}]_i$ during the Mg^{2+}-loading protocol described above (Figure 3.8A). It therefore seems that a maximum increase in R in the loading solution of less than 0.1 is unlikely to be the result of a large rise in $[Ca^{2+}]_i$.

The information obtained in the above experiments can be utilised to determine whether an increase $[Ca^{2+}]_i$, up to about 1 μM, affects $[Mg^{2+}]_i$ determined using mag-fura-2. To investigate the likelihood of such interference, myocytes, loaded with the AM ester of mag-fura-2 and bathed in normal Tyrode, were electrically stimulated to contract at a rate of 1 Hz. Cell contraction should be accompanied by an transient increase in $[Ca^{2+}]_i$ from its resting level of ~ 0.1 μM to ~ 1 μM. Figure 3.9 shows the averaged results from 3 such experiments. The figure depicts changes in $[Mg^{2+}]_i$ during a single action potential (average of 120 seconds). Despite the expected rise in $[Ca^{2+}]_i$ during contraction, $[Mg^{2+}]_i$ remained at about 0.8 mM and did not follow the typical pattern of Ca^{2+} spikes. To illustrate this further, a trace showing a typical Ca^{2+} spike (recorded in a different myocyte loaded with fura-2 AM ester) was superimposed on the $[Mg^{2+}]_i$ trace.

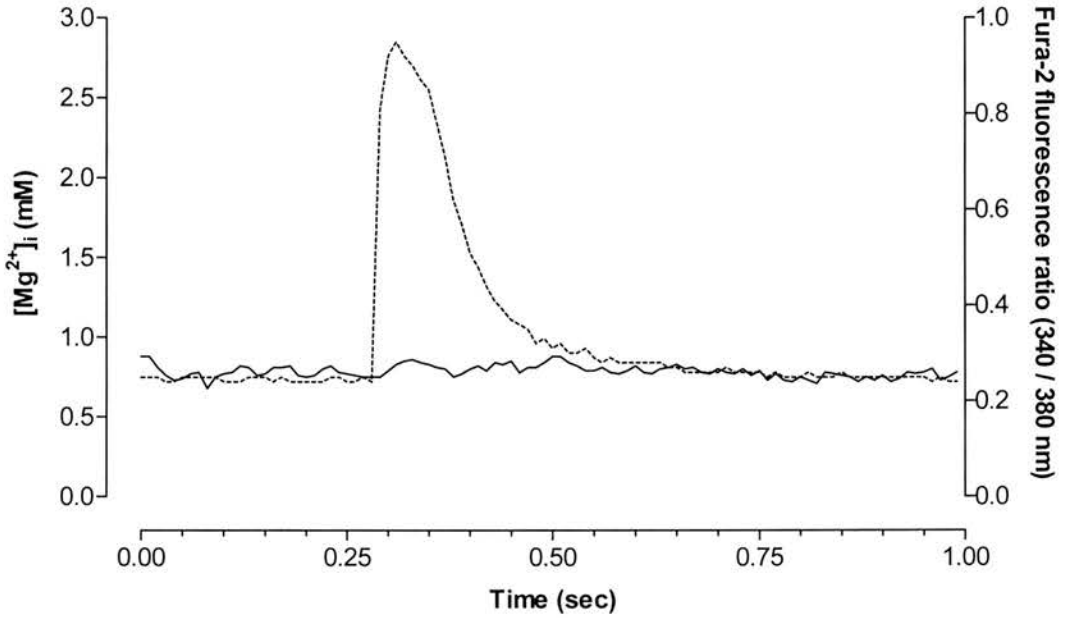

Figure 3.9. **Effect of Ca^{2+} spikes during action potentials on mag-fura-2 fluorescence**

A 120-second average of changes in $[Mg^{2+}]_i$ measured from 3 cells loaded with mag-fura-2 AM ester (solid trace), and stimulated to contract at a rate of 1 Hz in normal Tyrode at 37 °C. $[Mg^{2+}]_i$ remained at around 0.8 mM throughout the duration of the action potential. Note that the fluorescence signal from mag-fura-2 did not follow the characteristic pattern of Ca^{2+} spikes during action potentials (superimposed dotted trace), indicating lack of interference by changes in $[Ca^{2+}]_i$ in the range of ~ 0.1-1.0 μM, expected during the action potential, on mag-fura-2 fluorescence. Data points for both traces were sampled at a rate of 100 data points/sec.

In summary, the experiment shown in Figure 3.8 suggests that there is no substantial increase in $[Ca^{2+}]_i$ during the experimental protocol used to increase $[Mg^{2+}]_i$ above resting levels. A transient increase in $[Ca^{2+}]_i$ is expected on re-addition of Ca^{2+} to the superfusate following a period of Ca^{2+}-free superfusion. The experiments also suggest that increases in $[Ca^{2+}]_i$ up to 1 μM – for example during an action potential – had no measurable effect on $[Mg^{2+}]_i$ when determined using mag-fura-2. Therefore, it can be concluded that the fluorescence measured in mag-fura-2-loaded myocytes reflects to a large part, at least under the experimental protocols used in the present experiments, changes in $[Mg^{2+}]_i$.

3.3.5 Effect of changes in pH_i on $[Mg^{2+}]_i$

As described before, increasing $[Mg^{2+}]_i$ was achieved by removal of Na^+ and Ca^{2+} from the external medium in the presence of 30 mM $[Mg^{2+}]_o$. It is well established that removal of Na^+ also produces cellular acidification, mainly via inhibition of sarcolemmal Na^+/H^+ exchange (e.g. Ellis & MacLeod, 1985). It has also been suggested that changes in pH_i modulate $[Mg^{2+}]_i$ since Mg_i^{2+} and protons may share common intracellular binding sites (Freudenrich *et al.*, 1992a; Freudenrich *et al.*, 1992b; Silverman *et al.*, 1994). In order to examine the effect of alterations in pH_i on $[Mg^{2+}]_i$, cellular acidification was produced by (1) NH_4Cl prepulse method and (2) exposure to solutions containing 15 mM propionic acid. Exposure to NH_4Cl induces a transient intracellular alkalinisation followed by a rapid acidification on washout. In the case of propionic acid, the situation is reversed; initial acidification is followed by transient alkalinisation on removal of the acid.

Effect of NH_4Cl prepulse on $[Mg^{2+}]_i$

Superfusing cells with normal Tyrode containing 15 mM NH_4Cl (added to normal Tyrode without correction to osmolarity) resulted in a small decrease in $[Mg^{2+}]_i$ over a period of 7 minutes (0.08 ± 0.01 mM, n = 3) (Figure 3.10A). Upon removal of NH_4Cl a small transient increase in $[Mg^{2+}]_i$ accompanied the expected transient cytosolic acidification (0.05 ± 0.01 mM, n = 3). This increase in $[Mg^{2+}]_i$ recovered within 2-3 minutes to the control level in normal Tyrode.

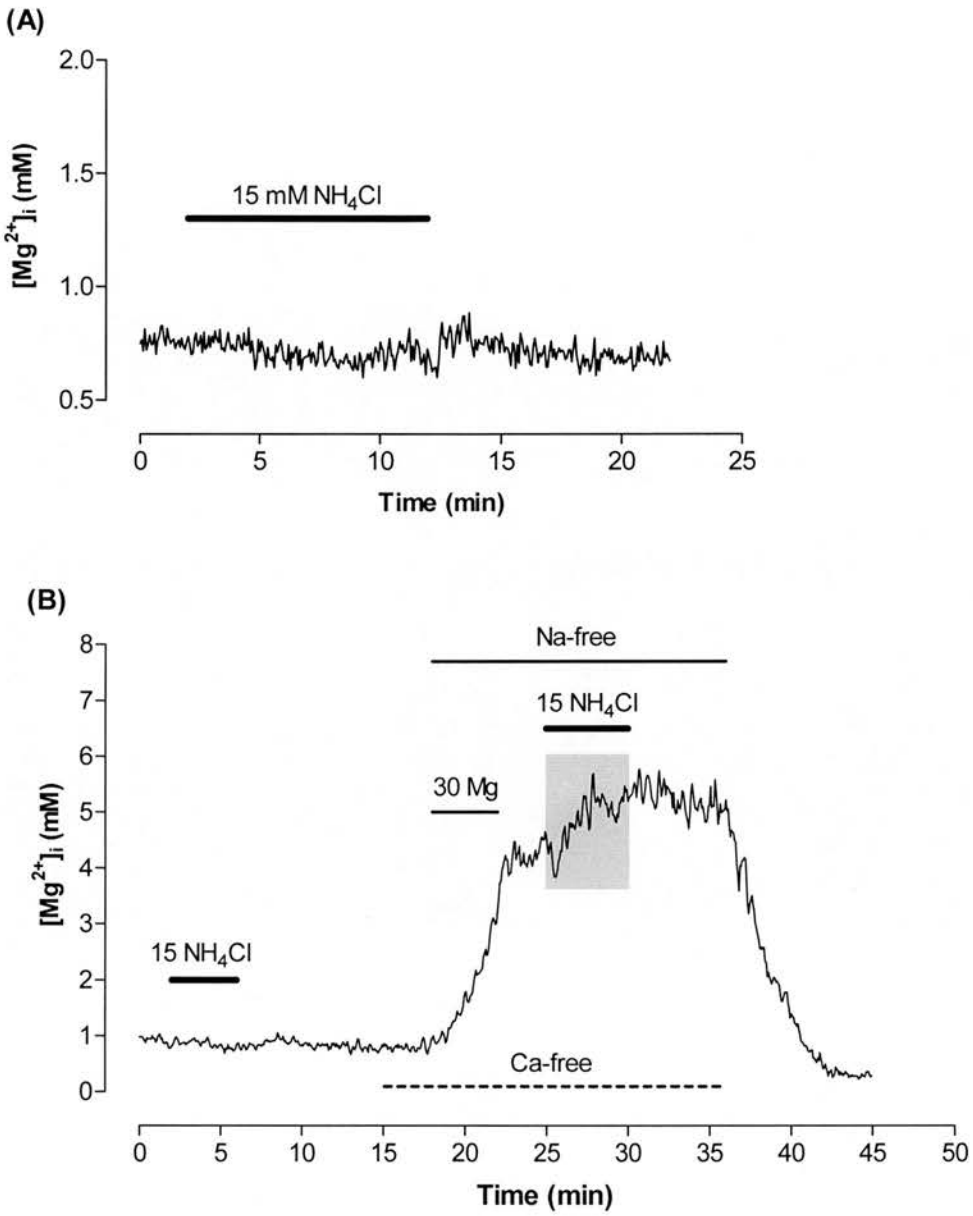

Figure 3.10. **Effect of NH_4Cl prepulse on $[Mg^{2+}]_i$**

(A) An average of 3 identical experiments from myocytes loaded with mag-fura-2 AM ester. A small decrease in $[Mg^{2+}]_i$ was observed on application of 15 mM NH_4Cl. Subsequent removal of NH_4Cl caused a transient increase in $[Mg^{2+}]_i$ that recovered within 3 minutes. **(B)** NH_4Cl application and subsequent removal at baseline $[Mg^{2+}]_i$ produced an effect similar to (A). However, application of NH_4Cl at elevated $[Mg^{2+}]_i$ produced a rise in $[Mg^{2+}]_i$ (shaded area), followed by a small decrease on washout.

The same protocol was repeated on cells where $[Mg^{2+}]_i$ has been raised. Figure 3.10B is one of 4 similar experiments in which initial exposure of Mg^{2+}-loaded cells to 15 mM NH_4Cl resulted in a rise in $[Mg^{2+}]_i$ (1.12 ± 0.48, n = 4). Subsequent removal of NH_4Cl had little effect on $[Mg^{2+}]_i$, although a small decrease was observed.

In summary, only small transient changes in $[Mg^{2+}]_i$ were observed in cells subjected to 15 mM NH_4Cl prepulse at baseline or high $[Mg^{2+}]_i$. Therefore, it is highly unlikely that the observed increase in $[Mg^{2+}]_i$ using the Mg^{2+}-loading protocol described earlier is the result of interference by protons on either mag-fura-2 binding affinity to Mg^{2+} or the displacement of Mg^{2+} from intracellular binding sites by protons.

Effect of propionic acid on $[Mg^{2+}]_i$

These experiments were carried out to investigate further the effect of changes in pH_i on intracellular Mg^{2+}. 15 mM propionic acid, added to normal Tyrode (without correction to osmolarity), caused a negligible increase in $[Mg^{2+}]_i$ when applied at baseline $[Mg^{2+}]_i$ (Figure 3.11A). In cells where $[Mg^{2+}]_i$ has been increased to around 4 mM, propionic acid caused a more significant increase in $[Mg^{2+}]_i$ that recovered to control levels in approximately 5 minutes (Figure 3.11B); mean increase in $[Mg^{2+}]_i$ was 1.60 mM (range 1.40 - 1.80, n = 2).

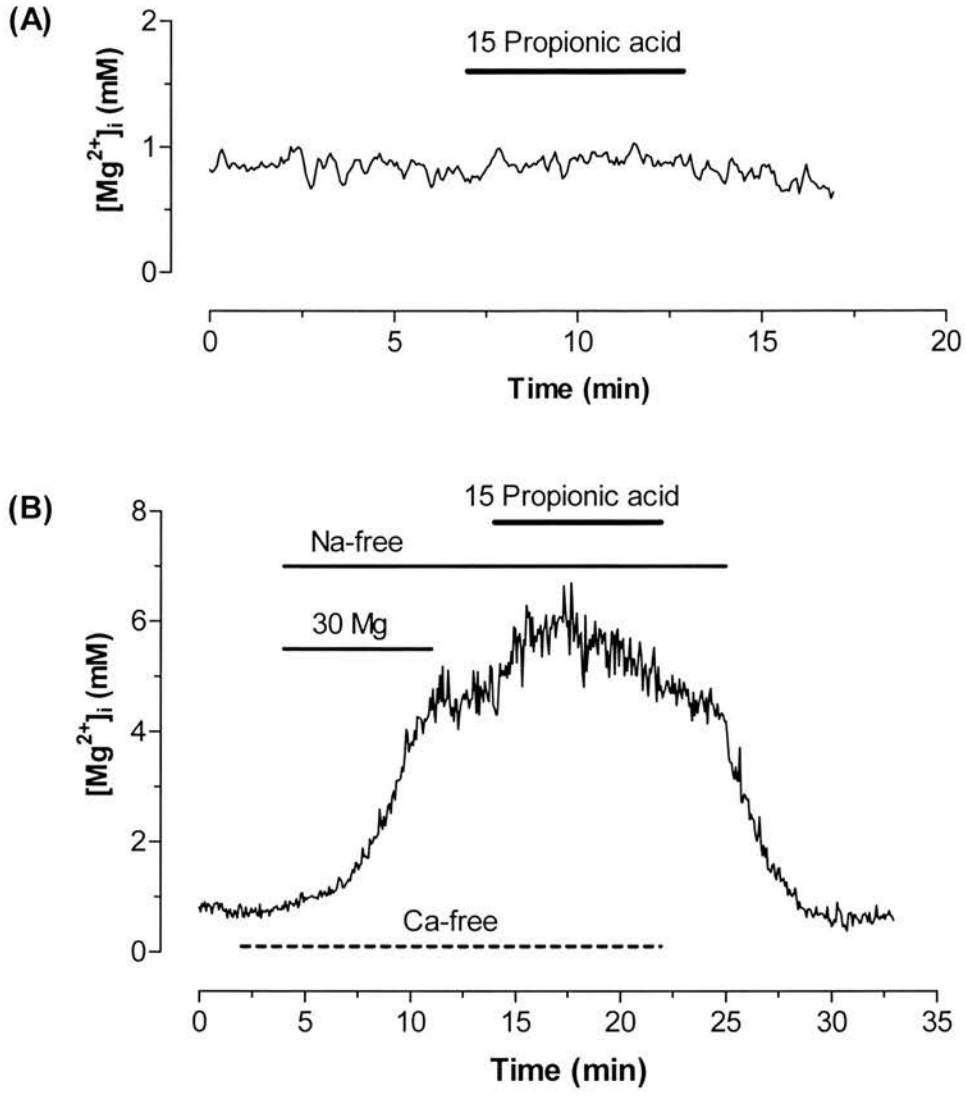

Figure 3.11. **Effect of propionic acid prepulse on $[Mg^{2+}]_i$**

All solutions are normal Tyrode unless otherwise indicated. **(A)** Addition of 15 mM propionic acid (added to normal Tyrode) at resting $[Mg^{2+}]_i$ resulted in a small increase in $[Mg^{2+}]_i$. **(B)** One of two similar experiments in which addition of propionic acid at elevated $[Mg^{2+}]_i$ (~ 4.5 mM) for 10 minutes caused an initial increase in $[Mg^{2+}]_i$ by around 1.5 mM, followed by recovery to pre-addition value. On removal of propionic acid, $[Mg^{2+}]_i$ continued to decline and stabilised around the "clamped" $[Mg^{2+}]_i$. $[Mg^{2+}]_i$ fully recovered to baseline on changing the solution to normal Tyrode.

3.4 DISCUSSION

The aim of this study was to examine the Na^+-dependence of $[Mg^{2+}]_i$ transport in quiescent rat ventricular myocytes. In this chapter the Na^+-dependence of $[Mg^{2+}]_i$ reduction was addressed. The results show that reduction of $[Mg^{2+}]_i$ in cells pre-loaded with Mg^{2+} was dependent on the presence and concentration of Na^+ in the external medium, where increasing $[Na^+]_o$ increases the rate of $[Mg^{2+}]_i$ reduction. These results are suggestive of the presence of a Na^+-dependent Mg^{2+} extrusion mechanism in rat heart. Aspects of the experiments presented in this chapter in addition to the methods used to obtain the myocytes and load them with fluorescent dye, will now be discussed.

3.4.1 Cell isolation

The most significant insult to the heart probably occurs during the time of stoppage of myocardial circulation, i.e. between removal of the heart and the inception of retrograde perfusion in a Langendorff fashion. It was therefore crucial to minimize the ischemic injury to the myocardium by shortening, as much as possible, the period of myocardial ischemia that occurs during complete cessation in coronary circulation. The average time between removal of the heart and canulation of the aorta was approximately 15 minutes, with the heart cooled in an ice-cold cardioplegic solution to prevent beating. This is crucial to prevent energy waste and cellular Na^+ loading via action potentials, since cooling most likely inactivates the Na^+/K^+ pump.

The damaging effects on the myocardium by ischemia results primarily from an increase in $[Ca^{2+}]_i$, secondary to an increase in $[Na^+]_i$ during ischemia. $[Na^+]_i$ has been found to increase during myocardial ischemia (Pike *et al.*, 1990; van Echteld *et al.*, 1991; Murphy *et al.*, 1991b) due to reduced capability of the sarcolemmal Na^+/K^+ ATPase to extrude Na^+ (Cross *et al.*, 1995), while Na^+ influx through the Na^+ channels continues (Van Emous *et al.*, 1997). Furthermore, ischemic acidosis may promote Na^+ entry via Na^+/H^+ exchange (Tani & Neely, 1989). Upon reperfusion of the myocardium $[Na^+]_i$ is expected to decrease rapidly (Van Emous *et al.*, 1998).

This reduction takes place mainly through the Na^+/K^+ ATPase that becomes fully functional immediately upon reperfusion, restoring $[Na^+]_i$ to pre-ischemic levels, although $[Na^+]_i$ recovery is marginally counteracted by enhanced Na^+ influx through the Na^+/H^+ exchanger (Van Emous *et al.*, 1998).

Current understanding attributes the events that take place during ischemia to a substantial reduction in the rate of ATP supply due to cessation of oxidative metabolism (Kammermeier *et al.*, 1982) and subsequent depletion of cellular glycogen stores (Fiolet *et al.*, 1984), which leads to a reduction in the Na^+/K^+- and Ca^{2+}-ATPase's capacities. On reperfusing the myocardium with an oxygen-rich medium, re-energisation of the tissue leads to contracture and possibly death of the cells.

Hypothermia is believed to have protective effects on the myocardium, mainly by slowing depletion of the high-energy phosphate stores (e.g. Piper, 2000). Therefore, Na^+ and Ca^{2+} overloading is likely to be reduced in the present study since the heart was kept in an ice-cold cardioplegic solution following removal.

It is crucially important to obtain a good perfusion of the heart. Poor perfusion of the myocardium was almost always associated with a poor cell yield. Perfusing the heart with the collagenase-containing solution appears to increase aortic pressure (Levi *et al.*, 1992) which possibly reflects vasoconstriction of the coronary arteries. One way to improve perfusion was to re-circulate the perfusate by passing the heart effluent back into the aorta. Levi *et al.*, (1992) found that by re-circulating the heart effluent, the aortic pressure decreases, suggesting vasodilatation of the coronaries. In addition, heparinisation of the animals prior to removal of the heart should also reduce the risk of blood clot development in the coronary arteries. Using these measures, namely heparinisation, cooling of the heart, shortening the period of ischemia, and recirculation of the heart effluent during Langendorff perfusion, should minimize injury to the myocardium. Once the cells were isolated, gradual introduction of Ca^{2+} in the bathing medium was necessary to prevent Ca^{2+} overloading. This was especially important since increased $[Ca^{2+}]_i$ might lead to a secondary increase in

$[Mg^{2+}]_i$, and therefore offsetting resting $[Mg^{2+}]_i$ to higher levels. Ca^{2+} overloading and the possible occurrence of the calcium paradox should also be reduced by the inclusion of taurine in the cell isolation solution. Taurine is believed to protect the heart from the adverse effects of excessive Ca^{2+} levels (Satoh, 1994). Taurine may both directly and indirectly help regulate $[Ca^{2+}]_i$ by modulating the activity of the voltage dependent Ca^{2+} channels, and by regulation of Na^+ channels. Taurine also acts on many other ion channels and transporters. Therefore, its action can be quite non-specific (Satoh & Sperelakis, 1998). The presence of taurine in adequate amounts significantly reduces the calcium-induced myocardial damage, probably by interaction between taurine and membrane proteins (Kramer *et al.*, 1981).

High yields of quiescent and Ca^{2+}-tolerant myocytes were obtained using this method. Healthy cells maintained a rod shape with clear cross-striation and well defined edges for up to 8 hours after isolation.

3.4.2 Effect of solutions on the membrane potential

Resting membrane potential of quiescent myocytes bathed in normal Tyrode measured in this study was –74 ± 2.9 mV (range –95 to –55, n = 14), slightly more positive than values obtained by Mubagwa *et al.* (1997) for rat ventricular myocytes at 37 °C (–82 ± 1.9 mV) and for guinea-pig ventricular myocytes (–82 ± 2.4 mV) (Levi, 1991) and closer to the value of –78 mV reported for isolated ferret ventricular trabeculae (Chapman *et al.*, 1983). It must be noted that these workers measured the resting membrane potential in solutions that contained 5.4 mM $[K^+]_o$, whereas 6 mM was used in the present experiments.

Removal of Ca^{2+} from normal Tyrode resulted in a significant depolarisation of cells (mean 36 ± 2.1 mV). This depolarisation is probably due to voltage-dependant Na^+ influx via L-type Ca^{2+}-channels in Ca^{2+}-free Tyrode (Chapman *et al.*, 1991) and/or influx through non-selective cation channel(s) normally blocked by physiological concentrations of divalent cations (Ca^{2+} and Mg^{2+}) (Mubagwa *et al.*, 1997). Tunstall *et al.* (1986), using ^{22}Na tracer, have shown that superfusing trout ventricular muscle preparations with nominally Ca^{2+}-free (10 nM) and Mg^{2+}-free Ringer solution

containing 137 mM [Na^+] at 20 °C results in an increase in $[Na^+]_i$ from a baseline concentration of 15 mM (kg wet weight)$^{-1}$ to 32 mM (kg wet weight)$^{-1}$. This increase in $[Na^+]_i$ occurred following 40 minutes perfusion, and reached ~ 60 mM (kg wet weight)$^{-1}$ after 60 minutes. This rise in $[Na^+]_i$ was also associated with the development of spontaneous and prolonged action potentials.

An increase in membrane permeability to Na^+ on removal of divalent cations from the bathing medium has also been suggested by Van Echteld *et al.* (1998) who used ^{23}Na NMR spectroscopy to monitor $[Na^+]_i$ in isolated, perfused rat hearts. They reported almost a ten-fold increase in $[Na^+]_i$ (from 7.3 ± 3.7 mM to 71.3 ± 15.6 mM) following perfusion with Ca^{2+}- and Mg^{2+}-free perfusate for 30 minutes. The authors found that addition of 1 mg/l verapamil completely prevented the rise in $[Na^+]_i$ (see e.g. Fig. 3 in van Echteld *et al.* 1998).

In the present study, the membrane potential in Ca^{2+}-free, 1 mM [Mg^{2+}] Tyrode stabilised around –38 mV. This was more negative than values obtained for Ringer solution lacking Mg^{2+} in frog atrial trabeculae (–10 mV) (Tunstall *et al.*, 1986). Switching from Ca^{2+}-free Tyrode to a similar solution but containing 5 mM Mg^{2+} restored the membrane potential to values close to the resting values in normal Tyrode. This is likely due to block by Mg^{2+} of L-type Ca^{2+}-channels (Tunstall *et al.*, 1986), which would attenuate further Na^+ entry. This may not be the only route for the block by divalent cations such as Mg^{2+}, as suggested by experiments carried out by Mubagwa *et al.* (1997). They have demonstrated that removing extracellular divalent cations increases membrane non-selective conductance to monovalent cations that could not be blocked by the L-type channel blocker, nifedipine. Chapman *et al.* (1986) found that reduction of $[Mg^{2+}]_o$ from 1 to 0.25 mM, in a Ca^{2+}-free solution, results in a five-fold increase in $[Na^+]_i$ in sheep Purkinje fibres. Moreover, Ca^{2+} channels become more permeable to Na^+ ions in the absence of both Ca^{2+} and Mg^{2+} than in the absence of Ca^{2+} alone in the superfusate (Rodrigo & Chapman, 1991).

In the present study, changing from Ca^{2+}-free Tyrode to a solution in which Na_o^+ was totally replaced with TMA in an equimolar amount, and $[Mg^{2+}]_o$ was increased to 5 mM, restored the membrane potential close to its resting values in normal Tyrode (Figure 3.6B). The difference in the membrane potential in 5 mM $[Mg^{2+}]$, Ca^{2+}-free Tyrode compared to that in 5 mM $[Mg^{2+}]_o$, Ca^{2+}- and Na^+-free Tyrode was not significant (mean difference was 5.7 mV in the negative direction when TMA was used to replace Na_o^+, $P > 0.1$). Therefore, it appears that 5 mM $[Mg^{2+}]_o$ is sufficient to protect cells against Na^+-overload and subsequent depolarisation.

Since the Na^+-dependence of $[Mg^{2+}]_i$ reduction was investigated in this study by introducing various $[Na^+]_o$, ranging between 28 and 140 mM, in a Ca^{2+}-free medium containing 1 mM $[Mg^{2+}]$, the membrane potential is not expected to depolarise severely, and Na^+ influx through either L-type Ca^{2+} channels or other non-selective channels should be small.

3.4.3 Mag-fura-2 loading

Unfortunately it is not possible to limit the indicator mag-fura-2 to the cytosol. There is evidence that the dye, introduced as the AM ester also permeates other cellular compartments such as the mitochondria and the SR. Cellular fractioning of mag-indo-1-loaded rat ventricular myocytes showed that around 60% of the indicator is in the cytosol while the remaining 40% is localised in the mitochondria (Silverman *et al.*, 1994). However, the same authors also found that altering total cellular loading by incubating isolated myocytes with varying concentrations of mag-indo-1 AM ester for varying times had no clear effect on mitochondrial compartmentation. In another study, Hongo *et al.* (1994) estimated the percentage of mag-fura-2 in the cytosol of rat ventricular myocytes loaded in a similar fashion to that used in this study at around 84%. Mitochondrial matrix free Mg^{2+} concentration ($[Mg^{2+}]_m$) maintained by respiring heart mitochondria is around 0.8 mM (Rutter *et al.*, 1990), i.e. similar to cytosolic $[Mg^{2+}]$.

It is assumed that the fluorescence measured here reflects changes in cytosolic $[Mg^{2+}]$, since a major fraction of mag-fura-2 seems to be localised in the cytosol. In

addition, factors known to cause significant changes in mitochondrial (discussed below) or total cell magnesium concentrations (mainly hormonal signals (Romani & Scarpa, 1992b) or uncouplers (Jung & Brierley, 1994)) were avoided.

3.4.4 Calibration of mag-fura-2

$[Mg^{2+}]_i$ was obtained directly from an *in vitro* calibration curve (Figure 2.2). Under these conditions it is assumed that mag-fura-2 AM ester has been completely hydrolysed in the cytosol and that the chemically synthesised mag-fura-2 (free acid) used in the calibration and the intracellularly-generated mag-fura-2 have the same dissociation constant. Although this may not be entirely true all the time for all cell types, *R* for *in vivo* and *in vitro* calibration seem to agree within 10% (Raju *et al.*, 1989). To ensure the reliability of $[Mg^{2+}]_i$ values, calibration was repeated every 2-3 months to account for changes to optics and light source that may occur over time. Mag-fura-2 was also recalibrated on changing any part of the optics, such as the excitation filters or the dichroic mirror.

3.4.5 Resting $[Mg^{2+}]_i$

The resting $[Mg^{2+}]_i$ in myocytes bathed in normal Tyrode at 37 °C was 0.75 ± 0.05 mM (n = 77). This is within the reported range of 0.47 to 0.85 mM (Table 1.1). There was no detectable change in $[Mg^{2+}]_i$ on removal of Ca^{2+} from normal Tyrode. Similar findings were obtained by other workers (Hongo *et al.*, 1994; Handy *et al.*, 1996; Tashiro & Konishi, 2000).

3.4.6 Mg^{2+}-loading

It appears that the permeability of the sarcolemma of cardiac cells to Mg^{2+} is low. Previous attempts to increase $[Mg^{2+}]_i$ by increasing $[Mg^{2+}]$ and/or lowering $[Na^+]$ in basic solutions were not very successful (Fry, 1986; Quamme & Rabkin, 1990; Hall *et al.*, 1991; Freudenrich *et al.*, 1992a; Buri *et al.*, 1993; Silverman *et al.*, 1994). Elevation of $[Mg^{2+}]_i$ was only seen upon removal of both Na^+ and Ca^{2+} from the high $[Mg^{2+}]$ superfusate. Increasing $[Mg^{2+}]_o$ to 30 mM resulted in increases in $[Mg^{2+}]_i$ as high as 9 mM in some experiments (e.g. Figure 3.2).

The difference in the magnitude of increases in $[Mg^{2+}]_i$ between this study and the study carried out by Handy *et al.* (1996) may be accounted for by the presence of a greater inward electrochemical gradient for the downhill movement of Mg^{2+} across the sarcolemma. The electrochemical equilibrium potential for Mg^{2+} when $[Mg^{2+}]_o$ is 30 mM and $[Mg^{2+}]_i$ is 0.75 mM is +48 mV, compared to +24 mV when $[Mg^{2+}]_o$ is set to 5 mM. The increase in $[Mg^{2+}]_i$ in Ca^{2+}- and Na^+-free conditions observed in these experiments implies that both Ca^{2+} and Na^+ at normal extracellular concentrations inhibit or significantly attenuate any detectable increase in $[Mg^{2+}]_i$. It also means that Mg^{2+} probably enters through routes partially or completely blocked by external Ca^{2+} and Na^+.

3.4.7 Effect of changes in pH_i on $[Mg^{2+}]_i$

To determine whether pH_i changes affect $[Mg^{2+}]_i$, pH_i was manipulated by NH_4Cl or the propionic acid prepulse method. Application of 15 mM NH_4Cl is expected to increase pH_i by about 0.5 units (Bountra *et al.*, 1990; Ng *et al.*, 1993). The expected initial alkalinisation produced by NH_4Cl was accompanied by a slight decrease in $[Mg^{2+}]_i$ at baseline levels. Similar results were also obtained in chick cardiac myocytes (Freudenrich *et al.*, 1992b) and guinea pig ventricular myocytes (Buri *et al.*, 1993), while no change was observed in rat ventricular myocytes (Silverman *et al.*, 1994). Washout of NH_4Cl or addition of propionic acid should cause a transient cellular acidosis by approximately 0.7 pH units (Bountra *et al.*, 1990; Freudenrich *et al.*, 1992b). This was accompanied by a small transient increase in $[Mg^{2+}]_i$ that recovered in 2 to 3 minutes (Figures 3.10A & 3.11A). Buri *et al.* (1993) previously described a similar effect of NH_4Cl removal on fluorescence measured from either mag-fura-2- or mag-fura-5-loaded guinea pig ventricular myocytes. The changes in $[Mg^{2+}]_i$ are likely to be the result of changes in $[H^+]_i$, where an increase in $[H^+]_i$ (intracellular acidosis) displaces Mg^{2+} from common intracellular binding sites. In addition, secondary increases in $[Ca^{2+}]_i$ as a result of intracellular acidification may also participate in displacing Mg_i^{2+}.

There is considerable evidence for a competition between H^+, Ca^{2+} and Mg^{2+} for common intracellular binding sites. $[Ca^{2+}]_i$ decreases as pH_i is made alkaline in the

presence of NH_4Cl. It then increases during cellular acidosis brought about by NH_4Cl removal (Bers & Ellis, 1982; Vaughan-Jones *et al.*, 1983). These effects of changes in pH_i on $[Ca^{2+}]_i$ are believed to be mediated by competition between the H^+ and Ca^{2+} for common intracellular binding sites (Vaughan-Jones *et al.*, 1983; Ellis & MacLeod, 1985). Another possible mechanism may involve intracellular sodium (Kim & Smith, 1988), where cellular acidosis causes efflux of H^+ in exchange for Na_o^+ via the Na^+/H^+ exchanger. The consequent increase in $[Na^+]_i$ inhibits Na^+/Ca^{2+} exchange and thereby results in an increase in $[Ca^{2+}]_i$. The net effect of intracellular acidification is an increase in $[H^+]_i$ and $[Ca^{2+}]_i$, both of which might displace Mg^{2+}, resulting in an apparent increase in $[Mg^{2+}]_i$. It is unlikely that NH_4^+ directly interferes with the excitation spectra of mag-fura-2 or the complexation of $MgATP^{2-}$ (Freudenrich *et al.*, 1992b). Also, the NH_4^+-evoked changes in pH_i are unlikely to change the binding affinity of Mg^{2+} to mag-fura-2 as long as these changes occurred within the pH-insensitive range of mag-fura-2 (6.4 to 7.8) (Freudenrich *et al.*, 1992b), which is most probably the case. Application of NH_4Cl to cells where $[Mg^{2+}]_i$ has been raised to about 4 mM produced an increase in $[Mg^{2+}]_i$ (Figure 3.10B). However, this increase could be due to release of Mg^{2+} from the mitochondria following alkalinisation (Günzel el al., 1997). The authors suggest that intracellular alkalinisation in leech neurons stimulates the mitochondrial permeability transition pore (MTP), which results in Mg^{2+} release from the mitochondria.

The increase in $[Mg^{2+}]_i$ of around 1.5 mM seen on the application of 15 mM propionic acid at elevated $[Mg^{2+}]_i$ (Figure 3.11B) is difficult to explain. However, one possibility is significant intracellular acidification. A marked decrease in pH_i (less than 6.5) causes an increase in the concentration of cytosolic protonated ATP ($HATP^{3-}$), which has a much lower affinity to Mg^{2+} than ATP^{4-}, therefore Mg^{2+} is liberated from the $MgATP^{2-}$ complex (Lüthi *et al.*, 1999; Günzel & Schlue, 2000). Since cells were loaded with Mg^{2+} in Ca^{2+}-free conditions, pH_i changes are expected to be minimal (Ellis & MacLeod, 1985) and would not significantly alter ATP binding to Mg^{2+}. In summary, the changes in $[Mg^{2+}]_i$ caused by NH_4Cl or propionic acid prepulse method appear to be genuine, however, these changes were small, and even if such a shift in pH_i occurs in Ca^{2+}- and Na^+-free conditions, they cannot

account for the high $[Mg^{2+}]_i$ values observed in cells exposed to the Mg^{2+}-loading protocol.

3.4.8 Interference by $[Ca^{2+}]_i$

Loading cells with Mg^{2+} was carried out under Ca^{2+}-free conditions, and hence trans-sarcolemmal Ca^{2+} influx can be ruled out. This study also investigated the influence of electrically stimulating myocytes on mag-fura-2 fluorescence. Figure 3.9 shows that even when $[Ca^{2+}]_i$ is expected to increase to around 1 μM during cell contraction, $[Mg^{2+}]_i$ remained around baseline level, and the pattern of Ca^{2+} transients was not picked up by mag-fura-2 fluorescence, indicating that changes in Mg^{2+} have a different time course and magnitude. Similar results were also obtained for mag-indo-1-loaded rat ventricular myocytes (Silverman *et al.*, 1994). The small increase in fura-2 *R* on superfusing cells with the loading solution (Figure 3.8A), is most likely due to an increase in $[Ca^{2+}]_i$ secondary to cellular acidification on removal of Na^+ from the superfusate. It must be stressed that an increase in $[Ca^{2+}]_i$ per se would only displace a small amount of Mg^{2+} from common binding sites. To this end, and as far as displacement of Mg^{2+} bound to ATP is concerned, Lüthi *et al.* (1999) estimated that increasing $[Ca^{2+}]$ to 10 μM would only increase $[Mg^{2+}]$ by 0.02 mM. Therefore, the observed effect on fura-2 *R* of exposing cells to the Mg-loading protocol is possibly a combined effect of displacement of Ca_i^{2+} by Mg^{2+} and protons from shared binding sites.

3.4.9 Interference by the mitochondria

This study avoided conditions that have been suggested to promote mitochondrial Mg^{2+} mobilisation. These include noradrenaline, adrenaline and other *β*- and α-adrenergic receptors agonists that result in Mg^{2+} efflux from cardiac and liver cells (Romani & Scarpa, 1990; Rodrigo & Chapman, 1991; Romani *et al.*, 1991). The authors suggested that increasing cytosolic cAMP level either directly through stimulation of adenylate cyclase by forskolin or addition of permeant cAMP analogues or indirectly via stimulation of *β*-adrenergic receptors by noradrenaline, adrenaline or by drugs like isoprenaline (β_2-adrenergic receptors agonist) results in significant cellular Mg^{2+} efflux. The authors also suggested that cAMP in turn

modulates the transport properties of adenine nucleotide translocase (ANT) in the inner membrane of the mitochondria allowing it to bind $MgATP^{2-}$ (instead of ATP) in exchange for cytosolic ADP (Fig. 1 in Romani & Scarpa (2000)). However, evidence for such conformational change is still lacking. ANT has also been shown to exhibit properties related to the sudden increase in the inner membrane permeability, known as permeability transition (PT) due to opening of the MTP (Woodfield *et al.*, 1998). MTP is defined as "a voltage-dependent cyclosporin A (CsA)-sensitive, high conductance inner membrane channel of unknown molecular structure" (Bernardi, 1999).

The consequences of MTP opening are dramatic. In its open state, it leads to an increase in the permeability of the inner membrane to solutes of molecular mass up to 1500 Da, collapse of the proton gradient, loss of matrix adenine and pyridine nucleotides and inhibition of ATP synthesis. In its full open state, the diameter and conductance of the MTP, studied in isolated liver mitochondria, can reach 3 nm (Massari & Azzone, 1972) and 1.3 nanosiemens respectively (Szabo & Zoratti, 1991). Detailed analysis of the PT is beyond the scope of this thesis. However, since MTP opening can result in loss of mitochondrial Mg^{2+} and Ca^{2+} (Riley & Pfeiffer, 1985) and therefore influence $[Mg^{2+}]_i$ directly or indirectly, factors that promote or inhibit MTP opening are of particular importance. Elevations in free mitochondrial matrix Ca^{2+} ($[Ca^{2+}]_m$) can lead to pore opening, an effect which can be counteracted by Mg^{2+} in a competitive manner, suggesting interactions at common binding site(s) (Haworth & Hunter, 1979). An increase in $[Ca^{2+}]_m$ is not expected in the present study since both Mg^{2+} loading and recovery were carried out in Ca^{2+}-free conditions, and an increase in mitochondrial free matrix Mg^{2+} ($[Mg^{2+}]_m$), which may occur following Mg^{2+}-loading, is likely to inhibit pore opening, in the absence of other factors known to promote permeability transition (PT), such as an increase in matrix pH (Bernardi *et al.*, 1992) or partial depolarisation of the inner membrane (Petronilli *et al.*, 1993).

It must be stressed that pore opening is under the influence of various inputs of stimulatory and inhibitory factors acting simultaneously, and whether PT will occur

under a given *in vivo* condition is not easy to predict. Evidence suggests the Mg^{2+} efflux from mitochondria has a pathway(s) distinctive from uptake. One possible pathway for Mg^{2+} efflux is through a Mg-ATP/P_i exchange mechanism. However, such a mechanism does not seem to operate in heart mitochondria (Aprille, 1993). A role for P_i in Mg^{2+} efflux has also been suggested in isolated respiring rat heart mitochondria, where increasing matrix P_i was found to stimulate Mg^{2+} loss, possibly by buffering matrix ADP, an inhibitor of PT, and protons. The combined effect of removal of ADP inhibition and elevation of pH could culminate in MTP opening and release of both Ca^{2+} and Mg^{2+} to the cytosol (Lapidus & Sokolove, 1994).

Therefore, in the absence of Ca_o^{2+} and factors that cause significant perturbation of $[Mg^{2+}]_t$ and/or $[Mg^{2+}]_i$, the increase in mag-fura-2 *R*, observed during superfusion of myocytes with the loading solution, appears to reflect a genuine increase in $[Mg^{2+}]_i$ arising from trans-sarcolemmal Mg^{2+} influx.

3.4.10 Na^+-dependence of $[Mg^{2+}]_i$ reduction

To balance the inward leak of Mg^{2+} into cardiac myocytes, a Mg^{2+} extrusion mechanism is required. The reduction of $[Mg^{2+}]_i$ in Mg^{2+}-loaded cells seen in these experiments (e.g. Figure 3.2) occurred against a Mg^{2+} electrochemical gradient and was specifically dependent upon the presence of Na^+ in the bathing solution. The rate of $[Mg^{2+}]_i$ reduction was dependent on $[Na^+]_o$, where increasing $[Na^+]_o$ increased the rate constant of $[Mg^{2+}]_i$ reduction (Figure 3.4). The fall in $[Mg^{2+}]_i$ in Mg^{2+}-loaded cells to its initial value did not require Ca_o^{2+}. In theory, $[Mg^{2+}]_i$ reduction could occur either as a result of Mg^{2+} efflux across the sarcolemma or redistribution among intracellular organelles at binding sites. In cardiac myocytes, the mitochondria and the SR represent the two major intracellular organelles.

The permeability of the SR to Mg^{2+} is low as determined *in situ* by electron probe microanalysis (Somlyo *et al.*, 1985), and may be transiently increased during contraction where it acts as the counter ion for Ca^{2+} release. However, the SR in rat ventricle represents only 3.5% of the total cell volume (Page, 1978; Page *et al.*, 1971), and although it is capable of effectively buffering Ca^{2+} following muscle

contraction, it is unlikely to function as an efficient uptake site for Mg^{2+} at basal $[Mg^{2+}]_i$.

The mitochondria in cardiac cells represent the second largest compartment after the cytosol, occupying around 35% of the total cell volume (Page, 1978), and is the site for ATP synthesis, in itself a Mg^{2+} buffer. The permeability of the mitochondrial inner membrane to cations is tightly regulated. Cation uptake by respiring mitochondria, including that of Mg^{2+} appears to be electrophoretically mediated, as a direct consequence of mitochondrial membrane potential ($\triangle\psi$), which is around 180 mV (negative inside). However, Mg^{2+} does not come to electrochemical equilibrium across the inner mitochondrial membrane. $[Mg^{2+}]_m$ is maintained at a level close to resting cytosolic $[Mg^{2+}]$; between 0.8 and 1.5 mM (Rutter *et al.*, 1990), while Jung *et al.* (1990) reported an average value of 0.5 mM. This implies that the electrophoretic uptake of Mg^{2+} by the mitochondria is balanced by an efflux mechanism(s), or that Mg^{2+} uptake is not electrophoretic in the first place.

Unfortunately, little is known about pathways for Mg^{2+} movement across the inner coupling membrane of the mitochondria and in the absence of measurements of these fluxes in intact isolated myocytes under conditions used here, one can only speculate, on the basis of available knowledge, as to what extent mitochondrial Mg^{2+} fluxes affect the rates of $[Mg^{2+}]_i$ elevation and reduction obtained in this study.

It appears that the electrophoretic uptake by respiring mitochondria of charged species including Mg^{2+} is very slow (Bernardi, 1999). Available evidence suggests that the respiration-dependent, uncoupler-sensitive uptake of Mg^{2+} by mitochondria occurs by diffusive leak pathways (Jung & Brierley, 1994). Mg^{2+} uptake is not inhibited by ruthenium red, a potent inhibitor of Ca^{2+} influx via the Ca^{2+}-uniport in isolated heart mitochondria (Brierley *et al.*, 1987), by diltiazem, which inhibits mitochondrial Na^+/Ca^{2+} exchange, and only partially inhibited by N,N`-dicyclohexylcarbodiimide (DCCD), an inhibitor of K^+/H^+ (Na^+) exchanger in rat liver mitochondria (Garlid *et al.*, 1986).

Mitochondrial Mg^{2+} uptake is largely inhibited in the presence of physiological concentrations of K^+ and other monovalent cations in the intermembrane space, even when heart mitochondria are treated with the exogenous electroneutral K^+/H^+ exchanger nigericin (Jung & Brierley, 1994; Bernardi, 1999). These observations support the hypothesis that Mg^{2+} uptake is mediated through diffusive leak in response to $\triangle\psi$ or through specific pathways not yet characterised, but probably not through routes preferred by K^+ and Ca^{2+}. Crompton *et al.* (1976) also found that when the extramitochondrial $[Mg^{2+}]$ is less that about 2.5 mM a net Mg^{2+} efflux was observed, whereas a net influx of Mg^{2+} occurred at $[Mg^{2+}]$ above 2.5 mM in the suspension medium. Brierley *et al.* (1987) confirmed these findings. This would also support the observation by Corkey *et al.* (1986) that raising extramitochondrial $[Mg^{2+}]$ to 2 mM did not result in a detectable increase in $[Mg^{2+}]_m$. Therefore, it is likely that the increase in $[Mg^{2+}]_i$ observed in the present study by subjecting isolated myocytes to the Mg-loading protocol will also result in an increase in mitochondrial $[Mg^{2+}]_m$. However, massive uptake of Mg^{2+} by mitochondria in this study is not expected to occur, since Mg^{2+} uptake has only been observed following addition of P_i and reagents that seem to increase the permeability of the inner mitochondrial membrane such as zinc, cadmium and mercury salts (Brierley, 1967; Brierley *et al.*, 1967).

Another concern probably applies to all studies employing mag-fura-2 AM ester to measure $[Mg^{2+}]_i$ in intact cells. Indicators introduced as AM esters, once inside the cell, may also permeate cell organelles and may not be hydrolysed by cytosolic esterases. In cardiac cells, due to the abundance of mitochondria, a fraction of the fluorescence signal may arise from mag-fura-2 trapped in the mitochondrial matrix. However, loading cells with the dye at room temperature should minimize uptake of the dye by mitochondria (Griffiths *et al.*, 1997).

It can be concluded that the rapid response of $[Mg^{2+}]_i$ to the change in $[Na^+]_o$ is most likely due to outward movement of Mg^{2+} across the sarcolemma, probably through a Na^+/Mg^{2+} antiport. Na^+/Mg^{2+} exchange has been suggested in various tissues as a Mg^{2+} extrusion mechanism (see Table 1.2 in General Introduction), and significant

evidence is building for a similar mechanism in the heart (Fry, 1986; Vormann & Günther, 1987; Romani *et al.*, 1993a; Handy *et al.*, 1996; Tashiro & Konishi, 2000) (see Sec. 3.1). A linear regression best describes the relationship between $[Na^+]_o$ and the rate constant ratio of the test $[Na^+]_o$ (28 to 98 mM) to 140 mM $[Na^+]_o$ (Figure 3.4). The slope of 1.02 ± 0.10 mM^{-1} obtained for this relationship suggests that the influx of a single Na^+ is required for the extrusion of a single Mg^{2+}, making the exchange mechanism through a putative Na^+/Mg^{2+} antiport electrogenic. This would also imply that the rate of Mg^{2+} extrusion is influenced by changes in the membrane potential, where depolarisation to voltages more positive than the antiport's reversal potential should accelerate Mg^{2+} extrusion. The voltage sensitivity of the putative Na^+/Mg^{2+} antiport is examined in more detail in Chapter 6. The effect of variable $[Na^+]_o$ *per se* on $[Mg^{2+}]_i$ recovery cannot be attributed to an effect of membrane potential, since decreasing $[Na^+]_o$ from 140 to 0 mM in Ca^{2+}-free Tyrode had negligible effect on the membrane potential (Figure 3.7.B).

In summary, the simplest explanation of the Na^+-dependence of $[Mg^{2+}]_i$ reduction observed in this study is a sarcolemmal Na^+/Mg^{2+} antiport, though these experiments do not rule out the involvement of other ions in the transport process. Analysis of the rate of Mg^{2+} reduction at various $[Na^+]_o$ indicates that the putative antiport has a 1 Na^+: 1 Mg^{2+} stoichiometry, and therefore would utilise changes in membrane potential during the cardiac cycle in addition to the Na^+ gradient across the sarcolemma to regulate $[Mg^{2+}]_i$ at around the measured resting values.

CHAPTER 4

SODIUM- AND MAGNESIUM-DEPENDENCE OF MAGNESIUM ELEVATION

4.1 INTRODUCTION

Although removal of external Na^+ and elevation of $[Mg^{2+}]_o$ should reverse a putative Na^+/Mg^{2+} antiport to operate in the Mg^{2+} influx mode, it is not clear whether Na^+/Mg^{2+} exchange is responsible for all or part of Mg^{2+} uptake in cardiac cells. Obviously, under physiological conditions, Mg^{2+} leak into cells is unlikely to be mediated by the putative Na^+/Mg^{2+} antiport. If the true stoichiometry of the antiport is 1 Na^+: 1 Mg^{2+} then in resting isolated ventricular myocytes the antiport would be close to its reversal potential (see Section 6.1). However, the antiport would promote Mg^{2+} influx only if the membrane potential was more negative than the exchanger's reversal potential. Although this might occur during the resting phase of cardiac cycle in myocytes, the main function of the putative antiport remains the removal of internal Mg^{2+} in exchange for external Na^+. Mg^{2+} influx through the antiport might, nevertheless, serve to alleviate or at least participate in correcting cellular Mg^{2+} depletion resulting from certain pathological conditions.

It is not clear whether Mg^{2+} influx in heart cells occurs via dedicated route(s) or is simply the inability of certain cation channels to exclude it entirely and thus mediate a slow but constant Mg^{2+} leak. The evidence in heart muscle is consistent with the view that Mg^{2+} may share Ca^{2+}-influx route(s), since removal of Ca^{2+} stimulates a rise in $[Mg^{2+}]_i$ (Handy *et al.*, 1996; Tashiro & Konishi, 2000). The stimulatory effect of removing external Na^+ on $[Mg^{2+}]_i$ rise is consistent with Mg^{2+} movement through a Na^+/Mg^{2+} antiport that reverses to mediate Mg^{2+} influx rather than its removal. It is also consistent with the possibility that Mg^{2+} might enter through Na^+ channels. These studies, however, do not necessarily rule out other uptake routes.

In this chapter, the effect of manipulating external $[Mg^{2+}]$ or $[Na^+]$ on the rate of $[Mg^{2+}]_i$ elevation in isolated, mag-fura-2-loaded rat ventricular myocytes will be addressed. The chapter is divided into three main sections, Na^+-dependence of $[Mg^{2+}]_i$ elevation, Mg^{2+}-dependence of $[Mg^{2+}]_i$ elevation and the effect of internal Na^+ depletion on $[Mg^{2+}]_i$ elevation.

4.2 MATERIALS AND METHODS

1. Mg^{2+}-loading solution: Cells were loaded with Mg^{2+} by superfusion with a modified Mg^{2+}-loading solution that contained various $[Na^+]_o$ (in mM: $MgCl_2$ 30; KCl 6; HEPES 10; glucose 10; NaCl 0 to 95; pH 7.4 at 37 °C adjusted with either HCl or NaOH). Where the concentrations of Na^+ or Mg^{2+} in the superfusate were manipulated, equimolar amounts of NMDG were added to maintain constant osmolarity.

4.3 RESULTS

A protocol has been developed to investigate the Na^+-dependence of Mg^{2+}-loading. Isolated cells where subjected to a Mg^{2+}-loading protocol twice and in some experiments three times. Figure 4.1 shows an example of one such experiment comparing Mg^{2+}-loading at two different $[Na^+]_o$. The main advantage of this protocol is that it permits the comparison of the maximum rate of $[Mg^{2+}]_i$ elevation at two or three different $[Na^+]_o$ within the same cell. Comparing the rate of $[Mg^{2+}]_i$ elevation between cells is less useful because of the variability in the ability of cells to load with Mg^{2+}. This was found to be the case whether cells were obtained from the same or different hearts.

4.3.1 Na^+-dependence of $[Mg^{2+}]_i$ elevation

The maximum rate of Mg^{2+}-loading at 0, 10 and 45 mM $[Na^+]_o$ was compared to that at $[Na^+]_o$ of 95 mM, all in the presence of 30 mM $[Mg^{2+}]_o$.

Typically a cell was subjected to a Mg^{2+} loading protocol twice (Figure 4.1). The first loading was carried out in the presence of 95 mM $[Na^+]_o$ and 30 mM $[Mg^{2+}]_o$. Once $[Mg^{2+}]_i$ has risen to an appreciable level above resting value, the solution was changed to normal Tyrode and $[Mg^{2+}]_i$ was allowed to recover to the initial level. This was maintained for a few minutes before a second loading was started using various $[Na^+]_o$ (0, 10 or 45 mM) while $[Mg^{2+}]_o$ was kept at 30 mM. In all the

experiments, loading was carried out in Ca^{2+}-free conditions. The maximum rate of $[Mg^{2+}]_i$ elevation (in mM min^{-1}) was calculated for the two loading conditions.

The data from all experiments of this type were compared using the one-way analysis of variance test (ANOVA). The results are summarised in Table 4.1. It is clear that Mg^{2+} loading in 0, 10 or 45 mM $[Na^+]_o$ is significantly greater than that in 95 $[Na^+]_o$. There appears to be little difference between the rates of $[Mg^{2+}]_i$ elevation at 0 and 10 mM $[Na^+]_o$ (P = 0.86). With an $[Na^+]_o$ of 45 mM there was not a significant inhibition of $[Mg^{2+}]_i$ elevation compared to 0 mM $[Na^+]_o$ in the presence of 30 mM Mg^{2+}. This was further investigated using a double loading protocol (Figures 4.3) in which a comparison between $[Mg^{2+}]_i$ elevation at 0 and 10 (Figure 4.3A), and 0 and 45 mM (Figure 4.3B) $[Na^+]_o$ was made. The results (Table 4.1) confirm that there is little difference in the mean maximum rate of $[Mg^{2+}]_i$ elevation between the $[Na^+]_o$ tested.

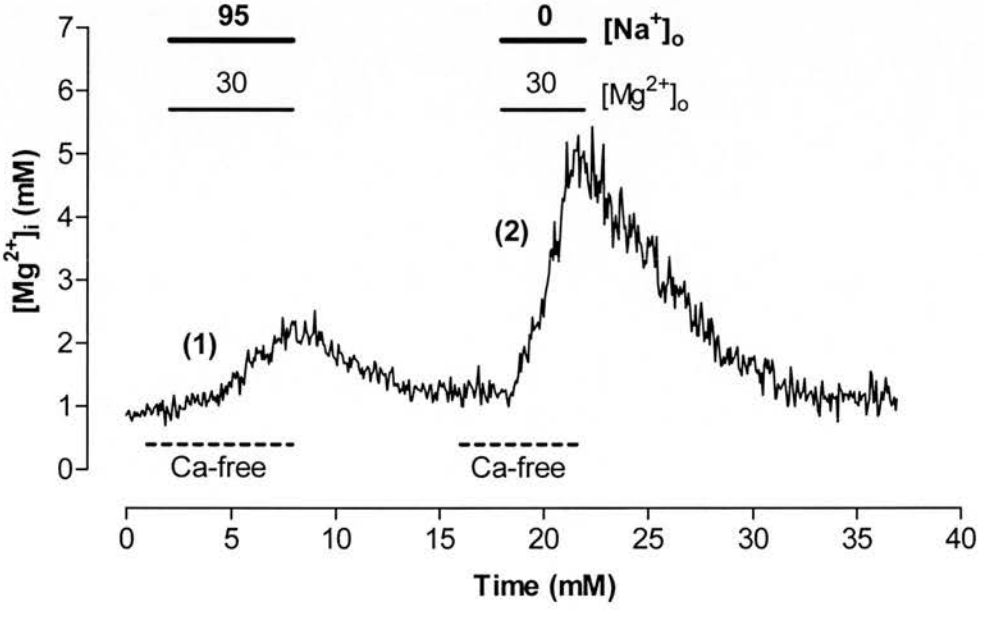

Figure 4.1. Comparison of Mg^{2+} loading at 95 and 0 mM $[Na^+]_o$

A fluorescence trace recorded from a single mag-fura-2-loaded ventricular myocyte. Unless otherwise specified, $[Mg^{2+}]_o$ = 1 mM, $[Na^+]_o$ = 140 mM and $[Ca^{2+}]_o$ = 1 mM. The cell was loaded with Mg^{2+} first in the presence of 95 mM $[Na^+]_o$ (1). $[Mg^{2+}]_i$ was then allowed to recover to the initial value before a second loading (2) in Na^+-free conditions was started. See text for more details.

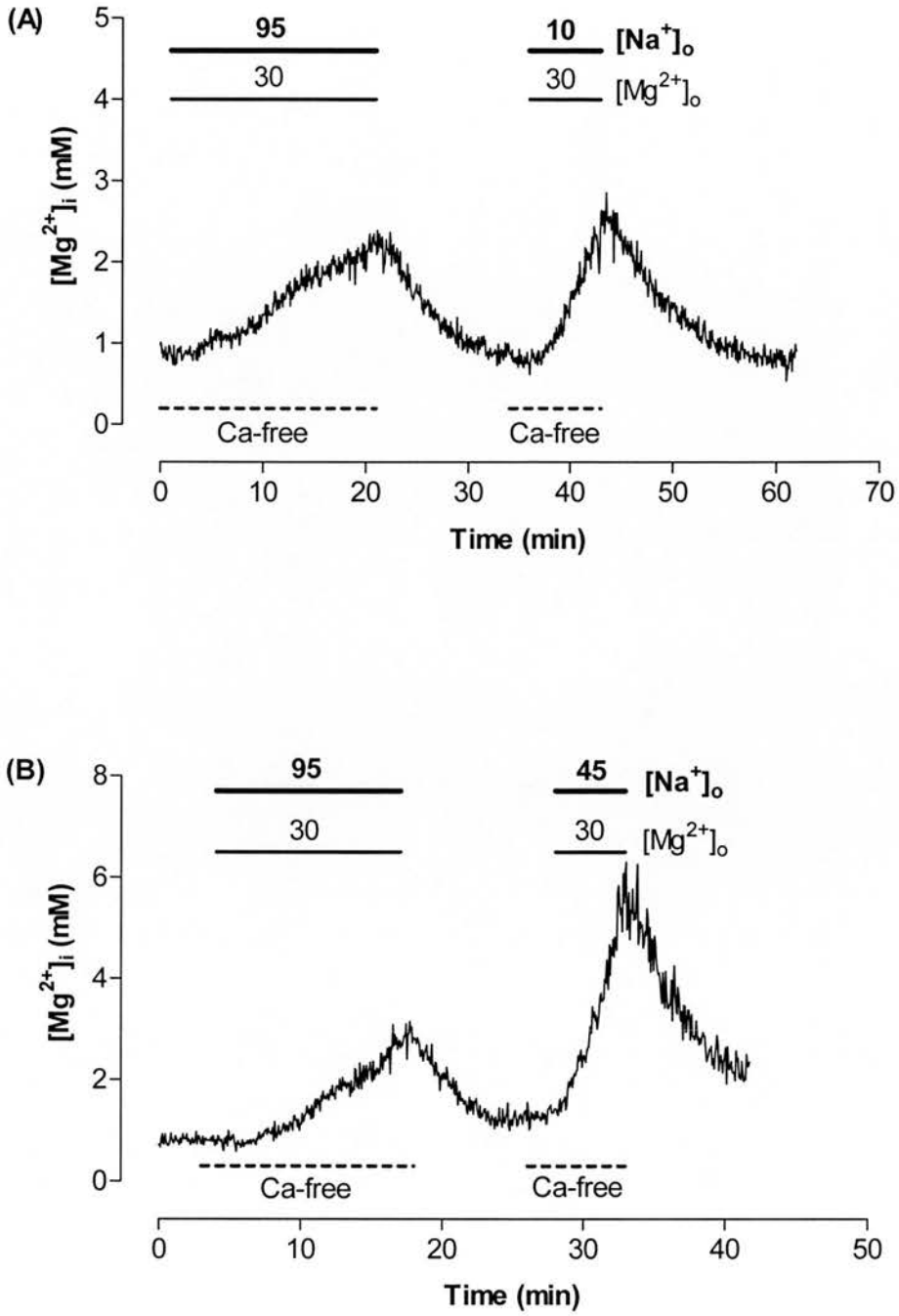

Figure 4.2. **Comparison of Mg^{2+}-loading at 10, 45, and 95 mM $[Na^+]_o$**

Comparing Mg^{2+}-loading at 10 mM $[Na^+]_o$ to 95 mM **(A)** and 45 mM $[Na^+]_o$ to 95 mM **(B)**.

Table 4.1. **Na^+-dependence of $[Mg^{2+}]_i$ elevation**

$[Na^+]_o$ (mM)	*Mean max. rate of $[Mg^{2+}]_i$ elevation ($mM.min^{-1}$)**	*Ratio **	*(n)*	*P***
0	0.71 ± 0.22	2.70 ± 0.42	6	0.01
95	0.25 ± 0.03			
10	0.67 ± 0.08	1.86 ± 0.05	4	0.01
95	0.36 ± 0.08			
45	0.58 ± 0.11	1.75 ± 0.17	4	0.05
95	0.33 ± 0.07			
0	0.56 ± 0.06	1.14 ± 0.04	3	0.33
10	0.49 ± 0.03			
0	0.74 ± 0.18	1.27 ± 0.18	4	0.14
45	0.49 ± 0.07			

* Mean ± S.E.M.

** Means were compared using the one-way analysis of variance test (ANOVA).

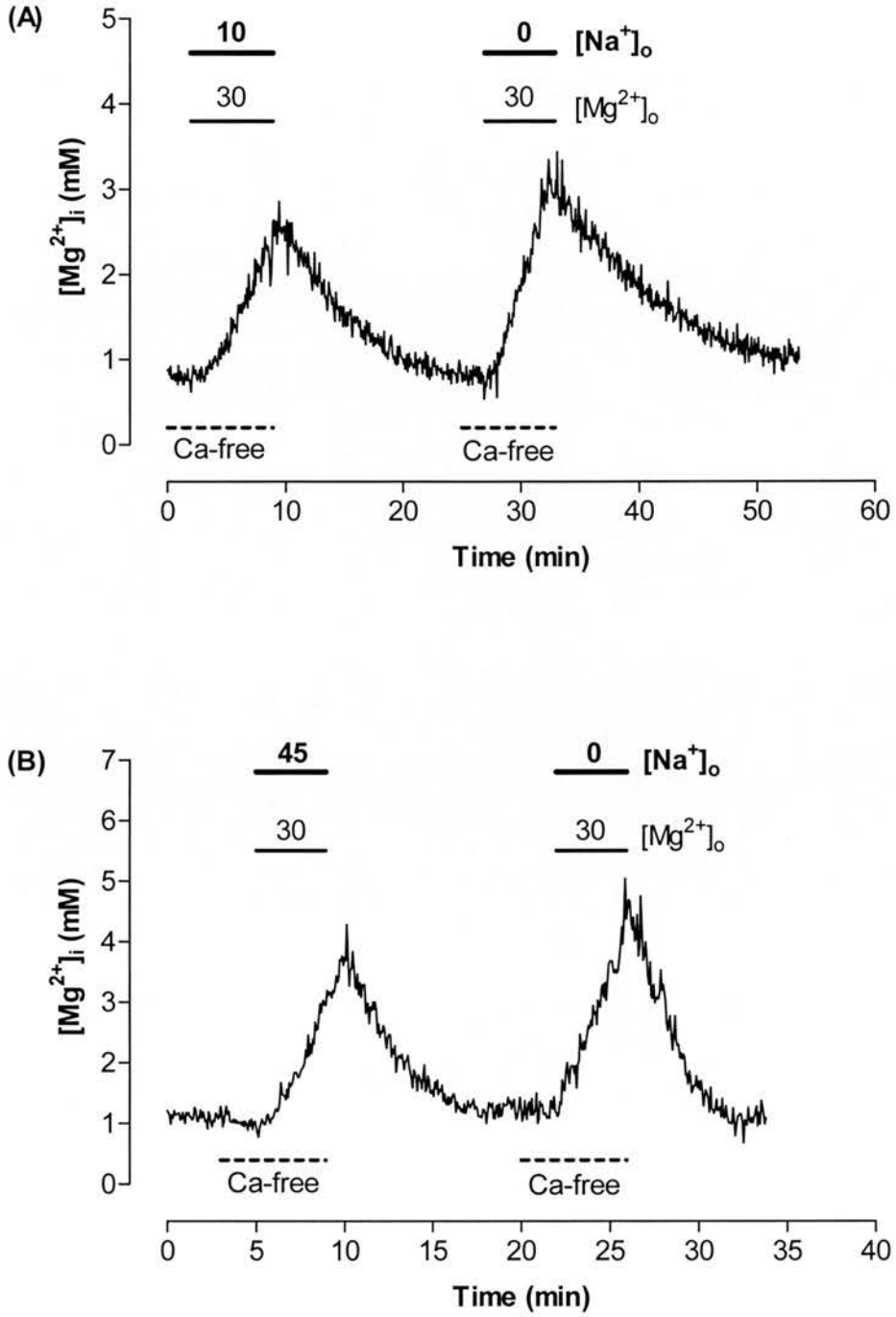

Figure 4.3. **Comparison of Mg^{2+}-loading at 0 and 10 mM and 0 and 45 mM $[Na^+]_o$**

Fluorescence signal depicting changes in $[Mg^{2+}]_i$ in mag-fura-2-loaded single ventricular myocytes. The rate of $[Mg^{2+}]_i$ elevation in Na^+-free loading solution was compared to that at 10 mM $[Na^+]_o$ **(A)** and 45 mM $[Na^+]_o$ **(B)** using double loading protocols.

A comparison of $[Mg^{2+}]_i$ elevation at all three $[Na^+]_o$ (0, 10 and 45 mM) was carried out using a triple loading protocol (Figure 4.4). Technically, this is a very demanding protocol for the cells. This is because of the possible detrimental effects of repeated exposure of the cell to Ca^{2+}-free medium. However, if carried out under continuous monitoring of the cell's structure, a triple loading protocol was useful. Figure 4.4 clearly shows the similarity in the rate of $[Mg^{2+}]_i$ elevation among the three conditions tested.

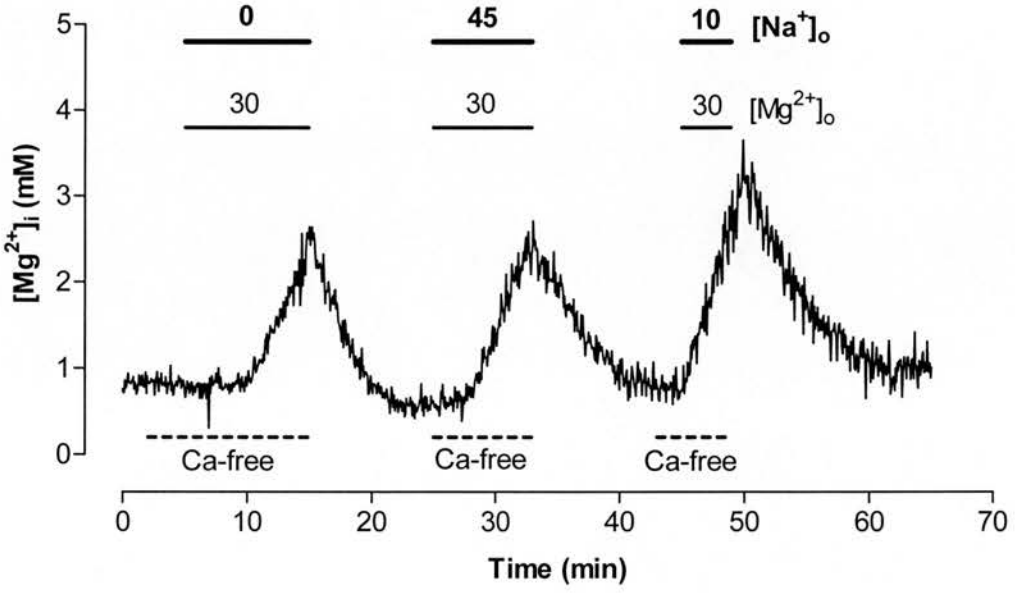

Figure 4.4. Comparison of Mg^{2+}-loading at 0, 10, and 45 mM $[Na^+]_o$

A single myocyte was subjected to the Mg^{2+}-loading protocol three times. Each time the concentration of external Na^+ was varied (dark bars) while the concentration of Mg^{2+} in the superfusate was kept at 30 mM. The diagram illustrates the lack of significant difference in the rate of $[Mg^{2+}]_i$ elevation among the three loading conditions. In this case, the rate of $[Mg^{2+}]_i$ elevation in Na^+-free conditions was 0.32 mM min^{-1}, 0.4 mM min^{-1} at 45 mM $[Na^+]_o$ and 0.42 mM min^{-1} at 10 mM $[Na^+]_o$.

Since most experiments compared the rate of $[Mg^{2+}]_i$ elevation at 95 mM $[Na^+]_o$ to that at either 0, 10 or 45 mM $[Na^+]_o$, the rate of $[Mg^{2+}]_i$ elevation at the lower external Na^+ concentrations was normalised to that at 95 mM and plotted against $[Na^+]_o$ (Figure 4.5). Although the data do not conclusively describe a kinetic model, the rate of $[Mg^{2+}]_i$ elevation appears to approach its maximum at external Na^+ concentrations below 45 mM. On the other hand, increasing $[Na^+]_o$ to 95 mM decreases Mg^{2+} loading significantly.

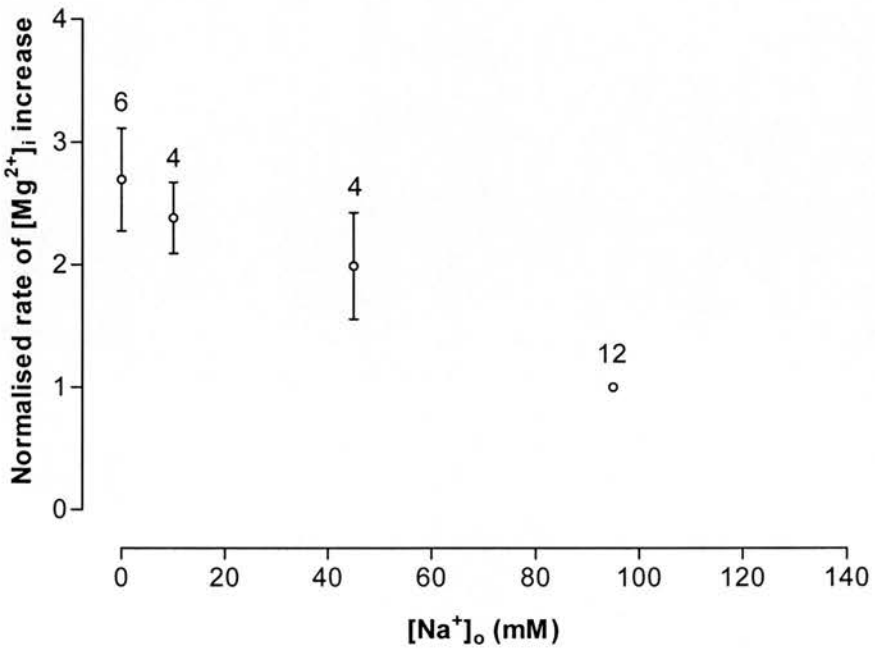

Figure 4.5. **Rate of $[Mg^{2+}]_i$ elevation as a function of $[Na^+]_o$**

Each data point is the statistical mean of (n) experiments (number above error bars) representing the ratio of the maximum rate of $[Mg^{2+}]_i$ elevation at the test $[Na^+]_o$ (0, 10 and 45) to that at 95 mM $[Na^+]_o$. The mean rate of $[Mg^{2+}]_i$ elevation at 95 mM $[Na^+]_o$ was 0.25 ± 0.03 mM min^{-1}.

4.3.2 Mg^{2+}- dependence of $[Mg^{2+}]_i$ elevation

Using similar loading protocols, the effect of manipulating $[Mg^{2+}]_o$ on the rate of $[Mg^{2+}]_i$ elevation was studied. However, in this case $[Na^+]_o$ was maintained at 95 mM during the Mg^{2+}-loading phase of the experiment. The rate of $[Mg^{2+}]_i$ elevation was measured at three different $[Mg^{2+}]_o$, 5, 15 and 30 mM. The rate of loading was either compared between 5 and 30 mM $[Mg^{2+}]_o$ (Figure 4.6A) or between 15 and 30 mM $[Mg^{2+}]_o$ (Figure 4.6B). The results (Table 4.2) show that the rate of Mg^{2+} loading in 30 mM Mg^{2+} is significantly higher ($P = 0.01$) than that in 5 or 15 mM $[Mg^{2+}]_o$.

Table 4.2. **Mg^{2+}-dependence of $[Mg^{2+}]_i$ elevation**

$[Mg^{2+}]_o$ (mM)	*Max. rate of $[Mg^{2+}]_i$ elevation ($mM.min^{-1}$)**	*Ratio**	*n*	*P***
5	0.11 ± 0.03	0.21 ± 0.05	5	0.01
30	0.50 ± 0.10			
15	0.23 ± 0.06	0.42 ± 0.08	4	0.01
30	0.55 ± 0.04			

* Mean ± S.E.M.

** Means were compared using the one-way analysis of variance test (ANOVA)

The results suggest that the rate of $[Mg^{2+}]_i$ elevation is higher with 30 mM external $[Mg^{2+}]$ and also it takes less time for $[Mg^{2+}]_i$ to be raised to appreciable levels above resting (permitting the study of Mg^{2+} efflux mechanism(s)). This is an important finding since experimentally raising $[Mg^{2+}]_i$ under conditions where the cell is continuously subjected to ultraviolet light and/or Ca^{2+}-free medium could have serious damaging effects. Therefore, limiting the time of cell exposure to either of these two conditions should always be an advantage. The results show that increasing the concentration of Mg^{2+} in the bathing medium increases the rate of $[Mg^{2+}]_i$ elevation. The relationship between the normalised maximum rate of $[Mg^{2+}]_i$ elevation (rate at 5 and 15 mM to that at 30 mM $[Mg^{2+}]_o$) and the concentration of external Mg^{2+} appears linear (Figure 4.7). The fitted regression line had a slope of $0.032 \pm 0.002\ mM^{-1}$.

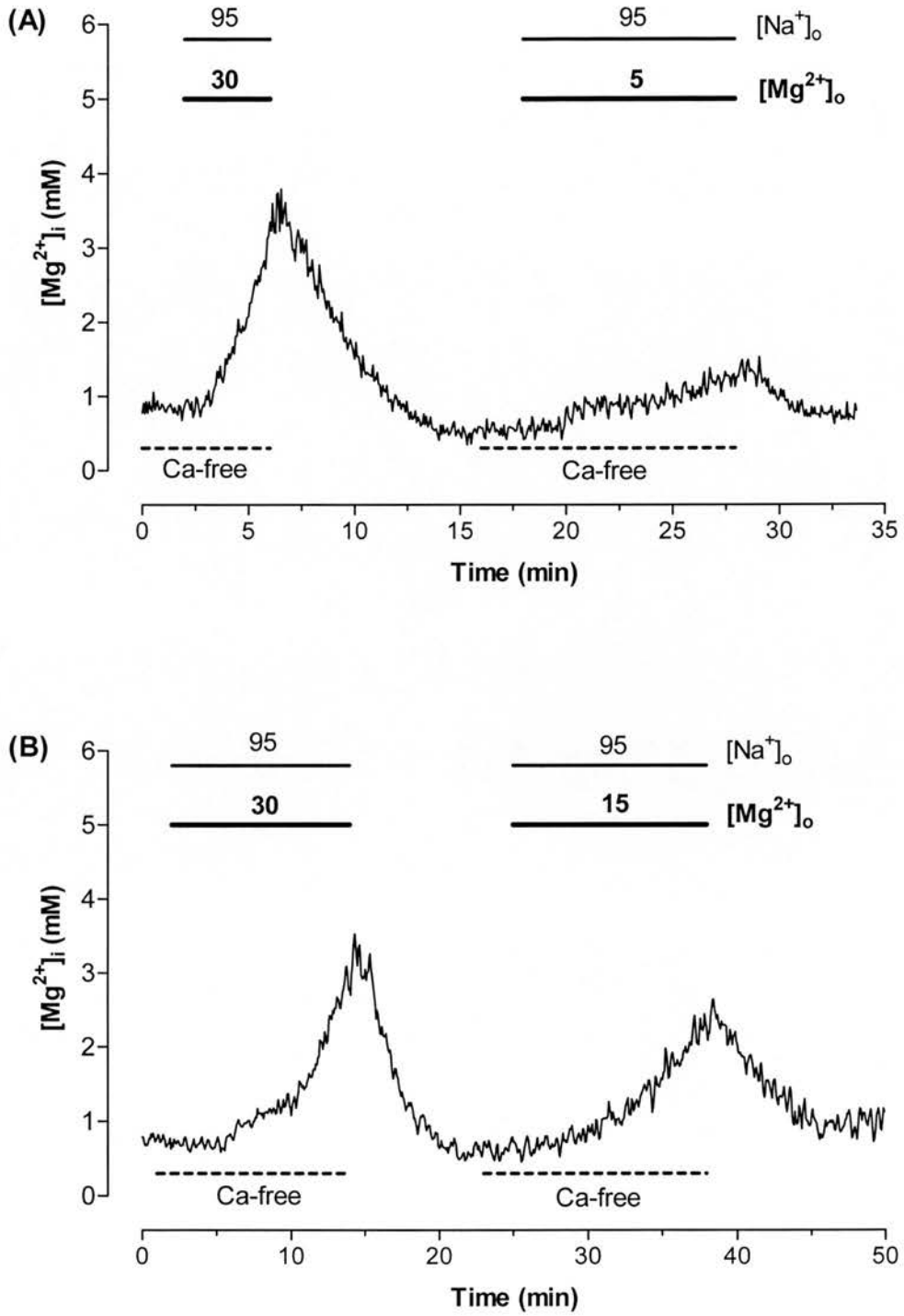

Figure 4.6. **Mg^{2+}-dependence of $[Mg^{2+}]_i$ elevation**

The rate of $[Mg^{2+}]_i$ elevation at 5 mM $[Mg^{2+}]_o$ was compared to that at 30 mM **(A)**, also, loading at 15 mM $[Mg^{2+}]_o$ was compared to that at 30 mM $[Mg^{2+}]_o$ **(B)**.

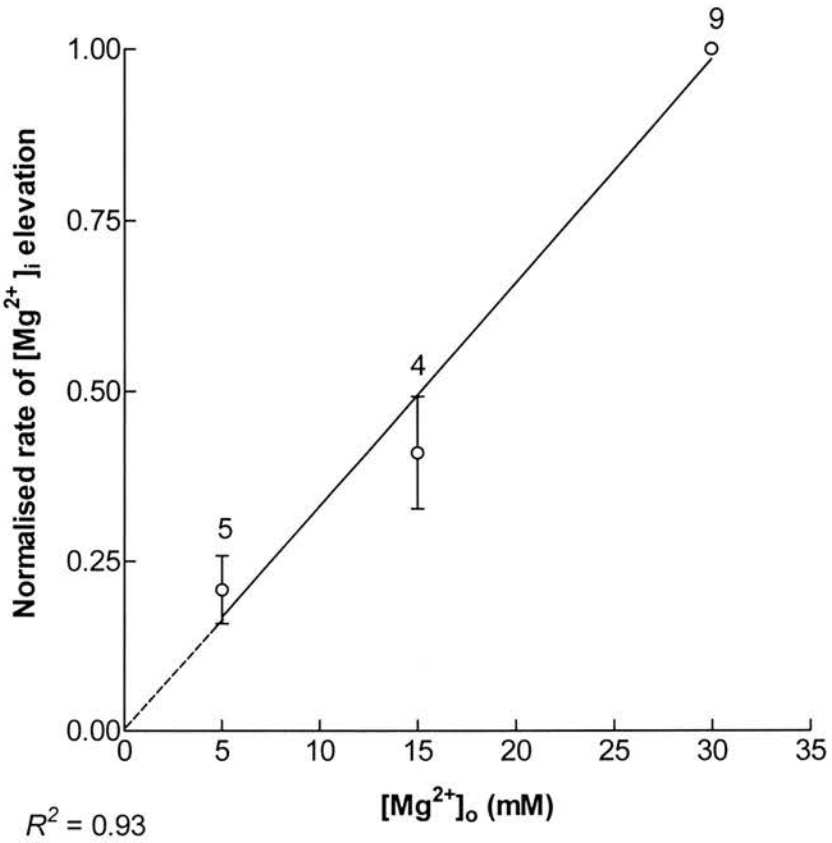

Figure 4.7. **The rate of $[Mg^{2+}]_i$ elevation as a function of $[Mg^{2+}]_o$**

The rate of $[Mg^{2+}]_i$ elevation at three different $[Mg^{2+}]_o$ (5, 15 and 30 mM) was calculated in mM min^{-1}. All the rates were normalised to the rate of $[Mg^{2+}]_i$ elevation at 30 mM $[Mg^{2+}]_o$ by obtaining the ratio of $[Mg^{2+}]_i$ elevation at 5 or 15 mM $[Mg^{2+}]_o$ to that at 30 mM. Each data point represents the statistical mean for n experiments (numbers above error bars). The fitted regression line has a slope of 0.032 ± 0.002 mM^{-1}. Note that the graph predicts a rate of approximately zero in 0 $[Mg^{2+}]_o$ (dashed line).

4.3.3 Effect of Intracellular Na^+ depletion on $[Mg^{2+}]_i$ elevation

These experiments were designed to obtain information on the extent of dependence of $[Mg^{2+}]_i$ elevation on $[Na^+]_i$. The cells were superfused with a Na^+-free solution (in mM: $MgCl_2$ 1, $CaCl_2$ 1, KCl 6, NMDG 140, HEPES 10, glucose 10; pH was adjusted using 6N HCl; the final $[Cl^-]$ was approximately 145 mM) for at least 10 minutes in order to deplete intracellular Na^+. Under these conditions, $[Na^+]_i$ is expected to drop close to zero mM (e.g. Ellis, 1977; Ellis & MacLeod, 1985). Then Ca^{2+} was also removed from the superfusate, 2 to 3 minutes before Mg^{2+} loading. Loading was carried out in the presence of 30 mM $[Mg^{2+}]_o$.

Three successful experiments were carried out using the above protocol, one of which was a double loading. The first two experiments (Figure 4.8) show almost identical responses. Following 13 minutes of Na^+-free superfusion, increasing $[Mg^{2+}]_o$ from 1 to 30 mM caused an unusually large and rapid rise in $[Mg^{2+}]_i$. The rise could not be attributed to cell damage since $[Mg^{2+}]_i$ fully recovered to the initial level when cells were returned to normal Tyrode at the end of the experiment. In addition the cells were continuously monitored for morphological changes throughout the course of the experiment for any sign of membrane damage or cell shortening. $[Mg^{2+}]_i$ increased from 0.9 to approximately 11 mM in just 4 minutes. Whatever the mechanism(s) responsible for this high Mg^{2+}-loading response, it is a reversible process that cannot be attributed to Na^+/Mg^{2+} exchange (see Discussion).

The third experiment (Figure 4.9) is a double Mg^{2+}-loading protocol, which was used to compare loading under normal and $[Na^+]_i$ depletion conditions. In the first loading, a similar approach to deplete internal Na^+ to the one just mentioned (Figure 4.8) was used. The second loading was carried out with the usual protocol, i.e. without removal of external Na^+ prior to superfusion with the Mg^{2+}-loading solution. The maximum rate of $[Mg^{2+}]_i$ elevation in the first loading was 0.08 mM min^{-1}, while that in the second loading was 0.09 mM min^{-1}. The response following superfusion with the loading solution observed in Figure 4.9 is quite different from the two previous experiments with regard to the magnitude and rate of rise in $[Mg^{2+}]_i$, and resembles the majority of experiments presented in this thesis.

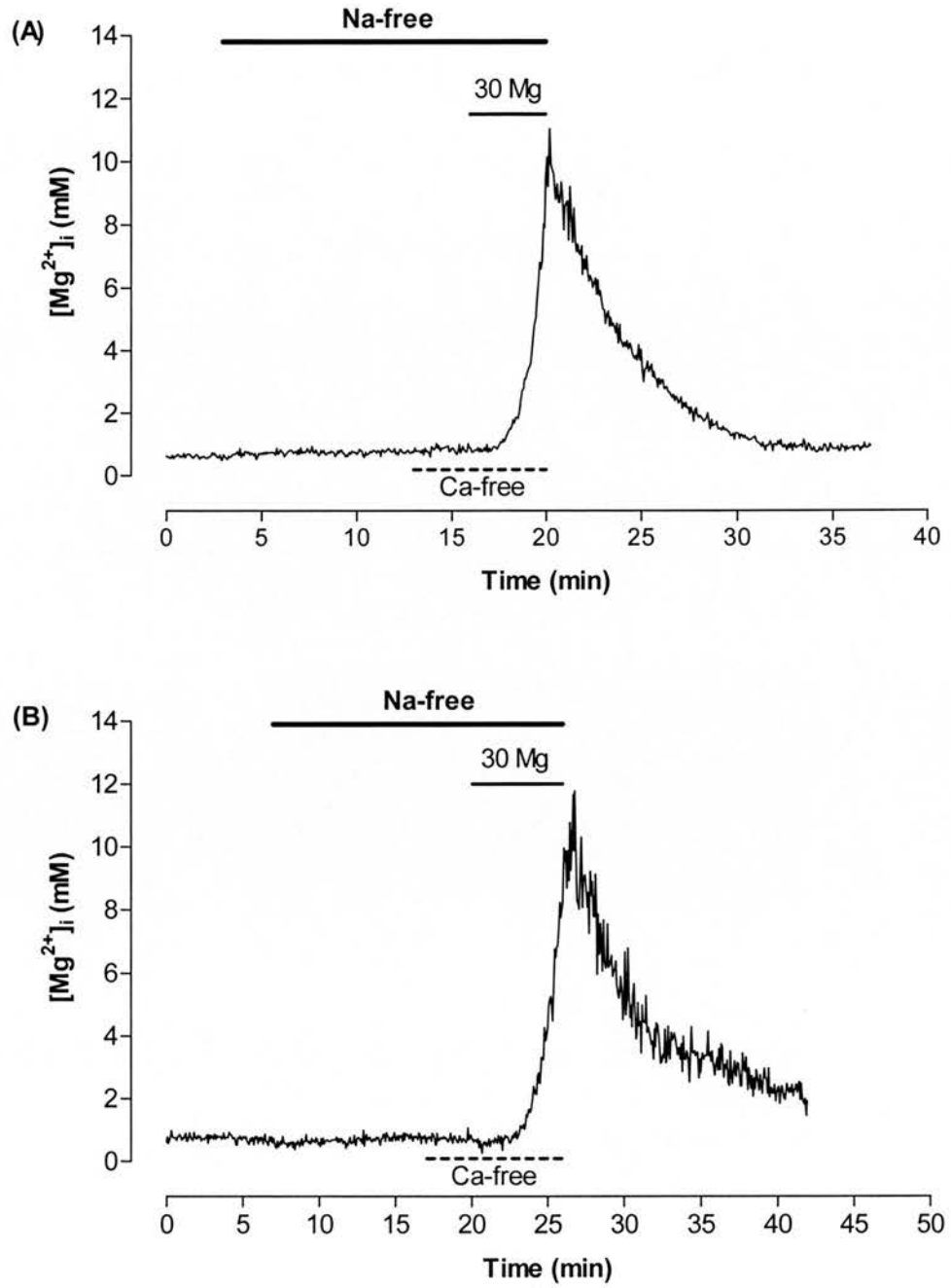

Figure 4.8. Effect of intracellular Na^+ depletion on Mg^{2+}-loading

Two experiments in which external Na^+ was removed for at least 10 minutes before 30 mM Mg_o^{2+} was introduced in the bathing medium. In both experiments, $[Mg^{2+}]_i$ increased at a very fast rate despite the low $[Na^+]_i$ expected following more than 10 minutes superfusion with Na^+-free medium. $[Mg^{2+}]_i$ recovered fully to the initial resting level **(A)**, and partially **(B)** once Na^+ was added to the superfusate.

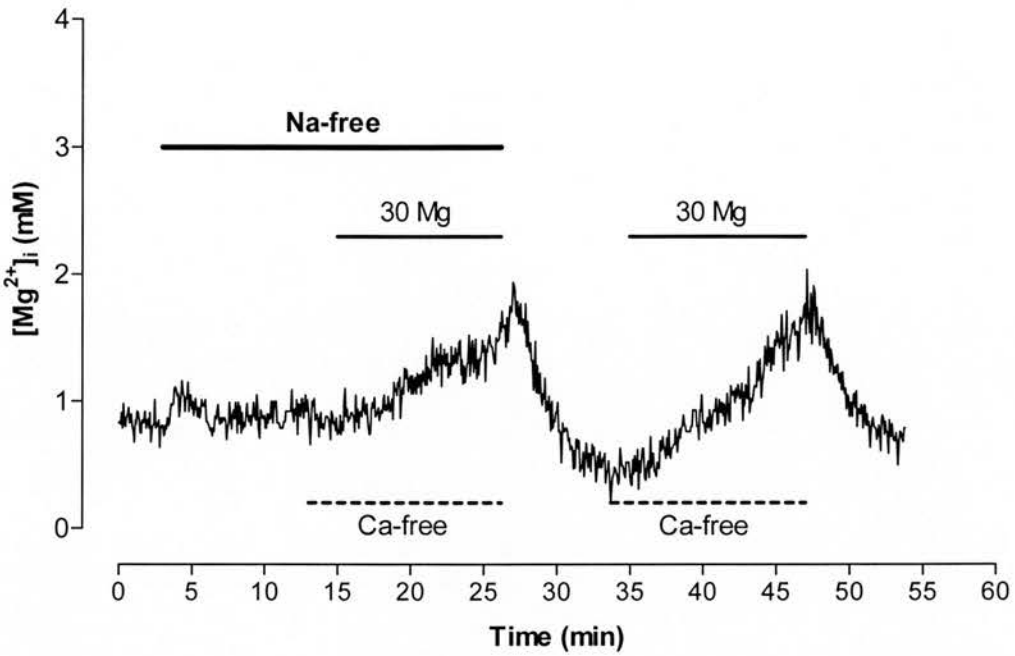

Figure 4.9. **Effect of intracellular Na^+ depletion on Mg^{2+} loading (double-loading protocol)**

Results from one experiment in which, the rate of $[Mg^{2+}]_i$ elevation was compared using a double Mg^{2+}-loading protocol. The first loading was carried out following 10 minutes superfusion with a Na^+-free solution. The initial rate of rise in $[Mg^{2+}]_i$ in both the first and second loading was approximately the same (0.08 and 0.09 mM min^{-1} respectively).

Regardless of the cause of variation in Mg^{2+}-loading, these experiments highlight the fact that depletion of internal Na^+ does not slow the rate of $[Mg^{2+}]_i$ elevation by cardiac myocytes under the loading conditions used here, as would be expected of elevation solely by reverse Na^+/Mg^{2+} exchange. This also means that reverse Na^+/Mg^{2+} exchange is not the only means of Mg^{2+} entry across the sarcolemma, and another route(s) probably exist.

4.4 Discussion

When cells with physiological Mg^{2+} contents are superfused or incubated with a Mg^{2+}-rich medium, no significant $[Mg^{2+}]_i$ elevation is detected despite a large electrochemical gradient favouring Mg^{2+} influx. The reason for this is three fold: low membrane permeability to Mg^{2+}, an intracellular buffering system that efficiently defends against changes in $[Mg^{2+}]_i$, and the presence of a powerful Mg^{2+} extrusion mechanism across the plasma membrane. Significant uncertainties still remain concerning the nature and properties of the putative Na^+/Mg^{2+} antiport, of which the question of reversibility is of special importance in relation to the experiments presented in this chapter. The idea of reversibility is supported by experiments in which $[Mg^{2+}]_i$ could be increased under conditions where the Na^+ gradient is outward (removal of external Na^+).

Mg^{2+} influx through an Na^+/Mg^{2+} antiport would be dependent on $[Na^+]_o$, $[Na^+]_i$, $[Mg^{2+}]_o$ and $[Mg^{2+}]_i$, as well as the membrane potential if the exchange process is electrogenic. Assuming a 1 Na^+: 1 Mg^{2+} stoichiometry, the relationship dictates that increasing $[Mg^{2+}]_o$ and/or decreasing $[Na^+]_o$ reverses the antiport into Mg^{2+} influx mode. The Mg^{2+}-loading protocol used to increase $[Mg^{2+}]_i$ in the experiments presented in the previous chapter and the modified protocols used in this chapter could mediate an increase in $[Mg^{2+}]_i$ through reversible Na^+/Mg^{2+} exchange. This concept will be discussed in more detail later in this section.

In the presence of 30 mM $[Mg^{2+}]_o$ loading was possible when $[Na^+]_o$ was as high as 95 mM (e.g. Figure 4.1). The rate increased more than two fold when Na_o^+ was either removed or decreased to either 10 or 45 mM. These results suggest that increasing $[Na^+]_o$ inhibits Mg^{2+} influx into cardiac cells. It was not possible to test the rate of $[Mg^{2+}]_i$ elevation in 140 mM in the presence of 30 mM external $[Mg^{2+}]$ since the solution would be significantly hypertonic. However, based on the results obtained the rate of $[Mg^{2+}]_i$ elevation is significantly reduced as $[Na^+]_o$ is increased to 95 mM (Figure 4.5). It is therefore possible that at physiological (or near physiological) $[Na^+]_o$, an increase in $[Mg^{2+}]_i$ would hardly be detectable using mag-

fura-2 as an indicator for Mg_i^{2+}. This would be consistent with results obtained by other workers using various methods to measure changes in $[Mg^{2+}]_i$ in cardiac tissue, in which either minor or no increase in $[Mg^{2+}]_i$ was detected in the presence of high $[Mg^{2+}]_o$ and physiological $[Na^+]_o$ in the bathing medium (Fry, 1986; Hall *et al.*, 1991; Buri *et al.*, 1993; Silverman *et al.*, 1994).

These findings could be explained as follows: at physiological $[Na^+]_o$, a putative Na^+/Mg^{2+} antiport would be operating in the forward mode, removing Mg^{2+} from the cell in exchange for external Na^+. Increasing $[Mg^{2+}]_o$ would increase Mg^{2+} entry into the cell and probably interfere with Na^+ binding to an external site on the antiport, although no direct evidence is available at present to support this. The net effect would be an increase in Mg^{2+} influx and a decrease in Mg^{2+} extrusion. This should lead to an increase in $[Mg^{2+}]_i$. However, the extrusion of Mg^{2+}, coupled with a powerful buffering system would defend the cell against a rise in $[Mg^{2+}]_i$ but not $[Mg^{2+}]_t$. This is supported by the fact that cells can lose or gain 5 to 10% of total cell magnesium content within minutes, yet these fluxes result in minor or no change in $[Mg^{2+}]_i$ (Romani & Scarpa, 2000). $[Mg^{2+}]_i$ would rise slowly using up the buffering capacity of the cytoplasm and causing redistribution of Mg^{2+} among intracellular organelles until $[Mg^{2+}]_i$ can no longer be stabilised. It may not be possible to detect a significant rise in $[Mg^{2+}]_i$ within an experimental time frame.

Experiments on ferret red blood cells (Flatman & Smith, 1991), rat liver plasma membrane vesicles (Cefaratti *et al.*, 2000), the squid axon (Mullins & Brinley, 1978), smooth muscle (Tashiro & Konishi, 1997b) and rat sublingual acini (Zhang & Melvin, 1996) have shown that reducing $[Na^+]_o$ stimulates the rate at which $[Mg^{2+}]_i$ increases. Removal of external Ca^{2+} has been found to enhance Mg^{2+} entry into cardiac myocytes (Handy *et al.*, 1996). A concomitant removal of external Na^+ results in even greater stimulation of Mg^{2+} entry. However, it is clear from the experiments presented here that complete removal of Na^+ from the bathing medium was not necessary to load myocytes with Mg^{2+}. It was possible to load cells even in solutions in which $[Na^+]$ and $[Mg^{2+}]$ were 95 and 5 mM respectively (Figure 4.6A). Under these conditions a putative Na^+/Mg^{2+} antiport with a 1 Na^+: 1 Mg^{2+}

stoichiometry would favour Mg^{2+} influx, at a resting membrane potential of –74 mV. Decreasing $[Na^+]_o$ further would increase the driving force for Mg^{2+} influx through the putative antiport. However, it is difficult to ascertain whether the increase in $[Mg^{2+}]_i$ seen under the loading conditions is due to Mg^{2+} influx through Na^+/Mg^{2+} antiport or through other routes, such as a Mg^{2+} channel, Na^+ channels, Ca^{2+} channels or other non-specific cation channel(s).

It is unlikely that a Na^+/Mg^{2+} antiport could sustain Mg^{2+} influx to the levels seen in the present experiments in Na^+-free conditions. Resting $[Na^+]_i$ in mammalian ventricular myocytes in normal saline measured using the fluorescent Na^+ indicator SBFI (Levi *et al.*, 1994; Ödblom & Handy, 2001), $^{23}Na^+$ NMR (Wittenberg & Gupta, 1985) or Na^+-selective microelectrodes (Mihailidou *et al.*, 1998) is between 8 and 11 mM. Superfusing rat ventricular myocytes with Na^+-free solution is expected to reduce $[Na^+]_i$ to about 3 mM in less than 10 minutes (Ödblom & Handy, 2001). Because of the reduction in the $[Na^+]$ gradient under such conditions, Mg^{2+} influx through reverse Na^+/Mg^{2+} exchange would also be reduced.

The best evidence against the absolute requirement for Na^+/Mg^{2+} exchange is probably the experiment shown in Figure 4.8. In this experiment, external Na^+ was removed for 13 minutes to deplete $[Na^+]_i$ before the loading phase was started. Yet, $[Mg^{2+}]_i$ increased from 0.9 mM to approximately 11 mM during a four-minute superfusion with the loading medium. This is roughly 2.5 mM min^{-1}. As far as Na^+/Mg^{2+} is concerned, there is simply not enough internal Na^+ to promote such a high rate of $[Mg^{2+}]_i$ elevation through reverse Na^+/Mg^{2+} exchange. Mg^{2+} rise is probably very high here as many Mg^{2+} binding sites would be occupied by Ca^{2+} following Ca^{2+} loading in the zero $[Na^+]$ solution.

Therefore, other routes of $[Mg^{2+}]_i$ elevation under the loading conditions probably exist to explain the high Mg^{2+} loads that were seen in most experiments presented in this report. The chemistry of Mg^{2+} poses a unique problem, which makes distinction between channel and carrier behaviour difficult. The best way to distinguish between channel and carrier behaviour is to calculate the turnover rate of a particular ion

passing through a plasma membrane. A high turnover number is good evidence for a channel. A typical conductance of a channel is at least 1 pA, corresponding to a turnover number of 6×10^6 monovalent ions per second (e.g. Hille, 1992). Most channels can pass much more. In contrast, an ion passing through a carrier protein can never approach such a rate. An example is the extrusion of Na^+ by the Na^+/K^+-ATPase, which has a turnover number of only 5×10^2 (Jorgensen, 1974). In the case of a carrier, the ion may have to bind to a site causing a conformational change of the transport protein molecule that allows the transport process to occur. The conformational change with each ion binding before the ion can be transported may be the rate-limiting step in the transport of an ion through an antiport or a symport.

In two experiments (Figure 4.8) where external Na^+ was removed for at least 10 minutes before superfusion with the loading solution, $[Mg^{2+}]_i$ increased at an exceptionally high rates. Although a carrier-mediated mechanism cannot be ruled out, the exceptionally high rates of $[Mg^{2+}]_i$ elevation suggest a channel-mediated process. $[Mg^{2+}]_i$ elevation is stimulated on reduction of $[Na^+]_o$ and removal of Ca_o^{2+} (Figure 4.5). Therefore, the simplest explanation for an $[Mg^{2+}]_i$ elevation route would involve Na^+ and/or Ca^{2+} channels. It is also possible that $[Mg^{2+}]_i$ elevation involves several pathways, some of which might only become activated under the experimental loading condition that are imposed on cells. Among those routes, the Na^+/Ca^{2+} exchanger is a possible candidate. There is evidence that Type I Na^+/Ca^{2+} exchanger might be involved in Mg^{2+} transport (Tashiro *et al.*, 2000). More details on the possible involvement of a Na^+/Ca^{2+} exchanger in Mg^{2+} transport will be presented in Chapter 5.

The relationship between external Mg^{2+} concentration and rate of rise in $[Mg^{2+}]_i$ appears linear (Figure 4.7). There is no indication that the transport process saturates. This provides more evidence for a channel-mediated uptake process. These results were expected since increasing $[Mg^{2+}]_o$ increases the electrochemical gradient that is already very large in favour of Mg^{2+} influx. However, it was interesting to record a slow but sustained increase in $[Mg^{2+}]_i$ upon increasing $[Mg^{2+}]_o$ from 1 to 5 mM in a solution that contained 95 mM $[Na^+]_o$ in Ca^{2+}-free conditions. These results contrast

with those obtained by Tashiro & Konishi (2000), who did not detect any change in $[Mg^{2+}]_i$ when single rat ventricular myocytes were bathed in a Na^+-free medium containing 10 mM $[Mg^{2+}]_o$ for 30 minutes. Their results also show no significant rise in $[Mg^{2+}]_i$ when $[Mg^{2+}]_o$ was raised to 30 mM (Figure 2 in Tashiro & Konishi (2000)). The difference in results between the present study and that by Tashiro & Konishi (2000) is not clear. It could be related to differences in the experimental temperature (37 °C in the present experiments versus 25 °C in theirs), cell isolation procedure or other factors that could affect the permeability of the cell membrane to Mg^{2+}.

In the majority of the experiments described here (e.g. Figures 3.2, 4.1 and 4.6B), the loading process appears to occur in two phases. An initial slow, followed by a much faster rise in $[Mg^{2+}]_i$. The initial slow component may reflect an initial effect of the intracellular buffering system. The early rise in Mg^{2+} might take place through reverse Na^+/Mg^{2+} exchange. This is supported by the observation by Handy *et al.* (1996) that when 10 μM imipramine is added to a loading solution containing 5 mM $[Mg^{2+}]$, and $[Mg^{2+}]_i$ was below 2 mM, a complete inhibition of $[Mg^{2+}]_i$ elevation was seen. In fact imipramine even caused a slight decrease in $[Mg^{2+}]_i$. However, once $[Mg^{2+}]_i$ exceeds a certain threshold, possibly between 1 and 2 mM, the rate of $[Mg^{2+}]_i$ elevation increases dramatically. Flatman & Smith (1996) previously observed an $[Mg^{2+}]_i$ "threshold" in ferret red blood cells – in this case 0.9 mM – where an extra Mg^{2+} permeability mechanism became apparent. In the present experiments this increase cannot be attributed to movement of Mg^{2+} through a Na^+/Mg^{2+} antiport for the reasons mentioned above.

The elevation in $[Mg^{2+}]_i$ is probably due to a rise in $[Mg]_t$ and not intracellular Mg^{2+} redistribution, Ca^{2+} interference with mag-fura-2 or other factors such as protons (see Chapter 3, Sections 3.4.7 to 3.4.9). This is also supported by the Mg^{2+}-dependence of $[Mg^{2+}]_i$ elevation (Figure 4.7), which predicts that at 0 $[Mg^{2+}]_o$ there would be no uptake. It is not clear what causes this apparent sudden change in membrane permeability to Mg^{2+}, and whether this process is triggered by the increase in $[Mg^{2+}]_i$, a decrease in $[Na^+]_i$ or saturation of intracellular buffers.

In summary, the experiments presented in this chapter were an attempt to understand how Mg^{2+} is transported into isolated ventricular myocytes. The results suggest:

- Reduction of $[Na^+]_o$ stimulates $[Mg^{2+}]_i$ elevation in high $[Mg^{2+}]_o$ and the absence of Ca_o^{2+}.
- $[Mg^{2+}]_i$ elevation falls significantly if $[Na^+]_o$ is increased above 45 mM.
- $[Mg^{2+}]_i$ elevation would probably be undetectable if the $[Na^+]_o$ was increased to 140 mM when mag-fura-2 is used to monitor changes in $[Mg^{2+}]_i$.
- The rate of rise of $[Mg^{2+}]_i$ increases linearly with $[Mg^{2+}]_o$.
- Reverse Na^+/Mg^{2+} exchange cannot account for the entire Mg^{2+} load seen in these experiments. Other routes of uptake must exist.
- The Mg^{2+} load observed in many experiments appears to occur in two phases. A slow phase $[Mg^{2+}]_i$ elevation followed by a much faster one.

CHAPTER 5

EFFECTS OF DRUGS ON MAGNESIUM TRANSPORT

5.1 INTRODUCTION

The data presented so far strongly suggests that Mg^{2+} extrusion in rat ventricular myocytes is Na^+-dependent, and most probably occurs through a sarcolemmal Na^+/Mg^{2+} antiport. The mechanisms that mediate $[Mg^{2+}]_i$ elevation on the other hand are less obvious. The experiments presented in the previous chapter suggest that $[Mg^{2+}]_i$ elevation might occur through a number of routes. At least some of the Mg^{2+} influx pathways are probably Ca^{2+} and/or Na^+ channels or carriers, since removal of these cations significantly stimulates elevations in $[Mg^{2+}]_i$ under Mg^{2+}-loading conditions. It is feasible that the putative Na^+/Mg^{2+} antiport might, under certain conditions (whether experimental of pathological), mediate Mg^{2+} influx in cardiac tissue. Unfortunately, the lack of specific inhibitor of Mg^{2+} transport system(s) hampered further characterisation of the pathways through which Mg^{2+} crosses the plasma membrane.

Féray & Garay (1988) made a significant contribution to the development of reagents that might inhibit Mg^{2+} transport. They examined the effects of tricyclic and non-tricyclic antidepressants on the Na^+-dependent Mg^{2+} efflux in Mg^{2+}-loaded human erythrocytes. They found that the Na^+-stimulated Mg^{2+} carrier is sensitive to tricyclic antidepressant drugs. Among the drugs tested, imipramine and dothiepine were the most potent. Today, an increasing number of researchers use imipramine to inhibit the Mg^{2+} carrier. Below is a brief account on the pharmacology of imipramine. This is followed by a description of the influence of some other drugs on Mg^{2+} fluxes and Na^+-dependent exchange processes.

Imipramine (tofranil), the first anti-depressant to be discovered, was found by accident in the late 1940s when new antihistamines were being tested (e.g. Pinder & Wieringa, 1993). Several other tricyclic antidepressants were subsequently produced once the chemistry of imipramine was known. Imipramine, is of the dibenzazepine type (10,11-dihydro-*N,N*-dimethyl-5*H*-dibenz[*b,f*]azepine-5-propanamine) (Figure 5.1).

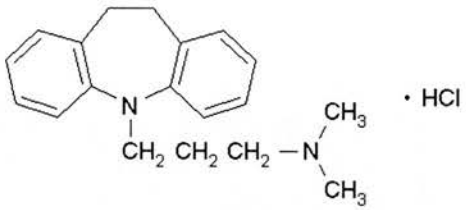

Figure 5.1. **Chemical structure of imipramine**

Imipramine is metabolised in the liver to an active compound called desipramine. It has been used in treatment of depression and childhood enuresis. It has also has been used in the management of neurogenic pain, attention-deficit hyperactivity disorder in children over age 6 years, eating disorders, and panic or phobic disorder (e.g. Pinder & Wieringa, 1993). The precise mechanism of action of tricyclic antidepressants is not fully understood. It is believed that imipramine and other tricyclic antidepressants interfere with the re-uptake of various neurotransmitters at the neuronal membrane. Following vesicular release, the biogenic amine neurotransmitters, noradrenaline, dopamine and serotonin, are removed from the synaptic cleft by selective and pharmacologically distinct transport proteins. These transporters, abbreviated NET, DAT and SERT, transport noradrenaline, dopamine and serotonin respectively. They are of particular clinical interest because they are the molecular targets for many anti-depressants including desipramine (Barker & Blakely, 1995) as well as drugs of abuse such as cocaine and the amphetamines (e.g. Saunders *et al.*, 2000). The molecular cloning of NET, DAT and SERT revealed that these transporters arise from single genes with homology to members of a larger sodium-dependent neurotransmitter transporter gene family (Blakely, 1997).

The availability of complementary deoxyribonucleic acids (cDNA) for NET, DAT and SERT has permitted detailed pharmacological study of each protein. SERT is most potently inhibited by selective serotonin reuptake inhibitors (Blakely, 1997). By inhibiting reuptake, drugs like imipramine enhance the action of noradrenaline and to a lesser extent serotonin at the postsynaptic receptor, thereby correcting a presumed deficit in the activity of these neurotransmitters.

Arrhythmias associated with imipramine usually occur after toxic doses, and they may result from the combination of the direct quinidine-like effect on cardiac function along with anticholinergic activity and noradrenaline potentiation (Pinder & Wieringa, 1993). In addition to the inhibitory effects imipramine has on a number of Na^+-dependent neurotransmitter transporters in the brain, other transporters are also sensitive to it at various concentrations. For example, imipramine has modest inhibitory activity against Na^+-K^+-$2Cl^-$ cotransport, Ca^{2+} -sensitive K^+ channels and K^+-Cl^- cotransport in human erythrocytes (Féray & Garay, 1988). Other Na^+-dependent transporters are poorly inhibited by imipramine. This inhibition usually requires high concentrations of the drug. The effect of imipramine on Na^+-dependent Mg^{2+} transport is well documented. Imipramine inhibits Na^+-dependent Mg^{2+} efflux and/or influx in a variety of tissues including human (Féray & Garay, 1988; Günther, 1993), ferret (Flatman & Smith, 1990; Flatman & Smith, 1991), rat (Günther, 1993; Günther & Vormann, 1995) and chicken (Günther, 1993) red blood cells, rat thymocytes (Günther, 1993), rat ventricular myocytes (Handy *et al.*, 1996; Tashiro & Konishi, 2000), liver cells (Cefaratti *et al.*, 1998; Tessman & Romani, 1998), Ehrlich ascites tumour cells (Wolf *et al.*, 1994a), and rat reticulocytes (Günther & Vormann, 1991).

The effective imipramine inhibitory concentration varies among tissues and sometimes even among reports studying the same tissue type. For example half-maximal inhibition of a Mg^{2+} carrier for human erythrocytes is 25 μM (Féray & Garay, 1988), while 500 μM has been used to partially inhibit Mg^{2+} efflux in ferret erythrocytes (Flatman & Smith, 1990) and Ehrlich ascites tumour cells (Wolf *et al.*, 1994a). In cardiac cells Handy *et al.* (1996) have shown that 10 μM imipramine was sufficient to completely abolish both $[Mg^{2+}]_i$ reduction and elevation in rat ventricular myocytes, while Tashiro & Konishi (2000) used 200 μM of the drug to achieve comparable inhibition, though at different $[Mg^{2+}]_i$, $[Mg^{2+}]_o$ and experimental temperature. Similar concentrations of imipramine also inhibit Na^+-stimulated Mg^{2+} efflux in rat liver plasma membrane vesicles (Cefaratti *et al.*, 1998).

Other drugs that inhibit Mg^{2+} transport include amiloride and quinidine. Amiloride is known to inhibit the Na^+/H^+ exchanger of vertebrate cells by acting competitively at the Na^+-binding site (Paris & Pouyssegur, 1983). The exchanger extrudes protons from cells using the inward $[Na^+]$ gradient as a driving force, resulting in intracellular alkalinisation. In 1967, Cragoe and co-workers reported the synthesis of amiloride and several amiloride analogues, pyrazine diuretics that inhibit the Na^+ channel in urinary epithelia. Since then, over 1000 different amiloride analogues have been synthesised and many of these were tested for their specificity and potency in inhibiting the renal Na^+ channel, Na^+/H^+ exchanger and Na^+/Ca^{2+} exchanger (Kleyman & Cragoe, 1988).

Amiloride (often in concentrations in the millimolar range) and quinidine were used to inhibit Na^+-dependent Mg^{2+} efflux in many tissues, including rat (Günther, 1993; Günther & Vormann, 1995; Ebel & Günther, 1999), ferret (Flatman & Smith, 1990; Flatman & Smith, 1996), human (Lüdi & Schatzmann, 1987; Günther, 1993), and chicken (Günther & Vormann, 1985; Günther, 1993) red blood cells. They were also found to have varying inhibitory effect on Mg^{2+} efflux in isolated perfused rat heart (Vormann & Günther, 1987; Howarth *et al.*, 1995), hepatocytes (Tessman & Romani, 1998), intact Ehrlich ascites tumour cells (Wolf *et al.*, 1994a), and leech neurons (Günzel & Schlue, 1996; Hintz *et al.*, 1999). In rat liver plasma membrane vesicles, amiloride, quinidine and imipramine inhibit both Na^+- and a Ca^{2+}-stimulated Mg^{2+} efflux (Cefaratti *et al.*, 1998). Amiloride and quinidine were also reported to inhibit Mg^{2+} uptake in certain tissues including erythrocytes (Flatman & Smith, 1991; Günther, 1993; Günther & Vormann, 1995; Flatman & Smith, 1996), rat reticulocytes (Günther & Vormann, 1991), and leech neurons (Hintz *et al.*, 1999).

The use of amiloride to inhibit Na^+-stimulated Mg^{2+} transport has many disadvantages. The most obvious drawback is its inhibition of the Na^+/H^+ exchanger at similar concentrations. Second, amiloride is fluorescent and this poses serious limitations on its use when changes in the fluorescence properties of a Mg^{2+} indicator is the only means by which $[Mg^{2+}]_i$ is being monitored. Non-fluorescent amiloride analogues, such as 5(N,N-hexamethylene)-amiloride, 5-(N,N-dimethyl)-amiloride

and 5-(N-ethyl-N-isopropyl)-amiloride could provide alternative means by which the drug might be used in Mg^{2+} transport studies employing fluorescence systems. However, these agents were ineffective in inhibiting Na^+-stimulated Mg^{2+} transport in some tissues (Wolf *et al.*, 1994a; Wolf *et al.*, 1994b; Günzel & Schlue, 1996).

Na^+-stimulated Mg^{2+} transport is not directly affected by the cardiac glycosides ouabain and strophanthidin. These agents do not seem to directly inhibit a Mg^{2+} carrying protein in cardiac (Fry, 1986; Freudenrich *et al.*, 1992a; Handy *et al.*, 1996) or smooth muscle (Tashiro & Konishi, 1997b). Ouabain does not affect Mg^{2+} transport in human (Féray & Garay, 1988) or ferret (Flatman & Smith, 1991) red blood cells. However, inhibition of the Na^+ pump by these agents increases $[Na^+]_i$ (e.g. Ellis, 1977) and that could lead to stimulation of Mg^{2+} uptake through a putative Na^+/Mg^{2+} antiport (Fry, 1986; Freudenrich *et al.*, 1992a; Handy *et al.*, 1996; Tashiro & Konishi, 1997b). Similarly, an increase in $[Na^+]_i$ should inhibit Mg^{2+} efflux through a Na^+/Mg^{2+} antiport. Therefore, the effect of ouabain and strophanthidin on Mg^{2+} transport is most probably an indirect one, resulting from the primary effect of these glycosides on the $[Na^+]$ gradient.

The properties of Na^+/Mg^{2+} exchange resemble in many ways those of Na^+/Ca^{2+} exchange. For example Na^+/Mg^{2+} exchange appears to be reversible, at least under some experimental conditions (Flatman & Smith, 1990; Günzel & Schlue, 1996), modulated by $[Ca^{2+}]_i$ (Romani *et al.*, 1993a), $[Na^+]_i$ (Levi, 1991; Handy *et al.*, 1996), and $[Ca^{2+}]_o$ and $[Na^+]_o$ (Handy *et al.*, 1996; Tashiro & Konishi, 2000), inhibited by amiloride (Vormann & Günther, 1987; Flatman & Smith, 1990; Flatman & Smith, 1996; Günzel & Schlue, 1996; Ebel & Günther, 1999; Hintz *et al.*, 1999), and in some tissues stimulated by intracellular ATP (Brinley & Mullins, 1968; Mullins & Brinley, 1978; Féray & Garay, 1986; Frenkel *et al.*, 1989; Rasgado-Flores *et al.*, 1994;).

A recent report suggests the Na^+/Ca^{2+} exchange molecule is capable of transporting Mg^{2+} instead of Ca^{2+} (Tashiro *et al.*, 2000). The authors used hamster lung fibroblasts expressing the cardiac Na^+/Ca^{2+} exchanger (cells were transfected with the cDNA of

the Na^+/Ca^{2+} exchanger isolated from canine heart). Their results suggest that cells expressing the Na^+/Ca^{2+} exchanger are capable of extruding Mg^{2+} in the presence of external Na^+. However, the authors found no direct evidence that the exchanger mediates Mg^{2+} influx through reverse-mode operation (Na^+ efflux). Nevertheless, their findings do not rule out such possibility.

In the present study myocytes were loaded with Mg^{2+} by superfusion with high $[Mg^{2+}]$ medium that is both Na^+- and Ca^{2+}-free. The absence of both Na^+ and Ca^{2+} in the external medium would inhibit both the forward and the reverse mode of the Na^+/Ca^{2+} exchanger. However, if in the absence of Ca^{2+}, Mg^{2+} binds to the Na^+/Ca^{2+} exchanger molecule and is transported into the cell in exchange for internal Na^+ (i.e. reverse-mode operation) then drug inhibition of this mode might inhibit or attenuate the rise in $[Mg^{2+}]_i$ during Mg^{2+}-loading.

Recently, a newly synthesised drug, 2-[2-[4-(4-nitrobenzyloxy)phenyl]-ethyl]isothiourea methanesulfonate (KB-R7943 mesylate or KBR) (Figure 5.2) was reported to potently and selectively inhibit the reverse mode of the Na^+/Ca^{2+} exchanger without affecting other Na^+-dependent transport systems or Na^+ channels (Iwamoto *et al.*, 1996).

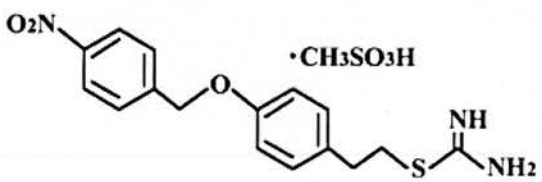

Figure 5.2. **Chemical structure of KB-R7943 (KBR)**

KBR only partially inhibits Na^+-dependent Ca^{2+} efflux (forward mode) at high concentrations (half maximal inhibition $\geq$ 30 μM) (Iwamoto *et al.*, 1996). In intact cardiomyocytes KBR was found to act primarily on external exchanger site(s) rather than transport sites and inhibition was non-competitive with respect to Ca^{2+} and Na^+ (Iwamoto *et al.*, 1996; Elias *et al.*, 2001).

Approximately 90% of Ca^{2+} influx via the reverse Na^{+}/Ca^{2+} exchanger operation in rat ventricular myocytes can be inhibited by 5 μM KBR at 36 °C (Satoh *et al.*, 2000) (half maximal inhibition = 1.2 to 2.4 μM), while Ladilov *et al.* (1999) reported complete inhibition in isolated rat ventricular myocytes with 20 μM KBR. Compared to its potent inhibition of outward exchanger currents (Ca^{2+} influx), KBR is far less effective at inhibiting inward Na^{+}/Ca^{2+} exchange currents. 10 μM KBR, inhibits only about 14% while 20 μM inhibits less than 20% of the exchanger's current (Elias *et al.*, 2001).

Not all isoforms of the Na^{+}/Ca^{2+} exchanger are inhibited by KBR with the same effectiveness. The mammalian Na^{+}/Ca^{2+} exchanger forms a multigene family comprising three isoforms, Type 1, Type 2 and Type 3 Na^{+}/Ca^{2+} exchanger. These isoforms share more than 70% identity in the overall amino acid sequences, and are thought to share the same membrane topology as well (Nicoll *et al.*, 1990; Li *et al.*, 1994; Nicoll *et al.*, 1996). Type 1 is highly expressed in the heart and brain and at lower levels in other tissues (Nicoll *et al.*, 1990). KBR is 3-fold more effective on Na^{+}/Ca^{2+} exchanger Type 3 than it is on Type 1 or 2 (Iwamoto & Shigekawa, 1998). This difference in the drug's effectiveness among the three isoforms is thought to be due to differences in a small number of residues in the α-2 repeat of the Na^{+}/Ca^{2+} exchanger molecule (Iwamoto *et al.*, 2001).

One interesting application of KBR is in the prevention of post-ischemic Ca^{2+} overload in ventricular myocytes, and subsequent cell injury (Satoh *et al.*, 2000). In fact any situation, which might lead to Ca^{2+} overload via reverse Na^{+}/Ca^{2+} exchange, is potentially preventable by KBR. An increasing number of studies are being conducted on the protective effects of KBR on various tissues, mainly following ischemic events. For example it protects against the damaging effects of reperfusion following myocardial ischemia (Ladilov *et al.*, 1999; Mukai *et al.*, 2000; Satoh *et al.*, 2000; Elias *et al.*, 2001) and suppresses ouabain-induced arrhythmias in guinea pig (Watano *et al.*, 1999). In ischemic acute renal failure, Ca^{2+} overload via reverse Na^{+}/Ca^{2+} exchange is followed by overproduction of endothelin-1, which is believed to play an important role in the pathogenesis of the ischemia/reperfusion-induced

acute renal failure. KBR thus indirectly prevents the sequence of events that leads to acute renal failure (Yamashita *et al.*, 2001a; Yamashita *et al.*, 2001b). KBR has also been reported to protect neurons against hypoxic/hypoglycaemic injury (Schroder *et al.*, 1999).

In summary, there is convincing evidence that KBR at concentrations ranging between 5 and 20 μM inhibits at least 90% of reverse Na^+/Ca^{2+} exchange. Inhibition is observed without prior incubation with the agent and is completely reversible one minute after removal of the drug from the bathing medium (Iwamoto *et al.*, 1996).

The experiments presented in this chapter examine the effects of 200 μM imipramine and 20 μM KBR on Mg^{2+} loading and Na^+-dependent $[Mg^{2+}]_i$ reduction in isolated, rat ventricular myocytes.

5.2 MATERIALS AND METHODS

1. Solutions: A 200 mM stock of imipramine was prepared by dissolving the solid in water. An appropriate volume of the stock was added to the desired solution to a final concentration of 200 μM. Imipramine was added to normal Tyrode, standard Mg^{2+}-loading solution or "clamp" solution immediately before the experiment.

2. KBR was dissolved in DMSO to make a 50 mM stock. Immediately before the experiment, the drug was added directly to the solutions to a final concentration of 20 μM and 0.04% (v/v) DMSO.

3. All solutions have otherwise the same composition as previously described in the General materials and methods.

5.3 RESULTS

Imipramine or KBR were added to the superfusate at concentrations that were previously shown (see section 5.1) to either inhibit Na^+/Mg^{2+} transport in the case of imipramine or the reverse mode of Na^+/Ca^{2+} exchanger in the case of KBR.

5.3.1 Effect of imipramine on $[Mg^{2+}]_i$ elevation

The maximum rate of $[Mg^{2+}]_i$ elevation in the Mg^{2+}-loading solution was compared in the presence and absence of 200 μM imipramine. $[Mg^{2+}]_i$ was initially raised in cells by superfusion with the Mg^{2+}-loading solution. $[Mg^{2+}]_i$ was then allowed to stabilise for a few minutes in a "clamp" solution before a second Mg^{2+} loading in the presence of 200 μM imipramine was started. Figure 5.3 shows one of three such successful experiments.

It is worth noting that since some cells did not respond to the Mg^{2+} loading protocol, application of imipramine at the outset of the experiment would lead to difficulty in the interpretation of the results, as it would not be possible to differentiate between a cell that does not load and one in which imipramine has inhibited Mg^{2+} loading. Therefore, this protocol ensures that imipramine is only applied to cells in which Mg^{2+} loading was shown to occur.

The maximum rate of $[Mg^{2+}]_i$ elevation at 30 mM $[Mg^{2+}]_o$ was 0.46 ± 0.2 mM min^{-1} (n = 3 cells from 2 hearts). When 200 μM imipramine was added to the Mg^{2+}-loading solution the rate of $[Mg^{2+}]_i$ elevation was not significantly affected. The maximum rate of $[Mg^{2+}]_i$ elevation in the presence of imipramine was 0.45 ± 0.2 mM min^{-1} (n = 3, $P = 0.22$). Therefore, it appears that imipramine at a concentration of 200 μM has no effect on the rate of rise of $[Mg^{2+}]_i$ in cells superfused with the Mg^{2+}-loading solution.

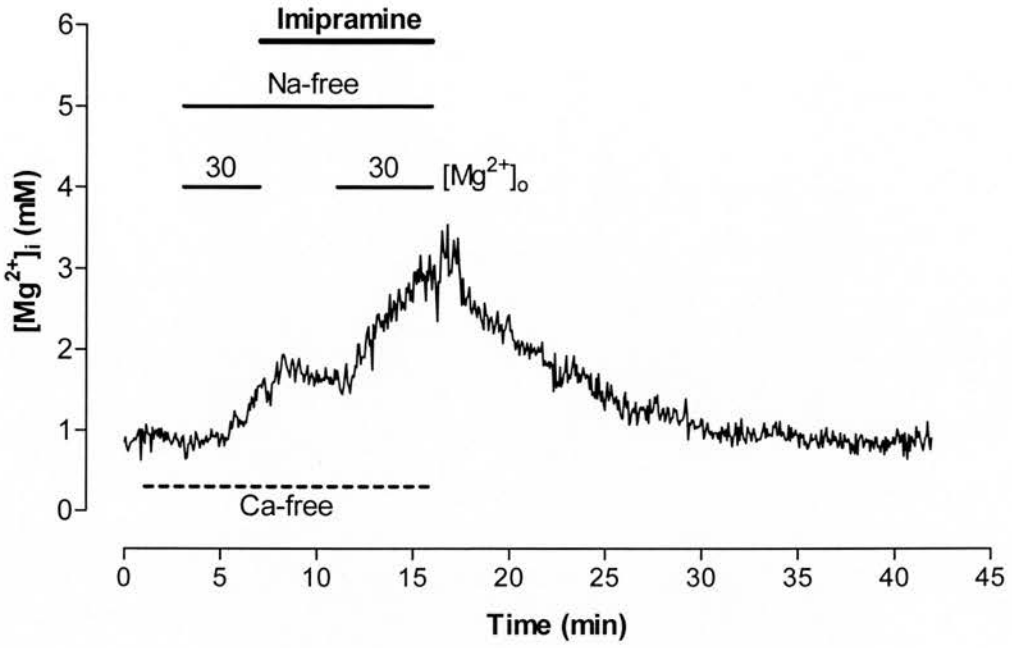

Figure 5.3. **Effect of imipramine on $[Mg^{2+}]_i$ elevation**

$[Mg^{2+}]_i$ was increased in two steps separated by a 5 minutes "clamp" period. 200 μM imipramine was applied from the beginning of the "clamp" phase until the end of the second loading. The drug had no effect on the rate of $[Mg^{2+}]_i$ rise over 5 minutes of high-$[Mg^{2+}]$ superfusion. The rate of $[Mg^{2+}]_i$ elevation during imipramine application was almost identical to that in imipramine-free conditions.

5.3.2 Effect of imipramine on $[Mg^{2+}]_i$ reduction

Unlike $[Mg^{2+}]_i$ elevation, imipramine had a profound effect on $[Mg^{2+}]_i$ reduction. Cells were loaded with Mg^{2+} as above, and $[Mg^{2+}]_i$ was "clamped" at the new elevated level for few minutes (Figure 5.4). 200 μM imipramine was added to the "clamp" solution to give time for binding of the drug to the putative Na^+/Mg^{2+} transporter. Re-addition of 140 mM $[Na^+]$ to the superfusate did not cause $[Mg^{2+}]_i$ to recover when 200 μM imipramine was also present. Recovery of $[Mg^{2+}]_i$ was only seen on withdrawal of imipramine from the bathing medium.

The rate constant of $[Mg^{2+}]_i$ change in the presence of imipramine was 0.003 ± 0.001 min^{-1} (n = 3), indicating a minor increase in $[Mg^{2+}]_i$. Removal of imipramine resulted in an immediate recovery of $[Mg^{2+}]_i$ towards initial levels. The rate constant of $[Mg^{2+}]_i$ reduction in normal Tyrode was 0.08 ± 0.01 min^{-1} (n=3), significantly higher than that at imipramine-containing Tyrode ($P < 0.05$). On average, resting $[Mg^{2+}]_i$ in these experiments was initially 0.68 ± 0.13 mM (n = 3). It recovered to 1.07 ± 0.11 mM (n = 3). Although statistically the difference was not significant ($P = 0.2$), the lack of complete recovery could indicate incomplete washout of imipramine.

5.3.3 Effect of KBR on $[Mg^{2+}]_i$ elevation

The effect of 20 μM of KBR, added to the Mg^{2+}-loading solution, on $[Mg^{2+}]_i$ elevation was assessed in cells loaded moderately or heavily with Mg^{2+}. At low Mg^{2+} loadings ($[Mg^{2+}]_i$ < 2 mM), application of 20 μM KBR almost entirely prevented further rise in $[Mg^{2+}]_i$ under Mg^{2+}-loading conditions (n = 3, $P < 0.05$) (Figure 5.5A). On returning to normal Tyrode, $[Mg^{2+}]_i$ recovered to the initial level. $[Mg^{2+}]_i$ continued to rise following withdrawal of the drug from the Mg^{2+}-loading solution, suggesting complete reversibility of the inhibitory effects of KBR on $[Mg^{2+}]_i$ elevation at low Mg^{2+} loadings (n = 1) (Figure 5.5B).

In contrast, addition of 20 μM KBR appeared to have little or no effect on $[Mg^{2+}]_i$ elevation when $[Mg^{2+}]_i$ was raised above 2 mM (Figure 5.6). The maximum rate of $[Mg^{2+}]_i$ elevation in drug-free loading solution was 0.93 ± 0.22 mM min^{-1} (n = 3),

while that in the same high-$[Mg^{2+}]$ medium but containing 20 μM KBR was 0.85 ± 0.13 mM min^{-1} (n = 3). The difference between the two rates was not significant (P = 0.17).

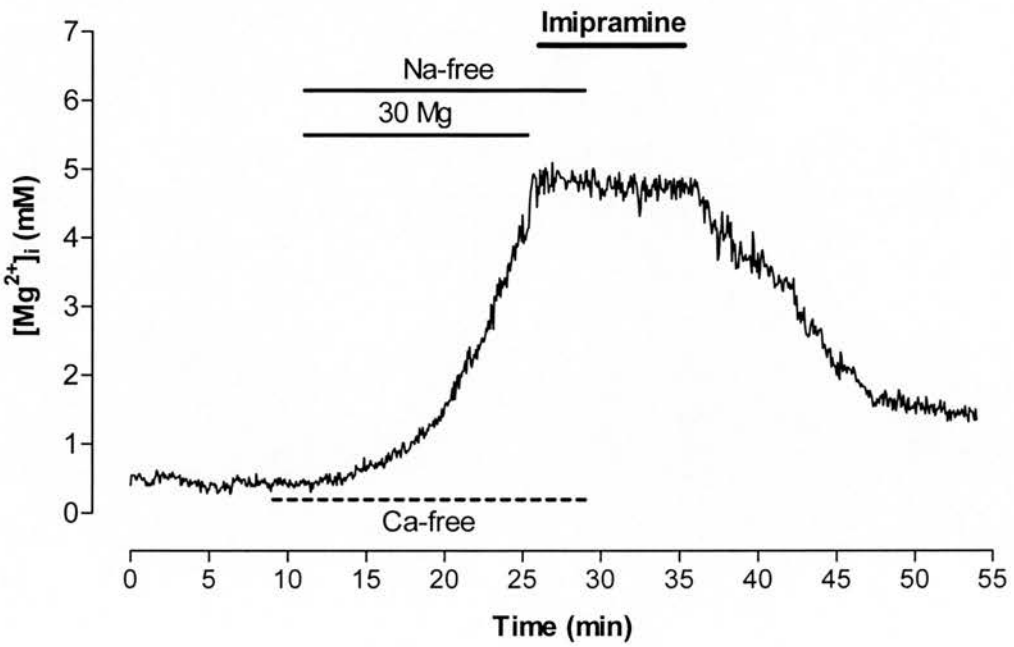

Figure 5.4. **Effect of imipramine on $[Mg^{2+}]_i$ reduction**

$[Mg^{2+}]_i$ was clamped at around 5 mM following 15 minutes superfusion with Mg^{2+}-loading solution, and the effect of 200 μM imipramine on $[Mg^{2+}]_i$ reduction was examined by adding the drug to normal Tyrode. Superfusion of the cell with the imipramine-containing Tyrode, completely inhibited $[Mg^{2+}]_i$ recovery. The cell recovered from the Mg^{2+}-load only on removal of the drug. In this experiment $[Mg^{2+}]_i$ did not fully recover to the initial level. This could be attributed to incomplete washout or to toxic effects of the drug.

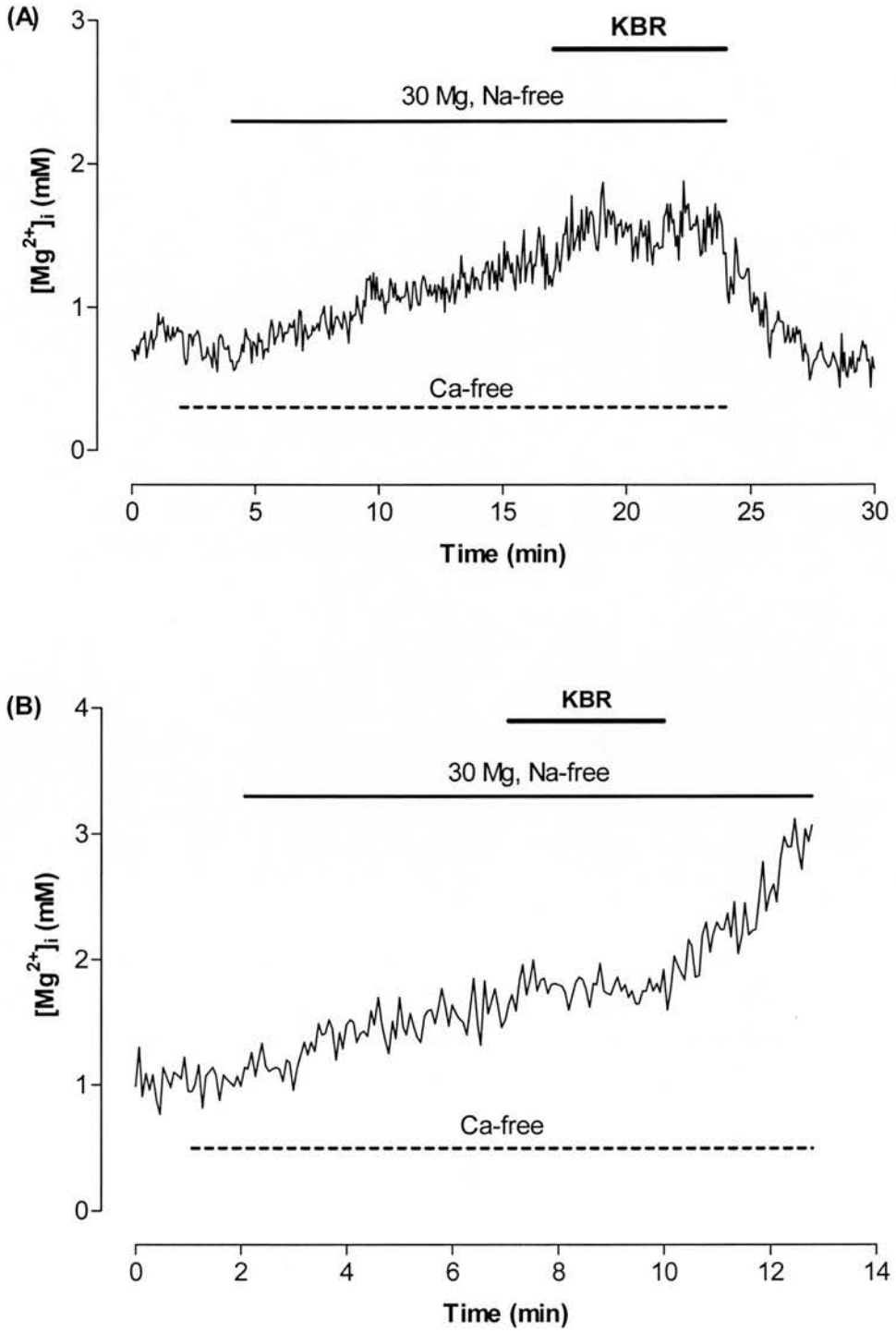

Figure 5.5. Effect of KBR on $[Mg^{2+}]_i$ elevation at low Mg^{2+}-loading

The application of 20 μM KBR slows further increase in $[Mg^{2+}]_i$ when applied during a "modest" Mg^{2+} load. The cell fully recovered from the Mg^{2+} load **(A)**. The inhibitory effect of the drug was completely reversible following its withdrawal **(B)**, in which case $[Mg^{2+}]_i$ continued to rise under the influence of the loading solution.

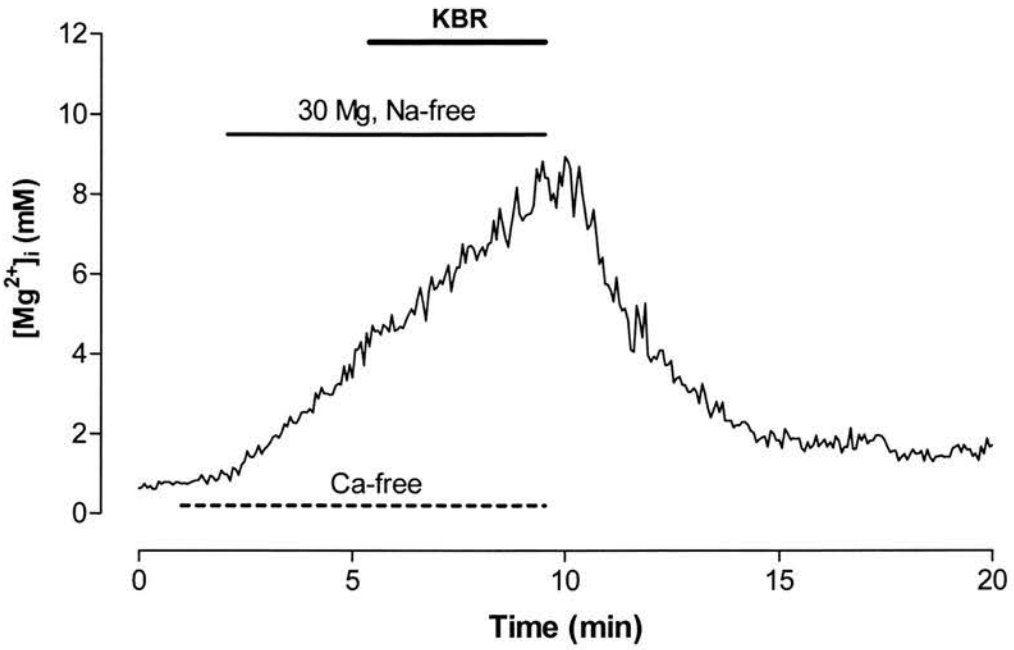

Figure 5.6. Effect of KBR on $[Mg^{2+}]_i$ elevation applied at high Mg^{2+} load

Application of 20 μM KBR following elevation of $[Mg^{2+}]_i$ to values exceeding 2 mM, had no significant effect on the rate of $[Mg^{2+}]_i$ elevation.

5.3.4 Effect of KBR on $[Mg^{2+}]_i$ reduction

These experiments were performed to obtain pharmacological evidence on the effect of KBR on the putative Na^+/Mg^{2+} antiport. $[Mg^{2+}]_i$ was raised in these cells to values appreciably higher than resting levels using the Mg^{2+}-loading solution. $[Mg^{2+}]_i$ was then "clamped" at the new elevated levels in the presence of 20 μM KBR to allow enough time for the drug to bind to its target site on the membrane. After a few minutes cells were allowed to recover from the high Mg^{2+} load in normal Tyrode, which also contained 20 μM KBR. The drug had no effect on $[Mg^{2+}]_i$ reduction and the recovery was almost complete in all experiments (n = 5) (Figure 5.7). The mean rate constant of $[Mg^{2+}]_i$ reduction was 0.32 ± 0.05 min^{-1} (n = 5), not significantly different from that obtained in normal Tyrode (0.34 ± 0.04 min^{-1} , n = 15, $P > 0.05$).

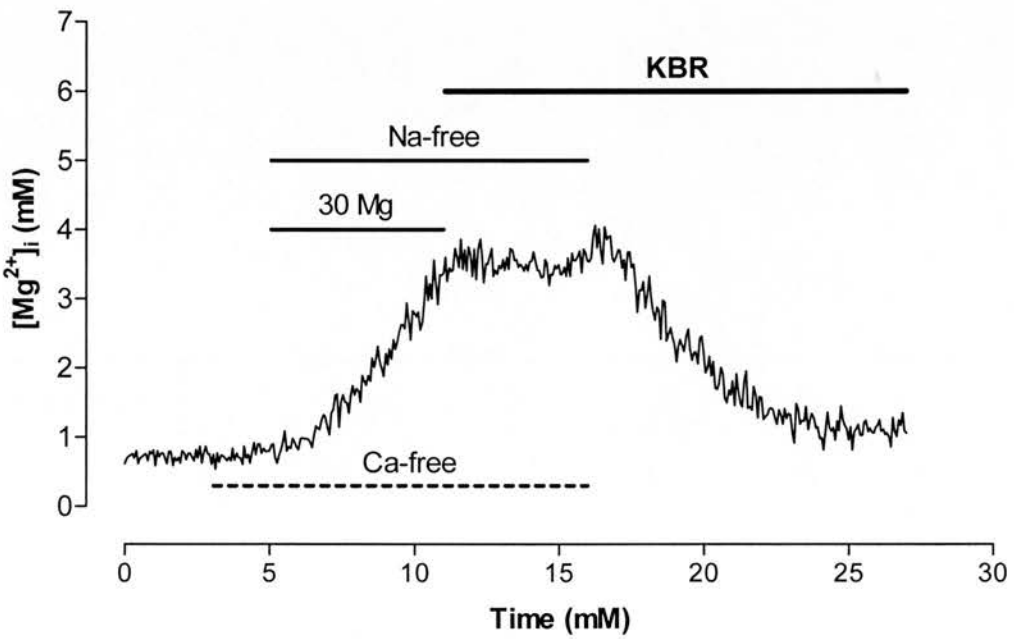

Figure 5.7. **Effect of KBR on $[Mg^{2+}]_i$ reduction**

The drug was applied 5 minutes before readdition of Na^+ to the medium to ensure adequate binding to target site(s). The recovery of $[Mg^{2+}]_i$ towards resting level was not affected by the presence of 20 μM KBR.

5.4 Discussion

There is substantial evidence that imipramine inhibits Na^+-stimulated Mg^{2+} efflux and/or influx in a variety of tissues (see section 5.1). In the present experiments 200 μM imipramine completely abolished the Na^+-stimulated $[Mg^{2+}]_i$ reduction (Figure 5.4). This is consistent with the observation by Handy *et al.* (1996) and Tashiro & Konishi (2000) who reported similar results in isolated rat ventricular myocytes.

The inhibition by imipramine of the Na^+-stimulated $[Mg^{2+}]_i$ reduction is most likely explained by the operation of a Na^+/Mg^{2+} exchange in rat ventricular myocytes. Both this study and the study by Tashiro & Konishi (2000) used 200 μM imipramine to achieve total inhibition of the Na^+-stimulated $[Mg^{2+}]_i$ reduction, although the experimental temperatures were different. The effect of other imipramine concentrations on $[Mg^{2+}]_i$ reduction were not tested in this study. However, Tashiro & Konishi (2000) calculated a half-inhibitory concentration of ~ 80 μM.

As discussed in Chapter 4 (Section 4.4), Mg^{2+}-loading appears to occur in two phases, an initial slow, followed by a faster one, with a possible $[Mg^{2+}]_i$ cut-off point at approximately 2 mM. The evidence from this study suggests that 200 μM imipramine does not inhibit $[Mg^{2+}]_i$ elevation when $[Mg^{2+}]_i$ is raised above 2 mM (Figure 5.3). Previously Handy *et al.* (1996) have shown that at a lower $[Mg^{2+}]_i$, 10 μM imipramine inhibited $[Mg^{2+}]_i$ elevation. However, a comparison between the results obtained in the present study and those Handy *et al.* (1996) is not straightforward. In the present study cells were loaded by superfusion with a Na^+- and Ca^{2+}-free solution containing 30 mM $[Mg^{2+}]$. Handy *et al.* (1996) loaded cells by superfusion with a similar solution but containing 5 mM $[Mg^{2+}]$, where Na^+ was replaced with K^+. Apart from the possible influence of K^+ on Mg^{2+} loading, which will be discussed in the next chapter, the results support the notion that the *early* rise in Mg^{2+} might occur through reverse Na^+/Mg^{2+} exchange, since imipramine (10 μM) was shown to inhibit such rise (Handy *et al.*, 1996). However, above the suggested 2 mM threshold, other – imipramine-insensitive – Mg^{2+} uptake mechanism(s) might dominate.

The effect of imipramine appeared to be reversible. In the majority of cells, subjected for about 10 minutes to 200 μM imipramine either during loading or recovery, $[Mg^{2+}]_i$ recovered to a slightly higher value than the initial level on withdrawal of the drug. This might indicate incomplete drug washout.

In summary, imipramine at a concentration of 200 μM completely inhibited the Na^+-stimulated $[Mg^{2+}]_i$ reduction, while the same concentration had no effect on Mg^{2+} loading. These results are consistent with the presence of a Na^+/Mg^{2+} antiport in mammalian cardiac myocytes as the principal mechanism of Mg^{2+} efflux. The lack of inhibition by imipramine of $[Mg^{2+}]_i$ elevation under loading conditions could be explained by the insensitivity of reverse Na^+/Mg^{2+} exchange to the drug, and therefore, does not necessarily rule out the influx of Mg^{2+} through the putative antiport.

KBR has produced contrasting results as far as $[Mg^{2+}]_i$ elevation is concerned. Below an $[Mg^{2+}]_i$ of about 2 mM, 20 μM KBR completely inhibited Mg^{2+}-loading (Figure 5.5), while little inhibitory effect was observed when the drug was applied at $[Mg^{2+}]_i$ above 2 mM (Figure 5.6). These results suggest that raising $[Mg^{2+}]_i$ from its resting (sub-millimolar) value to just below 2 mM may occur through the Na^+/Ca^{2+} exchanger working in reverse mode and carrying Mg^{2+} instead of Ca^{2+}. Alternatively, KBR may inhibit the putative Na^+/Mg^{2+} antiport, although evidence for such interaction is still lacking. However, if $[Mg^{2+}]_i$ was allowed to exceed 2 mM, other Mg^{2+} influx routes might become activated. These routes are not, or are very weakly, inhibited by 20 μM KBR.

The idea that Mg^{2+} and Ca^{2+} may share a common transporter is still speculative. As mentioned earlier in this chapter, it has been shown that the Na^+/Ca^{2+} exchanger can mediate Mg^{2+} efflux in exchange for Na_o^+ (Tashiro *et al.*, 2000). However, the same authors also concluded that Mg^{2+} influx in exchange for Na_i^+ might occur through reverse Na^+/Ca^{2+}. Under the present experimental conditions, Na_i^+ efflux either through reverse Na^+/Mg^{2+} or Na^+/Ca^{2+} exchange can only be supported during the

first few minutes of superfusion with the, Na^+-free, Mg^{2+} loading solution. Thereafter, $[Na^+]_i$ would be too low to promote Mg^{2+} influx through a Na^+-dependent exchange mechanism. The recorded increase in $[Mg^{2+}]_i$ observed prior to application of 20 μM KBR (Figures 5.5 A&B) occurred during the first 10 minutes in the loading solution. Therefore, since the rise in $[Mg^{2+}]_i$ was completely inhibited by KBR, $[Mg^{2+}]_i$ elevation might have occurred through reversal of the Na^+/Ca^{2+} exchanger carrying Mg^{2+} instead of Ca^{2+}. Another possibility is that KBR inhibited $[Mg^{2+}]_i$ elevation by inhibiting reverse Na^+/Mg^{2+} exchange. Similarities exist between KBR and imipramine with regard to their inhibitory action on the early rise of $[Mg^{2+}]_i$ under loading conditions. Imipramine, at a concentration of 10 μM, was found to inhibit the early increase in $[Mg^{2+}]_i$ associated with superfusing myocytes with a loading solution containing 5 mM $[Mg^{2+}]$ (Handy *et al.*, 1996). Currently, it is premature to speculate too far about the involvement of the Na^+/Ca^{2+} exchanger in Mg^{2+} transport. This is because while the effect of KBR on the Na^+/Ca^{2+} exchanger working in reverse mode is well established, no data are available on its action on a putative Na^+/Mg^{2+} exchanger molecule. Conversely, no information is available on the effect of imipramine on the Na^+/Ca^{2+} exchanger.

When Mg^{2+}-loaded cells were superfused with normal Tyrode, the Na^+/Ca^{2+} exchanger would be expected to operate in the forward or Ca^{2+} extrusion mode, which is only very weakly inhibited by KBR (Iwamoto *et al.*, 1996). The Na^+-dependent $[Mg^{2+}]_i$ reduction was insensitive to 20 μM KBR (Figure 5.7). This indicates that KBR does not affect the forward mode of a putative, reversible Na^+/Mg^{2+} antiport, just as it does not affect the forward mode of the Na^+/Ca^{2+} exchanger.

In summary, 20 μM KBR did not inhibit the Na^+-dependent $[Mg^{2+}]_i$ reduction and caused little or no inhibition of the rise in $[Mg^{2+}]_i$ at heavy loads. The main effect of KBR was however, seen on the early rise of $[Mg^{2+}]_i$ under loading conditions. The interpretations of the results are complicated by the lack of information on the actions of KBR and imipramine on the putative Na^+/Mg^{2+} antiport molecule and Na^+/Ca^{2+} exchanger respectively. More experiments are required to resolve this

issue, probably utilising the purification and transfection of the Na^+/Ca^{2+} exchanger molecule in less complicated systems than cardiac cells.

CHAPTER 6

VOLTAGE-DEPENDENCE OF MAGNESIUM TRANSPORT

6.1 INTRODUCTION

The relationship between membrane potential and the concentration of any ion at both sides of the membrane at equilibrium is given by the Nernst equation (e.g. Hille, 1992):

$$E_{ion} = \frac{RT}{zF} \ln \frac{[Ion]_o}{[Ion]_i} \quad \text{.....(1)}$$

where E_{ion} is the equilibrium potential, z is the charge of the ion, R is the gas constant, T is the absolute temperature, F is the Faraday's constant and $[Ion]_o$ and $[Ion]_i$ are the concentrations of the ion outside and inside the cell, respectively. The Nernst equation can be extended to calculate the equilibrium potential of an antiport. In this case the equilibrium potential, also known as the reversal potential (E_r), is the membrane potential at which the net flux of ions through the antiport is equal to zero. In the case of a Na^+/Mg^{2+} antiport, this is defined by the following equations (McGuigan *et al.*, 2002):

$$E_r = 2E_{Mg} - E_{Na} \quad \text{..... (2)} \quad \text{for 1 } Na^+/\text{ 1 } Mg^{2+} \text{ exchange}$$

or $$E_r = 2E_{Mg} - 3E_{Na} \quad \text{.....(3)} \quad \text{for 3 } Na^+/\text{ 1 } Mg^{2+} \text{ exchange}$$

where E_r is the reversal potential of the antiport and E_{Mg} and E_{Na} are the equilibrium potentials of Mg^{2+} and Na^+ ions across the cell membrane, respectively. Under normal physiological condition, E_r for 1 Na^+/ 1 Mg^{2+} antiport can be calculated using equation (2) after knowing E_{Mg} and E_{Na} in equation (1). For $[Mg^{2+}]_i$ = 0.75 mM, $[Mg^{2+}]_o$ = 1 mM, $[Na^+]_i$ = 10 mM and $[Na^+]_o$ = 140 mM; and RT/F at 37 °C = 26.73 mV:

E_{Mg} = +4 mV and E_{Na} = +70 mV

Using equation (2) gives a E_r = – 62 mV.

Since there is a net loss of one positive charge (carried by Mg^{2+}), membrane potentials more positive than – 62 mV result in Mg^{2+} efflux while more negative

potentials lead to Mg^{2+} influx through the antiport. If the same parameters were applied to a 3 Na^+/ 1 Mg^{2+} antiport, then the system will have a E_r of approximately +200 mV. However, since there is a net gain of one positive charge (carried by Na^+), membrane potentials more positive than E_r should lead to Mg^{2+} influx and vice versa. Therefore, apart from the difference in E_r between the two models, cell depolarisation increases Mg^{2+} efflux and decreases influx in the case of a 1 Na^+/ 1 Mg^{2+} antiport, while the opposite is true for a 3 Na^+/ 1 Mg^{2+} antiport. The accuracy of the calculated E_r in either case depends mainly on the true $[Na^+]_i$ and $[Mg^{2+}]_i$, and therefore unless $[Mg^{2+}]_i$ and $[Na^+]_i$ are measured reliably and simultaneously in the preparation, the E_r values calculated above should be considered approximate.

The Na^+-dependence of $[Mg^{2+}]_i$ reduction studied in chapter 3 suggests that Mg^{2+} is extruded from cardiac myocytes through a Na^+/Mg^{2+} antiport exchanging 1 Na^+ ion for each Mg^{2+} ion. This makes the antiport electrogenic and it should be sensitive to changes in membrane potential in the way described above. Therefore, quiescent myocytes (mean E_m = –74 mV) maintained in normal Tyrode will be expected to slowly accumulate Mg^{2+}. However, no detectable change in $[Mg^{2+}]_i$ was observed in myocytes bathed in normal Tyrode in this or other studies. This could reflect (1) low permeability of the sarcolemma to Mg^{2+} (2) insensitivity of mag-fura-2 to small changes in $[Mg^{2+}]_i$ and (3) a powerful intracellular buffering system, that defends the cell against changes in $[Mg^{2+}]_i$. The failure of experiments that attempted to manipulate $[Mg^{2+}]_i$ simply by raising $[Mg^{2+}]_o$ in an otherwise physiological medium underscores both the low permeability of the sarcolemma to Mg^{2+} as well as the effectiveness of this buffering system, which is mainly comprised of cytosolic ATP, polyanions and the mitochondria. Though Mg^{2+} intracellular buffering capacity might be capable of correcting small and slow changes in $[Mg^{2+}]_i$, it would be vulnerable to sudden and more profound alterations especially under pathological conditions such as ischemia. Therefore, it is questionable whether such a regulatory system, unaided by an active Mg^{2+} efflux mechanism, could maintain $[Mg^{2+}]_i$ under wide-ranging alterations in $[Mg^{2+}]_o$ and conditions that might affect intracellular buffering capacity.

Evidence in other cell types suggests that Mg^{2+} transport may occur through an electrogenic Na^+/Mg^{2+} antiport. Using imipramine Féray & Garay (1988) found evidence for the existence of a Na^+/Mg^{2+} exchange mechanism in human red blood cells which catalyses the exchange of 3 external Na^+ for each internal Mg^{2+} ion. In agreement with the previous authors Lüdi & Schatzmann (1987) found convincing evidence for the presence of an electrogenic Na^+/Mg^{2+} antiport in human red cells. However, Lüdi & Schatzmann (1987) and Frenkel *et al.* (1989) calculated a 1 to 1 coupling ratio for the transporter rather than 3 to 1, and suggested that the extrusion of Mg^{2+} from these cells has an absolute requirement for ATP as a direct source of energy. Flatman & Smith (1990) on the other hand estimated that 1 Na^+: 1 Mg^{2+} exchange explains maintenance of the physiological level of $[Mg^{2+}]_i$ in ferret red blood cell, where the role of ATP is limited to the activation of the transporter by protein phosphorylation rather than supplying energy for the transport process. From a thermodynamic point of view a 1 to 1 antiport in red cells provides a highly energy-efficient Mg^{2+} extrusion mechanism, and would not require energy input from ATP hydrolysis.

The situation is quite different in excitable cells such as nerve and muscle. The membrane potential in these tissues changes either continuously and rhythmically, as in the case of the heart, or frequently in tissues like smooth muscle and nerve. Therefore, an electrogenic transporter would be affected by the changes in membrane potential. The direction of a particular ion flux through the antiport depends mainly on the stoichiometry of the antiport, and the ions cotransported. For example the work on leech neurons provides strong evidence for the operation of an electrogenic antiport in excitable tissues (Günzel & Schlue, 1996; Günzel & Schlue, 2000). The authors found that $[Mg^{2+}]_i$ in leech neurons and neuropile glial cells may be regulated by a 1 Na^+: 1 Mg^{2+} antiport and an additional Na^+-independent process, and that the contribution of these two mechanisms towards Mg^{2+} extrusion varies in the different types of neurons. Their results were supported by experiments showing that depolarisation by voltage clamp accelerates the rate of Mg^{2+} loss from the cells while the opposite was observed on hyperpolarizing the cells.

In smooth muscle evidence for the presence of an electrogenic Na^+/Mg^{2+} antiport came from a study by Tashiro & Konishi (1997b) in which high $[K^+]$ medium was used to depolarise strips of longitudinal smooth muscle of guinea pig taenia cecum. As opposed to leech neurons, they found that the presence of high $[K^+]$ in the bathing medium accelerates the Na^+-dependent $[Mg^{2+}]_i$ rise, whereas the reverse is observed when preparations were bathed in a low $[K^+]$ medium. These observations are consistent with a 3 Na^+/ 1 Mg^{2+} exchange process, where depolarisation promotes an increase in $[Mg^{2+}]_i$, rather than the decrease expected with a 1 to 1 exchanger, although an effect of the $[K^+]$ *per se* on a Mg^{2+} transport mechanism cannot be entirely excluded.

The experiments by Tashiro & Konishi (2000) on isolated rat ventricular myocytes suggest that Mg^{2+} extrusion in the heart is a Na^+-dependent process exchanging 2 or more Na^+ for each Mg^{2+} ion. The authors have also found that cell depolarisation by high $[K^+]_o$ facilitates Na^+/Mg^{2+} exchange. The authors concluded that the presence of high $[K^+]$ in the bathing medium might lower $[Na^+]_i$ by stimulating Na^+ extrusion through the Na^+/K^+ ATPase, thereby increasing the driving force for the inwardly directed movement of Na^+ ions, or that extracellular K^+ may be directly involved in Mg^{2+} transport.

Involvement of K^+ in Mg^{2+} transport has been implicated in the squid giant axon (Rasgado-Flores *et al.*, 1994). The authors suggest that Cl^- and K^+ are cotransported to counteract charge movement across the cell membrane. They have presented evidence that intracellular K^+ and Cl^- are involved in a Mg^{2+}-dependent Na^+ efflux. Whether these observations point to a single $[Na^+ + K^+ + Cl^-]$-Mg^{2+} exchanger or are the result of multiple Mg^{2+} transporters working in combination is not clear.

Electroneutral Na^+/Mg^{2+} exchange mechanisms have also been suggested. The early work in squid axon suggest that depolarisation of the cell by increasing external $[K^+]$ does not affect either Mg^{2+} efflux (De Weer, 1976) or the Mg^{2+} content of axons (Caldwell-Violich & Requena, 1979), which suggests that Mg^{2+} transport in the squid axon is electroneutral. In chicken and turkey erythrocytes (Günther & Vormann,

1985) first reported the operation of a 2 Na^+/ 1 Mg^{2+} antiport in the plasma membrane of these cells. A similar stoichiometry has also been suggested in rat ventricular myocytes (Tashiro & Konishi, 2000).

The experiments presented in this chapter are an attempt to obtain information on the effect of cell depolarisation on the rates of $[Mg^{2+}]_i$ elevation and the Na^+-stimulated $[Mg^{2+}]_i$ reduction in cardiac myocytes. If the extrusion of $[Mg^{2+}]_i$ in cardiac cells is through an electrogenic Na^+/Mg^{2+} antiport then changes in the membrane potential should have a clear effect on the rate of $[Mg^{2+}]_i$ reduction in Mg^{2+}-loaded cells. The effect of cell depolarisation on the rate of $[Mg^{2+}]_i$ reduction should therefore provide clues on the stoichiometry of the putative Na^+/Mg^{2+} antiport. If depolarisation accelerates Mg^{2+} loss then this is suggestive of a 1 to 1 exchange process, while on a 3 to 1 Na^+/Mg^{2+} exchange, depolarisation should have an opposite effect. An electroneutral exchange mechanism (2 Na^+/ 1 Mg^{2+}) would not be affected by changes in the membrane potential.

The experiments will also look into the voltage-dependence of $[Mg^{2+}]_i$ elevation under loading conditions. The rate of $[Mg^{2+}]_i$ elevation might also be affected if an electrogenic Na^+/Mg^{2+} antiport, operating in reverse mode, is responsible for Mg^{2+} uptake. The cells were depolarised either by increasing $[K^+]_o$ or by the voltage clamp technique.

6.2 MATERIALS AND METHODS

1. Solutions: The high $[K^+]$, Mg^{2+}-loading solution contained (in mM): $MgCl_2$ 30, NMDG 70, KCl 70, HEPES 10, glucose 10; pH adjusted to 7.4 at 37 °C using HCl. High $[K^+]$ Tyrode contained (in mM): $MgCl_2$ 1, NaCl 64, KCl 70, HEPES 10, glucose 10; pH adjusted to 7.4 at 37 °C using NaOH. All other solutions are as previously described.

2. Voltage clamp: Isolated, mag-fura-2-loaded ventricular myocytes were voltage-clamped using the whole-cell configuration of the patch clamp technique. Electrodes were fabricated from thin-walled borosilicate glass capillaries (outer diameter 1.55 mm) using a 5-stage pulling process (see General Materials and Methods, Section 2.6.1). The tips of the pulled glass pipettes were heat-polished and had a resistance of 1 to 3 MΩ in normal Tyrode when filled with a solution designed to mimic the intracellular medium (in mM): potassium aspartate 120, KCl 20, NaCl 10, Mg.ATP 5, $CaCl_2$ 0.2, EGTA 10, HEPES 10. The pH was adjusted to 7.2 at 37 °C using KOH. The osmolarity was 320 ± 3 mOsm (n = 3). Once a whole-cell patch configuration was achieved, the series resistance was typically < 15 MΩ before compensation. No more than 50% of the series resistance was compensated. Voltage clamp was performed in the continuous single-electrode voltage clamp mode of the clamp unit.

6.3 RESULTS

6.3.1 Effect of high $[K^+]$ on $[Mg^{2+}]_i$ elevation

To examine the effect of high $[K^+]$ on $[Mg^{2+}]_i$ elevation, myocytes were superfused with the high $[K^+]$, Mg^{2+}-loading solution for a few minutes before changing over to the standard loading solution, which contained 6 mM $[K^+]$ (Figure 6.1). The maximum rate of $[Mg^{2+}]_i$ elevation achieved under the two conditions was then compared.

The maximum rate of $[Mg^{2+}]_i$ elevation in standard loading solution was 0.53 ± 0.06 mM min^{-1} (n = 8). This was significantly greater than the maximum rate of $[Mg^{2+}]_i$ elevation in the presence of 70 mM $[K^+]$ (0.13 ± 0.02 mM min^{-1}, $P < 0.01$).

6.3.2 Effect of high $[K^+]_o$ on $[Mg^{2+}]_i$ reduction

$[Mg^{2+}]_i$ was first increased in cells by superfusion with standard loading solution. $[Mg^{2+}]_i$ was "clamped" at the new level for a few minutes by reducing $[Mg^{2+}]$ in the superfusate from 30 to 1 mM (clamp solution). 70 mM Na^+ was then introduced in the bathing medium and $[Mg^{2+}]_i$ was allowed to recover towards baseline levels for approximately 5 minutes, before switching to a solution that contained the same $[Na^+]$ but in which $[K^+]$ was increased from 6 to 70 mM as shown in Figure 6.2.

The rate constant of $[Mg^{2+}]_i$ reduction at 70 mM $[Na^+]_o$ and normal $[K^+]_o$ was 0.10 ± 0.01 min^{-1} (n = 7). On increasing $[K^+]_o$ to 70 mM, the rate constant of $[Mg^{2+}]_i$ reduction increased to 0.38 ± 0.04 min^{-1} (n = 7). The increase was significant ($P <$ 0.01).

6.3.3 Effect of depolarisation by voltage clamp on $[Mg^{2+}]_i$ elevation

Single-electrode voltage clamp was used to further address the issue of the sensitivity of $[Mg^{2+}]_i$ elevation in cardiac myocytes to changes in membrane potential. Initially, myocytes were clamped at –80 mV in normal Tyrode and subjected to the standard loading protocol as previously described (Figure 6.3A). Once $[Mg^{2+}]_i$ was raised, the membrane potential was stepped to 0 mV.

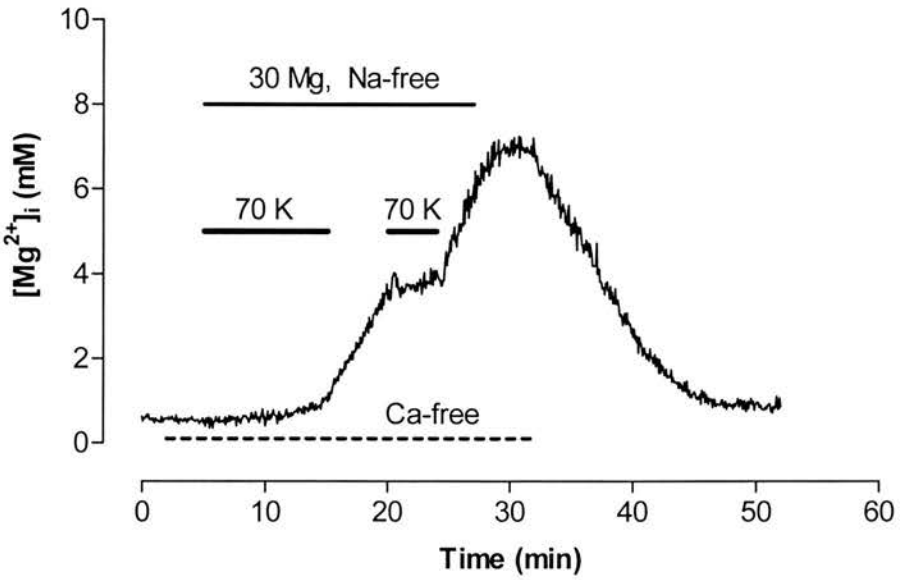

Figure 6.1. **Effect of high $[K^+]_o$ on $[Mg^{2+}]_i$ elevation**

Mag-fura-2 fluorescence trace showing changes in $[Mg^{2+}]_i$ during a protocol designed to examine the effect of cell depolarisation by 70 mM $[K^+]_o$ on the maximum rate of $[Mg^{2+}]_i$ elevation. In this experiment the protocol was repeated twice. The cell was first superfused with normal Tyrode for a few minutes, and then external Ca^{2+} was removed for 2 minutes before the bathing medium was changed to a loading solution containing 70 mM $[K^+]$. Over the next 12 minutes, $[Mg^{2+}]_i$ increased slightly above the initial level at a slow rate. However, when $[K^+]_o$ was reduced to 6 mM, the rate of increase in $[Mg^{2+}]_i$ increased significantly, and in 5 minutes a 4-fold increase in $[Mg^{2+}]_i$ was observed. The same protocol was then repeated over the next 10 minutes, showing a similar pattern. Unless otherwise specified (mM): $[K^+]_o$ = 6 mM, $[Na^+]_o$ = 140, $[Mg^{2+}]_o$ = 1 and $[Ca^{2+}]_o$ = 1. NMDG was substituted for Na^+.

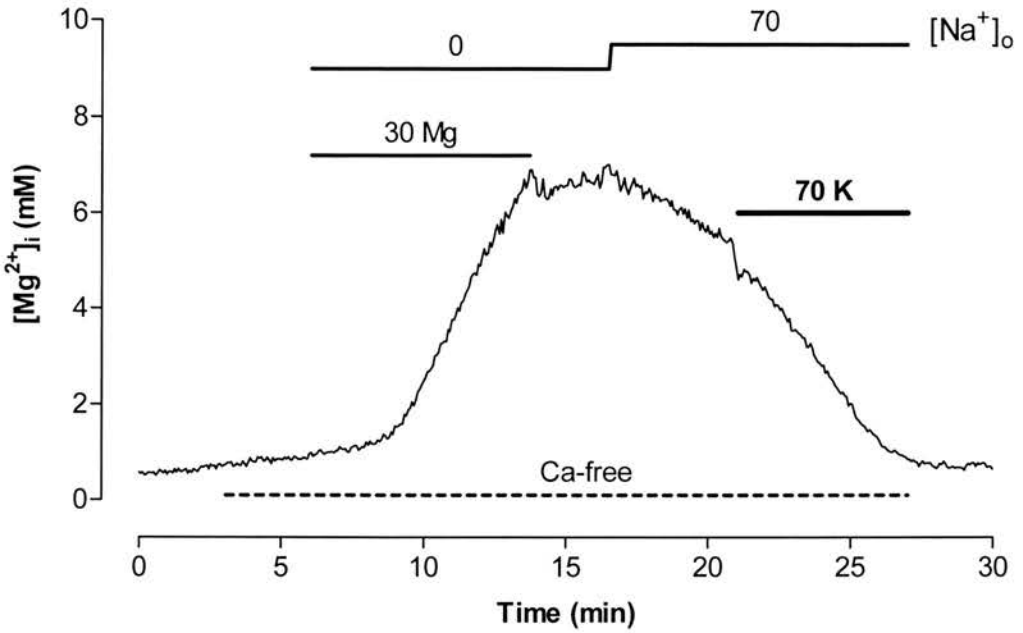

Figure 6.2. **Effect of high $[K^+]_o$ on $[Mg^{2+}]_i$ reduction**

The cell was first loaded with Mg^{2+} in the usual way. $[Mg^{2+}]_i$ in this case increased to about 7 mM over 8 minutes of superfusion with the loading solution. $[Mg^{2+}]_i$ was clamped at this new level for around 3 minutes before 70 $[Na^+]$ was introduced into the bathing medium. Almost immediately $[Mg^{2+}]_i$ began to decline. After 5 minutes of steady decline in $[Mg^{2+}]_i$, the concentration of K^+ in the superfusate was increased from 6 to 70 mM without changing the concentration of Na^+ which was kept at 70 mM to ensure that any change in the rate of decline in $[Mg^{2+}]_i$ is solely due to the high $[K^+]$. The rate of $[Mg^{2+}]_i$ reduction increased significantly over 7 minutes of superfusion with the high $[K^+]$ solution. Unless otherwise specified (mM): $[K^+]_o = 6$, $[Na^+]_o = 140$, $[Mg^{2+}]_o = 1$ and $[Ca^{2+}]_o = 1$.

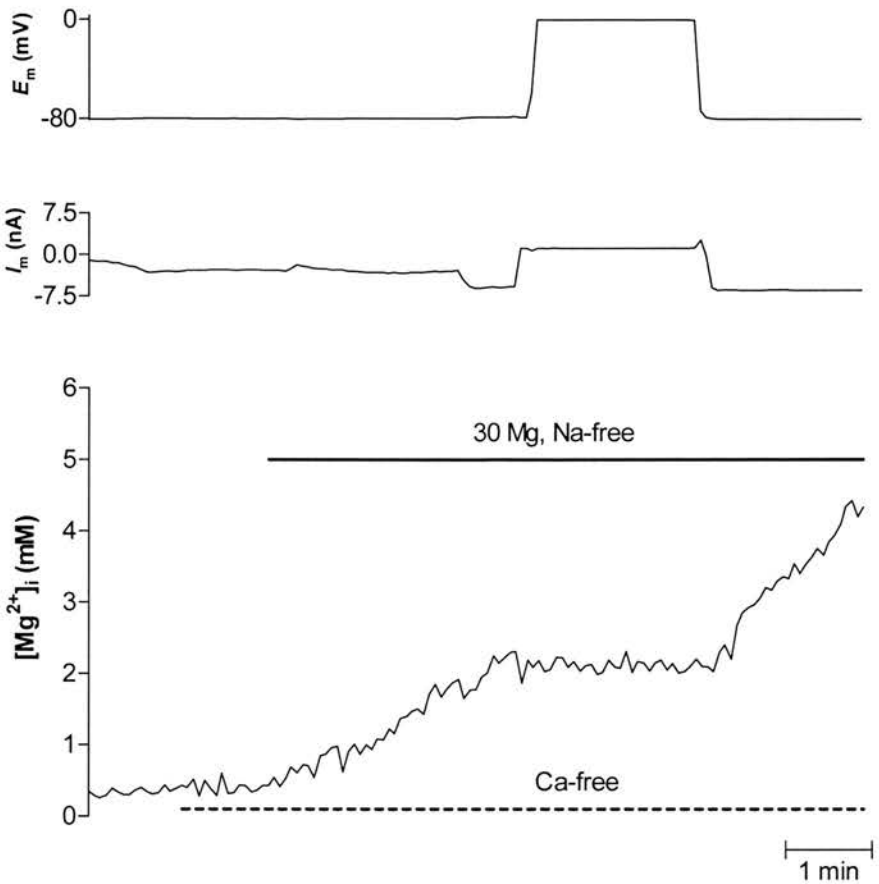

Figure 6.3A. **Effect of cell depolarisation on $[Mg^{2+}]_i$ elevation [1]**

One of three experiments showing the effect of cell depolarisation by voltage clamp on $[Mg^{2+}]_i$ elevation. The elevation was abolished (lower panel) when the cell was depolarised from –80 to 0 mV, and resumed on stepping the membrane potential back to –80 mV. The cell was voltage-clamped in the whole-cell configuration of the patch clamp technique. The patch pipette had a resistance of 3 MΩ in normal Tyrode when filled with the internal solution. Series resistance was less than 10 MΩ at the beginning of the experiment. The cell was voltage-clamped in continuous single-electrode voltage clamp mode.

Three successful experiments were performed in this way. At –80 mV and bathed in normal Tyrode, $[Mg^{2+}]_i$ remained stable and close to the previously measured resting levels. However, once the superfusate was changed to the Mg^{2+}-loading solution $[Mg^{2+}]_i$ began to increase at a maximum rate of 1.5 ± 0.48 mM min^{-1} (n = 3). On stepping the membrane potential, to 0 mV, the rate of $[Mg^{2+}]_i$ elevation reduced significantly (0.32 ± 0.10 mM min^{-1}, n = 3, $P < 0.05$). In one experiment (Figure 6.3A), depolarisation to 0 mV completely abolished the rise in $[Mg^{2+}]_i$, while in the other two experiments (one of which is shown is Figure 6.3B) $[Mg^{2+}]_i$ continued to increase, though at a much slower rate, following depolarisation. In the experiment shown in Figure 6.3B, the membrane potential was stepped from –80 to 0 mV and then from 0 to +50 mV. At +50 mV the rise in $[Mg^{2+}]_i$ was completely abolished. However, when the cell was clamped at –80 once more, $[Mg^{2+}]_i$ continued to rise for about 1 minute at a rate comparable to that at the beginning of the experiment. It is worth mentioning that when the cell voltage was clamped at +50 mV, the current increased dramatically and peaked at about 18 nA. This might be the cause of cell death shortly following stepping the holding potential to –80 mV. None of the cells used in these experiments survived to the stage of recovery from the high Mg^{2+} load, as all the cells died shortly after changing from the loading solution to normal Tyrode while held at –80 mV.

6.3.4 Effect of cell depolarisation by voltage clamp on $[Mg^{2+}]_i$ reduction

(Figure 6.4). Cells were voltage-clamped at –80 mV in normal Tyrode and then loaded with Mg^{2+} (Figure 6.4). $[Mg^{2+}]_i$ was allowed to recover in normal Tyrode towards resting levels. The membrane potential was then changed from –80 to 0 mV or as in the experiment shown in Figure 6.4, recovery in normal Tyrode was initially tested at 0 mV and then at –80 mV. A total of three cells were successfully clamped in this way. The rate constant of $[Mg^{2+}]_i$ recovery at –80 mV was 0.21 ± 0.1 min^{-1} (n = 3). Depolarising the cell from –80 to 0 mV significantly increased the rate constant of $[Mg^{2+}]_i$ reduction (to 0.7 ± 0.1 min^{-1}, n = 3, $P < 0.05$). Only one cell recovered fully from Mg^{2+} load to the initial $[Mg^{2+}]_i$ in normal Tyrode at –80 mV. The other two cells died before full recovery but remained morphologically healthy throughout the period of recording.

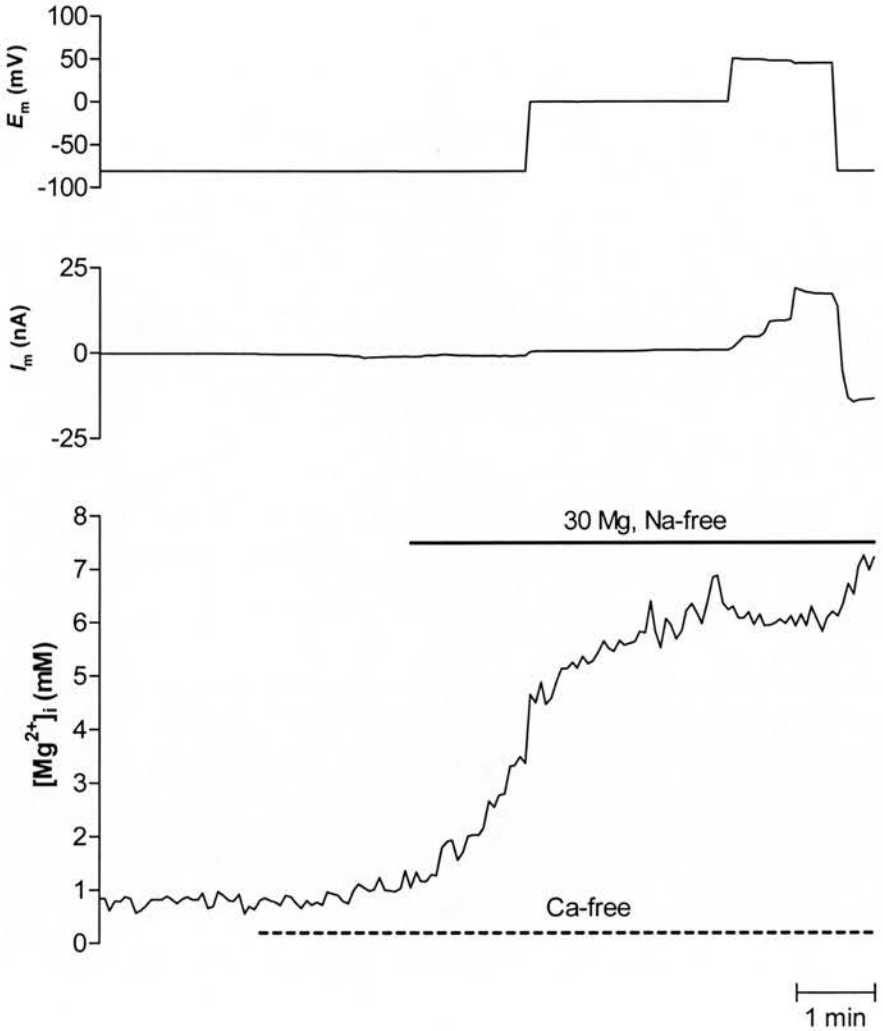

Figure 6.3B. **Effect of cell depolarisation on $[Mg^{2+}]_i$ elevation [2]**

One of two similar experiments showing the effect of cell depolarisation, by voltage clamp, on $[Mg^{2+}]_i$ elevation. In this case $[Mg^{2+}]_i$ was increased to around 5 mM. $[Mg^{2+}]_i$ elevation was reduced by about 80% (lower panel) when the cell was depolarised from –80 to 0 mV. The rate of $[Mg^{2+}]_i$ elevation decreased further when the cell was voltage-clamped to +50 mV. The cell was voltage-clamped in the continuous, single-electrode, whole-cell configuration of the patch clamp technique. The patch pipette had a resistance of 2 MΩ in normal Tyrode when filled with the internal solution. Series resistance was 12 MΩ at the beginning of the experiment.

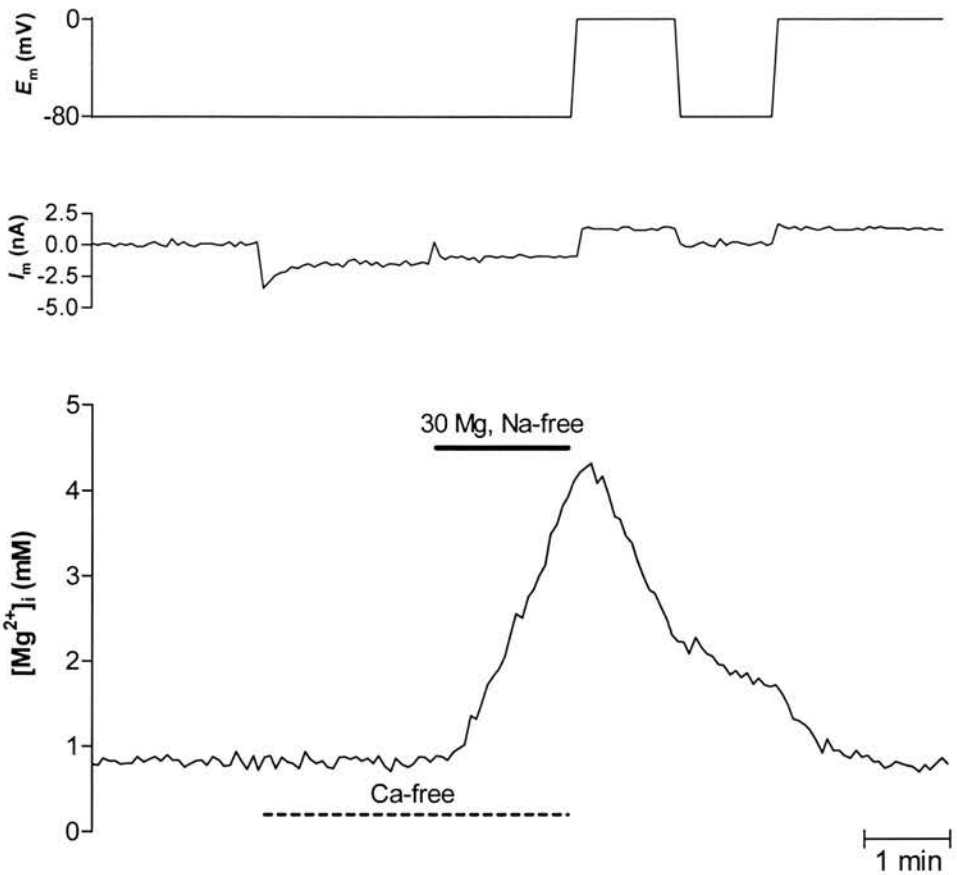

Figure 6.4. **Effect of cell depolarisation on $[Mg^{2+}]_i$ reduction**

Depolarising the cell from –80 mV to 0 mV accelerates the rate of $[Mg^{2+}]_i$ reduction. The cell was voltage-clamped in the whole cell configuration of the patch clamp technique. The patch pipette had a resistance of 5 MΩ in normal Tyrode when filled with the internal solution. Series resistance was less than 12 MΩ at the beginning of the experiment. The cell was voltage-clamped in continuous single-electrode voltage clamp mode.

6.4 Discussion

Two approaches were used to examine the effect of cell depolarisation on Mg^{2+} transport in isolated cardiac myocytes, superfusion with high $[K^+]$ solution and single-electrode voltage clamp. A similar effect on $[Mg^{2+}]_i$ elevation and reduction was observed with both approaches.

6.4.1 Effect of cell depolarisation on $[Mg^{2+}]_i$ elevation

Increasing $[K^+]_o$ to 70 mM in the Mg^{2+} loading solution is expected to depolarise the cell by as much as 50 mV (Chapman, 1973). Therefore, in 70 $[K^+]_o$ the membrane potential is probably around –20 mV. $[Mg^{2+}]_i$ elevation almost ceased under these conditions (Figure 6.1). This indicates that the mechanism(s) responsible for the $[Mg^{2+}]_i$ elevation under loading conditions is sensitive to depolarisation, high $[K^+]_o$ or both. Depolarising the cells either by voltage clamp or high $[K^+]$ had comparable effects on $[Mg^{2+}]_i$ elevation. Several models can be tested to try to understand the mechanism(s) responsible for $[Mg^{2+}]_i$ elevation including, a Na^+/Mg^{2+} antiport and a channel.

Mg^{2+} uptake through a Na^+/Mg^{2+} antiport

The difference between the experiments shown in Figures 6.3A and 6.3B was the variability in the degree of inhibition of $[Mg^{2+}]_i$ elevation caused by cell depolarisation. Cell depolarisation to 0 mV completely inhibited Mg^{2+} loading when $[Mg^{2+}]_i$ had been raised to 2 mM (Figure 6.3 A), whereas it only partially inhibited Mg^{2+} loading when $[Mg^{2+}]_i$ had been raised to 5 mM (Figure 6.3 B). The Nernst equation (see Section 6.1) can be used to test whether the effects of depolarisation in either case could be attributed to Mg^{2+} entry through a 1 Na^+/ 1 Mg^{2+} antiport operating in reverse mode. A 3 Na^+/ 1 Mg^{2+} antiport can be excluded since cell depolarisation would cause an increase in the rate of $[Mg^{2+}]_i$ elevation rather than a decrease.

Figure 6.5 shows the reversal potential (E_r) of a 1 Na^+/ 1 Mg^{2+} antiport, at various $[Mg^{2+}]_i$ values, in cells superfused with the Mg^{2+} loading solution.

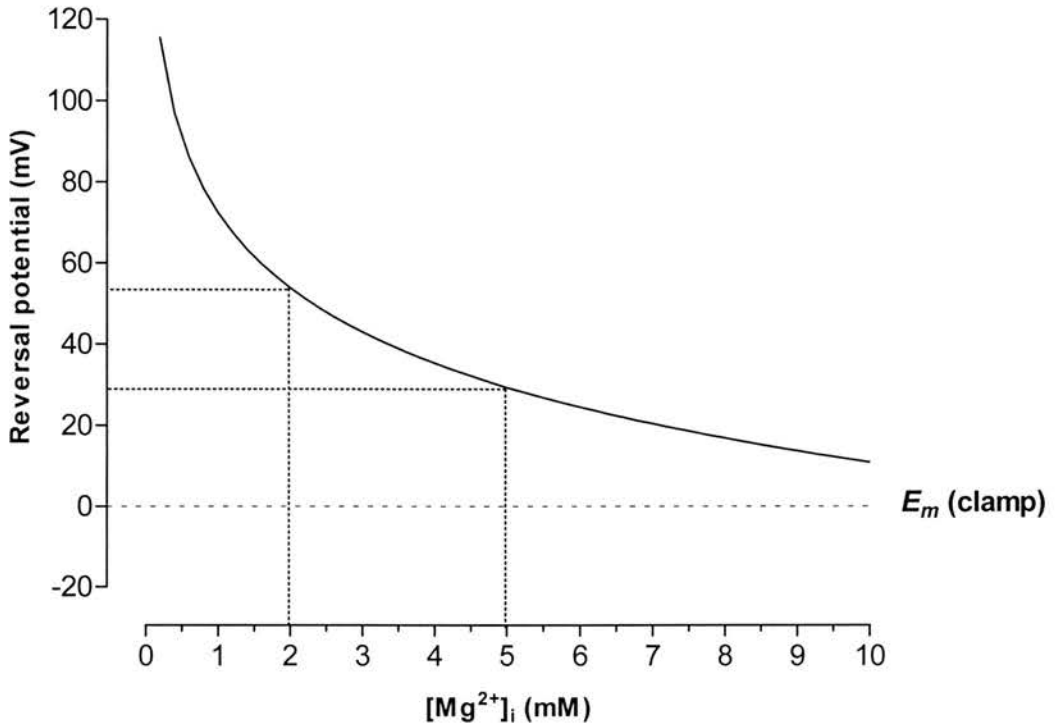

Figure 6.5. Reversal potential of a 1 Na^+/ 1 Mg^{2+} antiport under loading conditions

A model depicting the reversal potential of a putative Na^+/Mg^{2+} antiport with a 1 Na^+/ 1 Mg^{2+} stoichiometry, drawn according to the Nernst equation for reversal potential. The trace predicts the reversal potential of the antiport (zero net Mg^{2+} flux) at different $[Mg^{2+}]_i$ values. Intersect of horizontal and vertical dotted lines show the reversal potential of the antiport at $[Mg^{2+}]_i$ of 2 and 5 mM, under typical Mg^{2+}-loading conditions. As $[Mg^{2+}]_i$ increases the reversal potential becomes less positive. The diagram shows that at the clamp potential of 0 mV (dashed line) the antiport will not reverse at $[Mg^{2+}]_i$ of 2 or 5 mM, and should continue to mediate Mg^{2+} influx. This model is consistent with the idea that cell depolarisation reduces Mg^{2+} influx through reversal of the putative antiport under the Mg^{2+} loading conditions. The model was drawn assuming (in mM): $[Mg^{2+}]_o$ = 30, $[Na^+]_o$ = 1 and $[Na^+]_i$ = 0.5, at an experimental temperature of 37 °C.

In order to calculate E_r (equation (2) in Section 6.1), the internal and external concentrations of Na^+ and Mg^{2+} must be entered into the formula. Therefore, $[Mg^{2+}]_o$ was set at 30 mM ($[Mg^{2+}]$ in the loading solution), while $[Na^+]_i$ and $[Na^+]_o$ had to be set to arbitrary values. Removal of external Na^+ will decrease $[Na^+]_o$ to values close to 0 mM after some time. But since trace Na^+ will most likely be present, $[Na^+]_o$ was set to 1 mM. The concentration of internal Na^+ decreases to 0.34 mM after superfusing cardiac tissue with a nominally Na^+-free solution for long periods of time (Ellis & Macleod, 1985). Therefore, a value of 0.5 mM was chosen because of the shorter exposure of cells to Na^+-free conditions in the present experiments. For accurate calculation of E_r, both internal and external Na^+ concentrations should be determined. However, this would have been difficult to do under the current conditions.

The model predicts that where $[Mg^{2+}]_i$ has been increased to approximately 2 mM (Figure 6.3A) or 5 mM (Figure 6.3B), the antiport will have reversal potentials of +54 and +29 mV respectively. Therefore, with a Mg^{2+} load of 2 mM, depolarising the cell to 0 mV would not be sufficient to stop $[Mg^{2+}]_i$ elevation by reversal of a putative antiport alone. The complete cessation of uptake seen when cells were depolarised to 0 mV as in Figure 6.3A therefore suggests that other mechanisms might be involved.

At a Mg^{2+} load of 5 mM (Figure 6.3B), cell depolarisation to 0 mV significantly reduced the rate of $[Mg^{2+}]_i$ elevation. Depolarising the cell further to 50 mV completely stopped Mg^{2+} loading. In this case the effect of depolarisation on $[Mg^{2+}]_i$ elevation is consistent with Mg^{2+} entry through the putative Na^+/Mg^{2+} antiport operating in reverse mode as predicted by the model.

A possible explanation for the contrasting effect of cell depolarisation on $[Mg^{2+}]_i$ elevation under loading conditions (Figures 6.3 A & B) assumes a role for the intracellular Mg^{2+} buffering capacity, which is more powerful when $[Mg^{2+}]_i$ is 2 mM than when it is 5 mM, in defending the cell against an increase in $[Mg^{2+}]_i$. This is because the ability of the buffering system to "absorb" excess Mg^{2+} during loading

diminishes as more Mg^{2+} enters the cell. Thus a small flux of Mg^{2+} may not be detectable as a change of $[Mg^{2+}]_i$ at 2 mM whereas the same flux would be detectable at 5 mM. This might explain the apparent complete inhibition of $[Mg^{2+}]_i$ increase at 2 mM internal Mg^{2+} concentration where the influx of Mg^{2+} was masked by a powerful buffering system. At 5 mM $[Mg^{2+}]_i$ the same flux of Mg^{2+} was easily detectable because the buffering capacity has been overwhelmed.

Mg^{2+} uptake through a channel

A simple Mg^{2+} channel could in theory provide an influx/efflux route for Mg^{2+} in cardiac cells. Assuming Ca^{2+} and/or Na^+ or other major cations such as K^+ do not affect this channel, Mg^{2+} movement across this channel would depend on three parameters, $[Mg^{2+}]_i$, $[Mg^{2+}]_o$ and the membrane potential. Under typical loading conditions, a simple Mg^{2+} channel that allows movement of Mg^{2+} in both directions across the cell membrane would have a reversal potential of approximately +48 mV when $[Mg^{2+}]_i$ is 0.75 mM. The reversal potential of the channel becomes less positive as $[Mg^{2+}]_i$ increases (Figure 6.6). At 2 mM $[Mg^{2+}]_i$ the reversal potential is about +36 mV, which decreases to +24 mV as $[Mg^{2+}]_i$ approaches 5 mM.

In Figure 6.3A, the complete cessation of $[Mg^{2+}]_i$ increase is not compatible with a simple Mg^{2+}-permeable channel (Figure 6.6). However, as discussed above, a role for intracellular buffering sites cannot be excluded. The findings may be consistent with another model for Mg^{2+} uptake, namely a voltage-gated, Mg^{2+}-permeable channel. However, two other experiments (e.g. Figure 6.3B), where depolarisation did not completely abolish the rise of $[Mg^{2+}]_i$ when $[Mg^{2+}]_i$ was 5 mM, do not support this idea. The most likely explanation is that Mg^{2+} influx occurs through a variety of transporters. Here there would appear to be a dominant conductance that "switches off" when cells are depolarised. In this case, the observation that $[Mg^{2+}]_i$ continues to rise in some cells may show that other putative transporters that are still functioning and the difference in the response of cells to depolarisation may reflect that the density of these transporters varies among cells. This could in fact also explain the variability in Mg^{2+} loading among cells.

It is unlikely that reverse Na^+/Mg^{2+} exchange provides the main route for Mg^{2+} influx in the heart under the specific loading conditions. This is further supported by the fact that $[Na^+]_i$ in the cells studied is probably very low following superfusion with the Mg^{2+} loading solution (Ellis & MacLeod, 1985; Ödblom & Handy, 2001). Such a low level would not be expected to support reverse Na^+/Mg^{2+} exchange. However, a 1 Na^+/ 1 Mg^{2+} antiport might mediate Mg^{2+} influx under physiological or pathological conditions provided the antiport is reversible, especially since the calculated reversal potential of 1 Na^+/ 1 Mg^{2+} exchanger is very close to the resting membrane potential of ventricular myocytes bathed in normal Tyrode (Figure 6.7).

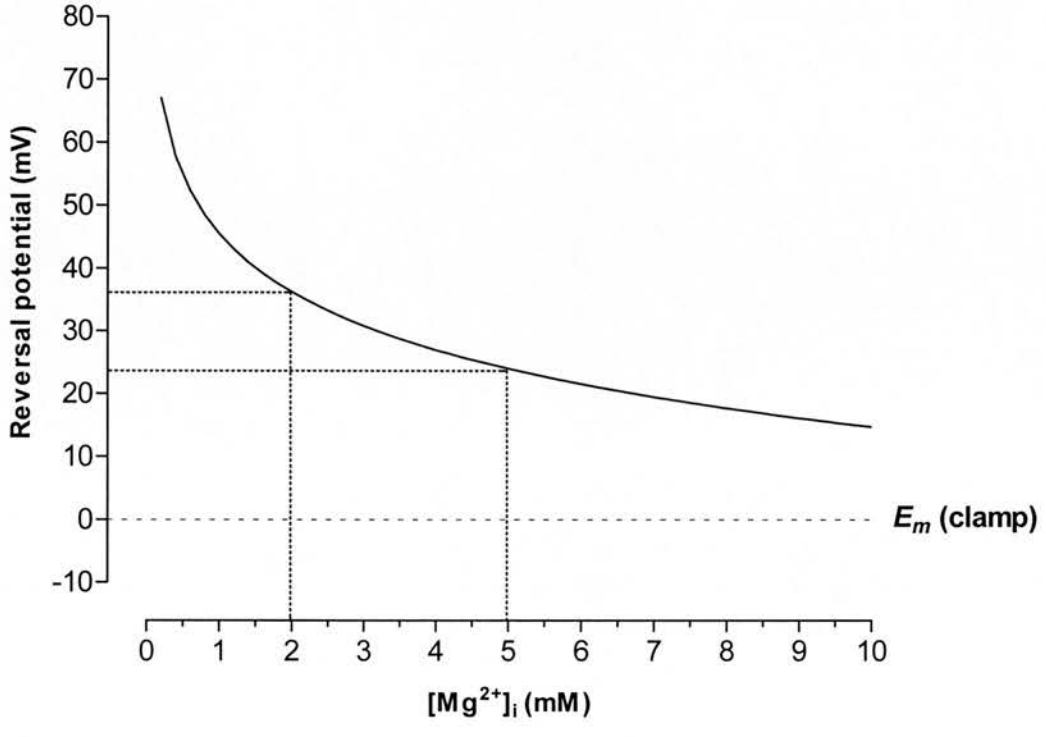

Figure 6.6. Reversal potential of a simple Mg^{2+} channel under loading conditions

Mg^{2+} uptake through a channel under loading conditions is reduced by cell depolarisation. The trace shows that as $[Mg^{2+}]_i$ increases the reversal potential becomes less positive. The reversal potential of a Mg^{2+} channel at 2 and 5 mM $[Mg^{2+}]_i$ (intersect of dotted horizontal and vertical lines) is positive to a holding potential of 0 mV, and therefore at E_m = 0 mV $[Mg^{2+}]_i$ should continue to increase beyond 5 mM. Whereas at a clamp voltage of +50 mV the equilibrium $[Mg^{2+}]_i$ should be less than 1 mM. The calculations were based on the Nernst equation for the electrochemical equilibrium of Mg^{2+} (E_{Mg}), assuming (in mM): $[Mg^{2+}]_o$ = 30, $[Na^+]_o$ = 1 and $[Na^+]_o$ = 0.5, at an experimental temperature of 37 °C.

Additionally, it must be remembered that since $[Na^+]_i$ was not measured, the models are a rough guide to the direction of Mg^{2+} movement across the cell membrane and its reversibility through either a 1 Na^+/ 1 Mg^{2+} antiport or a channel at a particular $[Mg^{2+}]_i$. The effect of the value assumed for $[Na^+]_i$ on the reversal potential of the putative Na^+/Mg^{2+} antiport is highlighted in Figure 6.7.

The experiments were technically demanding, since it was necessary to voltage-clamp the cells using low resistance patch pipettes for 15 to 30 minutes, while being subjected to the loading protocol and continuously illuminated with ultraviolet light. All these factors can affect the cells' viability and hence lower the rate of successful recordings. More experiments are required to further investigate the mechanism of $[Mg^{2+}]_i$ elevation and whether a voltage-gated Mg^{2+} channel is present in cardiac myocytes. It might be necessary, however, to improve on the experimental protocol to prolong cell survival and structural integrity during the course of the experiment.

In conclusion, the above experiments on the effect of cell depolarisation by voltage-clamping were an attempt to explore the mechanisms responsible for $[Mg^{2+}]_i$ elevation under the loading conditions used in this study. Ideally, calculation of the reversal potential of Mg^{2+} fluxes under controlled experimental conditions should provide clear answers as to the mechanisms responsible for Mg^{2+} flux. Unfortunately, these experiments were not conclusive in resolving the matter. The results suggest that the direction of $[Mg^{2+}]_i$ change under voltage clamp conditions is consistent with a 1 Na^+/ 1 Mg^{2+} antiport. However, $[Mg^{2+}]_i$ elevation in myocytes occurs through a variety of routes, perhaps predominantly through a voltage-gated, Mg^{2+}-permeable channel with contributions from reverse Na^+/Mg^{2+} exchange and Na^+ and Ca^{2+} channels.

6.4.2 Effect of cell depolarisation on $[Mg^{2+}]_i$ reduction

Increasing the $[K^+]_o$ or cell depolarisation increased the Na^+-dependent $[Mg^{2+}]_i$ reduction significantly (Figure 6.2 & 6.4). Again as in the case of $[Mg^{2+}]_i$ elevation, these results are consistent with the idea that membrane depolarisation enhances Mg^{2+} loss from Mg^{2+} loaded cells through a 1 Na^+/ 1 Mg^{2+} antiport.

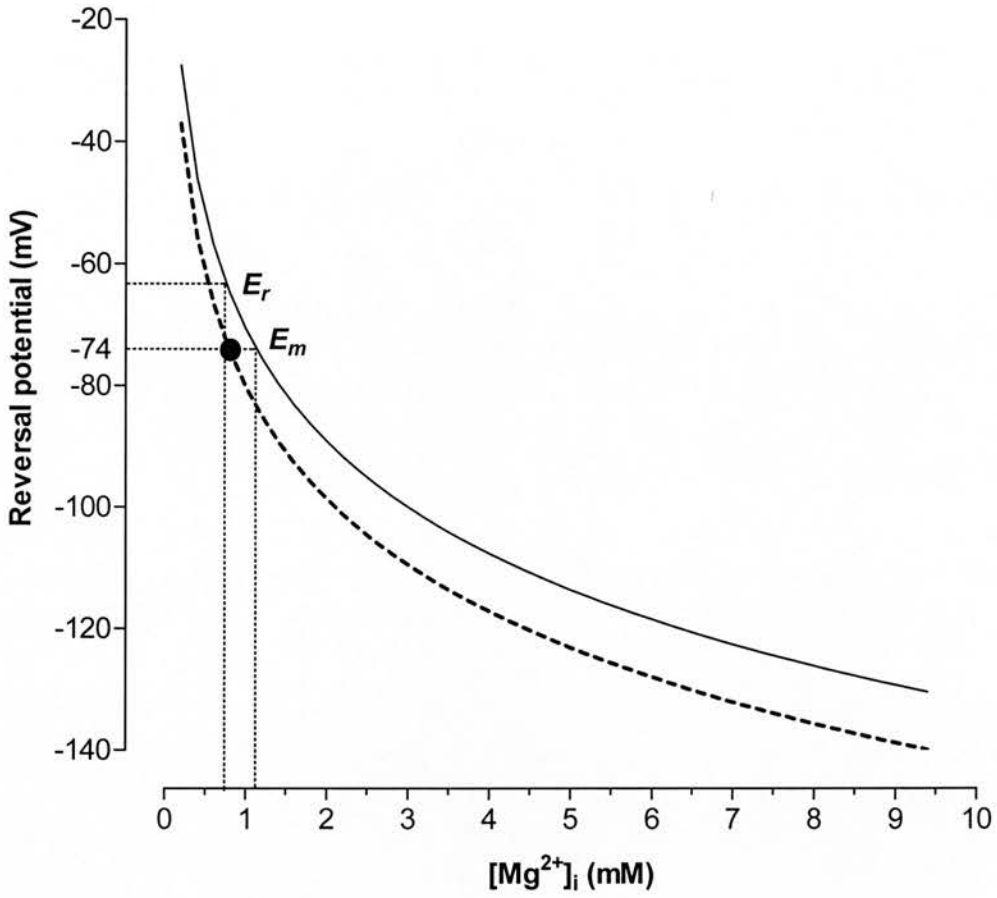

Figure 6.7. The reversal potential of a 1 Na^+/ 1 Mg^{2+} antiport under normal physiological conditions at various internal Mg^{2+} concentrations

Solid trace predicts the reversal potential of a 1 Na^+/ 1 Mg^{2+} antiport at various $[Mg^{2+}]_i$ in normal Tyrode at 37 °C. The reversal potential (E_r) at resting $[Mg^{2+}]_i$ of 0.75 mM is close to the resting membrane potential. The value E_r was calculated assuming $[Mg^{2+}]_o$= 1, $[Na^+]_o$ = 140, $[Na^+]_i$ = 10. Since $[Na^+]_i$ was not measured, E_r would change slightly for other internal Na^+ concentrations. Dashed trace predicts the reversal potential of the antiport at various $[Mg^{2+}]_i$ calculated assuming similar values for $[Mg^{2+}]_o$ and $[Na^+]_o$ but with $[Na^+]_i$ of 7 mM. In this case E_r when $[Mg^{2+}]_i$ is 0.75 mM is almost identical to membrane potential (●).

The results do not, however, exclude an effect of high $[K^+]_o$ on a putative Mg^{2+} transporter, nor do the results exclude an effect on $[Na^+]_i$ and hence the $[Na^+]$ gradient utilised by the putative Na^+/Mg^{2+} antiport. There is no evidence suggesting that K^+ interacts directly with the Mg^{2+} transport molecule. However, since Na^+ is the most likely counter ion on a sarcolemmal Mg^{2+} transporter, changes in $[Na^+]_i$ are expected to influence the rate of Mg^{2+} transport through a Na^+/Mg^{2+} exchange process. The effects of increasing $[K^+]_o$ on the rate constant of the Na^+-stimulated $[Mg^{2+}]_i$ reduction are likely to be due to depolarisation of the cell and to a less extent to alterations of $[Na^+]_i$. The membrane potential would be expected to become more positive (by as much as 50 mV) when $[K^+]_o$ is raised from 6 to 70 mM (Chapman, 1973, Ellis, 1977). This depolarisation is likely to be rapid and occurs within a few seconds. Cell depolarisation alone should increase the rate at which Mg^{2+} is extruded from the cell through a 1 Na^+/ 1 Mg^{2+} antiport. Increasing $[K^+]_o$ also results in a decrease in $[Na^+]_i$. This decrease is fairly rapid and reaches a steady state in less than 10 minutes, while the greatest decrease occurs in the first 2 minutes (e.g. Ellis, 1977). The decrease in $[Na^+]_i$ following superfusion with the high $[K^+]$ medium is probably mainly due to the decreased electrical gradient for inward movement of Na^+, since the Na^+/K^+ pump is almost saturated at 6 mM $[K^+]_o$ (Gadsby, 1984).

It is worth mentioning that the aim of these experiments was to obtain information on the effects of cell depolarisation on Mg^{2+} transport, since superfusing preparations with a medium containing high $[K^+]$ is technically less demanding than the voltage clamp technique. Therefore, the results are of a qualitative nature and should not be interpreted otherwise.

The results of the high $[K^+]$ experiments were followed by the more powerful method of depolarising the cell by the voltage clamp technique. In three successful experiments the rate constant of $[Mg^{2+}]_i$ reduction was greater when cells were depolarised to 0 mV than when they were held at –80 mV (Figure 6.4). These results confirmed the observations with the high $[K^+]_o$ experiments that depolarisation increases the rate of $[Mg^{2+}]_i$ reduction in Mg^{2+}-loaded myocytes. The data suggest

that extrusion of Mg^{2+} in cardiac cells occurs through a Na^+-dependent mechanism that is sensitive to changes in the membrane potential.

If a Na^+/Mg^{2+} antiport was solely responsible for these observations then the transporter results in a net loss of one positive charge. The simplest coupling ratios for a potential-dependent Na^+/Mg^{2+} antiport are 1 Na^+: 1 Mg^{2+} or 3 Na^+: 1 Mg^{2+}. A 3 Na^+/ 1 Mg^{2+} antiport would carry a net positive charge into the cell, and thus cell depolarisation should reduce Mg^{2+} efflux through the antiport (Figure 6.8). That implies that as the membrane potential becomes more positive $[Mg^{2+}]_i$ increases, which is opposite to the observed effects of depolarisation shown in Figure 6.4. Another factor that argues against a 3:1 stoichiometry is the amount of energy provided by 3 Na^+ ions to extrude 1 Mg^{2+} ion. It is estimated that 14.24 kJ is required to remove one mole of Mg^{2+} (McGuigan *et al.*, 2002). Three moles of Na^+ provide approximately 40 kJ, making the exchange process highly energy-inefficient.

On the other hand, cell depolarisation should increase Mg^{2+} efflux or reduce influx through a 1 to 1 antiport depending on $[Mg^{2+}]_i$ (Figure 6.7). Under quiescent conditions, where the membrane potential is around –74 mV, a 1 Na^+/1 Mg^{2+} antiport may struggle to maintain $[Mg^{2+}]_i$ at the measured mean resting value of 0.75 mM, since the calculated equilibrium $[Mg^{2+}]_i$ is 1.14 mM. However, the antiport is potential-dependent and over the heart cycle, depolarisation during systole should enhance Mg^{2+} efflux and the antiport could maintain a lower $[Mg^{2+}]_i$ than the value calculated at the resting membrane potential. Moreover, extrusion of Mg^{2+} through a 1 to 1 antiport system has the advantage of being dependent on the heart rate. As the heart rate increases the mean membrane potential becomes more positive and that helps keep $[Mg^{2+}]_i$ at a lower value than that calculated at a membrane potential of –74 mV. This has the benefit of offsetting an increase in $[Mg^{2+}]_i$ brought about by an increase in breakdown of ATP and liberation of bound Mg^{2+} during muscle contraction and an increase in $[Na^+]_i$ as heart rate increases. Therefore, under normal physiological conditions, a 1 Na^+/ 1 Mg^{2+} exchange should provide a highly energy-efficient Mg^{2+} efflux mechanism that would be capable of maintaining $[Mg^{2+}]_i$ at around the measured value.

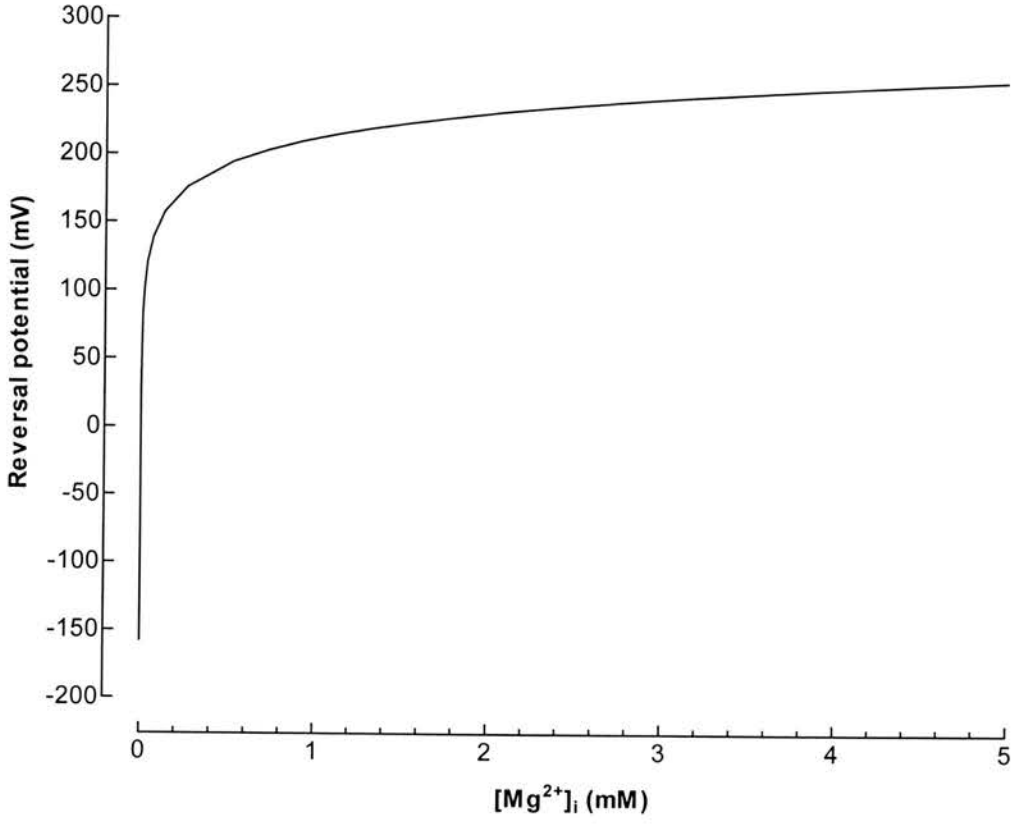

Figure 6.8. The reversal potential of 3 Na^+/ 1 Mg^{2+} antiport at various $[Mg^{2+}]_i$

The model depicts the reversal potential of a Na^+/Mg^{2+} antiport with a 3 to 1 stoichiometry calculated according to the Nernst equation assuming (in mM): $[Na^+]_o$ = 140, $[Mg^{2+}]_o$ = 1 and $[Na^+]_i$ = 10. The model shows that at a reversal potential equal to the resting membrane potential (–74 mV), the equilibrium $[Mg^{2+}]_i$ is in the nano-molar range (too small to be accurately shown). More positive membrane voltages (cell depolarisation) favours an increase in $[Mg^{2+}]_i$ (the antiport reverses direction to mediate Mg^{2+} influx).

It must be remembered though that the calculation of the reversal potential would be significantly affected by the assumed value for $[Na^+]_i$, which wasn't measured under the conditions used in this study. Whether the antiport would be capable of maintaining $[Mg^{2+}]_i$ within the normal range in a physiological solution depends critically on the true $[Mg^{2+}]_i$ and $[Na^+]_i$. At a particular $[Mg^{2+}]_i$ slight differences in $[Na^+]_i$ would also change E_r. For a 1 Na^+/ 1 Mg^{2+} antiport, E_r ranges between –72 mV to –52 mV for $[Na^+]_i$ between 7 and 15 respectively.

The extrusion of Mg^{2+} in cardiac cells though mechanisms other than a Na^+/Mg^{2+} antiport is possible. There is evidence that Mg^{2+} efflux occurs through Na^+-independent pathway(s). Leonhard-Marek *et al.* (1998) have suggested that extrusion of Mg^{2+} in sheep rumen epithelium is probably through an electroneutral 2 H^+/ 1 Mg^{2+} antiport, which they found was sensitive to short chain fatty acids and CO_2. Involvement of Cl^- in a Mg^{2+} transporter has also been suggested in hepatocytes (Romani *et al.*, 1993b), human and rat erythrocytes (Günther & Vormann, 1990), vertebrate intestinal epithelium (Bijvelds *et al.*, 1998) and cardiac myocytes (Ödblom & Handy, 1999). The contribution of bicarbonate ions (HCO_3^-) in extrusion of intracellular free Mg^{2+} has been implicated in isolated rat ventricular myocytes (Ödblom & Handy, 1999), where a DIDS-sensitive Mg^{2+}/HCO_3^- symport was suggested. The present study does not provide independent evidence relating to the involvement of HCO_3^- in either influx or efflux of Mg^{2+}, since none of the solutions used contained added bicarbonate.

In conclusion, the effects of cell depolarisation on the Na^+-dependent $[Mg^{2+}]_i$ reduction are consistent with the operation of a Na^+/Mg^{2+} antiport in the plasma membrane of rat ventricular myocytes, exchanging one Na^+ for each Mg^{2+} ion. Probably the best way to determine the true stoichiometry of the putative Na^+/Mg^{2+} antiport in the heart is to measure the membrane potential, $[Mg^{2+}]_i$ and $[Na^+]_i$ simultaneously in the same cell. Unfortunately, currently there are no fluorescent dyes for Na^+ that can be used together with mag-fura-2 in the same cell. This is because of overlap of the spectral properties of the two dyes and separation of emitted light from the two dyes is not possible. However, ion-selective

microelectrodes, although technically more demanding, could provide an alternative method to measure the concentration of the two ions in the same cell without cross interference.

$[Mg^{2+}]_i$ elevation on the other hand does not appear to occur solely through reverse Na^+/Mg^{2+} exchange. The increase in $[Mg^{2+}]_i$ during cell loading could be the result of Mg^{2+} entry through multiple influx routes. This would probably account for the failure to attribute the potential-dependence of Mg^{2+} loading to a single uptake process.

An important difference between the experiments studying the effect of voltage clamp on $[Mg^{2+}]_i$ reduction and those on Mg^{2+} loading is the presence and absence of external Ca^{2+}, respectively. With normal (or near normal) $[Ca^{2+}]_o$ the membrane conductance and selectivity to external cations falls within the normal range. Whereas superfusing cells with a nominally Ca^{2+}-free medium (for example during Mg^{2+} loading), increases the conductance of Ca^{2+} channels to cations such as Na^+ and Mg^{2+} significantly (e.g. Tunstall *et al.*, 1986). This could be the cause of the relatively higher current passed into the cells during loading. This is evident in Figure 6.3B when cells were voltage-clamped to +50 mV. However, when voltage-clamping the cells in the presence of external Ca^{2+}, as in the case of $[Mg^{2+}]$ recovery, the permeability of the membrane and the selectivity of the Ca^{2+} channels should remain relatively unaltered. Thus the current injected by the clamp unit to achieve comparable holding potentials should also be less. Therefore, while removal of Ca^{2+} might have adversely affected cells subjected to the loading protocol under voltage clamp, and hence the voltage-dependence of $[Mg^{2+}]_i$ elevation, it is unlikely that the same has occurred in cells depolarised by voltage clamp during recovery of $[Mg^{2+}]_i$. Therefore, the observed effects of the membrane potential on the Na^+-dependent $[Mg^{2+}]_i$ reduction most likely occurred in healthy, viable myocytes.

CHAPTER 7
GENERAL DISCUSSION

7.1 TECHNICAL NOTES

Our system only allowed us to plot the ratio of fluorescence resulting from excitation at 340 to that at 380 nm. The background fluorescence was measured from a cell-free area on the cover slip at the end of the experiment, and this value was later subtracted from individual data points before calculating the actual *R*. The background fluorescence from the cell-free area and from cells not loaded with mag-fura-2 AM ester are not significantly different as assessed in preliminary experiments. The use of dye-free cells in estimation of background fluorescence is also expected to introduce an error in the calculation of $[Mg^{2+}]_i$ due to variability of cells' dimensions. $[Mg^{2+}]_i$ was determined and plotted using *R* directly from an *in vitro* calibration curve. This was only performed once the experiment was completed and further processing of the raw data carried out. Recording changes in $[Mg^{2+}]_i$ using this method proved to be reliable and reproducible. However, this method still needs to be developed to enable us to monitor changes in *R* and $[Mg^{2+}]_i$ simultaneously during the course of the experiment. This can be achieved by adding new hardware and software components to our current system. The hardware component should allow us to electronically subtract the background fluorescence prior to recording from cells, whereas the software should utilise the measured *R* to calculate and display $[Mg^{2+}]_i$ values based on a pre-defined calibration formula and parameters. There is an obvious advantage to be able to determine $[Mg^{2+}]_i$ during the course of an experiment. For example it would be possible to "clamp" $[Mg^{2+}]_i$ at a desired value during Mg^{2+} loading of the cell. This should increase the reliability and reproducibility of the experiments by preventing overloading of the cells with Mg^{2+}. Also, when cells are recovering from a high-Mg^{2+} load, it would be possible to accurately judge when to intervene, for example by changing the extracellular milieu or the holding potential, in cases where cells are voltage-clamped. Such improvements are attainable and are in fact in the process of implementation.

7.1.1 The reliability of mag-fura-2 as an intracellular Mg^{2+} indicator

Over the past 15 years, reported values for $[Mg^{2+}]_i$ in myocardium have varied widely, ranging between 0.4 to 3.5 mM (Wu *et al.*, 1981; Hess *et al.*, 1982; Blatter &

McGuigan, 1986; Fry, 1986; Murphy *et al.*, 1989; Buri *et al.*, 1993; Handy *et al.*, 1996; Tashiro & Konishi, 2000; Almulla *et al.*, 2001). At present there appears to be a consensus on the free cytosolic Mg^{2+} concentration in the myocardium. Experimental results show that $[Mg^{2+}]_i$ in the heart is in the sub-millimolar range (Table 1.1). The mean value measured using mag-fura-2 in this study has been 0.75 mM, which agrees well with measurements previously made in rat ventricular myocytes by other workers using the same technique (Hongo *et al.*, 1994; Handy *et al.*, 1996; Tashiro & Konishi, 2000). Since its introduction more than 10 year ago (Raju *et al.*, 1989), mag-fura-2 has been used with relative reliability to measure $[Mg^{2+}]_i$ in isolated cells. Provided serious perturbations in $[Ca^{2+}]_i$ are avoided, values for $[Mg^{2+}]_i$ obtained using mag-fura-2 are consistent with other techniques such as Mg^{2+}-sensitive microelectrodes (Buri *et al.*, 1993) and NMR (Murphy *et al.*, 1989). The main problems with mag-fura-2 are calibration and selectivity over Ca^{2+}.

Although differences between *in vivo* and *in vitro* calibrations might exist, the direction of $[Mg^{2+}]_i$ changes should remain unaffected by these differences regardless of the absolute magnitude of $[Mg^{2+}]_i$ changes.

The fluorescence signal measured from cells in the present study was assumed to arise mainly from the cytosol. If mag-fura-2 also permeates other cellular compartments such as the SR or the mitochondria, then the measured fluorescence would be the average signal obtained from these cellular compartments. In the present study, the distribution of the dye in cardiac cells following loading with the AM ester was not studied and preferential loading of the cytosol, for example by directly injecting the free acid analogue of the indicator, was not attempted. To this end, it would be worthwhile to examine the distribution of mag-fura-2 in isolated cardiac myocytes using confocal microscopy. This would be especially useful in cardiac cells, where the density of the mitochondria is particularly high.

The problem of indiscriminate loading of mag-fura-2 AM ester in single cells can be a serious one if a major proportion of the dye depicts changes in cell organelles rather than the cytosol. Direct injection of the mag-fura-2 into the cytosol is

technically more demanding than ester loading, but could be attempted especially if cells were to be voltage-clamped at the same time. In this way the patch pipette could be used to load the cells with mag-fura-2 in addition to controlling cell voltage. Despite all the uncertainties related to loading of organelles with the dye, by avoiding factors that perturb either SR Ca^{2+} or mitochondrial Mg^{2+}, the data presented in this study should still reflect genuine changes in $[Mg^{2+}]_i$. (see also Chapter 3, Sections 3.4.8 and 3.4.9).

A new class of fluorescent Mg^{2+} indicators has recently been developed (Otten *et al.*, 2001). The newly synthesised indicators are derivatives of fluorinated quinolones, widely used as antibiotics, which are known to chelate Mg^{2+}. The authors have synthesised a series of new 4-oxo-4H-quinolizine-3-carboxylic acid derivatives. The main advantage of the new indicators is their insensitivity to Ca^{2+} even in the millimolar range, as well as having dissociation constants for Mg^{2+} at around 1 mM. Among the compounds synthesised, one was found to be suitable for ratiometric fluorescence measurement, as it possesses a large shift in emission spectra (23 nm) upon complexation with Mg^{2+}, with an isosbestic point around 437 nm. However, at the time of writing, no data has been published on the reliability of these compounds in the measurement of $[Mg^{2+}]_i$ in biological systems. It remains to be seen whether the new fluorophore will circumvent a major problem often related to the use of mag-fura-2 in the measurement of $[Mg^{2+}]_i$, namely sensitivity to Ca^{2+}. Until such data becomes available, mag-fura-2 remains one of the most reliable and easiest methods currently available to measure changes in $[Mg^{2+}]_i$ in a wide range of cell types.

7.2 Mg^{2+} HOMEOSTASIS IN MAMMALIAN HEART

In the following section an attempt will be made to summarise the current state of Mg^{2+} research in the heart based on the previous and the present studies and to highlight potentials for future work that would bolster our understanding of $[Mg^{2+}]_i$ regulation in heart cells.

7.2.1 $[Mg^{2+}]_i$ elevation

Throughout this report the term "$[Mg^{2+}]_i$ elevation" has been used to indicate a rise in $[Mg^{2+}]_i$, although the technique used does not demonstrate that Mg^{2+} has in fact crossed the sarcolemma. The most obvious criticism of this approach is the possibility that the change in $[Mg^{2+}]_i$ was the result of interference by other cations, mainly Ca^{2+} and H^+, with the dye and uptake and release of Mg^{2+} by intracellular organelles, mainly the mitochondria. This was the main reason for using the term "elevation" and not "uptake" to express an increase in $[Mg^{2+}]_i$. However, there is convincing evidence from the present work and from studies by others to suggest that many of the factors mentioned above would not, or only minimally, affect the measurements of $[Mg^{2+}]_i$ made using mag-fura-2.

Probably the most frequently criticised aspect of $[Mg^{2+}]_i$ measurement using mag-fura-2, is the sensitivity of the dye to Ca_i^{2+}. This issue is still the focus of much controversy. The study of Hurley *et al.* (1992) on rat pancreatic and submandibular gland acini was in favour of the view that Ca^{2+} interference severely limits the use of mag-fura-2 in the measurement of $[Mg^{2+}]_i$. The authors suggested that when $[Ca^{2+}]_i$ and $[Mg^{2+}]_i$ are changing simultaneously, a change in the amount of Ca^{2+} that is less than 1% of the change in the amount of Mg^{2+} would interfere substantially with measurement of $[Mg^{2+}]_i$ in cells loaded with mag-fura-2.

On the other hand Li & Quamme (1997) found that the mag-fura-2 signal decreased in rat ventricular myocytes as $[Ca^{2+}]_i$ increased. The authors demonstrated that even when myocytes were electrically-stimulated to contract at 0.5 Hz, $[Mg^{2+}]_i$ remained at baseline values, and only transient increases equivalent to 0.1 mM change in $[Mg^{2+}]_i$ were recorded with each cell contraction. This is most likely attributed to the Ca^{2+} transients accompanying cell contraction. Such low level of interference would be lost in the background noise of the signal recorded from cells in the present study. This was evident from the experiments conducted on electrically-stimulated myocytes loaded with mag-fura-2 AM (Figure 3.9), where a very small increase in $[Mg^{2+}]_i$ was recorded with cell contraction. Our results therefore concur with that of

Li & Quamme (1997) and support the notion that increases in $[Ca^{2+}]_i$, even during cell contraction, do not interfere with the measured values for $[Mg^{2+}]_i$.

Further evidence that such interference is only minimal came from the study by Silverman *et al.* (1994), who found that Ca^{2+} only marginally interferes with mag-indo-1 fluorescence. The authors suggest that only under unusual circumstances of massive cellular Ca^{2+} loading, as may occur with prolonged severe energy depletion, the indicator might respond to a rise in $[Ca^{2+}]_i$, giving an apparent rise in $[Mg^{2+}]_i$. The reported K_d for the binding of Mg^{2+} to mag-indo-1 ranges between 1.4 (Rutter *et al.*, 1990) and 2.7 mM (Haugland, 1999), close to values reported for mag-fura-2. Also, like mag-fura-2, mag-indo-1 binds Ca^{2+} with higher affinity (K_d = 23 μM) (Rutter *et al.*, 1990) that is also comparable to that reported for mag-fura-2 (Raju *et al.*, 1989). Kennedy (1998) compared the signal registered by both ion-selective microelectrodes and mag-fura-2 on snail neurons. The author found that only significant perturbation of $[Ca^{2+}]_i$, such as by impalement of the cell by the microelectrode and/or activating Ca^{2+} channels by voltage-clamping the preparation to 0 mV, resulted in interference with mag-fura-2 and to a lesser extent with the Mg^{2+}-ISME.

Ca^{2+} interference would be much less significant under conditions in which small changes in $[Ca^{2+}]_i$ are accompanied by much larger changes in $[Mg^{2+}]_i$, which is the most likely case in the present study. It was also possible to demonstrate that both the Ca^{2+} and Mg^{2+} signals as measured by fura-2 and mag-fura-2, respectively, do not follow a similar time course. This is evident in Figure 3.9.

Probably a better approach to resolve the issue of the magnitude of Ca_i^{2+} interference with mag-fura-2 fluorescence in cardiac cells is to measure changes in $[Mg^{2+}]_i$ simultaneously by Mg^{2+}-selective microelectrodes and mag-fura-2.

In summary, the most likely cause of the increase in mag-fura-2 fluorescence recorded during the Mg^{2+}-loading protocol is a trans-sarcolemmal movement of Mg^{2+} into the cytosol. This is believed to be the case for the following reasons:

- Loading was carried out in Ca^{2+}-free conditions.
- In the majority of experiments, the time course of the rise in fluorescence ratio is consistent with a slow influx process that could not be attributed to Ca^{2+} release from intracellular stores.
- The change in fluorescence signal was not the result of pH_i changes as discussed in Chapter 3, Section 3.4.7.
- Movement of Mg^{2+} from the mitochondria to the cytosol can be excluded since factors that promote such shift were avoided.
- Ca^{2+} release from the SR is minimised in Ca^{2+}-free conditions (Somlyo *et al.*, 1985). The SR contains only a small amount of the total cell magnesium and is unlikely to account for the magnitude of the increase in fluorescence ratio seen in most experiments.
- Increasing $[Mg^{2+}]_o$ increases the rate and magnitude of $[Mg^{2+}]_i$ elevation (Figure 4.8). The relationship between $[Mg^{2+}]_o$ and $[Mg^{2+}]_i$ predicts zero increase in $[Mg^{2+}]_i$ at zero external Mg^{2+}.

The routes through which Mg^{2+} penetrates heart cells are still a matter of speculation. However, the results presented here suggest that there are multiple pathways. The rate of $[Mg^{2+}]_i$ elevation in cells superfused with the Mg^{2+}-loading solution decreases as $[Na^+]_o$ increases (Figure 4.5), suggesting a role for Na^+ channels and reverse Na^+/Mg^{2+} exchange in mediating Mg^{2+} uptake. Other studies on heart cells also support this possibility (Handy *et al.*, 1996; Tashiro & Konishi, 2000). The lack of inhibition by imipramine of Mg^{2+} loading does not necessarily rule out Mg^{2+} entry through reverse Na^+/Mg^{2+} exchange, as the drug might act differently when the exchange protein is operating in the forward mode. Mg^{2+} might also enter the cell through reversal of the Na^+/Ca^{2+} exchanger carrying Mg^{2+} in place of Ca^{2+}. There is evidence that the reverse Na^+/Ca^{2+} exchange inhibitor, KBR, inhibits $[Mg^{2+}]_i$ elevation at modest Mg^{2+} loads, while it only slightly affects loading at higher loads (Figures 5.5 and 5.6). The dependence of $[Mg^{2+}]_i$ elevation on membrane potential suggests a Mg^{2+} voltage-gated channel might also be present in the sarcolemma of heart cells.

Taken together, these results could also explain the fact that the Na^+-dependence of $[Mg^{2+}]_i$ elevation was not consistent with a single transport process (Figure 4.5). Evidence obtained in tissues other than the heart suggests that a Mg^{2+}-permeable channel or a carrier mechanism might indeed exist in cardiac myocytes. A Mg^{2+} channel has been suggested in *Paramecium* (Preston, 1990). Putative Mg^{2+} channels have been described in the proximal tubule of the kidney and from the brush border of proximal intestinal epithelium of fish (Freire *et al.*, 1996; Bijvelds *et al.*, 2001). Stout *et al.* (1996) have also described a Mg^{2+} uptake mechanism in forebrain neurons from foetal rats. Their results suggest that glutamate-stimulated increases in $[Mg^{2+}]_i$ that occur in the absence of Na_o^+ and Ca_o^{2+} and in the presence of high $[Mg^{2+}]_o$ result from Mg^{2+} entry through NMDA (N-methyl-D-aspartate)-activated ion channels. Recently, Mg^{2+}-permeable channels were cloned from yeast (Graschopf *et al.*, 2001). The transport protein, known as "Alr1p" was considered the first known candidate for a Mg^{2+} transport system in eukaryotic cells. It was also found to be distantly related to the bacterial CorA Mg^{2+} transporter family. However, in the heart, and despite more than three decades of research, a Mg^{2+} transporter has not yet been characterised and cloned.

The present study underlined the complexity of the situation in cardiac tissue in relation to Mg^{2+} uptake pathways, and hopefully with the emergence of more specific inhibitors and Mg^{2+} indicators in the future, a better dissection of those pathways will be possible.

7.2.2 $[Mg^{2+}]_i$ reduction

As with influx, the term " efflux" has been avoided for the same reasons mentioned above. "$[Mg^{2+}]_i$ reduction" was used instead to describe the results. In this case too, there is convincing evidence that $[Mg^{2+}]_i$ reduction was almost certainly due to Mg^{2+} extrusion rather than intracellular redistribution of Mg^{2+}. The possibility of Ca^{2+} interference can hardly be entertained here since in the majority of the experiments $[Mg^{2+}]_i$ reduction occurred under conditions where Ca^{2+} was present in the external

medium. An artifact caused by Ca^{2+} should cause in increase in the fluorescence ratio. Therefore, since $[Mg^{2+}]_i$ reduction was detected as a decrease in the fluorescence ratio on superfusion with normal Tyrode, this cannot be attributed to an artifactual effect of Ca^{2+}. Control measurements carried out by Handy *et al.* (1996) indicated that re-addition of external Ca^{2+} causes small increases in $[Ca^{2+}]_i$, which were normally below the 1 μM needed to cause direct interference with mag-fura-2 (Hurley *et al.*, 1992). The authors also observed that changes in $[Ca^{2+}]_i$ were rapid and occurred only at the point of solution change. The experiment shown in Figure 3.8A supports these observations, although, the $[Ca^{2+}]_i$ transient seems to occur over a period of approximately 2 minutes. Intracellular Mg^{2+} buffering and hence $[Mg^{2+}]_i$ is expected to be only transiently affected by the transient $[Ca^{2+}]_i$ rise. This should not, however, affect the calculation of $[Mg^{2+}]_i$ reduction rate constant where Ca^{2+} was present in the recovery solution, since the first 2 minutes of recording following introduction of external Ca^{2+} were not included in the calculations.

In experiments studying the Na^+-dependence of $[Mg^{2+}]_i$ reduction, $[Mg^{2+}]_i$ recovery was carried out in Ca^{2+}-free conditions (for example Figure 3.2). This was important since the rate of Mg^{2+} extrusion by the putative Na^+/Mg^{2+} antiport would be indirectly affected by the action of the Na^+/Ca^{2+} exchanger. Therefore, since the goal of the experiments was to compare the rate of $[Mg^{2+}]_i$ recovery at the "test" (28 to 98 mM) external Na^+ concentration to that at 140 mM, the experimental protocol was designed to minimise alterations in $[Na^+]_i$, caused by varying degrees of Na^+/Ca^{2+} exchange activity, during the recovery phase.

Fluxes of Mg^{2+} between the cytosol and the mitochondria were also minimised by avoiding factors that might cause such fluxes, including low ionic strength solutions and stimulation by cAMP (Brierley *et al.*, 1987; Romani & Scarpa, 1992a; Jung & Brierley, 1994). Mg^{2+} fluxes between the cytosol and the SR must be small, first because it contains little Mg^{2+} (Somlyo *et al.*, 1985) and second, such fluxes should be minimised in the absence of large changes in $[Ca^{2+}]_i$, the likely counter ion for Mg^{2+} (Salama & Scarpa, 1985; Romani & Scarpa, 1992b; Vormann & Günther,

1993). Most of the issues related to intracellular redistribution of Mg^{2+} have been discussed in Chapter 3.

For all these reasons, the reduction of $[Mg^{2+}]_i$ in Mg^{2+}-loaded myocytes is most likely the result of trans-sarcolemmal Mg^{2+} efflux. The following section will focus on the possible mechanisms through which Mg^{2+} is extruded and potential experimental work that would help resolve the issue.

There is substantial evidence that extrusion of Mg^{2+} in the heart is Na^+-dependent. A similar process has also been suggested in a large number of tissues (Table 7.1). The work carried out in the past decade, particularly the past 6 years has put forward convincing evidence in favour of a Na^+/Mg^{2+} antiport in the sarcolemma of cardiac myocytes from different species.

The following evidence from the present experiments substantiates those earlier findings:

- Recovery of $[Mg^{2+}]_i$ in Mg^{2+}-loaded cells was strictly dependent on $[Na^+]_o$, where increasing $[Na^+]_o$ increases the rate constant of $[Mg^{2+}]_i$ reduction.
- No recovery was observed in Na^+-free conditions.
- The Na^+-dependent $[Mg^{2+}]_i$ recovery was completely inhibited by 200 μM imipramine.

An attempt was also made to determine the stoichiometry of Na^+/Mg^{2+} exchange in isolated rat ventricular myocytes. It was shown that $[Mg^{2+}]_i$ reduction was potential-dependent, where cell depolarisation accelerates Mg^{2+} loss (Figure 6.4). These observations were consistent with an antiport that extrudes 1 Mg^{2+} ion in exchange for 1 Na^+ ion, with a resultant loss of one positive charge. As discussed in Chapter 6, extrusion of Mg^{2+} via such antiport would partly be assisted by the cardiac cycle where during part of the cycle the membrane potential would be above the reversal potential of the antiport, and hence the antiport will be effluxing Mg^{2+} (Figure 6.7).

Table 7.1. Tissues in which Na^+-dependent Mg^{2+} efflux mechanisms have been suggested.

Tissue	*Reference*
Heart muscle	
Rat	(Vormann & Günther, 1987; Murphy *et al.*, 1991a; Handy *et al.*, 1996; Tashiro & Konishi, 2000; Almulla *et al.*, 2001)
Ferret and guinea pig	(Fry, 1986)
Smooth muscle	
Tenia cecum	(Tashiro & Konishi, 1997b)
Mesenteric artery	(Touyz & Schiffrin, 1996)
Red blood cells	
Chicken and turkey	(Günther & Vormann, 1985)
Ferret	(Flatman & Smith, 1991)
Hamster	(Xu & Willis, 1994)
Human	(Günther & Vormann, 1985; Féray & Garay, 1986; Lüdi & Schatzmann, 1987; Féray & Garay, 1988)
Rat	(Günther *et al.*, 1990)
Other tissues	
Barnacle muscle	(Baker & Crawford, 1972)
Squid axon	(DiPolo & Beauge, 1988)
Leech neuron	(Günzel & Schlue, 1996)
Rat Liver	(Günther & Hollriegl, 1993; Cefaratti *et al.*, 1998; Tessman & Romani, 1998; Fagan & Romani, 2001)
Thymocytes	(Günther & Vormann, 1992)
Lymphocytes	(Wolf *et al.*, 1997)
HL-60 promyelocytic leukemia cells	(Wolf *et al.*, 1998)
Erlich ascites cells	(Wolf *et al.*, 1994a; Wolf *et al.*, 1994b)
Sublingual mucous acini	(Zhang & Melvin, 1996)
Rabbit ileum brush border	(Tashiro & Konishi, 1997b)
Paramecium tetraurelia	(Clark *et al.*, 1997)

7.3 OTHER Mg^{2+} EXTRUSION MECHANISMS

It is unclear whether other ions are also involved in the regulating $[Mg^{2+}]_i$ in the heart. Ödblom & Handy (1999) found that $[Mg^{2+}]_i$ rises to higher values in DIDS-treated rat ventricular myocytes compared to DIDS-free controls. The authors attributed the difference in Mg^{2+}-loading to inhibition of a Mg^{2+} efflux pathway, possibly HCO_3^--Mg^{2+} symport that would normally be active under Mg^{2+}-loading conditions. A small contribution from other intracellular anions such as Cl^-, supplied from the external medium by the Cl^-/HCO_3^- exchanger, in Mg^{2+} extrusion was also suggested by the authors. This pathway was suggested by the authors as an additional $[Mg^{2+}]_i$ regulation mechanism supporting the putative Na^+/Mg^{2+} antiport and not replacing it.

Studies on Mg^{2+}-loaded erythrocytes show that, in addition to Na^+/Mg^{2+} antiport, a Na_o^+-independent Cl^--coupled transport mechanism exists for Mg^{2+} efflux, which is sensitive to anion transport inhibitors (Günther & Vormann, 1989a; Günther & Vormann, 1989b; Günther & Vormann, 1990). An anion-dependent and DIDS sensitive Mg^{2+} transport pathway has also been suggested in basolateral plasma membrane vesicles of fish enterocyte (Bijvelds *et al.*, 1996), and brush border membrane vesicles of rabbit ileum (Juttner & Ebel, 1998). Whether a similar pathway is present in cardiac cells requires further investigations.

The involvement of Ca^{2+} in Mg^{2+} transport in the heart probably requires more attention. Handy *et al.* (1996) observed that $[Mg^{2+}]_i$ recovery in Mg^{2+}-loaded myocytes was incomplete in the absence of external Ca^{2+}. This was attributed by the authors to possible interaction of Ca_o^{2+} with the Mg^{2+} extrusion mechanism, probably by competing with Mg^{2+} for the Na^+/Mg^{2+} antiport, contribution to Mg^{2+} efflux through a putative Ca^{2+}/Mg^{2+} antiport, or activation of the extrusion mechanism. These findings were not substantiated by the present experiments where much larger Mg^{2+} loads were used. $[Mg^{2+}]_i$ reduction was not found to be affected by the presence or absence of external Ca^{2+}. Complete recovery of $[Mg^{2+}]_i$ occurred under

both conditions. The existence of a non-reversible Ca^{2+}/Mg^{2+} antiport has been suggested in rat liver plasma membrane vesicles (Cefaratti *et al.*, 1998; Cefaratti *et al.*, 2000), however, no attempts have been made to determine the presence of a similar mechanism in the heart.

7.4 Conclusion:

Figure 7.1 summarises the various influx/efflux pathways that participate in regulating $[Mg^{2+}]_i$ in mammalian cardiac myocytes. $[Mg^{2+}]_i$ is believed to be regulated by concerted action of various cellular components. In the short term, changes in $[Mg^{2+}]_i$ around the normal level could be adjusted by movement of Mg^{2+} between the cytosol and intracellular organelles, and the cytosol and other Mg^{2+} binding sites such as ATP and polyanions. However, in the long term $[Mg^{2+}]_i$ is regulated by the putative sarcolemmal Na^+/Mg^{2+} antiport. Extrusion of Mg^{2+} is the main function Na^+/Mg^{2+} antiport. This is supported by inhibition by imipramine of Mg^{2+} efflux. Reversal of Na^+/Mg^{2+} exchange might take place under conditions, most probably pathological in origin, where cellular Mg^{2+} deficiency occurs. The inhibition by KBR of Mg^{2+} uptake might be evidence of reversibility of Na^+/Mg^{2+} exchange if the drug was found to inhibit the putative Na^+/Mg^{2+} antiport as well. However, to date, no information is available to substantiate, or otherwise, this observation.

The evidence from the Na^+-dependence of $[Mg^{2+}]_i$ reduction and the voltage-sensitivity of $[Mg^{2+}]_i$ reduction suggests the influx of one Na^+ ion is required for the extrusion of one Mg^{2+} ion through a Na^+/Mg^{2+} antiport.

Entry of Mg^{2+} is most probably through several pathways. These include a voltage-sensitive Mg^{2+} channel, Ca^{2+} channels, Na^+ channels, Na^+/Mg^{2+} antiport operating in reverse mode, the Na^+/Ca^{2+} exchanger operating in reverse mode and carrying Mg^{2+} instead of Ca^{2+} and possibly other, yet unidentified, leak pathways.

The present study was successful in developing multi-loading experimental protocols that could be utilised to address several questions related to Mg^{2+} influx/efflux mechanisms in isolated cardiac myocytes, and possibly other cell types. These protocols could be used to compare the effect of various drugs, ionic composition of external media, experimental temperature, and other variables to control conditions in the same cell.

Problems related to the usage of mag-fura-2 in the measurement of changes in $[Mg^{2+}]_i$, most importantly preferential loading of the cytosol, also need to be addressed using more sophisticated techniques. One such technique is microinjection of the free acid form of the dye directly into the cytosol. This method should ensure more accurate measurements of $[Mg^{2+}]_i$ changes without risking loading of cell organelles. Injection of mag-fura-2 free acid should also resolve some of the issues related to Mg^{2+} fluxes between the cytosol and the cell organelles, especially if used in conjunction with drugs that affect Mg^{2+} uptake/release by these organelles.

The cellular distribution of mag-fura-2 following loading of the AM ester analogue of the dye is best studied using confocal microscopy. This technique should also prove useful in determining the optimal dye concentration and incubation time used to load cells, without risking loading cellular structures.

Future Mg^{2+} research must be directed towards answering basic questions regarding pathways of Mg^{2+} transport in the heart. For example, are other ions involved in providing energy for Mg^{2+} extrusion besides Na^+? What is the true stoichiometry of Na^+/Mg^{2+} exchange? Is the Na^+/Ca^{2+} exchanger involved in Mg^{2+} influx/efflux? Is there a Mg^{2+}-selective channel analogous to other cation channels?

The synthesis of more specific inhibitors of Mg^{2+} transport and better fluorescent dyes would undoubtedly help in finding definite answers to some of the above questions.

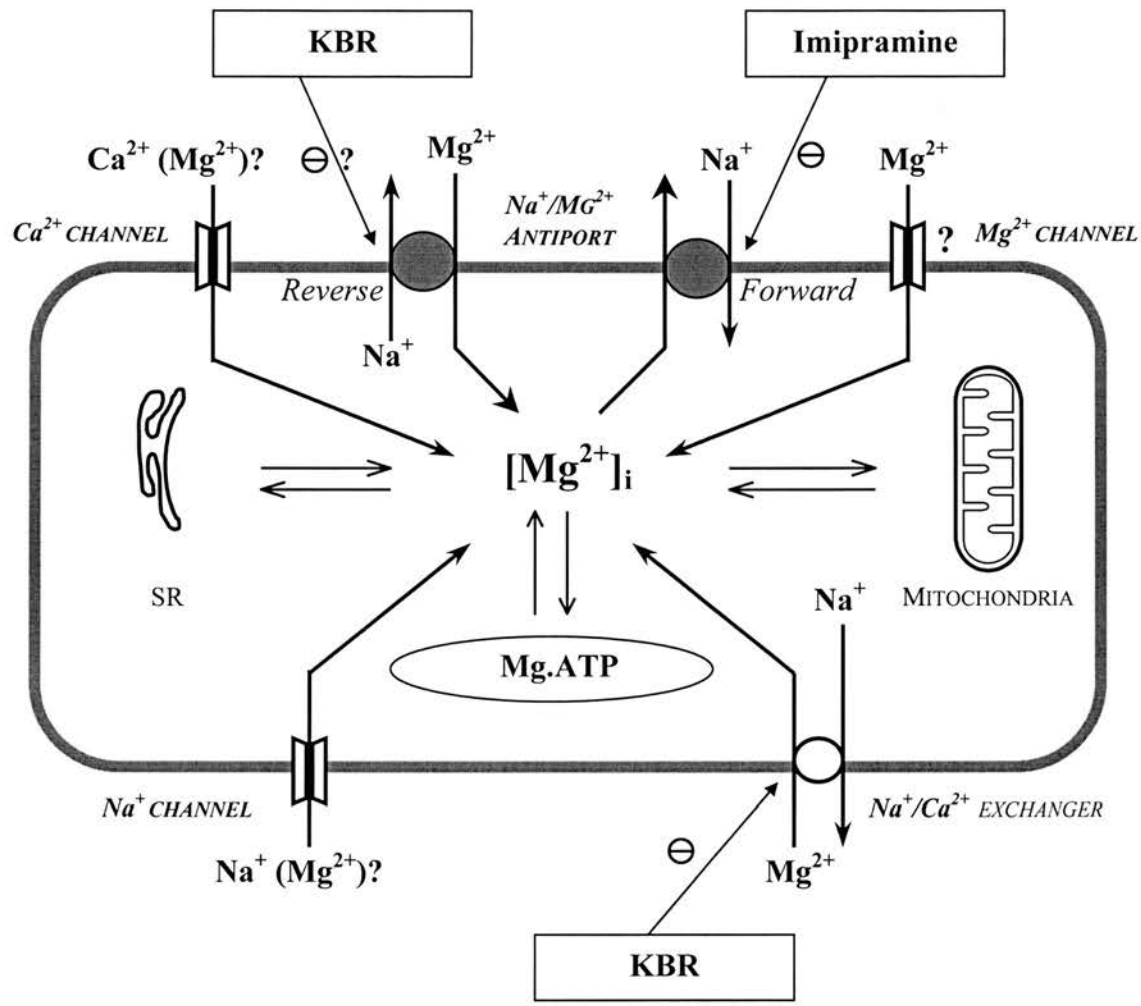

Figure 7.1. **Schematic diagram of possible Mg^{2+} influx/efflux pathways**

See text for details.

REFERENCES

AGUS, Z.S., KELEPOURIS, E., DUKES, I. & MORAD, M. (1989). Cytosolic magnesium modulates calcium channel activity in mammalian ventricular cells. *American Journal of Physiology* **256**, C452-C455.

ALMULLA, H.A., FLATMAN, P.W. & ELLIS, D. (2001). Sodium-dependent magnesium transport in isolated rat ventricular myocytes. *Journal of Physiology* **531.P**, 186P.

ALTURA, B.T. & ALTURA, B.M. (1995). Ionised magnesium measurements in serum, plasma and whole blood in health and disease. In *Advances in magnesium research: 1, Magnesium in cardiology*, ed. SMETANA, R., pp. 538-546. London: John Libbey & Company Ltd.

AMLER, E., TEISINGER, J. & SVOBODA, P. (1987). Mg^{2+}-induced changes of lipid order and conformation of (Na^+ + K^+)-ATPase. *Biochimica et Biophysica Acta* **905**, 376-382.

APRILLE, J.R. (1993). Mechanism and regulation of the mitochondrial ATP-Mg/P_i carrier. *Journal of Bioenergetics & Biomembranes* **25**, 473-481.

ASCHERIO, A., RIMM, E.B., HERNAN, M.A., GIOVANNUCCI, E.L., KAWACHI, I., STAMPFER, M.J. & WILLETT, W.C. (1998). Intake of potassium, magnesium, calcium, and fiber and risk of stroke among US men. *Circulation* **98**, 1198-1204.

BABCOCK, D.F., FIRST, N.L. & LARDY, H.A. (1976). Action of ionophore A23187 at the cellular level. Separation of effects at the plasma and mitochondrial membranes. *Journal of Biological Chemistry* **251**, 3881-3886.

BAKER, P.F. & CRAWFORD, A.C. (1972). Mobility and transport of magnesium in squid giant axons. *Journal of Physiology* **227**, 855-874.

BARKER, E.L. & BLAKELY, R.D. (1995). Norepinephrine and serotonin transporters: Molecular targets of anti-depressant drugs. In *Psychopharmacology: The Fourth Generation of Progress*, eds. BLOOM, F. & KUPFER, D., pp. 321-333. New York: Raven Press.

BEAN, B.P. (1989). Classes of calcium channels in vertebrate cells. *Annual Review of Physiology* **51**, 367-384.

BERNARDI, P. (1999). Mitochondrial transport of cations: channels, exchangers, and permeability transition. *Physiological Reviews* **79**, 1127-1155.

BERNARDI, P., VASSANELLI, S., VERONESE, P., COLONNA, R., SZABO & ZORATTI, M. (1992). Modulation of the mitochondrial permeability transition pore. Effect of protons and divalent cations. *Journal of Biological Chemistry* **267**, 2934-2939.

BERS, D.M. (1991). Ca influx via sarcolemmal Ca channels. In *Excitation-contraction coupling and cardiac contractile force*, ed. BERS, D.M., pp. 57-62. Kluwer Academic Publishers.

BERS, D.M. & ELLIS, D. (1982). Intracellular calcium and sodium activity in sheep heart Purkinje fibres. Effect of changes of external sodium and intracellular pH. *Pflugers Archiv.- European Journal of Physiology* **393**, 171-178.

BERS, D.M., LEDERER, W.J. & BERLIN, J.R. (1990). Intracellular Ca transients in rat cardiac myocytes: role of Na-Ca exchange in excitation-contraction coupling. *American Journal of Physiology* **258**, C944-C954.

BEYENBACH, K.W. (1990). Transport of magnesium across biological membranes. *Magnesium &.Trace Elements.* **9**, 233-254.

BIJVELDS, M.J., FLIK, G. & KOLAR, Z.I. (1998). Cellular magnesium transport in the vertebrate intestine. *Magnesium Research* **11**, 315-322.

BIJVELDS, M.J., KOLAR, Z.I. & FLIK, G. (2001). Electrodiffusive magnesium transport across the intestinal brush border membrane of tilapia (Oreochromis mossambicus). *European Journal of Biochemistry* **268**, 2867-2872.

BIJVELDS, M.J., KOLAR, Z.I., WENDELAAR, B.S. & FLIK, G. (1996). Magnesium transport across the basolateral plasma membrane of the fish enterocyte. *Journal of Membrane Biology* **154**, 217-225.

BLAKELY, R.D. (1997). Regulation of antidepressant-sensitive serotonin transporters. In *Neurotransmitter Transporters: Structure, Function and Regulation*, ed. REITH, M.E.A., pp. 29-72. NJ: Humana Press Inc.

BLATTER, L.A. & MCGUIGAN, J.A. (1986). Free intracellular magnesium concentration in ferret ventricular muscle measured with ion selective micro-electrodes. *Quarterly Journal of Experimental Physiology* **71**, 467-473.

BOND, M., VADASZ, G., SOMLYO, A.V. & SOMLYO, A.P. (1987). Subcellular calcium and magnesium mobilization in rat liver stimulated in vivo with vasopressin and glucagon. *Journal of Biological Chemistry* **262**, 15630-15636.

BOUNTRA, C., POWELL, T. & VAUGHAN-JONES, R.D. (1990). Comparison of intracellular pH transients in single ventricular myocytes and isolated ventricular muscle of guinea-pig. *Journal of Physiology* **424**, 343-365.

BRANDT, P.W., REUBEN, J.P. & GRUNDFEST, H. (1972). Regulation of tension in the skinned crayfish muscle fiber. II. Role of calcium. *Journal of General Physiology* **59**, 305-317.

BRIERLEY, G.P. (1967). Ion transport by heart mitochondria. VII. Activation of the energy-linked accumulation of Mg^{++} by Zn^{++} and other cations. *Journal of Biological Chemistry* **242**, 1115-1122.

BRIERLEY, G.P., DAVIS, M. & JUNG, D.W. (1987). Respiration-dependent uptake and extrusion of Mg^{2+} by isolated heart mitochondria. *Archives of Biochemistry & Biophysics* **253**, 322-332.

BRIERLEY, G.P., JACOBUS, W.E. & HUNTER, G.R. (1967). Ion transport by heart mitochondria. 8. Activation of the adenosine triphosphate-supported accumulation of Mg^{++} by Zn^{++} and by rho-chloromercuriphenylsulfonate. *Journal of Biological Chemistry* **242**, 2192-2198.

BRINLEY, F.J.J. (1973). Calcium and magnesium transport in single cells. *Federation Proceedings* **32**, 1735-1739.

BRINLEY, F.J.J. & MULLINS, L.J. (1968). Sodium fluxes in internally dialyzed squid axons. *Journal of General Physiology* **52**, 181-211.

BRINLEY, F.J.J., SCARPA, A. & TIFFERT, T. (1977). The concentration of ionized magnesium in barnacle muscle fibres. *Journal of Physiology* **266**, 545-565.

BRONZETTI, G., DELLA CROCE, C. & DAVINI, T. (1995). Magnesium: its role in cellular functions - A review. *Journal of Environmental Pathology, Toxicology &.Oncology* **14**, 197-204.

BURI, A., CHEN, S., FRY, C.H., ILLNER, H., KICKENWEIZ, E., MCGUIGAN, J.A., NOBLE, D., POWELL, T. & TWIST, V.W. (1993). The regulation of intracellular Mg^{2+} in guinea-pig heart, studied with Mg^{2+}-selective microelectrodes and fluorochromes. *Experimental Physiology* **78**, 221-233.

BURI, A. & MCGUIGAN, J.A. (1990). Intracellular free magnesium and its regulation, studied in isolated ferret ventricular muscle with ion-selective microelectrodes. *Experimental Physiology* **75**, 751-761.

CALDWELL-VIOLICH, M. & REQUENA, J. (1979). Magnesium content and net fluxes in squid giant axons. *Journal of General Physiology* **74**, 739-752.

CAMPBELL, D.L., GILES, W.R. & SHIBATA, E.F. (1988). Ion transfer characteristics of the calcium current in bull-frog atrial myocytes. *Journal of Physiology* **403**, 239-266.

CEFARATTI, C., ROMANI, A. & SCARPA, A. (1998). Characterization of two Mg^{2+} transporters in sealed plasma membrane vesicles from rat liver. *American Journal of Physiology* **275**, C995-C1008.

CEFARATTI, C., ROMANI, A. & SCARPA, A. (2000). Differential localization and operation of distinct Mg^{2+} transporters in apical and basolateral sides of rat liver plasma membrane. *Journal of Biological Chemistry* **275**, 3772-3780.

CHAPMAN, R.A. (1973). The ionic dependence of the strength and spontaneous relations of the potassium contracture induced in the heart of the frog Rana pipiens. *Journal of Physiology* **231**, 209-232.

CHAPMAN, R.A., CORAY, A. & MCGUIGAN, J.A. (1983). Sodium/calcium exchange in mammalian ventricular muscle: a study with sodium-sensitive micro-electrodes. *Journal of Physiology* **343**, 253-276.

CHAPMAN, R.A., FOZZARD, H.A., FRIEDLANDER, I.R. & JANUARY, C.T. (1986). Effects of Ca^{2+}/Mg^{2+} removal on a_iNa, a_iK, and tension in cardiac Purkinje fibres. *American Journal of Physiology* **251**, C920-C927.

CHAPMAN, R.A., SULEIMAN, M.S., RODRIGO, G.C. & TUNSTALL, J. (1991). The calcium paradox: a role for $[Na]_i$, a cellular or tissue basis, a property unique to the Langendorff perfused heart? A bundle of contradictions. *Journal of Molecular & Cellular Cardiology* **23**, 773-777.

CLARK, K.D., HENNESSEY, T.M., NELSON, D.L. & PRESTON, R.R. (1997). Extracellular GTP causes membrane-potential oscillations through the parallel activation of Mg^{2+} and Na^+ currents in Paramecium tetraurelia. *Journal of Membrane Biology* **157**, 159-167.

CORKEY, B.E., DUSZYNSKI, J., RICH, T.L., MATSCHINSKY, B. & WILLIAMSON, J.R. (1986). Regulation of free and bound magnesium in rat hepatocytes and isolated mitochondria. *Journal of Biological Chemistry* **261**, 2567-2574.

CRAGOE, E.J.J., WOLTERSDORF, O.W.J., BICKING, J.B., KWONG, S.F. & JONES, J.H. (1967). Pyrazine diuretics. II. N-amidino-3-amino-5-substituted 6-halopyrazinecarboxamides. *Journal of Medical Chemistry* **10**, 66-75.

CROMPTON, M., CAPANO, M. & CARAFOLI, E. (1976). Respiration-dependent efflux of magnesium ions from heart mitochondria. *Biochemical Journal* **154**, 735-742.

CROSS, H.R., RADDA, G.K. & CLARKE, K. (1995). The role of Na^+/K^+ ATPase activity during low flow ischemia in preventing myocardial injury: a ^{31}P, ^{23}Na and ^{87}Rb NMR spectroscopic study. *Magnetic Resonance in Medicine* **34**, 673-685.

DE WEER, P. (1976). Axoplasmic free magnesium levels and magnesium extrusion from squid giant axons. *Journal of General Physiology* **68**, 159-178.

DEITMER, J.W. & ELLIS, D. (1978). Changes in the intracellular sodium activity of sheep heart Purkinje fibres produced by calcium and other divalent cations. *Journal of Physiology* **277**, 437-453.

DIPOLO, R. & BEAUGE, L. (1988). An ATP-dependent Na^+/Mg^{2+} countertransport is the only mechanism for Mg extrusion in squid axons. *Biochimica et Biophysica Acta* **946**, 424-428.

DURLACH, J. (1988). Magnesium research: a brief historical account. *Magnesium Research* **1**, 91-95.

EBEL, H. & GÜNTHER, T. (1999). Characterization of Mg^{2+} efflux from rat erythrocytes non-loaded with Mg^{2+}. *Biochimica et Biophysica Acta* **1421**, 353-360.

ELIAS, C.L., LUKAS, A., SHURRAW, S., SCOTT, J., OMELCHENKO, A., GROSS, G.J., HNATOWICH, M. & HRYSHKO, L.V. (2001). Inhibition of Na^{+}/Ca^{2+} exchange by KB-R7943: transport mode selectivity and antiarrhythmic consequences. *American Journal of Physiology - Heart & Circulatory Physiology* **281**, H1334-H1345.

ELLIS, D. (1977). The effects of external cations and ouabain on the intracellular sodium activity of sheep heart Purkinje fibres. *Journal of Physiology* **273**, 211-240.

ELLIS, D. & MACLEOD, K.T. (1985). Sodium-dependent control of intracellular pH in Purkinje fibres of sheep heart. *Journal of Physiology* **359**, 81-105.

FAGAN, T.E. & ROMANI, A. (2001). α_1-Adrenoceptor-induced Mg^{2+} extrusion from rat hepatocytes occurs via Na^{+}-dependent transport mechanism. *American Journal of Physiol Gastrointest Liver Physiol* **280**, G1145-G1156.

FÉRAY, J.C. & GARAY, R. (1986). An Na^{+}-stimulated Mg^{2+}-transport system in human red blood cells. *Biochimica et Biophysica Acta* **856**, 76-84.

FÉRAY, J.C. & GARAY, R. (1988). Demonstration of a Na^{+}: Mg^{2+} exchange in human red cells by its sensitivity to tricyclic antidepressant drugs. *Naunyn-Schmiedebergs Archives of Pharmacology* **338** , 332-337.

FINDLAY, I. (1987). ATP-sensitive K^{+} channels in rat ventricular myocytes are blocked and inactivated by internal divalent cations. *Pflugers Archiv - European Journal of Physiology* **410**, 313-320.

FIOLET, J.W., BAARTSCHEER, A., SCHUMACHER, C.A., CORONEL, R. & TER WELLE, H.F. (1984). The change of the free energy of ATP hydrolysis during global ischemia and anoxia in the rat heart. Its possible role in the regulation of transsarcolemmal sodium and potassium gradients. *Journal of Molecular & Cellular Cardiology* **16**, 1023-1036.

FLATMAN, P.W. (1984). Magnesium transport across cell membranes. *Journal of Membrane Biology* **80**, 1-14.

FLATMAN, P.W. (1991). Mechanisms of magnesium transport. *Annual Review of Physiology* **53**, 259-271.

FLATMAN, P.W. & LEW, V.L. (1980). Magnesium buffering in intact human red blood cells measured using the ionophore A23187. *Journal of Physiology* **305**, 13-30.

FLATMAN, P.W. & SMITH, L.M. (1990). Magnesium transport in ferret red cells. *Journal of Physiology* **431**, 11-25.

FLATMAN, P.W. & SMITH, L.M. (1991). Sodium-dependent magnesium uptake by ferret red cells. *Journal of Physiology* **443**, 217-230.

FLATMAN, P.W. & SMITH, L.M. (1996). Magnesium transport in magnesium-loaded ferret red blood cells. *Pflugers Archive-European Journal of Physiology* **432**, 995-1002.

FLIK, G., VAN DER VELDEN, J.A. & KOLAR, Z.I. (1993). Radiotracer probes in cellular magnesium transport studies. In *Magnesium and the Cell*, ed. BIRCH, N.J., pp. 80-90. London: Academic Press.

FORD, L.E. & PODOLSKY, R.J. (1972). Intracellular calcium movements in skinned muscle fibres. *Journal of Physiology* **223**, 21-33.

FOX, C., RAMSOOMAIR, D. & CARTER, C. (2001). Magnesium: its proven and potential clinical significance. *Southern Medical Journal* **94**, 1195-1201.

FRAKES, M.A. & RICHARDSON, L.E.2. (1997). Magnesium sulfate therapy in certain emergency conditions. *American Journal of Emergency Medicine* **15**, 182-187.

FREIRE, C.A., KINNE, R.K., KINNE-SAFFRAN, E. & BEYENBACH, K.W. (1996). Electrodiffusive transport of Mg across renal membrane vesicles of the rainbow trout Oncorhynchus mykiss. *American Journal of Physiology* **270**, F739-F748.

FRENKEL, E.J., GRAZIANI, M. & SCHATZMANN, H.J. (1989). ATP requirement of the sodium-dependent magnesium extrusion from human red blood cells. *Journal of Physiology* **414**, 385-397.

FREUDENRICH, C.C., MURPHY, E., LEVY, L.A., LONDON, R.E. & LIEBERMAN, M. (1992b). Intracellular pH modulates cytosolic free magnesium in cultured chicken heart cells. *American Journal of Physiology* **262**, C1024-C1030.

FREUDENRICH, C.C., MURPHY, E., LIU, S. & LIEBERMAN, M. (1992a). Magnesium homeostasis in cardiac cells. *Molecular & Cellular Biochemistry* **114**, 97-103.

FRY, C.H. (1986). Measurement and control of intracellular magnesium ion concentration in guinea pig and ferret ventricular myocardium. *Magnesium* **5**, 306-316.

FRY, C.H. & PROCTOR, A.V. (1993). The effect of magnesium on excitable tissues. In *Magnesium and the Cell*, ed. BIRCH, N.J., pp. 217-234. London: Academic Press.

GADSBY, D.C. (1984). The Na/K pump of cardiac cells. *Annual Review of Biophysics & Bioengineering* **13**, 373-398.

GARFINKEL, L., ALTSCHULD, R.A. & GARFINKEL, D. (1986). Magnesium in cardiac energy metabolism. *Journal of Molecular & Cellular Cardiology* **18**, 1003-1013.

GARLID, K.D., DIRESTA, D.J., BEAVIS, A.D. & MARTIN, W.H. (1986). On the mechanism by which dicyclohexylcarbodiimide and quinine inhibit K^+ transport in rat liver mitochondria. *Journal of Biological Chemistry* **261**, 1529-1535.

GILBERT, D.L. (1960). Magnesium Equilibrium in Muscle. *Journal of General Physiology* **43**, 1103-1118.

GOW, I.F., LATHAM, T., ELLIS, D. & FLATMAN, P.W. (1995). Measurement of intracellular ionized magnesium concentration in myocytes isolated from the septomarginal band of sheep hearts. *Magnesium Research* **8**, 223-232.

GRASCHOPF, A., STADLER, J.A., HOELLERER, M.K., EDER, S., SIEGHARDT, M., KOHLWEIN, S.D. & SCHWEYEN, R.J. (2001). The yeast plasma membrane protein Alr1 controls Mg^{2+} homeostasis and is subject to Mg^{2+}-dependent control of its synthesis and degradation. *Journal of Biological Chemistry* **276**, 16216-16222.

GRIFFITHS, E.J., STERN, M.D. & SILVERMAN, H.S. (1997). Measurement of mitochondrial calcium in single living cardiomyocytes by selective removal of cytosolic indo 1. *American Journal of Physiology* **273**, C37-C44.

GROVER, S. & HAMEL, E. (1994). The magnesium-GTP interaction in microtubule assembly. *European Journal of Biochemistry* **222**, 163-172.

GRYNKIEWICZ, G., POENIE, M. & TSIEN, R.Y. (1985). A new generation of Ca^{2+} indicators with greatly improved fluorescence properties. *Journal of Biological Chemistry* **260**, 3440-3450.

GÜNTHER, T. (1986). Functional compartmentation of intracellular magnesium. *Magnesium* **5**, 53-59.

GÜNTHER, T. (1993). Mechanisms and regulation of Mg^{2+} efflux and Mg^{2+} influx. *Mineral & Electrolyte Metabolism* **19**, 259-265.

GÜNTHER, T. & HOLLRIEGL, V. (1993). Na^+- and anion-dependent Mg^{2+} influx in isolated hepatocytes. *Biochimica et Biophysica Acta* **1149**, 49-54.

GÜNTHER, T. & VORMANN, J. (1985). Mg^{2+} efflux is accomplished by an amiloride-sensitive Na^+/Mg^{2+} antiport. *Biochemical & Biophysical Research Communications* **130**, 540-545.

GÜNTHER, T. & VORMANN, J. (1989a). Characterization of Mg^{2+} efflux from human, rat and chicken erythrocytes. *FEBS Letters* **250**, 633-637.

GÜNTHER, T. & VORMANN, J. (1989b). Na^+-independent Mg^{2+} efflux from Mg^{2+}-loaded human erythrocytes. *FEBS Letters* **247**, 181-184.

GÜNTHER, T. & VORMANN, J. (1990). Characterization of Na^+-independent Mg^{2+} efflux from erythrocytes. *FEBS Letters* **271**, 149-151.

GÜNTHER, T. & VORMANN, J. (1991). Mg^{2+} influx into Mg^{2+}-depleted reticulocytes. *Magnesium & Trace Elements* **10**, 17-20.

GÜNTHER, T. & VORMANN, J. (1992). Activation of Na^+/Mg^{2+} antiport in thymocytes by cAMP. *FEBS Letters* **297**, 132-134.

GÜNTHER, T. & VORMANN, J. (1995). Reversibility of Na^+/Mg^{2+} antiport in rat erythrocytes. *Biochimica et Biophysica Acta* **1234**, 105-110.

GÜNTHER, T., VORMANN, J. & HOLLRIEGL, V. (1990). Characterization of Na^+-dependent Mg^{2+} efflux from Mg^{2+}-loaded rat erythrocytes. *Biochimica et Biophysica Acta* **1023**, 455-461.

GÜNZEL, D., DURRY, S. & SCHLUE, W.R. (1997). Intracellular alkalinization causes Mg^{2+} release from intracellular binding sites in leech Retzius neurones. *Pflugers Archiv - European Journal of Physiology* **435**, 65-73.

GÜNZEL, D. & SCHLUE, W.R. (1996). Sodium-magnesium antiport in Retzius neurones of the leech Hirudo medicinalis. *Journal of Physiology* **491**, 595-608.

GÜNZEL, D. & SCHLUE, W.R. (2000). Mechanisms of Mg^{2+} influx, efflux and intracellular 'muffling' in leech neurones and glial cells. *Magnesium Research* **13**, 123-138.

GUPTA, R.K., GUPTA, P. & MOORE, R.D. (1984). NMR studies of intracellular metal ions in intact cells and tissues. *Annual Review of Biophysics & Bioengineering* **13**, 221-246.

HAGIWARA, N., IRISAWA, H. & KAMEYAMA, M. (1988). Contribution of two types of calcium currents to the pacemaker potentials of rabbit sino-atrial node cells. *Journal of Physiology* **395**, 233-253.

HAHIN, R. & CAMPBELL, D.T. (1983). Simple shifts in the voltage dependence of sodium channel gating caused by divalent cations. *Journal of General Physiology* **82**, 785-805.

HALL, S.K. & FRY, C.H. (1992). Magnesium affects excitation, conduction, and contraction of isolated mammalian cardiac muscle. *American Journal of Physiology* **263**, H622-H633.

HALL, S.K., FRY, C.H., BURI, A. & MCGUIGAN, J.A. (1991). Use of ion-sensitive microelectrodes to study intracellular free magnesium concentration and its regulation in mammalian cardiac muscle. *Magnesium & Trace Elements* **10**, 80-89.

HAMILL, O.P., MARTY, A., NEHER, E., SAKMANN, B. & SIGWORTH, F.J. (1981). Improved patch-clamp techniques for high-resolution current recording from cells and cell-free membrane patches. *Pflugers Archiv - European Journal of Physiology* **391**, 85-100.

HANDY, R.D., GOW, I.F., ELLIS, D. & FLATMAN, P.W. (1996). Na-dependent regulation of intracellular free magnesium concentration in isolated rat ventricular myocytes. *Journal of Molecular & Cellular Cardiology* **28**, 1641-1651.

HARTZELL, H.C. & WHITE, R.E. (1989). Effects of magnesium on inactivation of the voltage-gated calcium current in cardiac myocytes. *Journal of General Physiology* **94**, 745-767.

HAUGLAND, R. (1999). Intracellular Ion Indicators. In Fluorescent and Luminescent Probes for Biological Activity: A Practical Guide to Technology for Quantitative Real-Time Analysis, ed. MASON, W.T., pp. 34-43. Academic Press.

HAWORTH, R.A. & HUNTER, D.R. (1979). The Ca^{2+}-induced membrane transition in mitochondria. II. Nature of the Ca^{2+} trigger site. *Archives of Biochemistry & Biophysics* **195**, 460-467.

HEATON, F.W. (1993). Distribution and function of magnesium within the cell. In *Magnesium and the Cell*, ed. BIRCH, N.J., pp. 121-136. London: Academic Press.

HENNEKENS, C.H., ALBERT, C.M., GODFRIED, S.L., GAZIANO, J.M. & BURING, J.E. (1996). Adjunctive drug therapy of acute myocardial infarction--evidence from clinical trials. *New England Journal of Medicine* **335**, 1660-1667.

HERZOG, W.R. & SEREBRUANY, V.L. (1996). How magnesium therapy may influence clinical outcome in acute myocardial infarction: review of potential mechanisms. *Coronary Artery Disease* **7**, 364-370.

HESS, P., METZGER, P. & WEINGART, R. (1982). Free magnesium in sheep, ferret and frog striated muscle at rest measured with ion-selective micro-electrodes. *Journal of Physiology* **333**, 173-188.

HILLE, B. (1992a). Calcium channels. In *Ionic Channels of Excitable Membranes*, ed. pp. 83-114. Sinauer Associates Inc., Sunderland, Massachusetts.

HILLE, B. (1992). Counting Channels. In *Ionic Channels of Excitable Membranes*, ed. pp. 315-336. Sinauer Associates Inc., Sunderland, Massachusetts.

HILLE, B. (1992b). *Ionic Channels of Excitable Membranes, ed.* Sinauer Associates Inc., Sunderland, Massachusetts.

HINTZ, K., GÜNZEL, G. & SCHLUE, W.R. (1999). Na^{+}-dependent regulation of the free Mg^{2+} concentration in neuropile glial cells and P neurones of the leech Hirudo medicinalis. *Pflugers Archiv - European Journal of Physiology* **437**, 354-362.

HIRANO, Y., FOZZARD, H.A. & JANUARY, C.T. (1989). Characteristics of L- and T-type Ca^{2+} currents in canine cardiac Purkinje cells. *American Journal of Physiology* **256**, H1478-H1492.

HONGO, K., KONISHI, M. & KURIHARA, S. (1994). Cytoplasmic free Mg^{2+} in rat ventricular myocytes studied with the fluorescent indicator furaptra. *Japanese Journal of Physiology* **44**, 357-378.

HORIE, M., IRISAWA, H. & NOMA, A. (1987). Voltage-dependent magnesium block of adenosine-triphosphate-sensitive potassium channel in guinea-pig ventricular cells. *Journal of Physiology* **387**, 251-272.

HOWARTH, F.C., SINGH, J., WARING, J.J., HUSTLER, B.I. & BAILEY, M. (1995). Effects of monovalent cations, pH and temperature on the dissociation constant (KD) for the fluorescent indicator mag-fura-2 at different excitation wavelengths. *Magnesium Research* **8**, 299-306.

HU, Z.M., BUHRER, T., MULLER, M., RUSTERHOLZ, B., ROUILLY, M. & SIMON, W. (1989). Intracellular magnesium ion selective microelectrode based on a neutral carrier. *Analytical Chemistry* **61**, 574-576.

HURLEY, T.W., RYAN, M.P. & BRINCK, R.W. (1992). Changes of cytosolic Ca^{2+} interfere with measurements of cytosolic Mg^{2+} using mag-fura-2. *American Journal of Physiology* **263**, C300-C307.

HUSER, J., BLATTER, L.A. & LIPSIUS, S.L. (2000). Intracellular Ca^{2+} release contributes to automaticity in cat atrial pacemaker cells. *Journal of Physiology* **524**, 415-422.

ISIS-4 COLLABORATIVE GROUP (1991). Fourth International Study of Infarct Survival: protocol for a large simple study of the effects of oral mononitrate, of oral captopril, and of intravenous magnesium. *American Journal of Cardiology* **68**, 87D-100D.

IWAMOTO, T., KITA, S., UEHARA, A., INOUE, Y., TANIGUCHI, Y., IMANAGA, I. & SHIGEKAWA, M. (2001). Structural domains influencing sensitivity to isothiourea derivative inhibitor KB-R7943 in cardiac Na^{+}/Ca^{2+} exchanger. *Molecular Pharmacology* **59**, 524-531.

IWAMOTO, T. & SHIGEKAWA, M. (1998). Differential inhibition of Na^{+}/Ca^{2+} exchanger isoforms by divalent cations and isothiourea derivative. *American Journal of Physiology* **275**, C423-C430.

IWAMOTO, T., WATANO, T. & SHIGEKAWA, M. (1996). A novel isothiourea derivative selectively inhibits the reverse mode of Na^{+}/Ca^{2+} exchange in cells expressing NCX1. *Journal of Biological Chemistry* **271**, 22391-22397.

JOHNSON, A.D., ELDER, H.Y., NICHOLSON, W.A.P. & MCGUIGAN, J.A.S. (1997). The distribution of Mg in ferret ventricular cells in Tyrode solution and on Na^{+} removal. *Journal of Physiology* **505.P**, 92P.

JORGENSEN, P.L. (1974). Isolation and characterization of the components of the sodium pump. *Quarterly Reviews of Biophysics* **7**, 239-274.

JUNG, D.W., APEL, L. & BRIERLEY, G.P. (1990). Matrix free Mg^{2+} changes with metabolic state in isolated heart mitochondria. *Biochemistry* **29**, 4121-4128.

JUNG, D.W. & BRIERLEY, G.P. (1994). Magnesium transport by mitochondria. *Journal of Bioenergetics & Biomembranes* **26**, 527-535.

JUTTNER, R. & EBEL, H. (1998). Characterization of Mg^{2+} transport in brush border membrane vesicles of rabbit ileum studied with mag-fura-2. *Biochimica et Biophysica Acta* **1370**, 51-63.

KAMMERMEIER, H., SCHMIDT, P. & JUNGLING, E. (1982). Free energy change of ATP-hydrolysis: a causal factor of early hypoxic failure of the myocardium? *Journal of Molecular & Cellular Cardiology* **14**, 267-277.

KENNEDY, H.J. (1998). Intracellular Mg^{2+} regulation in voltage-clamped Helix Aspersa neurons measured with Mag-Fura-2 and Mg^{2+}-sensitive microelectrodes. *Experimental Physiology* **83**, 449-460.

KERRICK, W.G. & DONALDSON, S.K. (1972). The effects of Mg^{2+} on submaximum Ca^{2+} -activated tension in skinned fibers of frog skeletal muscle. *Biochimica et Biophysica Acta* **275**, 117-122.

KIM, D. & SMITH, T.W. (1988). Cellular mechanisms underlying calcium-proton interactions in cultured chick ventricular cells. *Journal of Physiology* **398**, 391-410.

KLEYMAN, T.R. & CRAGOE, E.J.J. (1988). Amiloride and its analogues as tools in the study of ion transport. *Journal of Membrane Biology* **105**, 1-21.

KRAMER, J.H., CHOVAN, J.P. & SCHAFFER, S.W. (1981). Effect of taurine in calcium paradox and ischemic heart failure. *American Journal of Physiology* **240**, H238-H246.

LADILOV, Y., HAFFNER, S., BALSER-SCHAFER, C., MAXEINER, H. & PIPER, H.M. (1999). Cardioprotective effects of KB-R7943: a novel inhibitor of the reverse mode of Na^{+}/Ca^{2+} exchanger. *American Journal of Physiology* **276**, H1868-H1876.

LANTER, F., ERNE, D., AMMANN, D. & SIMON, W. (1980). Neutral carrier based ion-selective electrode for intracellular magnesium activity studies. *Analytical Chemistry* **52**, 2400-2402.

LAPIDUS, R.G. & SOKOLOVE, P.M. (1994). The mitochondrial permeability transition. Interactions of spermine, ADP, and inorganic phosphate. *Journal of Biological Chemistry* **269**, 18931-18936.

LATTANZIO, F.A.J. & BARTSCHAT, D.K. (1991). The effect of pH on rate constants, ion selectivity and thermodynamic properties of fluorescent calcium and magnesium indicators. *Biochemical & Biophysical Research Communications* **177**, 184-191.

LEONHARD-MAREK, S., GABEL, G. & MARTENS, H. (1998). Effects of short chain fatty acids and carbon dioxide on magnesium transport across sheep rumen epithelium. *Experimental Physiology* **83**, 155-164.

LEVI, A.J. (1991). The effect of strophanthidin on action potential, calcium current and contraction in isolated guinea-pig ventricular myocytes. *Journal of Physiology* **443**, 1-23.

LEVI, A.J., LEE, C.O. & BROOKSBY, P. (1994). Properties of the fluorescent sodium indicator "SBFI" in rat and rabbit cardiac myocytes. [see comments]. *Journal of Cardiovascular Electrophysiology* **5**, 241-257.

LEVI, A.J., LEE, C.O., HANCOX, J., ISSBERNER, J. & WANG, X. (1992). A method for obtaining a high yield of healthy myocytes from the ventricle and atrioventricular node of isolated rabbit hearts. *Journal of Physiology* **452**, 157P.

LEVINE, B.S. & COBURN, J.W. (1984). Magnesium, the mimic/antagonist to calcium. *New England Journal of Medicine* **310**, 1253-1255.

LEVY, L.A., MURPHY, E., RAJU, B. & LONDON, R.E. (1988). Measurement of cytosolic free magnesium ion concentration by ^{19}F NMR. *Biochemistry* **27**, 4041-4048.

LI, H.Y. & QUAMME, G.A. (1997). Caffeine decreases intracellular free Mg^{2+} in isolated adult rat ventricular myocytes. *Biochimica et Biophysica Acta* **1355**, 61-68.

LI, Z., MATSUOKA, S., HRYSHKO, L.V., NICOLL, D.A., BERSOHN, M.M., BURKE, E.P., LIFTON, R.P. & PHILIPSON, K.D. (1994). Cloning of the NCX2 isoform of the plasma membrane Na^{+}-Ca^{2+} exchanger. *Journal of Biological Chemistry* **269**, 17434-17439.

LONDON, R.E. (1991). Methods for measurement of intracellular magnesium: NMR and fluorescence. *Annual Review of Physiology* **53**, 241-258.

LÜDI, H. & SCHATZMANN, H.J. (1987). Some properties of a system for sodium-dependent outward movement of magnesium from metabolizing human red blood cells. *Journal of Physiology* **390**, 367-382.

LÜTHI, D., GÜNZEL, D. & MCGUIGAN, J.A. (1999). Mg-ATP binding: its modification by spermine, the relevance to cytosolic Mg^{2+} buffering, changes in the intracellular ionized Mg^{2+} concentration and the estimation of Mg^{2+} by ^{31}P-NMR. *Experimental Physiology* **84**, 231-252.

LUX, H.D., CARBONE, E. & ZUCKER, H. (1990). Na^+ currents through low-voltage-activated Ca^{2+} channels of chick sensory neurones: block by external Ca $^{2+}$ and Mg^{2+}. *Journal of Physiology* **430**, 159-188.

MASON, W.T. (1999). Fluorescent and Luminescent Probes for Biological Activity: A Practical Guide to Technology for Quantitative Real-Time Analysis. Academic Press.

MASSARI, S. & AZZONE, G.F. (1972). The equivalent pore radius of intact and damaged mitochondria and the mechanism of active shrinkage. *Biochimica et Biophysica Acta* **283**, 23-29.

MATSUDA, H., SAIGUSA, A. & IRISAWA, H. (1987). Ohmic conductance through the inwardly rectifying K channel and blocking by internal Mg^{2+}. *Nature* **325**, 156-159.

MCDONALD, T.F., CAVALIE, A., TRAUTWEIN, W. & PELZER, D. (1986). Voltage-dependent properties of macroscopic and elementary calcium channel currents in guinea pig ventricular myocytes. *Pflugers Archiv - European Journal of Physiology* **406**, 437-448.

MCGUIGAN, J.A., ELDER, H.Y., GUNZEL, D. & SCHLUE, W.R. (2002). Magnesium homeostasis in heart: A critical reappraisal. *Journal of Clinical Basic Cardiology* **5**, 5-22.

MCKEEHAN, W.L. & MCKEEHAN, K.A. (1980). Calcium, magnesium, and serum factors in multiplication of normal and transformed human lung fibroblasts. *In Vitro* **16**, 475-485.

MEISSNER, G. & HENDERSON, J.S. (1987). Rapid calcium release from cardiac sarcoplasmic reticulum vesicles is dependent on Ca^{2+} and is modulated by Mg^{2+}, adenine nucleotide, and calmodulin. *Journal of Biological Chemistry* **262**, 3065-3073.

MIHAILIDOU, A.S., BUHAGIAR, K.A. & RASMUSSEN, H.H. (1998). Na+ influx and Na(+)-K+ pump activation during short-term exposure of cardiac myocytes to aldosterone. *American Journal of Physiology* **274**, C175-C181.

MOTA DE FREITAS, D. & DORUS, E. (1993). Techniques for measuring magnesium in tissues from hypertensive, psychiatric and neurological patients. In *Magnesium and the Cell*, ed. BIRCH, N.J., pp. 51-79. London: Academic Press.

MUBAGWA, K., STENGL, M. & FLAMENG, W. (1997). Extracellular divalent cations block a cation non-selective conductance unrelated to calcium channels in rat cardiac muscle. *Journal of Physiology* **502**, 235-247.

MUKAI, M., TERADA, H., SUGIYAMA, S., SATOH, H. & HAYASHI, H. (2000). Effects of a selective inhibitor of Na^+/Ca^{2+} exchange, KB-R7943, on reoxygenation-induced injuries in guinea pig papillary muscles. *Journal of Cardiovascular Pharmacology* **35**, 121-128.

MULLINS, L.J. & BRINLEY, F.J. (1978). Magnesium influx in dialyzed squid axons. *Journal of Membrane Biology* **43**, 243-250.

MURPHY, E., FREUDENRICH, C.C. & LIEBERMAN, M. (1991a). Cellular magnesium and Na/Mg exchange in heart cells. *Annual Review of Physiology* **53**, 273-287.

MURPHY, E., PERLMAN, M., LONDON, R.E. & STEENBERGEN, C. (1991b). Amiloride delays the ischemia-induced rise in cytosolic free calcium. *Circulation Research* **68**, 1250-1258.

MURPHY, E., STEENBERGEN, C., LEVY, L.A., RAJU, B. & LONDON, R.E. (1989). Cytosolic free magnesium levels in ischemic rat heart. *Journal of Biological Chemistry* **264**, 5622-5627.

NAKATANI, K. & YAU, K.W. (1988). Calcium and magnesium fluxes across the plasma membrane of the toad rod outer segment. *Journal of Physiology* **395**, 695-729.

NG, L.L., DAVIES, J.E. & QUINN, P. (1993). Intracellular pH regulation in isolated myocytes from adult rat heart in HCO^{3-}-containing and HCO^{3-}-free media. *Clinical Science* **84**, 133-139.

NICOLL, D.A., LONGONI, S. & PHILIPSON, K.D. (1990). Molecular cloning and functional expression of the cardiac sarcolemmal Na^{+}-Ca^{2+} exchanger. *Science* **250**, 562-565.

NICOLL, D.A., QUEDNAU, B.D., QUI, Z., XIA, Y.R., LUSIS, A.J. & PHILIPSON, K.D. (1996). Cloning of a third mammalian Na^{+}-Ca^{2+} exchanger, NCX3. *Journal of Biological Chemistry* **271**, 24914-24921.

ÖDBLOM, M.P. & HANDY, R.D. (1999). A novel DIDS-sensitive, anion-dependent Mg^{2+} efflux pathway in rat ventricular myocytes. *Biochemical & Biophysical Research Communications* **264**, 334-337.

ÖDBLOM, M.P. & HANDY, R.D. (2001). Effect of external magnesium on intracellular free sodium: Na^{+} flux via Na^{+}/Mg^{2+} antiport is masked by other Na^{+} transport systems in rat cardiac myocytes. *Magnesium Research* **14**, 3-9.

OTTEN, P.A., LONDON, R.E. & LEVY, L.A. (2001). 4-oxo-4H-quinolizine-3-carboxylic acids as Mg^{2+} selective, fluorescent indicators. *Bioconjugate Chemistry* **12**, 203-212.

PAGE, E. (1978). Quantitative ultrastructural analysis in cardiac membrane physiology. *American Journal of Physiology* **235**, C147-C158.

PAGE, E., MCCALLISTER, L.P. & POWER, B. (1971). Stereological measurements of cardiac ultrastructures implicated in excitation-contraction coupling. *Proceedings of the National Academy of Sciences of the United States of America* **68**, 1465-1466.

PAGE, E. & POLIMENI, P.I. (1972). Magnesium exchange in rat ventricle. *Journal of Physiology* **224** , 121-139.

PAOLISSO, G. & BARBAGALLO, M. (1997). Hypertension, diabetes mellitus, and insulin resistance: the role of intracellular magnesium. *American Journal of Hypertension* **10**, 346-355.

PARIS, S. & POUYSSEGUR, J. (1983). Biochemical characterization of the amiloride-sensitive Na^+/H^+ antiport in Chinese hamster lung fibroblasts. *Journal of Biological Chemistry* **258**, 3503-3508.

PETRONILLI, V., COLA, C. & BERNARDI, P. (1993). Modulation of the mitochondrial cyclosporin A-sensitive permeability transition pore. II. The minimal requirements for pore induction underscore a key role for transmembrane electrical potential, matrix pH, and matrix Ca^{2+}. *Journal of Biological Chemistry* **268**, 1011-1016.

PIKE, M.M., KITAKAZE, M. & MARBAN, E. (1990). ^{23}Na-NMR measurements of intracellular sodium in intact perfused ferret hearts during ischemia and reperfusion. *American Journal of Physiology* **259**, H1767-H1773.

PINDER, R.M. & WIERINGA, J.H. (1993). Third-generation antidepressants. *Medicinal Research Reviews* **13**, 259-325.

PIPER, H.M. (2000). The calcium paradox revisited: an artefact of great heuristic value. *Cardiovascular Research* **45**, 123-127.

POLAK, P. (1989). Photonuclear production of ^{28}Mg ($\rightarrow{}^{28}$Al). *Journal of Labelled Compounds and Radiopharmaceuticals* **26**, 173-174.

PRESCOTT, A.R., COMERFORD, J.G., MAGRATH, R., LAMB, N.J. & WARN, R.M. (1988). Effects of elevated intracellular magnesium on cytoskeletal integrity. *Journal of Cell Science* **89**, 321-329.

PRESTON, R.R. (1990). A magnesium current in Paramecium. *Science* **250**, 285-288.

QUAMME, G.A. (1993). Magnesium homeostasis and renal magnesium handling. *Mineral & Electrolyte Metabolism* **19**, 218-225.

QUAMME, G.A. & RABKIN, S.W. (1990). Cytosolic free magnesium in cardiac myocytes: identification of a Mg^{2+} influx pathway. *Biochemical & Biophysical Research Communications* **167**, 1406-1412.

RABBANI, L.E. & ANTMAN, E.M. (1996). The role of magnesium therapy in acute myocardial infarction. *Clinical Cardiology* **19**, 841-844.

RAJU, B., MURPHY, E., LEVY, L.A., HALL, R.D. & LONDON, R.E. (1989). A fluorescent indicator for measuring cytosolic free magnesium. *American Journal of Physiology* **256**, C540-C548.

RASGADO-FLORES, H., GONZALEZ-SERRATOS, H. & DESANTIAGO, J. (1994). Extracellular Mg^{2+}-dependent Na^{+}, K^{+}, and Cl^{-} efflux in squid giant axons. *American Journal of Physiology* **266**, C1112-C1117.

REID, S.S. & COWAN, J.A. (1990). Biostructural chemistry of magnesium ion: characterization of the weak binding sites on tRNA(Phe)(yeast). Implications for conformational change and activity. *Biochemistry* **29**, 6025-6032.

REUBEN, J.P., BRANDT, P.W., BERMAN, M. & GRUNDFEST, H. (1971). Regulation of tension in the skinned crayfish muscle fiber. I. Contraction and relaxation in the absence of Ca (pCa is greater than 9). *Journal of General Physiology* **57**, 385-407.

RILEY, W.W. & PFEIFFER, D.R. (1985). Relationships between Ca^{2+} release, Ca^{2+} cycling, and Ca^{2+}-mediated permeability changes in mitochondria. *Journal of Biological Chemistry* **260**, 12416-12425.

RODRIGO, G.C. & CHAPMAN, R.A. (1991). The calcium paradox in isolated guinea-pig ventricular myocytes: effects of membrane potential and intracellular sodium. *Journal of Physiology* **434**, 627-645.

ROGERS, R.A. & MAHAN, P.E. (1959). Exchange of radioactive magnesium in the rat. *Proceedings of the Society of Experimental Biology and Medicine* **100**, 235-239.

ROMANI, A., DOWELL, E. & SCARPA, A. (1991). Cyclic AMP-induced Mg^{2+} release from rat liver hepatocytes, permeabilized hepatocytes, and isolated mitochondria. *Journal of Biological Chemistry* **266**, 24376-24384.

ROMANI, A., MARFELLA, C. & SCARPA, A. (1992). Regulation of Mg^{2+} uptake in isolated rat myocytes and hepatocytes by protein kinase C. *FEBS Letters* **296**, 135-140.

ROMANI, A., MARFELLA, C. & SCARPA, A. (1993a). Regulation of magnesium uptake and release in the heart and in isolated ventricular myocytes. *Circulation Research* **72**, 1139-1148.

ROMANI, A., MARFELLA, C. & SCARPA, A. (1993b). Hormonal stimulation of Mg^{2+} uptake in hepatocytes. Regulation by plasma membrane and intracellular organelles. *Journal of Biological Chemistry* **268**, 15489-15495.

ROMANI, A. & SCARPA, A. (1990). Hormonal control of Mg^{2+} transport in the heart. *Nature* **346**, 841-844.

ROMANI, A. & SCARPA, A. (1992a). cAMP control of Mg^{2+} homeostasis in heart and liver cells. *Magnesium Research* **5**, 131-137.

ROMANI, A. & SCARPA, A. (1992b). Regulation of cell magnesium. *Archives of Biochemistry &.Biophysics* **298**, 1-12.

ROMANI, A.M. & SCARPA, A. (2000). Regulation of cellular magnesium. *Frontiers in Bioscience* **5**, D720-D734.

ROUILLY, M., RUSTERHOLZ, B., SPICHIGER, U.E. & SIMON, W. (1990). Neutral ionophore-based selective electrode for assaying the activity of magnesium in undiluted blood serum. *Clinical Chemistry* **36**, 466-469.

RUDE, R.K. & OLDHAM, S.B. (1990). The Metabolic and Molecular Basis of Acquired Disease. In *Disorders of magnesium metabolism*, eds. COHEN, R.D., LEWIS, B., ALBERTI, K. & ET AL, pp. 1124London: Bailliere Tindall.

RUTTER, G.A., OSBALDESTON, N.J., MCCORMACK, J.G. & DENTON, R.M. (1990). Measurement of matrix free Mg^{2+} concentration in rat heart mitochondria by using entrapped fluorescent probes. *Biochemical Journal* **271**, 627-634.

SALAMA, G. & SCARPA, A. (1985). Magnesium permeability of sarcoplasmic reticulum. Mg^{2+} is not countertransported during ATP-dependent Ca^{2+} uptake by sarcoplasmic reticulum. *Journal of Biological Chemistry* **260**, 11697-11705.

SARIS, N.E., MERVAALA, E., KARPPANEN, H., KHAWAJA, J.A. & LEWENSTAM, A. (2000). Magnesium. An update on physiological, clinical and analytical aspects. *Clinica Chimica Acta* **294**, 1-26.

SATOH, H. (1994). Cardioprotective actions of taurine against intracellular and extracellular calcium-induced effects. *Advances in Experimental Medicine & Biology* **359**, 181-196.

SATOH, H., GINSBURG, K.S., QING, K., TERADA, H., HAYASHI, H. & BERS, D.M. (2000). KB-R7943 block of Ca^{2+} influx via Na^{+}/Ca^{2+} exchange does not alter twitches or glycoside inotropy but prevents Ca^{2+} overload in rat ventricular myocytes. *Circulation* **101**, 1441-1446.

SATOH, H. & SPERELAKIS, N. (1998). Review of some actions of taurine on ion channels of cardiac muscle cells and others. *General Pharmacology* **30**, 451-463.

SAUNDERS, C., FERRER, J.V., SHI, L., CHEN, J., MERRILL, G., LAMB, M.E., LEEB-LUNDBERG, L.M., CARVELLI, L., JAVITCH, J.A. & GALLI, A. (2000). Amphetamine-induced loss of human dopamine transporter activity: an internalization-dependent and cocaine-sensitive mechanism. *Proceedings of the National Academy of Sciences of the United States of America* **97**, 6850-6855.

SCHRODER, U.H., BREDER, J., SABELHAUS, C.F. & REYMANN, K.G. (1999). The novel Na^{+}/Ca^{2+} exchange inhibitor KB-R7943 protects CA1 neurons in rat hippocampal slices against hypoxic/hypoglycemic injury. *Neuropharmacology* **38**, 319-321.

SERRANO, J.R., DASHTI, S.R., PEREZ-REYES, E. & JONES, S.W. (2000). Mg^{2+} block unmasks Ca^{2+} /Ba^{2+} selectivity of alpha1G T-type calcium channels. *Biophysical Journal* **79**, 3052-3062.

SHECHTER, M., HOD, H., MARKS, N., BEHAR, S., KAPLINSKY, E. & RABINOWITZ, B. (1990). Beneficial effect of magnesium sulfate in acute myocardial infarction. *American Journal of Cardiology* **66**, 271-274.

SHEU, S.S., SHARMA, V.K. & BANERJEE, S.P. (1984). Measurement of cytosolic free calcium concentration in isolated rat ventricular myocytes with quin 2. *Circulation Research* **55**, 830-834.

SHIMONI, Y., CLARK, R.B. & GILES, W.R. (1992). Role of an inwardly rectifying potassium current in rabbit ventricular action potential. *Journal of Physiology* **448**, 709-727.

SILVERMAN, H.S., DI LISA, F., HUI, R.C., MIYATA, H., SOLLOTT, S.J., HANFORD, R.G., LAKATTA, E.G. & STERN, M.D. (1994). Regulation of intracellular free Mg^{2+} and contraction in single adult mammalian cardiac myocytes. *American Journal of Physiology* **266**, C222-C233.

SLAYMAN, C.L., MOUSSATOS, V.V. & WEBB, W.W. (1994). Endosomal accumulation of pH indicator dyes delivered as acetoxymethyl esters. *Journal of Experimental Biology* **196**, 419-438.

SOMLYO, A.V., MCCLELLAN, G., GONZALEZ-SERRATOS, H. & SOMLYO, A.P. (1985). Electron probe X-ray microanalysis of post-tetanic Ca^{2+} and Mg^{2+} movements across the sarcoplasmic reticulum in situ. *Journal of Biological Chemistry* **260**, 6801-6807.

STARON, K. (1985). Condensation of the chromatin gel by cations. *Biochim Biophys Acta* **825**, 289-298.

STORM, W. & ZIMMERMAN, J.J. (1997). Magnesium deficiency and cardiogenic shock after cardiopulmonary bypass. *Annals of Thoracic Surgery* **64**, 572-577.

STOUT, A.K., LI-SMERIN, Y., JOHNSON, J.W. & REYNOLDS, I.J. (1996). Mechanisms of glutamate-stimulated Mg^{2+} influx and subsequent Mg^{2+} efflux in rat forebrain neurones in culture. *Journal of Physiology* **492**, 641-657.

SZABO, I. & ZORATTI, M. (1991). The giant channel of the inner mitochondrial membrane is inhibited by cyclosporin A. *Journal of Biological Chemistry* **266**, 3376-3379.

TANI, M. & NEELY, J.R. (1989). Role of intracellular Na^{+} in Ca^{2+} overload and depressed recovery of ventricular function of reperfused ischemic rat hearts. Possible involvement of H^{+}-Na^{+} and Na^{+}-Ca^{2+} exchange. *Circulation Research* **65**, 1045-1056.

TASHIRO, M. & KONISHI, M. (1997a). Basal intracellular free Mg^{2+} concentration in smooth muscle cells of guinea pig tenia cecum: intracellular calibration of the fluorescent indicator furaptra. *Biophysical Journal* **73**, 3358-3370.

TASHIRO, M. & KONISHI, M. (1997b). Na^+ gradient-dependent Mg^{2+} transport in smooth muscle cells of guinea pig tenia cecum. *Biophysical Journal* **73**, 3371-3384.

TASHIRO, M. & KONISHI, M. (2000). Sodium gradient-dependent transport of magnesium in rat ventricular myocytes. *American Journal of Physiology - Cell Physiology* **279**, C1955-C1962.

TASHIRO, M., KONISHI, M., IWAMOTO, T., SHIGEKAWA, M. & KURIHARA, S. (2000). Transport of magnesium by two isoforms of the Na^+-Ca^{2+} exchanger expressed in CCL39 fibroblasts. *Pflugers Archiv - European Journal of Physiology* **440**, 819-827.

TESSMAN, P.A. & ROMANI, A. (1998). Acute effect of EtOH on Mg^{2+} homeostasis in liver cells: evidence for the activation of an Na^+/Mg^{2+} exchanger. *American Journal of Physiology* **275**, G1106-G1116.

TOUYZ, R.M. & SCHIFFRIN, E.L. (1996). Angiotensin II and vasopressin modulate intracellular free magnesium in vascular smooth muscle cells through Na^+-dependent protein kinase C pathways. *Journal of Biological Chemistry* **271** , 24353-24358.

TSIEN, R.W., BEAN, B.P., HESS, P. & NOWYCKY, M. (1983). Calcium channels: mechanisms of beta-adrenergic modulation and ion permeation. *Cold Spring Harbor Symposia on Quantitative Biology* **48 Pt 1**, 201-212.

TSIEN, R.Y. (1980). New calcium indicators and buffers with high selectivity against magnesium and protons: design, synthesis, and properties of prototype structures. *Biochemistry* **19**, 2396-2404.

TSIEN, R.Y. (1988). Fluorescence measurement and photochemical manipulation of cytosolic free calcium. *Trends in Neurosciences* **11**, 419-424.

TUNSTALL, J., BUSSELEN, P., RODRIGO, G.C. & CHAPMAN, R.A. (1986). Pathways for the movements of ions during calcium-free perfusion and the induction of the 'calcium paradox'. *Journal of Molecular & Cellular Cardiology* **18**, 241-254.

VAN ECHTELD, C.J., KIRKELS, J.H., EIJGELSHOVEN, M.H., VAN DER MEER, P. & RUIGROK, T.J. (1991). Intracellular sodium during ischemia and calcium-free perfusion: a ^{23}Na NMR study. *Journal of Molecular & Cellular Cardiology* **23**, 297-307.

VAN ECHTELD, C.J., VAN, E., JG, JANSEN, M.A., SCHREUR, J.H. & RUIGROK, T.J. (1998). Manipulation of intracellular sodium by extracellular divalent cations: a ^{23}Na and ^{31}P NMR study on intact rat hearts. *Journal of Molecular & Cellular Cardiology* **30**, 119-126.

VAN EMOUS, J.G., NEDERHOFF, M.G., RUIGROK, T.J. & VAN ECHTELD, C.J. (1997). The role of the Na^+ channel in the accumulation of intracellular Na^+ during myocardial ischemia: consequences for post-ischemic recovery. *Journal of Molecular & Cellular Cardiology* **29**, 85-96.

VAN EMOUS, J.G., SCHREUR, J.H., RUIGROK, T.J. & VAN ECHTELD, C.J. (1998). Both Na^+-K^+ ATPase and Na^+-H^+ exchanger are immediately active upon post-ischemic reperfusion in isolated rat hearts. *Journal of Molecular & Cellular Cardiology* **30**, 337-348.

VAUGHAN-JONES, R.D., LEDERER, W.J. & EISNER, D.A. (1983). Ca^{2+} ions can affect intracellular pH in mammalian cardiac muscle. *Nature* **301**, 522-524.

VORMANN, J. & GÜNTHER, T. (1987). Amiloride-sensitive net Mg^{2+} efflux from isolated perfused rat hearts. *Magnesium* **6**, 220-224.

VORMANN, J. & GÜNTHER, T. (1993). Magnesium transport mechanisms. In *Magnesium and the Cell*, ed. BIRCH, N.J., pp. 137-155. London: Academic Press.

WACKER, W.E. (1969). The biochemistry of magnesium. *Annals of the New York Academy of Sciences* **162**, 717-726.

WATANO, T., HARADA, Y., HARADA, K. & NISHIMURA, N. (1999). Effect of Na^+/Ca^{2+} exchange inhibitor, KB-R7943 on ouabain-induced arrhythmias in guinea-pigs. *British Journal of Pharmacology* **127**, 1846-1850.

WEBER, A., HERZ, A. & REISS, I. (1969). The role of magnesium in the relaxation of myofibrils. *Biochemistry* **8**, 2266-2271.

WENDT-GALLITELLI, M.F. & ISENBERG, G. (1989). X-ray microanalysis of single cardiac myocytes frozen under voltage-clamp conditions. *American Journal of Physiology* **256**, H574-H583.

WHANG, R. (1993). Clinical perturbations in magnesium metabolism-hypomagnesaemia and hypermagnesaemia. In *Magnesium and the cell*, ed. BIRCH, N.J., pp. 5-14. Academic press limited.

WHANG, R., HAMPTON, E.M. & WHANG, D.D. (1994). Magnesium homeostasis and clinical disorders of magnesium deficiency. *Annals of Pharmacotherapy* **28**, 220-226.

WHITE, R.E. & HARTZELL, H.C. (1988). Effects of intracellular free magnesium on calcium current in isolated cardiac myocytes. *Science* **239**, 778-780.

WHITE, R.E. & HARTZELL, H.C. (1989). Magnesium ions in cardiac function. Regulator of ion channels and second messengers. *Biochemical Pharmacology* **38**, 859-867.

WILLIAMS, B.A. & BEATCH, G.N. (1997). Magnesium shifts voltage dependence of activation of delayed rectifier I_K in guinea pig ventricular myocytes. *American Journal of Physiology* **272**, H1292-H1301.

WILLIAMS, D.A., CODY, S.H. & DUBBIN, P.N. (1999). Introducing and calibrating fluorescent probes in cells and organelles. In *Fluorescent and Luminescent Probes for Biological Activity: A Practical Guide to Technology for Quantitative Real-Time Analysis*, ed. MASON, W.T., pp. 321-334. Academic Press.

WILLIAMS, R.J.P. (1970). The biochemistry of sodium, potassium, magnesium, and calcium. *Quarterly reviews - Chemical society* **24**, 331-365.

WILLIAMS, R.J.P. (1993). Magnesium: An Introduction to its Biochemistry. In *Magnesium and the Cell*, ed. BIRCH, N.J., pp. 15-30. London: Academic Press.

WILLIAMSON, J.R., WILLIAMS, R.J., COLL, K.E. & THOMAS, A.P. (1983). Cytosolic free Ca^{2+} concentration and intracellular calcium distribution of Ca^{2+}-tolerant isolated heart cells. *Journal of Biological Chemistry* **258**, 13411-13414.

WITTENBERG, B.A. & GUPTA, R.K. (1985). NMR studies of intracellular sodium ions in mammalian cardiac myocytes. *Journal of Biological Chemistry* **260**, 2031-2034.

WOLF, F.I., COVACCI, V., BRUZZESE, N., DI FRANCESCO, A., SACCHETTI, A., CORDA, D. & CITTADINI, A. (1998). Differentiation of HL-60 promyelocytic leukemia cells is accompanied by a modification of magnesium homeostasis. *Journal of Cellular Biochemistry* **71**, 441-448.

WOLF, F.I., DI FRANCESCO, A. & CITTADINI, A. (1994a). Characterization of magnesium efflux from Ehrlich ascites tumor cells. *Archives of Biochemistry & Biophysics* **308**, 335-341.

WOLF, F.I., DI FRANCESCO, A., COVACCI, V. & CITTADINI, A. (1994b). cAMP activates magnesium efflux via the Na/Mg antiporter in ascites cells. *Biochemical & Biophysical Research Communications* **202**, 1209-1214.

WOLF, F.I., DI FRANCESCO, A., COVACCI, V. & CITTADINI, A. (1997). Regulation of magnesium efflux from rat spleen lymphocytes. *Archives of Biochemistry & Biophysics* **344**, 397-403.

WOODFIELD, K., RUCK, A., BRDICZKA, D. & HALESTRAP, A.P. (1998). Direct demonstration of a specific interaction between cyclophilin-D and the adenine nucleotide translocase confirms their role in the mitochondrial permeability transition. *Biochemical Journal* **336**, 287-290.

WOODS, K.L. & FLETCHER, S. (1994). Long-term outcome after intravenous magnesium sulphate in suspected acute myocardial infarction: the second Leicester Intravenous Magnesium Intervention Trial (LIMIT-2). *Lancet* **343**, 816-819.

WOODS, K.L., FLETCHER, S., ROFFE, C. & HAIDER, Y. (1992). Intravenous magnesium sulphate in suspected acute myocardial infarction: results of the second Leicester Intravenous Magnesium Intervention Trial (LIMIT-2). *Lancet* **339**, 1553-1558.

WU, J.Y. & LIPSIUS, S.L. (1990). Effects of extracellular Mg^{2+} on T- and L-type Ca^{2+} currents in single atrial myocytes. *American Journal of Physiology* **259**, H1842-H1850.

WU, S.T., PIEPER, G.M., SALHANY, J.M. & ELIOT, R.S. (1981). Measurement of free magnesium in perfused and ischemic arrested heart muscle. A quantitative phosphorus-31 nuclear magnetic resonance and multiequilibria analysis. *Biochemistry* **20**, 7399-7403.

XU, W. & WILLIS, J.S. (1994). Sodium transport through the amiloride-sensitive Na-Mg pathway of hamster red cells. *Journal of Membrane Biology* **141**, 277-287.

YAMASHITA, J., ITOH, M., KURO, T., KOBAYASHI, Y., OGATA, M., TAKAOKA, M. & MATSUMURA, Y. (2001a). Pre- or post-ischemic treatment with a novel Na^{+}/Ca^{2+} exchange inhibitor, KB-R7943, shows renal protective effects in rats with ischemic acute renal failure. *Journal of Pharmacology & Experimental Therapeutics* **296**, 412-419.

YAMASHITA, J., OGATA, M., TAKAOKA, M. & MATSUMURA, Y. (2001b). KB-R7943, a selective Na^{+}/Ca^{2+} exchange inhibitor, protects against ischemic acute renal failure in mice by inhibiting renal endothelin-1 overproduction. *Journal of Cardiovascular Pharmacology* **37**, 271-279.

ZHANG, G.H. & MELVIN, J.E. (1996). Na^{+}-dependent release of Mg^{2+} from an intracellular pool in rat sublingual mucous acini. *Journal of Biological Chemistry* **271**, 29067-29072.

ZHANG, S., SAWANOBORI, T., ADANIYA, H., HIRANO, Y. & HIRAOKA, M. (1995). Dual effects of external magnesium on action potential duration in guinea pig ventricular myocytes. *American Journal of Physiology* **268**, H2321-H2328.

PUBLICATIONS

ALMULLA, H.A., FLATMAN, P.W. & ELLIS, D. (2001). Sodium-dependent magnesium transport in isolated rat ventricular myocytes. *Journal of Physiology* **531.P**, 186P.

FLATMAN, P.W., ALMULLA, H., ELLIS, D. (2001). The role of sodium-magnesium antiport in magnesium homeostasis in the mammalian heart. In *Advances in Magnesium Research, Nutrition & Health,* ed. RAYSSIGUIER, Y., MAZUR, A., DURLACH, J., pp. 39-45. John Libbey & Company Ltd.

FLATMAN, P.W., ELLIS, D., ALMULLA, H. (2001). Magnesium homeostasis in the mammalian heart. *Magnesium Research* **14(1)**, 84-85.